Precise quantitation of PTEN by immuno-MRM: a tool to resolve the PTEN biomarker controversy in many cancers and hepatic disorders

by

Sahar Mahmoud Ibrahim

Experimental medicine department, McGill University, Montreal

December 2022

A thesis submitted to McGill University in partial fulfillment of the requirements of the degree of

DOCTOR OF PHILOSOPHY

Table of Contents

Abstract

The tumor suppressor PTEN is the main negative regulator of the PI3K/AKT signalling pathway, commonly found downregulated in some diseases and cancer subtypes such as breast cancer (BC). The degree of PTEN downregulation studied in mice models was found to be proportional to the tumor severity in a dose-dependent manner. However, conflicting immunohistochemistry (IHC) and western blot (WB) data have sparked a controversy about the clinical significance of PTEN's use as a biomarker to predict poor outcomes, resistance to several therapeutics as well as to select patients for combinatorial therapy with PI3K pathway inhibitors. Such techniques lack the inter-laboratory standardization, and high precision required to correlate minor PTEN-expression changes in tumors to clinical data. Mass spectrometry (MS)-based techniques especially multiple reaction monitoring (MRM) has garnered much interest from researchers as well as lately from hospitals and clinical labs. The high sensitivity, specificity, and great dynamic range are characteristic advantages of MS-based techniques. In addition, adding stable isotope-labeled standards has enabled "absolute quantitation" of the analytes and therefore highly precise and accurate assays. In a robust LC-MRM method for protein quantitation, a 'proteotypic' peptide released upon proteolytic digestion is quantified as a surrogate. With the development of more affordable and reliable instruments, MS has become less expensive and has a simpler setup than other methods. Moreover, MS has outperformed and, in some cases, replaced conventional techniques such as immunoassays. The FDA has approved MS for use as a diagnostic method for the identification of microbes, newborn screening, therapeutic drug monitoring, and vitamin D. In this work, I developed and analytically validated (*i*) a fully standardized, and robust microflow-MRM assay for the precise quantitation of PTEN. Because its high sensitivity was still insufficient to reliably quantify low PTEN levels in tumor samples, I further refined my PTEN MRM assay by developing a preceding anti-peptide antibody-based immuno-enrichment step to enrich my target peptide and improve its detectability prior to MS analysis. This immuno-MRM (iMRM) strategy enabled the precise quantitation of PTEN-expression in cells, fresh frozen- and formalin-fixed paraffin-embedded (FFPE) tissues, down to 0.1 fmol/10 µg of extracted protein, with high inter- and intra-day precision. I further developed (*ii*) a novel two-point internal calibration (2-PIC) strategy avoiding the need for external calibration of MRM data, which comes along with several shortcomings. The 2-PIC strategy has demonstrated high flexibility and robustness that fits well for clinical application, as the

suboptimal use of either surrogate matrices or additional patient material for external calibration can be avoided, while concurrently reducing instrument time and cost. Next, (*iii*) I used my 2-PIC iMRM assay to quantify PTEN in cell lines, fresh frozen-, and formalin-fixed paraffin-embedded (FFPE) patient/PDX tissues samples. PTEN protein levels in HER+2 BC PDX samples determined by iMRM correlate well with semi-quantitative IHC and WB data that were obtained under non-realistic ideal conditions. iMRM, however, allowed the precise quantitation of PTEN -- even in samples that were deemed to be PTEN-negative by IHC or WB -- while requiring substantially less tumor tissue than WB. This is particularly relevant because the extent of PTEN down-regulation in tumors has been shown to correlate with severity. Finally, to evaluate the full potential of my PTEN assay (*iv*) I determined PTEN protein levels in triple-negative BC PDX samples that were treated with paclitaxel and carboplatin to compare their PTEN concentrations with the PDXs' response to therapy. I could demonstrate that metastatic tumors showed a good correlation (r^2=0.86) between paclitaxel response and the determined PTEN concentrations.

Abstrait

Le suppresseur de tumeur PTEN est le principal régulateur négatif de la signalisation PI3K/AKT/mTOR. PTEN est couramment trouvé régulé à la baisse dans certains sous-types de maladies et de cancers tels que le cancer du sein (BC) en raison de plusieurs mécanismes transcriptionnels et post-transcriptionnels. Les données contradictoires d'immunohistochimie (IHC) et de western blot (WB) ont suscité une controverse sur le rôle de PTEN en tant que biomarqueur pronostique et prédictif dans ces cancers. Cela a entravé la précision requise pour corréler les modifications mineures de l'expression de PTEN dans les tumeurs aux données cliniques. Les techniques basées sur la spectrométrie de masse (MS), en particulier la surveillance des réactions multiples (MRM), ont suscité beaucoup d'intérêt de la part des chercheurs ainsi que, récemment, des hôpitaux et des laboratoires cliniques. La sensibilité élevée, la spécificité et la grande plage dynamique sont des avantages caractéristiques des MS techniques. De plus, l'ajout d'étalons marqués par des isotopes stables a permis une "quantification absolue" des analytes et donc des dosages très précis et exacts. Dans une méthode LC-MRM robuste pour la quantification des protéines, un peptide « protéotypique » libéré lors de la digestion protéolytique est quantifié en tant que substitut. Avec le développement d'instruments plus abordables et plus fiables, la MS techniques est devenue moins chère et sa configuration est plus simple que les autres méthodes. De plus, MS a surpassé et, dans certains cas, remplacé les techniques conventionnelles telles que les dosages immunologiques. Dans ce travail, j'ai développé et validé analytiquement (i) un test microflow-MRM entièrement standardisé et robuste pour la quantification précise de PTEN. Parce que sa haute sensibilité était encore insuffisante pour quantifier de manière fiable les faibles niveaux de PTEN dans les échantillons de tumeurs, j'ai encore affiné mon test PTEN MRM en développant une étape précédente d'immuno-enrichissement à base d'anticorps anti-peptide pour enrichir mon peptide cible et améliorer sa détectabilité. Analyse. Cette stratégie immuno-MRM (iMRM) a permis la quantification précise de l'expression de PTEN dans les cellules, les tissus frais congelés et FFPE, jusqu'à 0,1 fmol/10 µg de protéine extraite, avec une inter- et précision intra-journalière. J'ai ensuite développé (ii) une nouvelle stratégie d'étalonnage interne en deux points (2-PIC) évitant le besoin d'un étalonnage externe des données MRM, qui s'accompagne de plusieurs lacunes. La stratégie 2-PIC a démontré une flexibilité et une robustesse élevées qui conviennent bien à l'application clinique, car l'utilisation sous-optimale de matrices de substitution ou de

matériel patient supplémentaire. Ensuite, (iii) j'ai utilisé mon test 2-PIC iMRM pour quantifier le PTEN dans des lignées cellulaires, des échantillons de tissus de patients/PDX frais congelés et fixés au formol inclus en paraffine (FFPE). PTEN niveaux dans les échantillons HER+2 BC PDX déterminés par iMRM sont bien corrélés avec les données IHC et WB semi-quantitatives qui ont été obtenues dans des conditions idéales non réalistes. L'iMRM, cependant, a permis la quantification précise de PTEN - même dans les échantillons jugés négatifs pour PTEN par IHC ou WB - tout en nécessitant beaucoup moins de tissu tumoral que WB. Ceci est particulièrement pertinent car il a été démontré que l'étendue de la régulation à la baisse de PTEN dans les tumeurs est corrélée à la gravité. Enfin, pour évaluer le plein potentiel de mon test PTEN (iv), j'ai déterminé PTEN niveaux dans des échantillons BC PDX triple négatifs qui ont été traités avec du paclitaxel et du carboplatine pour comparer leurs concentrations de PTEN avec la réponse des PDX au traitement. J'ai pu démontrer que les tumeurs métastatiques montraient une bonne corrélation ($r^2 = 0,86$) entre la réponse au paclitaxel et les concentrations de PTEN déterminées.

Acknowledgements

First and foremost, I would like to praise and thank Allah, the almighty, who has granted countless blessing, knowledge, and opportunity to the writer, so that I have been finally able to accomplish the thesis. This thesis would not have been possible without the hard work and support of many talented people. Firstly, I would like to thank my supervisors Dr. Gerald Batist and Dr. Christoph Borchers for their guidance and encouragement throughout this project. I am very grateful for the help of Dr. Rene Zahedi, who closely supervised all the experiments and work related to this thesis, and always had time to give his expert advice and answer questions. I am truly lucky to have such an intelligent and supportive mentor in mapping my PhD journey. I would like to thank my research advisory committee members, Dr. Elizabeth MacNamara, Dr. Shaun Eintracht, and Dr. Chantal Autexier for their insightful guidance. I would also like to thank Dr. Carol Parker, Dr. Andre Leblanc, Dr. Vincent Richard, Dr. Evgeniy Petrotchenko, Connie Sobsey, Dr. Vanessa Gaspar, Vincent Lacasse, and Hannah Meltzer for their support and advice along the way.

I wish to extend a special thank you to Dr. Mark Basik and Dr. Adriana Aguilar for providing the cell lines, FFPE and fresh frozen tissue breast cancer PDX samples along with their data on PTEN copy number variants, as well as the triple-negative breast cancer PDX samples' response data to paclitaxel and carboplatin. I would like to acknowledge Cathy Lan and Dr. Catherine Chabot who conducted the Western Blot PTEN quantitation from cell lines and fresh frozen breast cancer tissue samples. I am very grateful to Dr. Alan Spatz and Dr. Manuela Pelmus who conducted the H&E and PTEN IHC examination of the FFPE tissue slides. I would also like to acknowledge Bjorn Frohlich, who conducted the iMALDI experiments which contributed to further validation of our two-point internal calibration strategy. I would like to deeply thank Georgia Mitsa, whose optimized protocol of protein extraction from FFPE cores was critical for applying my PTEN iMRM method to test FFPE tissue samples. I would like to acknowledge Dr. Oliver Poetz for developing the anti-peptide monoclonal antibodies we used in our assay. I would like to thank Carol Parker for her expert advice and assistance with editing this thesis.

This research was funded by Genome Canada through the Genomics Technology Platform (GTP: 264PRO). We are also grateful for support from the Warren Y. Soper Charitable Trust and the Alvin Segal Family Foundation to the Jewish General Hospital (Montreal, Quebec, Canada).

I would like to thank my family for their endless patience, support and many motivational speeches they gave me to be able to finish my PhD project.

Contribution to original knowledge

This thesis is intended to introduce to the scientific medical community, including clinicians as well, an anti-peptide immuno-multiple reaction monitoring assay with superior sensitivity and precision of PTEN quantitation. This, for the first time, allows us to discriminate the subtle differences in PTEN protein expression in a standardized manner, which is imperative for inter-laboratory comparisons. Importantly, this method makes it possible to conduct large-scale and cross-laboratory projects, which is greatly needed for testing and validating the clinical benefits of using PTEN as a biomarker in many different types of cancers, including breast cancer, colorectal cancer, and hepatocellular carcinoma, to name a few, as well as several non-neoplastic hepatic disorders. Moreover, the assay has the capacity to be fully automated it is hoped that it will be translated to clinical diagnostics, especially since MRM methods on triple quadrupole instruments, with high flow rate chromatographic separations, are already well established in clinical labs and the use of this technique in clinical labs has been increasing over the past several years. Also, the assay uses a new internal calibration strategy. The goal of this new strategy is to replace and to avoid the drawbacks of the conventional multipoint external calibration, especially for immuno-mass spectrometry assays applied to precious patients' tissue samples for the streamlined quantitation of low-abundance proteins. The two-point internal calibration (2PIC) only uses two peptide isotopologues as internal standards, and has no matrix effect issues. At the same time, it decreases the cost and the turnaround time, as well as the burden of preparing multiple calibration standards with every batch of samples. These advantages are of great value in clinical diagnostics. It is important, however, to note that the analytical quality of the assay will only be maintained if the standards are in the linear range.

Also, this thesis introduces, for the first time, the "absolute PTEN protein concentration" of several commercially available breast cancer and colorectal cell lines. During several years of analyzing samples from patients with hepatocellular carcinoma, colorectal metastases, and various non-neoplastic hepatic disorders, I have documented a significant variation of PTEN protein concentrations in these disorders. It is therefore hoped that this assay will help to improve the stratification of patients with these disorders, as a step forward towards personalized medicine.

Despite the limited number of samples tested, I have found a very clear positive correlation between the PTEN level and the response to paclitaxel in the metastatic BC PDX samples. This

indicates that the PTEN iMRM assay may allow the validation of PTEN as a predictive biomarker if enough samples are available to be tested, where cumulative results can be analyzed as in meta- or mega-analysis.

Contribution of authors

I did nearly all of the work described in this thesis. I performed all of the research and experiments related to the selection of the surrogate peptide and its product ions. Then I developed the LC-MRM method and did the optimization of its LC and MS parameters. I developed and optimized the anti-peptide immuno-enrichment step using the anti-peptide monoclonal antibodies developed by Dr. Oliver Poetz. All of the LC-MRM validation experiments were done by me, as well as all of the LC-MRM experiments that were used for validating the two-point internal calibration strategy in comparison with the external calibration. Bjorn Frohlich performed all the PTEN iMALDI experiments.

I was responsible for all of the steps and details of carrying out the experiments; the sample preparation including the standards made of the synthetic peptides, embedding the fresh frozen samples in OCT blocks and their protein extraction, as well as the protein extraction of cell lines, FFPE cores. For the extraction of proteins from FFPE cores, I used the protocol that was developed and optimized by Georgia Mitsa. Also, I did all of the sample preparation related to the bottom-up proteomics experiments, including denaturation, reduction, alkylation, and tryptic digestion, as well as sample purification, followed by all sample preparation related to the antipeptide immuno-enrichment step. I performed all of the LC-MRM analysis of all of the samples including the standards, the quality control samples, and the cell line and tissue samples (from patients or PDXs). This also included instrument maintenance and calibration, in addition to the troubleshooting of technical problems relating to the instrument.

Throughout the research project, I performed all of the proteomics data analysis, as well as the correlation and statistical analysis of the results. I prepared all the figures and all of the drafts for the first versions of the manuscripts and presentations. I actively contributed to the modifications made during several internal revision cycles (mainly requested by Dr. Rene Zahedi and Dr. Christoph Borchers)., as well as revisions requested by the reviewers of the manuscripts submitted to journals.

Members of the Research Pathology Core Facility at the JGH took care of all of the steps related to FFPE block preparation, punching out cores, H&E staining, PTEN IHC staining and Human mitochondria IHC staining. Dr. Alan Spatz and Dr. Manuela Pelmus performed all of the pathological examination needed and the IHC semiquantitative analysis.

Cathy Lan and Dr. Catherine Chabot from Translational Research Laboratory at the Lady Davis institute developed the cell lines and performed the PTEN and HER2 WB analyses. Marguerite Buchanan established the PDXs, followed their growth, and documented all results related to therapy response after doing all the calculations needed. PTEN copy number variant data was provided by Dr. Adriana Aguilar from CytoScan-HD analysis at Centre for Applied Genomics at Sick Kids Hospital.

The concept and design of the experiments and thesis subject was the result of the collective work of myself, Dr. René Zahedi, Dr. Christoph Borchers, and Dr. Gerald Batist, who were also the supervisors of the entire study.

Discussing the results and the interpretation of the data was the most time-consuming part of the project. This was done by me, with the assistance of Dr. Adriana Maguier, and Dr. Rene Zahedi., Dr. Christoph Borchers, and Dr. Gerald Batist.

Introduction

Since 1997, when PTEN (phosphatase and tensin homolog deleted on chromosome 10) was isolated for the first time and identified as a tumor suppressor, PTEN has attracted significant attention [1]. Being the main negative regulator of the PI3K/AKT pathway and one of the most important tumor suppressors, PTEN plays an important role in carcinogenesis and cancer severity. Therefore, it was proposed as a good candidate for a prognostic and predictive biomarker in many cancer subtypes [2]. Moreover, its function as a metabolic regulator boosts PTEN's prognostic and predictive role in cancer and in many other disorders such as insulin resistance, hepatitis, non-alcoholic fatty liver, and cirrhosis [3].

PTEN has not yet been validated as a biomarker despite the very promising data shown in many preclinical studies. This is due to several reasons: (i) PTEN deletion or loss of function mutations are not common in many cancer subtypes such as breast cancer, colorectal cancer, hepatocellular carcinoma, and prostate cancer as well as in non-neoplastic hepatic disorders. Instead, PTEN is commonly found downregulated via several transcriptional and posttranscriptional mechanisms. Accordingly, genomic data alone is insufficient to determine PTEN status in these cancer types [4]. (ii) Interestingly, a slight reduction of PTEN protein expression in mouse models was found to be sufficient to induce cancer, and the degree of reduction correlated with cancer severity in a dose-dependent manner [5].

While determining PTEN protein expression, (iii) several clinical studies showed many conflicting data that have sparked a controversy about PTEN's role as a prognostic and predictive biomarker in the above-mentioned cancer types and hepatic disorders. Carbognin et al. reasoned that the major source of the conflicting data on PTEN was the lack of standardization of the methods used to determine PTEN expression and neither the type of assay nor the protocols used for a single type of assay were consistent and reproducible across these studies [6]. Conventional methods, such as immunohistochemistry (IHC) and western blot [7] [7] techniques are associated with a variety of analytical and preanalytical shortcomings and generally lack standardization, high precision, and throughput. Thus, these assays do not have the precision required to correlate minor PTEN-expression changes in patients' samples with their clinical data. Moreover, both of these techniques do not provide a clear 'absolute' measure of PTEN expression and are instead 'relative' and subjective. These shortcomings have prevented the

cross-laboratory and cross-study comparison of data on PTEN expression, or the large-scale integrative projects needed for biomarker validation. Thus, there is an urgent need for an improved, robust, accurate, and validated method that allows the standardized and precise quantitation of actual PTEN protein expression in tissue samples – a method with high throughput capacity and which will therefore allow the clear discrimination of subtle differences in PTEN expression in clinical samples. Only this type of method will enable the thorough study of PTEN's role as a biomarker for diagnostic and prognostic purposes in precision oncology.

In general, proteins are the functional biomolecules which accurately represent the phenotype, which are the targets of many drugs, and which can act as biomarkers. Many comparative studies have found that correlations between RNA and protein levels are relatively weak and uncertain, or only moderately positive [8-13], while in studies involving cancer, the results are contradictory [12, 14, 15]. Therefore, determination of the protein levels provides a more comprehensive understanding of the pathology and more accurately reflects the tissue phenotype. However, the quantitative measurement of proteins using traditional techniques such as WB and IHC and other immunoassays has several limitations. For example, the performance of the antibodies in the immunoassays is a major source of inaccuracy. Antibodies can lack specificity and hence cannot distinguish between similar homologues and sequence variants arising from polymorphisms and mutations. They may fail to recognize an antigen, for example, due to an unusual post-translational modification (PTM) pattern. Some of these modifications can also interfere with the antibody binding to the protein [16].

IHC has many other issues besides antibody specificity. The fixation process can lead to molecular deformations which can hinder recognition by antibodies, particularly in glutaraldehyde-based fixation [17]. Additionally, sample fixation has the potential to induce artificial patterns, particularly for signalling PTMs such as protein phosphorylation, or, conversely, may fail to preserve these. For example, the IHC methods for detecting programmed death-ligand 1 (PD-L1), an important companion diagnostic for immune checkpoint therapies, can suffer severely from interference due to endogenous PD-L1 glycosylation patterns that prevent proper epitope recognition, leading to underestimation of PD-L1 expression levels [18]. One of the most serious drawbacks of IHC is that the results are often interpreted in a semi-

quantitative manner and hence always suffer from subjectivity and irreproducibility, [19] despite the continuous efforts to improve standardization [20].

Mass spectrometry (MS), particularly targeted MS, is increasingly being used for quantifying specific proteins and peptides in clinical specimens. Multiple reaction monitoring (MRM)-based assays are specific, can be multiplexed and precise, and they also can be standardized, reproduced, and distributed across laboratories and instruments. By identifying and determining the intensities of precursor and product ions of the selected proteotypic peptide and its isotopically labeled internal standard, MRM-MS allows a highly precise quantitation of the protein of interest [21]. The use of internal standards, typically a synthetic variant of the target peptide that is stable-isotope labeled and that is spiked into a sample at known concentration, enables the 'absolute' quantitation (i.e. concentration determination) of the endogenous target protein levels. As a result, MRM has been considered to be one of the most effective tools available for quantitative clinical proteomics, and has been proposed as the future alternative to standard antibody-based clinical assays [22].

Therefore, my first aim was to develop and optimize an MRM assay that was precise and sensitive enough to detect the low-abundance signaling protein PTEN in clinical samples.

The surrogate peptide or the" proteotypic peptide", which uniquely represents the target protein to be used for PTEN quantitation, was first selected with the help of proteomics databases and enforcing many rules [23]. The actual precursor ion selection (NNIDDVVR; 472.7434++) was based on data acquired from a data dependent acquisition [24] experiment using digested recPTEN, followed by a Parallel reaction monitoring (PRM) experiment to allow selecting the product ions form the peptide as the most abundant ions. The PTEN surrogate peptide NNIDDVVR was selected as ideal target to develop a highly sensitive liquid chromatography (LC)-MRM method, after querying proteomics databases, enforcing specific sequence and peptide criteria [23], and analyzing recombinant PTEN to validate a good signal response. Then an LC-MRM method for the NNIDDVVR peptide was developed on an Agilent 6495 triple quadrupole mass spectrometer, and the LC conditions and collision energies for individual MRM transitions were optimized to reduce analysis time and improve sensitivity. Unfortunately, although the

sensitivity of the assay was high, it was still not sufficient to quantify endogenous PTEN in different cell lines.

Typical steps to improve the sensitivity of MS-based assays include (i) the reduction of LC-MS flow rates, (ii) fractionation of samples prior LC-MS, or (iii) enrichment strategies prior to LC-MS analysis. Options (i) and (ii), however, are not in agreement with the high robustness and reproducibility required for clinical translation. In contrast, enrichment strategies can be used, particularly if they can be automated and well-controlled. Enrichment of PTEN on the protein level, however, is difficult to control, due to the lack of appropriate standards to compensate for variations in protein recovery. In contrast, peptide-based enrichment strategies can be well-controlled through the spike-in of a stable isotope labeled internal standard of the target peptide prior to enrichment. I therefore decided to generate an anti-peptide antibody targeted against NNIDDVVR in order to develop an immuno-MRM assay (iMRM) with very high sensitivity. The immuno-enrichment step significantly increased the sensitivity and successfully allowed endogenous PTEN quantitation.

The second aim of my work was to couple the PTEN iMRM assay to a calibration strategy that allows endogenous PTEN quantitation with high precision and accuracy. External calibration is the standard calibration method for quantitative MS assays. However, surrogate matrices are often used for external calibration especially, based on the assumption that an analyte's LC-MS response is the same in different types of samples, thus ignoring a major source of error in external calibration, i.e., matrix effects. In this way, the external calibration strategy using a surrogate matrix has inherent limitations for the analysis of clinical specimens where sample amount is typically limited. Furthermore, mimicking the matrix of a PTEN iMRM assay in order to generate a representative external calibration curve is challenging, as the background obtained after immuno-enrichment depends strongly on both the antibody used and the sample. I therefore developed and validated an internal calibration strategy that uses two isotopologues (i.e. stable isotope labeled internal standards with a different mass shift) at different concentrations in order to quantify the protein of interest, i.e. two-point internal calibration (2-PIC). By avoiding the cost and burden of preparing multiple calibration standards with every batch of samples, this calibration strategy adds more advantages to the PTEN iMRM assay and increases its potentials to be used in clinical labs.

Having developed a sensitive and robust iMRM method based on the new 2-PIC strategy, the next aim was to fully validate the assay to ensure its robustness before using it to quantify PTEN in clinical samples. For this purpose, I performed a set of experiments to evaluate the robustness, reproducibility, and precision/accuracy of the assay. I followed the Clinical Proteomic Tumor Analysis Consortium [25] guidelines for targeted MS to generate the response curve, to determine the the repeatability and the selectivity, and to the assessment of selectivity using multiple biological replicates of the matrix of interest. I also evaluated the recovery with the anti-peptide immuno-enrichment step added to the MRM workflow before testing the overall accuracy of the assay using different known amounts of a commercially available recombinant PTEN.

Then I used this validated iMRM method to quantify PTEN in different clinical specimens and to test its efficacy compared to WB and IHC. I started with three cell lines derived from HER2 breast cancer PDXs and three commercially available cell lines representing different BC subtypes: luminal B, luminal A, and triple-negative basal. I next evaluated the capacity of our iMRM assay to quantify PTEN levels in tissues. I therefore analyzed metastatic colorectal cancer (mCRC) and surrounding healthy hepatic tissues from three different patients in order to evaluate the assay's capability to discriminate between PTEN concentrations in the tumor area from its concentration in surrounding liver tissues. I furtherly applied PTEN iMRM to samples where a higher variability of PTEN expression could be expected, in order to test the capability of the assay for discriminating between BC patients with to different PTEN protein levels. I analyzed, in triplicate, samples derived from HER2+BC PDX models (13 samples), including biological replicates. Each sample was tested using both fresh frozen and formalin fixed paraffin embedded tissues (FFPE). PTEN protein levels determined by iMRM were found to correlate well with semiquantitative IHC and WB data. iMRM, however, allowed the precise quantitation of PTEN even in samples that were deemed to be PTEN negative by IHC or WB, while requiring substantially less tumor tissue than WB.

The BC patient stratification using PTEN level determined with our iMRM assay encouraged me to test additional clinical samples with other disorders where PTEN protein have been demonstrated to be a promising biomarker candidate. I, therefore analyzed several fresh frozen tissue samples of patients with colorectal cancer and different benign hepatic tumors where we found high variation in PTEN level.

The PTEN's role as a predictive biomarker across multiple tumor types for response to different cancer therapeutics has been given also special attention. From several preclinical and clinical BC studies [26-28], it has been deduced that the PTEN protein expression level is a promising potential clinical biomarker in BC for prediction of the resistance to endocrine and anti-HER2 therapies, and for selecting patients for combinatorial therapy with PI3K pathway inhibitors. However, several other studies have failed to report either an association between PTEN protein levels and prognosis in BC patients or an association with treatment response to various BC therapeutics in clinical trials.

Thus, one of the most important potential applications of my PTEN iMRM assay was to test this predictive role of PTEN and to be able to either validate it clinically, or to reject that role and save the time, money and effort that researchers might be uselessly spending. I therefore wanted to test some BC-PDXs treated with paclitaxel and carboplatin to evaluate whether there was a clinically significant correlation between PTEN protein concentration and response to therapeutics. Despite the limited number of samples tested, I found a very clear positive correlation between PTEN level and response to paclitaxel in the metastatic BC PDX samples. This shows that this PTEN iMRM assay may allow the validation of PTEN as a predictive biomarker as well as a prognostic one if enough samples are available to be tested and then cumulative results can be analyzed as in meta- or mega-analysis.

Literature review

The PI3K/AKT/mTOR pathway is one of the most commonly dysregulated signaling pathways in a variety of cancers. This pathway controls key cellular processes, such as metabolism, motility, growth, and proliferation, that support the survival, expansion, and dissemination of cancer cells. It is therefore a key target for therapeutic inhibition [29].

The pathway starts with PI3K activation (see Figure 1). Three of the class I catalytic isoforms (For p110α, β and δ; collectively known as the class IA subgroup) associate with regulatory subunits whose SH2 domains bind to phosphor-tyrosyl residues on growth factor receptors or adaptor proteins such as IRS1. The other catalytic isoform (p110γ; known as class IB) associates with regulatory subunits (p101, p87) that mediate binding to βγ subunits of heterotrimeric G proteins following activation of G protein-coupled receptors (GPCRs) [30-32]. The activated catalytic isoforms of PI3K allow the production of the second messenger phosphatidylinositol-3,4,5-triphosphate (PI3,4,5-P3; PIP3) through phosphorylation of the substrate phosphatidylinositol-4,5-bisphosphate (PI-4,5-P2; PIP2). This is the reaction that is reversed by PTEN's lipid phosphatase activity which converts PIP3 back to PIP2 and inhibits the pathway activation. PIP3 then recruits a subset of signaling proteins that have pleckstrin homology (PH) domains to the membrane, including protein serine/threonine kinase-3′-phosphoinositide-dependent kinase 1 (PDK1) and AKT [29].

AKT, on its own, regulates several cellular processes involved in cell survival and cell cycle progression. The AKT/ mammalian target of rapamycin (mTOR) signaling is one of the most important pathways downstream AKT that have been commonly found activated in many cancers. AKT directly phosphorylates the tumor suppressor tuberin (TSC2) relieving the inhibitory effects of the TSC1-TSC2 complex on Ras homolog enriched in brain (Rheb) and mTOR complex 1 (mTORC1). The mTORC1 mediates phosphorylation of the ribosomal S6 kinases (S6K1/2) and the eIF4E-binding proteins (4EBP1/2) stimulating mRNA translation and, ultimately, cell growth and proliferation. Also, mTOR signaling regulates immune cell differentiation and plays an important role in tumor metabolism [32-34].

Furthermore, AKT can induce cell survival through inactivating pro-apoptotic factors such as BAD and Procaspase-9, as well as the Forkhead family of transcription factors that induce the expression of other pro-apoptotic factors, such as Fas-ligand (FasL) [31]. AKT also activates the

IκB kinase [35], a positive regulator of the survival factor NFκB. For cell growth and proliferation, AKT has several targets involved in protein synthesis, glycogen metabolism, and cell cycle regulation, including mTOR, glycogen synthase kinase-3 (GSK3), insulin receptor substrate-1 (IRS-1), the cyclin-dependent kinase inhibitors p21CIP1/WAF1 and p27KIP1. AKT triggers a network that positively regulates G1/S cell cycle progression through inactivation of GSK3-β, leading to increased cyclin D1, and inhibition of the Forkhead family transcription factors and the tumor suppressor tuberin (TSC2) [36].

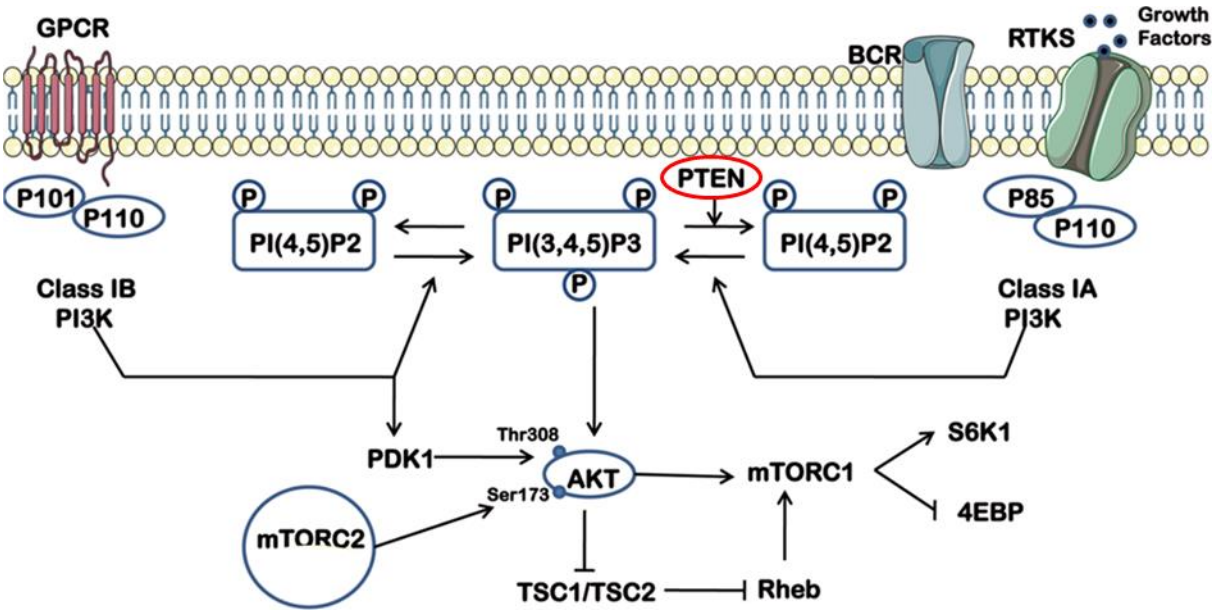

Figure 1: **As a major downstream effector of receptor tyrosine kinase (RTK) and G protein-coupled receptors, PI3K activates various downstream effectors by generating phospholipids, thereby transducing signals of various growth factors and cytokines into intracellular information.** The main lipid substrate of PTEN is PIP 3 and PTEN acts as a negative regulator of PI3K/AKT signaling. Among the upstream signaling networks, AKT inactivates TSC1/2 and activates mTORC1. mTORC2 directly phosphorylates AKT at S473 leading to its complete activation. This activation of the PI3K/Akt pathway is opposed by PTEN (Figure adapted from Liu et al.)[2].

Due to the pathway's critical functions that can be tumorigenic once it is overstimulated, the pathway's activity is carefully controlled by several negative regulators including tuberous TSC1, TSC2, and liver kinase B1 (LKB1). However, the most important negative regulator of the pathway is PTEN [30].

PTEN protein biology, localization and functions

The canonical PTEN protein contains 403-amino acids where the amino-terminal region shares sequence homology with the actin filament capping protein TENSIN (hence its name: "tensin homolog") and the putative tyrosine-protein phosphatase AUXILIN. PTEN was identified as a protein tyrosine phosphatase (PTP) due to its sequence homology in the catalytic domain to members of the PTP family [37].

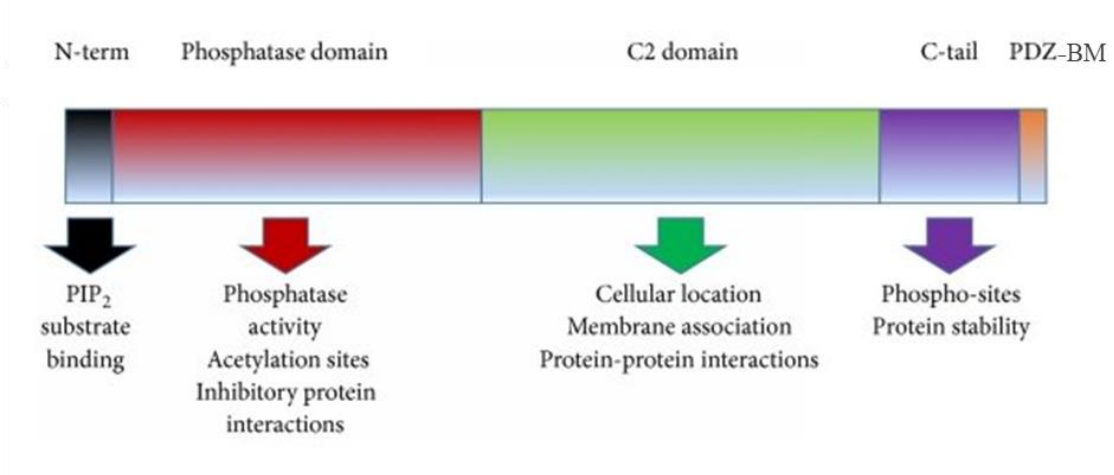

Figure 2: **Protein domains of PTEN.** PTEN has five distinct domains, consisting of (i) an N-terminal PIP binding domain, (ii) the phosphatase domain responsible for its enzymatic activity and containing acetylation sites responsible for regulating this phosphatase activity, (iii) the regulatory C2 domain responsible for PTEN's cellular location and protein-protein interactions including those that modify enzyme activity or localization, (iv) the less understood C-tail containing phosphorylation sites thought to be critical for PTEN's stability, and finally (v) the C-terminal PDZ-binding motif (PDZ-BM) domain (Figure adapted from Jerde et al.)[38].

PTEN is composed of five functional domains (see Figure 2): (i) **a short N-terminal phosphatidylinositol (PtdIns)(4,5)P2-binding domain (PBD)** that ensures selective binding of PTEN to the inner leaflet of the plasma membrane [39], (ii) **a catalytic phosphatase domain** that contains the PI(3,4,5)P3 catalytic binding site, including the P-loop consisting of the signature HCXXGXXR motif, common with members of protein tyrosine phosphatases (PTP) family, (iii) **a C2 lipid/membrane-binding domain**, (iv) **a C-terminal tail** containing Pro, Glu, Ser and Thr (PEST) sequences that have regulatory features for PTEN stability and activity, (v) **a class I PDZ-binding (PDZ-BD)** that acts as a protein-protein interaction motif [3, 37].

Recently, two transitional isoforms of PTEN have been identified and both are found to be longer than canonical PTEN and translated from alternative start sites upstream from the

canonical AUG start site [40]. **(i) PTEN-Long (PTEN-L) or PTENα** has 173 amino acids added to N-terminus of the canonical sequence, contains a secretion sequence that allow PTEN exit, exist, and function outside the cell. This allows PTEN-L to exert its tumor suppressive functions on adjacent cells as a paracrine interaction. However, the canonical PTEN protein can be secreted in exosomes, and can therefore interact with cells away from its origin. Additionally, PTEN-L is found localized in the mitochondria, where it interacts with PTEN-induced putative kinase 1 (PINK1) and hence regulates mitochondrial function, energy production, and mitophagy [37, 41]. **(ii) PTEN-β** has 146 amino acids added to the canonical N-terminus. This isoform was identified in the nucleolus, where it dephosphorylates nucleolin and thus inhibits transcription of ribosomal DNA, biogenesis of ribosomes, and, therefore, cell proliferation [42].

PTEN is a dual lipid and protein phosphatase, with its main substrate being PIP3. The discovery of PIP3 as PTEN substrate was a cornerstone in understanding PTEN biology and its main function as a negative regulator of the proto-oncogenic PI3K–AKT–mTOR signaling pathway. Because the majority of PTEN is present in the cytosol and nucleus, the mechanism of PTEN localization to the plasma membrane has been thoroughly studied. It has been found that dephosphorylation of PTEN's C-terminal tail residues exposes its surface cationic residues and accommodates an open conformation resulting in rapid electrostatic membrane binding [43]. Once PTEN binds to PIP2 with its PBD binding domain, it exhibits a sliding movement looking for PIP3. The lipid phosphatase motif of PTEN dephosphorylates PIP3 at the 3′ position and converts it back to PIP2, leading to a reduction of PIP3 production and a reduction of signals that depend on PIP3. Thus, PTEN opposes PI3K which catalyzes the reaction from PIP2 to PIP3 [39]. PTEN has a role in regulating cell polarity and migration where PIP3 acts as a secondary messenger [37]. PTEN protein substrates and the physiological relevance of their dephosphorylation are being extensively studied but are not yet fully established. For example, it has been found that PTEN directly dephosphorylates residues on itself (increasing its own activity) [37] and several other protein substrates, such as phosphoglycerate kinase 1 (PGK1) [44], cAMP-responsive element-binding protein 1 (CREB1), proto-oncogene tyrosine-protein kinase SRC [45], and insulin receptor substrate 1 (IRS1) [46]. In the cytoplasm, PTEN also functions as a scaffolding protein where it has been found to be involved in calcium-mediated apoptosis [47], as well as transcriptional activation of the oncogenic tumor necrosis factor (TNF)–nuclear factor-κB (NF-κB) pathway [48].

PTEN translocates into the nucleus through various mechanisms, including passive diffusion, and nuclear import mediated by certain post-translational modifications (PTMs) such as phosphorylation, sumoylation, or monoubiquitylation [37]. In response to DNA damage, nuclear PTEN promotes p53 acetylation to control cellular proliferation and positively upregulate RAD51, a key protein involved in double-strand break (DSB) repair [49]. Nuclear PTEN also promotes (i) genomic stability by binding to centromere protein C (CENPC), as well as (ii) tumor-suppressive activity of the anaphase-promoting complex (APC/C)– CDC20 homologue 1(CDH1) complex [49].

PTEN and cell metabolism

Recently, many studies were conducted on PTEN's role in glycolysis, gluconeogenesis, glycogen synthesis, lipid metabolism, as well as mitochondrial metabolism [3]. PTEN regulates the cellular energy expenditure by reducing cellular uptake of glucose and glutamine while increasing mitochondrial oxidative phosphorylation. Hence, it drives an "anti-Warburg state" in which less glucose is taken up, but it is more efficiently directed to the mitochondrial Krebs cycle. Thus, PTEN counteracts cancer cell metabolic reprogramming [44, 50].

PTEN and the tumor microenvironment

Tumor cells stimulate the infiltration of immune cells into the tumor microenvironment (TME) in order to induce an inflammatory response. This includes growth factors and the secretion of chemokines which, unfortunately, can promote tumor development, progression, and metastasis [50]. Also, during a cancer's induction and progression phases, stromal cells in the TME undergo metabolic reprogramming, altering their phenotype. The interaction between cancer and stromal/immune cells may result in a tumor-permissive or non-permissive TME. Recent studies have shed light on PTEN's role in TME regulation: PTEN has been found to affect (i) the metabolic reprogramming and autophagy of cancer cells, (ii) the immune composition of the TME, as well as (iii) the immune composition the stromal cells. Together, the overall effect of PTEN loss of function shifts the balance towards an immunosuppressive TME [2]. Therefore, PTEN expression and function may refine the prediction of sensitivity/resistance to immune checkpoint inhibition-based therapeutic strategies such as inhibitors of PD-L1 [51, 52], PD-1[53] and CTLA-4 [7, 54].

PTEN and autophagy

It has been found that autophagy-deficient tumors are also PTEN-deficient but notably are wild-type for p53. This further increased our understanding of the crucial protective role of PTEN. Many studies are currently being conducted to reveal the molecular mechanisms behind the relationship between PTEN and autophagy [55].

In conclusion, there are many PTEN functions that are independent of the PI3K/AKT pathway, but which have direct impact on cancer development and progression. Therefore, predicting the effects of PTEN deficiency is very complex because these go far beyond mechanisms that are related to the level of activated AKT.

Regulation of PTEN expression:

PTEN is subject to a wide range of molecular regulatory mechanisms.

PTEN and its genetic alterations.

The PTEN gene is located at chromosome 10q23.31. Mutations have been found throughout PTEN, including large deletions, small deletions or insertions, and point mutations. Allelic losses can result in complete deletion of the PTEN locus, whereas small deletions or insertions and point mutations can produce several truncated PTEN mutants that are functionally impaired [56]. Inherited (germline) loss-of-function mutations in the PTEN gene are rare and highly penetrant. These were originally identified in patients of Cowden disease which is characterized by multiple hamartomas in the skin, mucous membranes, breast, thyroid, and endometrium with increased risk of breast, thyroid, and endometrial cancers. Later germline PTEN mutations have been shown to be associated with more diverse human pathologies, now collectively named as PTEN Hamartoma Tumor Syndrome (PHTS) [57]. Somatic PTEN gene alterations are more frequent in some cancer types such as endometrial cancer (35%), glial tumors (32%) and prostate cancer (17%). In many other cancer types, such as lung, breast, and hepatocellular cancer, patients rarely harbor PTEN somatic mutations [4] and PTEN is downregulated through other mechanisms that are discussed below.

PTEN regulation at the transcriptional level.

PTEN silencing occurs through the hypermethylation of its promoter area, reducing PTEN expression in various cancers such as breast and colorectal cancers. PTEN transcription is also

regulated by various transcriptional factors which are either positive regulators (e.g., p53 and early growth-response protein 1(EGR1)) or negative regulators (e.g., NF-κB and C-repeat binding factor 1(CBF1)) [58].

The regulation of PTEN at the post-transcriptional level.

Numerous microRNAs (miRNAs) negatively regulate PTEN expression. For example, miR21 downregulates PTEN in a variety of human tumors, including hepatocarcinoma, ovarian, and lung cancers. miR25 negatively regulates PTEN levels in melanoma cells. In addition, miRNA regulatory networks also enable oncogenes such as MYC to suppress PTEN protein levels through induction of miR106b~25 miRNA cluster, miR-19, and miR200c [37]. Interestingly, PTEN is also positively regulated by networks of competitive endogenous RNAs (ceRNAs), which include various coding RNAs and non-coding RNAs with partial sequence homology to PTEN and the PTEN pseudogene 1 (PTENP1) mRNAs. The ceRNAs act as a decoy for PTEN-targeting miRNAs, thereby boosting PTEN expression [37, 58].

PTEN regulation by post-translational modifications (PTMs) and protein-protein interaction

PTEN is fine-regulated by a large number of PTMs as well as protein-protein interactions, some of which are summarized in Table 1. For example, PTEN phosphorylation and ubiquitination govern its stability and activity through its subcellular localization. Multiple kinases including CK2 and GSK3β are capable of phosphorylating the PTEN–C-terminal tail that induces a closed conformation and increases PTEN stability but decreases its activity. Conversely, dephosphorylation PTEN with leads to its recruitment to the membrane and hence increase its interaction with PDZ domain-containing proteins. Membrane-associated PTEN is more active but less stable [59].

Regarding PTEN turnover, polyubiquitinated PTEN remains in the cytoplasm and is targeted for degradation by the proteasome, whereas monoubiquitylation of PTEN has been found to regulate import of PTEN into the nucleus **[60]**.

Table 1: Regulation of PTEN by post-translational modifications and interactions with other proteins

Examples of PTEN PTMs that regulate PTEN activity	PTEN region involved	Effects on PTEN regulation
Ubiquitylation [61]	N-terminal and C2 domain	• Polyubiquitylation leading to protein degradation • Monoubiquitylation to facilitate nuclear import
Phosphorylation [62]	C-terminal	• Promotes a closed and stable conformation • Decrease membrane interaction and phosphatase activity
Oxidation [3]	Phosphatase domain (C124)	Inhibits lipid phosphatase activity
S-nitrosylation [63]	N-terminal	• Inhibits lipid phosphatase activity • Decreases protein stability
Acetylation [64]	• Phosphatase domain (K125 and K128) • C-terminal domain (K163) • C-terminal domain (K402)	• Inhibits lipid phosphatase activity • Increases association with plasma membrane •Increases interactions with PDZ-domain-containing interactors
Sumoylation [65]	• C2 domain (K266) • C2 domain (K254)	• Increases association with plasma membrane • Induces nuclear import
Examples of PTEN Interacting proteins that regulate PTMs that regulate PTEN function	**PTEN region involved**	**Effects on PTEN regulation**
SIPL1* [66]	N-terminus and C-terminus	Inhibits lipid Phosphatase activity
MC1R** [67]	C2 domain	Increases PTEN stability
β-arrestins [68]	C2 domain	Increases PTEN membrane recruitment and activity
Myosin V [69]	C-terminal tail	Increases PTEN membrane recruitment and activity

*SIPL1: shank-interacting protein like 1.

**MC1R: melanocortin receptor 1.

PTEN paradigm of tumor suppression

It has been established that PTEN paradigm as a tumor suppressor differs from other well-known tumor suppressors such as retinoblastoma RB (representing the two-hit paradigm where loss of one allele induces cancer susceptibility and loss of two alleles induces cancer) and p53 (representing the one hit paradigm, also called classical haploinsufficiency where loss of one allele is sufficient for induction of cancer) [5]. In the case of PTEN, a new paradigm was discovered which has two characteristics: quasi-sufficiency and obligate haploinsufficiency. Quasi-sufficiency refers to the impairment of PTEN tumor suppression and hence induction of cancer after subtle downregulation of expression (a 20% reduction in the PTEN protein level) without loss of even one allele. The more the PTEN is downregulated, the more the cancer becomes aggressive and poorly differentiated[70].

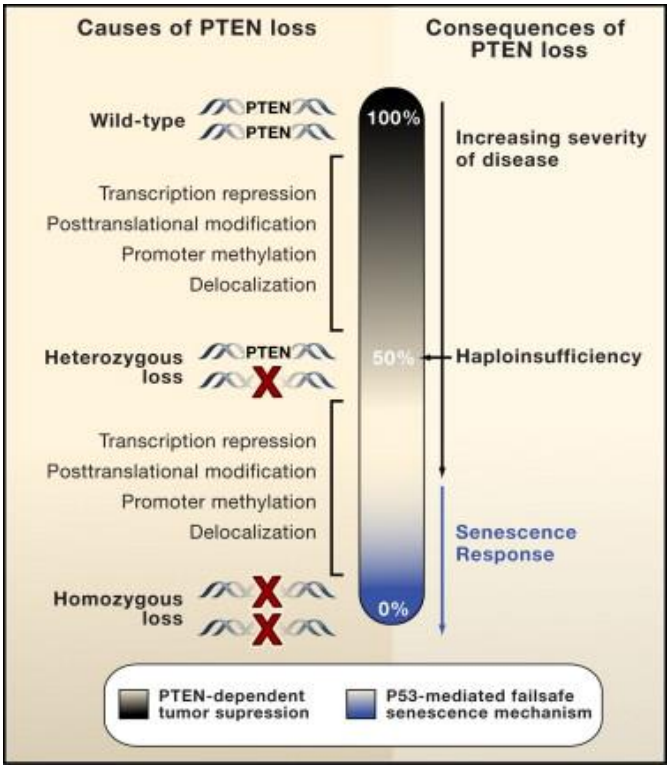

Figure 3: **The continuum model of PTEN.** PTEN tumor suppressor genes a continuum of expression level exists that result in a gradient of loss-of-function and increase of malignancy. (Figure adapted from Salmena et al.) [71].

Obligate haploinsufficiency occurs when PTEN haploinsufficiency is more tumorigenic than its complete loss, due to the activation of cellular senescence following the complete loss of PTEN

expression. However, in advanced cancers with p53 mutation or loss, PTEN loss-induced cellular senescence (PICS) does not occur and the complete loss of PTEN enhances proliferation and tumorigenesis to a greater degree than haploinsufficiency [5]. This can explain why complete loss of PTEN is rare in many cancer subtypes and why it is only common in advanced stages of cancer. Understanding this also explains the urgent need for a precise and highly sensitive quantitative assay that can assess and score subtle differences in PTEN expression in order to allow accurate diagnostics and the prediction of cancer severity.

PTEN role in several diseases and cancer subtypes

PTEN's role in breast cancer

Breast cancer (BC) is a worldwide health burden. In 2018, 2.1 million females were newly diagnosed with breast cancer. This means that breast cancer accounts for one out of four cancer cases in women [72]. Current systemic treatment for breast cancer is based upon its molecular subtypes. For instance, luminal A (that represents the histological phenotype: ER+, PR+, HER2-, Ki67-) and luminal B (ER+, PR+, HER+/−, Ki67+) subtypes are treated mainly with endocrine therapy, including aromatase inhibitors, selective estrogen receptor mediators (SERM), or selective estrogen receptor degraders (SERD) [73]. HER2-targeting drugs such as lapatinib, pertuzumab, ado-trastuzumab-emtansine, and most recently neratinib represent the main targeted treatments for the HER2 over-expressing subtype (ER-, PR-, HER2+) [74, 75]. It has recently been suggested that the most aggressive subtype; triple negative breast cancer (TNBC), which represents 15% all BC cases, is not actually a single disease, but rather is a collection of different ontology profiles. Therefore, TNBC is now further subdivided into six subtypes (basal like 1, basal like 2, mesenchymal, mesenchymal stem-like, luminal androgen receptor (LAR), immunomodulatory and unstable) according to the Lehmann classification [76]. For most TNBC subtypes, chemotherapy is the only approved systemic treatment. While chemotherapy is usually considered to biologically unselective, TNBC cases with BRCA1/2 mutations have been found to be platinum sensitive [77]. Despite effective breast cancer screening programs and the improvement of patient outcomes since the widespread use of the systemic treatment options mentioned above, BC is the leading cause of cancer death in over 100 countries [72]. This may be explained by *de novo* and acquired resistance that remains a huge challenge for effective treatment.

The PI3K/AKT pathway, forms a convergence point between all clinical subtypes of breast cancer and shows abnormality in 70% of breast cancers, where at least one of this pathway's components displays an aberration which plays a great role in therapy resistance [78]. Furthermore, the activation of the PI3K/AKT can stimulate the estrogen receptor ER in a ligand-independent manner, and is therefore associated with the luminal B subtype, tamoxifen resistance, and worse outcomes [79].

In HER2-overexpressing breast cancer, the PI3K/AKT pathway has been implicated in the resistance to anti-HER2 therapies and pathway inhibition is required for their anti-tumor activity[80, 81]. In TNBC, the common feature found in its various subtypes is the hyperactivation of the PI3K/AKT pathway [82]. Therefore, the PI3K/AKT pathway is a target for therapeutic intervention in all breast cancer subtypes, and several clinical trials are currently underway which involve different components of the pathway, such as PI3K, AKT(allosteric inhibitors such as MK2206, and ATP-competitive inhibitors such as capivasertib and ipatasertib), or mTOR (e.g., gefitinib, erlotinib, everolimus) or dual inhibitors [83-85]. However, in order to increase the treatment efficiency of all of these therapeutics that target the PI3K/AKT pathway, accurate predictive biomarkers for the therapeutic response are urgently needed in order to better select patients who can benefit most from the therapy. One of the most important biomarker candidates for this purpose is PTEN, and PTEN has been continuously researched over the past several years, in order to examine its efficacy as a clinical biomarker. For example, the potential use of PTEN loss in predicting resistance to the PI3Kα inhibitor alpelisib has been studied on liquid biopsies, with encouraging results [86]. Furthermore, in the phase 2 LOTUS clinical trial, inoperable, locally advanced or metastatic primary TNBC patients were recruited and treated with paclitaxel plus either ipatasertib (AKT inhibitor) or placebo, and in the low PTEN expression subset, median PFS was prolonged by ipatasertib [87].

As discussed before regarding PTEN's quasi-sufficiency, it has been found that a slight reduction of PTEN protein expression in mice was sufficient to induce BC, and the extent of PTEN reduction showed a correlation with cancer severity in a dose-dependent manner [5]. Many studies have shown that in BC, somatic PTEN mutations are rare (between 2-5%) while downregulated PTEN protein levels (determined by IHC) are much more common -- i.e., between 40-50% of all cases [27, 56]. Many studies have also shown that PTEN expression level significantly correlates

with lower tumor size as well as better outcomes [27, 88]. Even a moderate reduction in PTEN levels, as determined by reverse-phase protein array (RPPA), enhances a global change of gene expression profiles toward the luminal B subtype and endocrine resistance [79]. In HER2-overexpressing BC, PTEN protein expression correlated with response to anti--HER2 therapies such as trastuzumab, with a loss of PTEN inducing the epithelial-mesenchymal transition (EMT) and transforming HER2+ to a triple negative breast cancer [28, 89].

From all of the examples given above and from many other preclinical and clinical studies, it has been deduced that PTEN protein expression level is a promising potential clinical biomarker for BC that can be used (i) for prognosis, (ii) for prediction of resistance to endocrine and anti-HER2 therapies, and (iii) for selecting patients for combinatorial therapy with PI3K pathway inhibitors. However, several other studies have failed to report either an association between PTEN protein levels and prognosis in BC patients [90, 91], or an association with treatment response to various BC therapeutics in clinical trials. Because of these conflicting data, PTEN's role as a BC biomarker is still controversial [92, 93] despite its being a very promising candidate.

PTEN's role in colorectal cancer (CRC)

Colorectal cancer (CRC) is the third most deadly and the fourth most commonly diagnosed cancer in the world with nearly 2 million new cases and about 1 million deaths expected in 2018 [72]. Some CRC biomarkers are already in use and many others continue to be evaluated for their role in cancer screening, early detection of disease recurrence, and as prognostic and predictive factors [94]. In the 2000s and early 2010s, many studies were conducted to evaluate PTEN as a CRC biomarker. As a prognostic factor, loss of PTEN expression has been found to be more frequent in CRCs with liver metastases, and showed a significant association with the advanced Tumor, Node, Metastasis TNM stage and lymph node metastasis [95]. Lin et al., also showed that PTEN expression correlated with the cancer's histological grade and the distant metastasis [96]. Almost the same findings were demonstrated by Li et al. where low PTEN expression was associated with larger tumor size, invasion depth, lymphatic invasion, lymph node metastasis, and higher Dukes staging scores [97]. In addition, Zhou et al. have demonstrated that decreased PTEN expression was associated with sporadic microsatellite instability in tumors where mismatch repair deficiency has been detected [98].

Systematic treatment of CRC includes immunotherapy and targeted therapy in addition to the conventional chemotherapeutics. Targeted therapeutics include the anti-vascular endothelial growth factor-A (anti–VEGF-A) antibody bevacizumab [99], the VEGF-A, VEGF-B, and placental growth factor inhibitor aflibercept [100],the multi-kinase inhibitor regorafenib that has a dual targeted VEGFR2-TIE2 tyrosine kinase inhibition[100], and the anti-epidermal growth factor receptor (anti-EGFR) antibodies cetuximab and panitumumab [94]. Anti-EGFR antibodies clearly improved mCRC treatment and patient survival rate. RAS and BRAF mutational status determination and their negative predictive impact toward anti-EGFRs, improved the clinical response rate. However, many other predictive factors are being evaluated for boosting treatment efficiency. Initially, some studies showed that PTEN loss can predict resistance to anti-EGFRs such as cetuximab [101-103]. However more recent and comprehensive studies did not confirm these findings or show any benefit from PTEN analysis in predicting anti-EGFRs in CRC. This explains why the American Society of Clinical Oncology in 2006 [104] and the European Society for Medical Oncology (ESMO) in 2012 [105] considered PTEN as a potential predictive factor in mCRC, while in 2017, ASCO guidelines demonstrated insufficient evidence to recommend analysis of PTEN expression by IHC or detecting PTEN gene deletion by fluorescence in situ hybridization (FISH)] in CRC for patients who are being considered for therapy selection outside of a clinical trial [106].

PTEN expression was also evaluated for predicting response to bevacizumab. In the absence of PTEN, which usually counteracts PI3K, aberrant PI3K activity upregulates hypoxia-inducible factor 1 alpha (HIF1α), resulting in increased VEGF expression [107]. Therefore, bevacizumab-based regimens might be more effective in patients affected by mCRC with a loss of PTEN expression. More recently, mCRC therapeutics such as mTOR inhibitors (temsirolimus) or BRAF and MEK inhibitors in patients affected by BRAF V600-mutant mCRCs showed, in some studies, a correlation between PTEN expression level and response [107, 108].

PTEN's role in liver diseases

As PTEN is an important regulator of lipogenesis, glucose metabolism, and hepatocyte homeostasis in the liver, its deficiency was found to be associated with several pathological and functional changes including insulin hypersensitivity, hepatomegaly, steatohepatitis, and non-

alcoholic fatty liver disease (NAFLD), which is now considered as the most common liver disease worldwide [109].

Furthermore, it has been shown that PTEN plays an important role in the severity of viral hepatitis infections and the development of their complications. In hepatitis B which is a global public health threat, and the world's most common serious liver infection, it has been found that hepatitis B virus (HBV)-encoded X antigen (HBxAg) and HBV polymerase (HBp) can downregulate PTEN which, in turn, increases PD-L1 expression in hepatocytes, eventually leading to upregulation of PD-1 in T cells and the subsequent inhibition of the T cell response responsible for HBV clearance [110]. Moreover, HBV infection has been found to upregulate several miRNAs, including miR-3 and miR-181a, which downregulate PTEN expression and thereby inhibit apoptosis and induce HCC and increases its invasion. [111]. Infection with hepatitis C virus (HCV) is a prevalent infection worldwide which can be unnoticed and then lead to serious liver damage. PTEN has been demonstrated to interact with the virus, inhibiting its replication and secretion [24, 112]. Furthermore, treatment of HCV-infected hepatocytes with extracellular PTEN-Long protein has been found to inhibit HCV replication in a dose-dependent manner [113]. HCV infection, in turn, was found to regulate PTEN as shown in an *in-vitro* study where the HCV core domain I protein increased the lipid phosphatase activity of PTEN [112].

PTEN’s role in liver cancers

Liver cancer is the sixth most-diagnosed cancer and the fourth leading cause of cancer death worldwide in 2018 [72]. Hepatocellular carcinoma (HCC) is the most common primary liver cancer and is considered to be an aggressive cancer with very low survival rate [114], with hepatitis B, hepatitis C, and aflatoxin exposure being its major risk factors [72]. Early-stage HCC can be treated curatively by liver transplantation where the tumor is removed together with any liver tissue showing pathological changes that predispose to cancer [114]. Thus, in patients suffering from the different benign hepatic disorders that predispose to HCC, there has been a remarkable impact of surveillance on improving the overall survival of patients with HCC, as has been demonstrated in different observational studies [115]. Many biomarkers, including PTEN, are being studied for use in predict which hepatic patients have a high risk of developing HCC where close follow up is urgently needed [116]. Dysregulated PTEN expression is observed with obesity, insulin resistance, diabetes, hepatitis B virus/hepatitis C virus infections, and excessivealcohol consumption, while

PTEN downregulation has been associated with the occurrence, development, and prognosis of HCC [117]. Furthermore, PTEN expression was negatively associated with HCC pathological grading, liver function grading (Child-Pugh grading), and the presence of cancer thrombi. HCC patients with low levels of PTEN or complete loss of PTEN protein expression often have elevated levels of the alpha-fetoprotein AFP and develop metastases [118, 119]. These findings and many others have highlighted the potential role of PTEN as a prognostic biomarker in HCC.

Therapeutic targeting of cancers with loss of PTEN function

Determination of tumor PTEN status is quite important not only as a prognostic indicator but, more importantly, for selecting patients for targeted therapeutics who have a higher chance of a positive response. In the following, I will discuss some of the therapeutics and therapeutic strategies that can be used for PTEN deficient tumors or disorders.

RTK/PI3K pathway-targeted therapeutics

Many studies have shown that PTEN loss confers resistance to trastuzumab and other targeted therapeutics used in treating HER+2 breast cancers. Therefore, several clinical trials have been conducted where a drug that blocks a signaling node downstream of PI3K was added to abrogate the effects of PTEN loss. These trials included mTOR inhibitors (such as temsirolimus), pan-PI3K inhibitors (such as buparlisib) or AKT inhibitors (such as capivasertib) [120]. In CRC, clinical trials were also conducted to overcome resistance to EGFR inhibitors caused by PTEN deficiency by adding PI3K/AKT/mTOR pathway inhibitors [121].

While PTEN deficiency has been associated with increased sensitivity to PI3K pathway inhibitors in preclinical studies on selected cancer subtypes, clinical data from patients has resulted in mixed results. This can be largely attributed to the techniques (DNA sequencing, FISH or IHC) used in these trials to determine PTEN concentrations in clinical samples [122].

Therapeutics targeting tumors with lost PTEN genomic activity

Poly (ADP-ribose) polymerase inhibitors (PARPi) are used as cancer therapeutics, especially for tumors with deficient homologous recombination (HR) repair such as endometrial cancers. Many preclinical studies have confirmed that tumors with loss of PTEN function are defective in HR, and therefore the use of PARPi can provide synergistic lethality in case of PTEN deficiency

[123]. However, clinical studies have shown conflicting results regarding the effect of PTEN deficiency on the sensitivity of PARPi or a combination of PARPi and PI3K inhibitors [124-126].

Restoring normal PTEN expression levels

PTEN-Long as discussed above is a membrane-permeable lipid phosphatase that enters other cells and antagonizes PI3K signaling. Thus, it can be used as a new therapeutic agent/strategy by which PTEN-L may be delivered to cancer cells to treat patients with PTEN-deficient cancers [127]. Other therapeutic strategies to restore PTEN phosphatase activity involve (i) the use of statins to upregulate PTEN mRNA levels [128], (ii) the use of the mRNA of the PTEN pseudogene PTENP1 to sequester miRNAs that repress PTEN translation [129], and (iii) therapies that target proteins that interact with and inhibit PTEN, including P-REX2a (PIP3 dependent RAC exchanger factor 2a) and SIPL1 (shank-interacting protein-like 1).

Challenges in determining tumor PTEN status

PTEN genomic versus proteomic data

As mentioned previously, loss-of-function mutations in PTEN occur in only a fraction of PTEN-deficient tumors, and PTEN is commonly found downregulated through several transcriptional and post-transcriptional mechanisms. Thus, DNA sequencing or other genomic based techniques alone are not enough to determine a tumor's PTEN status. It is therefore necessary to quantify PTEN protein expression as well as its post-translational modifications.

Determination of PTEN protein level using antibody-based assays

The antibody-based assays are still considered the most reliable and widely available platform in clinical laboratories for protein tumor markers. Immunoassays including enzyme-linked immunosorbent assay (ELISA) and immuno-chemiluminescence used in automated platform represents the gold standard technique for many protein tumor markers including cancer antigen-15-3 (CA15-3) in breast cancer (BC), α-fetoprotein (AFP) in hepatocellular carcinoma (HCC), cancer antigen-125 (CA-125) in ovarian cancer, carcinoembryonic antigen (CEA) in colon cancer and prostate-specific antigen (PSA) in prostate cancer [19]. However, there are many limitations inherent to immunoassays such as interference by autoantibodies, cross-reactivity and hook effect, which can adversely affect clinical management [130].

IHC is a powerful method for investigating protein expression and localization within tissues. IHC is easy to perform, relatively inexpensive and several automated staining platforms are available. Since staining results can be viewed using a conventional bright-field microscope, protein expression can be evaluated in the context of tissue morphology. This has a special importance for PTEN because of his cytoplasmic and nuclear localization. Furthermore, since staining is permanent, slides can be stored [131]. Thus, it is the main method used for determining PTEN protein levels in clinical samples [127]. Despite being continuously refined, IHC has major sources of bias, including: (i) pre-analytical elements: All steps of tissue processing prior to IHC, can affect and introduce irreproducibility in the IHC results. This includes prolonged ischemia, delayed fixation, and variability in the type and length of fixation as well as thickness of sections [132]; (ii) analytical elements: There is considerable variability in antibody specificity and performance [133]. Also, the antigen retrieval method may enhance the result or destroy the target substance of interest [134]. Moreover, the detection systems and IHC stains are not standardised worldwide; (iii) post-analytical elements include interpretation and reporting of the results: Visual interpretation of the conventional IHC slides is based on qualitative and semiquantitative evaluation. There are several visual scoring/counting systems of the IHC results including ordinal categories (0, +1, +2, +3), estimated percent positivity, H-score, and the Allred system. However, scoring variability that comes from being subjective is a major limitation that every pathologist should be aware of. Many PTEN preclinical studies have also been conducted with Western blotting [7]. WB also suffers from major drawbacks, such as the lack of standardization and the low throughput that interferes both with its clinical use and also with achieving reproducible results in research. Also, the high background and the inconsistent expression levels of housekeeping reference proteins in both homogeneous and heterogeneous tissues, are major technical problems [135]. Importantly, the quantitative data provided by WB is just a measure of relative protein abundance that needs good normalization of the signal and does not allow comparison of expression levels across experiments or even laboratories. Moreover, the quality of the quantitative data obtained via WB is not comparable to the quality obtained with targeted MS techniques, which is vastly superior for several reasons. (i) Quality of the assay: quantitation by WB is based on a single reagent (antibody) that may be poorly characterized. Often, neither its affinity for the antigen nor the epitope are known or disclosed. Furthermore, WB suffers from the inability to evaluate and control the performance of the assay in individual experiments,

while MRM-MS assays make use of internal standards (isotopically labeled reference peptides) which are used not only for 'absolute' quantitation, but which also allow the researcher to specifically control the quality and performance of the entire workflow from sample preparation to data analysis. (ii) Quality of the results: protein quantitation via WB depends on a single signal: the intensity of a band on the blot without having reliable information on its specificity (i.e., whether it represents the quantity of the actual target protein, an unspecific signal, or a combination thereof). (iii) Performance characteristics: each method is characterized by several performance characteristics such as limit of detection, linear dynamic range, ability to multiplex, and reproducibility. For most of these characteristics, MS-based methods now outperform Western blotting [136], and often these criteria are not even tested or defined for WB as used in most laboratories.

Mass Spectrometry-based assays and quantitation of signaling proteins:

Liquid chromatography-mass spectrometry (LC-MS) is now an established platform for protein quantitation. Over the last decade, great advances have been made in the technological aspects of this technique, while much effort has also been made to optimize and properly combine different analytical tools to allow protein quantitation. While the required sensitivity, selectivity, precision, and best possible accuracy for a particular system are often achieved the actual accuracy is always difficult to demonstrate [137]. In particular, the robustness of a specific workflow and the required instrumentation have been important determinants that have expanded the use of LC-MS for the quantitation of proteins/peptides, not only in fundamental research but, recently and more importantly, in clinical labs [138].

In MS-based proteomics, two fundamental approaches are currently employed: top-down and bottom-up proteomics. In top-down proteomics, intact proteins or large fragments are analyzed by mass spectrometry. Top-down MS has specific applications due to its high technological demands, but it also has limited sensitivity and limitations with regard to protein size. It is currently only used by few laboratories that are mainly focused on technology development with regards to qualitative rather than quantitative proteomics. Bottom-up proteomics relies on the analysis of peptides generated upon proteolytic digestion of protein samples. It is the most common proteomic workflow, largely because of technical advantages of separating, analyzing, and identifying shorter peptides rather than intact proteins. Bottom-up proteomics can be used

for either for untargeted or "discovery" proteomics, or for targeted proteomics of a pre-selected group of "proteotypic" peptides representing a smaller group of proteins. While both targeted and untargeted proteomics experiments can provide quantitative results, untargeted quantitation usually produces only relative quantitation – i.e., protein quantitative ratios or relative changes (up or down regulation). In contrast, targeted proteomics, with stable-isotope labeled analogues of each target peptide, can provide information on the absolute amount of the protein/peptide present or the concentration of a protein within the sample.[139]. Untargeted (or "shotgun") proteomics is often used for relative quantitation and biomarker *discovery*. Targeted proteomics is typically used for highly selective and high-throughput analysis of one or more target proteins and is typically used for biomarker *validation* on a larger number of samples.

Targeted MS, specifically multiple reaction monitoring (MRM) and parallel reaction monitoring (PRM), have gained popularity in the last decade. MRM in particular is a robust MS technique that used comparably inexpensive and robust MS instrumentation (e.g., triple quadrupoles) for measurements. MRM was selected as the method of the year in 2012 by Nature Methods for its analytical performance, including its accuracy, and its high specificity to discriminate (e.g., between different isoforms), its reproducibility and sensitivity together with the possibility to perform multiplexed analyses. For the abovementioned reasons and more, MRM is largely considered as a valid future alternative to standard clinical assays [140-141].

Multiple reaction monitoring (MRM)

MRM is a targeted MS approach that has been used for decades in clinical reference laboratories for accurate quantitation of small molecules in plasma/serum/urine. More recently, this approach has been applied to the measurement of candidate biomarker proteins concentration in plasma and cell lysates. The MRM approach combined with stable isotope labelled standards (SIS) can be used to develop multiplexed, high throughput, accurate, and sensitive assays for multiple targets (30-100) and applied to a large number of samples [142]. MRM in combination with SIS peptides is the most-used method for absolute targeted quantitation of proteins by MS [143-145].

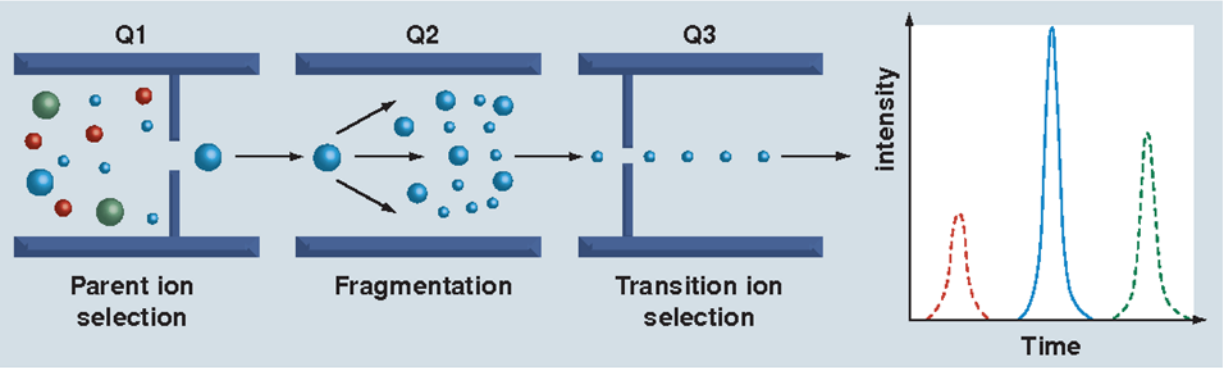

Figure 4: Schematic diagram of triple quadrupole mass spectrometer used for multiple reaction monitoring (MRM). Q represents a quadrupole in a triple quadrupole mass spectrometer. Three targeted peptides eluting at different retention times are monitored by MRM-MS (coloured in red, blue and green). MS/MS in Q2 illustrates the fragments in the second quadrupole Q2 (collision cell) for one of the three peptides (blue). An MRM-MS assay offers multiplexing capability of many target analytes in a single high-pressure liquid chromatography run. [146].

MRM assays are performed on triple quadrupole (QQQ) mass spectrometers (Figure 4) where a peptide ion of interest (the precursor ion) with a targeted m/z is preselected by the mass filter Q1. The second quadrupole serves as a collision cell Q2 to break the peptide into fragments. The third quadrupole functions as a second mass filter for specified m/z fragments from the initial precursor peptide. Each of these precursor-fragment ion pairs is termed a “transition,” and the transition intensity is recorded by the detector. The coelution of multiple fragment ions from a single precursor peptide is required to confirm the specific identification of the peptide of interest. The total peak area reflects the relative abundance of the peptide. Multiple targeted fragment ions resulting from multiple precursor ions can be monitored in a given sample, and the overall process is therefore termed multiple reaction monitoring [144, 147].

Assay development is an iterative process that involves the selection of proteotypic peptides. Proteotypic peptides are those peptides in a protein sequence that uniquely represent the targeted proteins or protein isoform and are most likely to provide good MS-based measurements for protein identification and quantitation [148]. There are selection criteria that consider key characteristics to enhance the specificity and maximum sensitivity of the assay and to minimize interference. For example, selection of peptides that are (i) free of known mutations or single nucleotide ploymorphisms, (ii) unique to the target protein or to the isoforms that need to be targeted by the assay, (iii) between 7 and 25 amino acid residues long, (iv) not containing

residues susceptible to modification during sample preparation, such as methionine (oxidation) [23, 149].

After selecting the peptide targets for the assay, stable isotope labeled analogues of these peptides are synthesized to be used as internal standards. Multiple fragments from a single parent peptide are selected and used for a given peptide to provide increased specificity (Figure 4). MRM acquisition parameters are then optimized so that sensitive and accurate quantitation can be performed without interference from other components in the sample. Finally, MRM assays must be characterized to determine the technical reproducibility, the selectivity, and the concentration range of the linear response over which quantitation can be performed [143]. The quantitation is typically performed by comparing the peak areas of the transitions of the endogenous peptide to those of the internal standards providing high specificity as well as high precision and accuracy in quantitation. The use of SIS peptides allows the normalization of the endogenous peptide's signal and therefore compensates for issues that are often hard to control, such as sample-specific ion suppression, or spray instabilities in electrospray ionization (ESI). Furthermore, these highly purified and previously quantified internal standards allow "definitive quantitation" a term that refers to the possibility of calculating the absolute protein concentrations for unknown samples through using a well-characterized reference standard along with a calibration curve. Moreover, compared to antibody-based assays, MRM assays are easy to multiplex, are able to distinguish modified and unmodified forms of the protein, and can be developed with a very high success rate, significantly shorter lead times and significantly lower costs, along with the high reproducibility required for use in clinical and preclinical research [145, 150].

Importantly, MRM has been evaluated in several systematic studies and has been demonstrated to be a highly reproducible analytical platform for targeted proteomics analysis. For example, the Clinical Proteomic Tumor Analysis Consortium [25] of the National Cancer Institute (NCI) has investigated the standardization and analytical validation of targeted protein assays in intra- and inter-laboratory settings and has demonstrated robust analytical performances of MRM assays on different instruments and across different laboratories [151].

Despite the high sensitivity that can be achieved with MRM assays, higher sensitivity is sometimes needed to detect low-abundance signaling proteins in compound matrices. The

coupling of MRM with immuno-enrichment of the targeted protein seems to be a very promising analytical method allowing more sensitivity and dynamic range [143, 144].

Immuno-MRM assays

First proposed by Nelson et al. in 1995, an elegant and straightforward approach that greatly enhances sensitivity and precision of any given protein analysis, while concurrently enabling "absolute" quantitation of protein levels, is to combine immuno-enrichment with MS [152]. Instead of using conventional anti-*protein* antibodies that are accompanied by a variety of shortcomings, we and others use anti-*peptide* antibodies to capture a proteotypic peptide of the target protein, after proteolytic digestion of the sample(s) [152]. This allows us to immuno-enrich target peptide sequences, including those that are not exposed on the surface of the protein, and also allows more stringent sample clean-up including washing, leading to considerably cleaner samples with lower background signals and interferences. Importantly, immuno-MS also allows the use of the corresponding SIS peptide as internal standard, as it is co-captured and co-enriched during the immuno-enrichment process together with its endogenous counterpart. Both the SIS and the endogenous peptide (END) have the same physicochemical properties and show the same behavior during all steps of the sample preparation and chromatography but can be distinguished by MS due to their different masses. Therefore, SIS peptides not only enable quantifying endogenous protein concentrations, as discussed above, but can also be used as internal standards to determine, e.g., immuno-enrichment recovery. This is a crucial control-step that is virtually impossible for anti-protein immuno-enrichment, where even a full-length SIS protein may not represent the exact proteoform(s) present in the sample of interest [153].

MS quantitation and the calibration strategy

Mass spectrometry (MS) measurements are not inherently calibrated. Researchers use various calibration methods to assign meaning to the signal intensities and to improve precision [154]. As discussed above, in proteomics laboratories where targeted peptide quantitation is performed, stable isotopically labeled peptides (one per analyte) are often added to the samples and used as internal standards; a strategy known as the single-point calibration. This strategy allows the confident identification of the endogenous peptide, and its quantity is infer by direct comparison to the internal standard assuming that both the endogenous and the internal standard peptides are within the linear range of quantitation. This approach has several drawbacks, including the fact

that the linear dependency between peptide areas and concentrations only occurs in a limited sample-dependent range of concentrations. Therefore, continuous adjustment of the internal standard abundances is required -- mainly for samples that exhibit a high variability of endogenous peptide abundances. This presents a major limitation, especially in high throughput projects or in clinical routines [21, 155]. External multipoint standard curves (external calibration) have alleviated some of these limitations and have become a standard calibration method for quantitative MS assays. The synthetic version of the endogenous target peptide (added in different levels, usually to a buffer solution) and its heavy stable isotope labeled peptide (constant level in each point) are used to generate the points/standards of the calibration curve. The same amount of the heavy stable isotope labeled peptide is added to all of the "real" samples, so one can determine the analyte concentration using the calibration curve if the measured signal and the actual peptide quantity are well matched, and if the signal is above the lower limit of quantitation and within the linear range. In this way, samples can be run in batches with calibration curves embedded in each batch, but this adds much effort, cost, and lowers the throughput of the assay. The most important limitation for using the external calibration is the matrix effect, which can affect the accuracy of the assay. [156] The matrix effect is the effect of other components in the sample co-eluting with the analyte and altering the analytical results. This effect is particularly marked in complex mixes/samples such as plasma or tissue samples. In cases where blank matrices identical to the sample are available, external calibration can be conducted as described above using internal standards labeled with isotopes and matrix matched calibration standards. However, sample-to-sample variability in composition hinders the *complete* elimination of the matrix effect especially for the quantitation of low-abundance analytes. When blank matrices are not available (as is the case for precious patient tissue samples), a surrogate matrix, i.e., a representative sample matrix, is often used for preparing the standards for external calibration. As such, it is often either impossible or not feasible to eliminate matrix effects completely, and external calibration should only be used when matrix effects can be expected to be low [157].

Recently, several groups have presented the use of multipoint internal calibration (MPIC) in clinical LC-MS/MS assays as an alternative to external calibration, mainly to eliminate the need for batch-mode analysis. Among them, Hoffman et al. validated the use of MPIC on LC-MS/MS assays for methotrexate quantitation in serum using four variants of labeled methotrexate [158]. For

targeted proteomics, Chiva et al. incorporated five different isotopically labeled peptide standards for internal calibration and demonstrated the applicability of this method for the high precision MRM-based quantitation of HER2 in FFPE samples [155]. Importantly, this MPIC strategy has several advantages including (i) more accuracy in analyte quantitation, where both standards and the analyte signals affected by the same matrix (sample matrix), (ii) increasing the throughput of the assay by decreasing the turnaround time as well as eliminating the batch mode analysis, (iii) being well-suited for the generation of ready-to-use biomarker kits for clinical applications. However, using five different isotopically labeled peptides adds a significant cost to the clinical assay as generation, purification, and quantitation of these isotopically labeled peptides is expensive [159].

Immuno-MS assays and internal calibration

A challenging aspect of generating a representative external calibration curve for immuno-MS assays is that the background obtained after immuno-enrichment is strongly dependent upon both the antibodies used and the sample [160]. Despite the fact that in anti-peptide immune-MS assays, the isotopically labeled peptide standard and the endogenous peptide co-elute with the same efficiency, unanticipated off-target binding of antibodies can induce significant interference and suppression in clinical samples. External calibration with a surrogate matrix, including BSA and E.coli digests can be used [161], but the matrix is completely different from the composition and amount of co-enriched digest from tissue samples and thus may affect the assay's precision and accuracy. At the same time, it is virtually impossible to prove on a case-by-case basis that a particular external calibration works for every combination of immuno-MS assay and patient tissue sample.

The necessity for running full calibration curves in each sample batch as "ideal" has also been challenged.[162] This practice might be even more questionable for precision-medicine assays which often demand timely analysis and thus are likely to be analyzed individually rather than in large batches. Since iMRM and iMALDI have the great advantage of co-enriching SIS and END peptides with the same efficiency, we evaluated the benefit of using two SIS isotopologues at different concentrations in order to quantify the protein of interest using internal calibration. Our rationale for the use of only two SIS isotopologues for immuno-MS was to keep the costs for clinical assays low without compromising precision, as (i) generation, purification, and

quantitation of SIS peptides is costly, and (ii) spiked-in SIS will compete with endogenous peptides for antibody-occupancy, and thus has the potential to either reduce peptide recoveries or require the use of additional antibody.

The first manuscript presents the newly developed anti-peptide PTEN immune-MRM method for the NNIDDVVR (472.7434++) peptide and how I used it, in a series of experiments, to demonstrate the flexibility and robustness of the two-point internal calibration (2-PIC), a new calibration strategy that uses two isotopologues. The 2-PIC calibration strategy, in comparison with the external calibration, allows endogenous PTEN quantitation with high precision and accuracy while reducing the instrument time and cost as well as overcoming the inherent limitations of using external calibration with surrogate matrices for the analysis of clinical specimens with limited sample amounts.

Using Two Peptide Isotopologues as Internal Standards for the Streamlined Quantification of Low-Abundance Proteins by Immuno-MRM and Immuno-MALDI

Sahar Ibrahim[1], Bjoern Froehlich[2], Adriana Aguilar-Mahecha[3], Raquel Aloyz[3,4,5], Oliver Poetz[6,7], Mark Basik[3,4,5], Gerald Batist[3,5], René P. Zahedi[1*], Christoph H. Borchers[1,2,5,8*].

[1] Segal Cancer Proteomics Centre, Lady Davis Institute, Jewish General Hospital, McGill University, Montréal, Québec, Canada.

[2] University of Victoria-Genome British Columbia Proteomics Centre, University of Victoria, Victoria, Canada

[3] Segal Cancer Center, Lady Davis Institute for Medical Research, Sir Mortimer B. Davis Jewish General Hospital, McGill University, Montréal, Québec, Canada

[4] Division of Experimental Medicine, McGill University, Montréal, Québec, Canada.

[5] Gerald Bronfman Department of Oncology, Jewish General Hospital, McGill University, Montréal, Québec, Canada

[6] NMI Natural and Medical Sciences Institute at the University of Tuebingen, Reutlingen, Germany.

[7] SIGNATOPE GmbH, Reutlingen, Germany

[8] Center for Computational and Data-Intensive Science and Engineering, Skolkovo Institute of Science and Technology, Moscow 121205, Russia

Introduction

Major advances in instrumentation and methods for MS-based proteomics have enabled the relative quantitation of 1000s of proteins across different samples and conditions [1-3]. In many cases, however, relative quantitation -- showing only up/down-regulation of a protein compared to a control -- may not be sufficient, and a more precise determination of the actual protein concentration, i.e. the expression level is required [4-6] This is of particular importance in precision oncology. Since not all patients' tumors have pharmacologically tractable alterations in their DNA, a deeper understanding of cancer biology -- at the level of proteins and their post-translational modifications -- may help to determine whether these proteins might either be drug targets, or serve as diagnostic, prognostic or predictive biomarkers [6,7].

The phosphatase and tensin homolog (PTEN) protein, a tumor suppressor which negatively regulates the PI3K/mTOR pathway, is an important example: Despite the low incidence of PTEN mutations and deletions in breast, prostate, and colon cancer, PTEN expression is commonly found to be downregulated in these tumors [8]. Importantly, PTEN downregulation correlates with the severity of these cancers in a dose-dependent manner [9]. These findings make PTEN a good biomarker candidate for prognosis, as well as for predicting the response to therapeutics that target the PI3K/mTOR pathway.

Typically, immunohistochemistry (IHC) is used to evaluate PTEN expression in patient clinical samples, but it lacks the sensitivity, specificity, and precision to distinguish subtle differences in protein expression levels between tumors. These shortcomings of IHC have hindered the accurate correlation of PTEN expression with disease severity, and thus have prevented PTEN's approval as a biomarker.

Whether a target protein can be quantified or even detected by MS strongly depends on the dynamic range that can be covered in a given type of analysis. Great advances have been made to expand the dynamic range of MS -- and thus enable and improve the quantitation of low abundance proteins -- however, this often requires pre-fractionation, or state-of-the-art instrumentation and technology which may not always be available [2,10,11]. In particular, the robustness of a specific workflow and of the required instrumentation are important determinants for clinical MS, which is in stark contrast to fundamental research, that is constantly pushing technological boundaries [12-14].

First proposed by Nelson et al., an elegant and straightforward approach that greatly enhances sensitivity and precision of any given protein analysis, while concurrently enabling "absolute" quantitation of protein levels, is to combine immuno-enrichment with MS [15]. Instead of using conventional anti-protein antibodies that are accompanied by a variety of shortcomings, we [16-18] and others [19] used anti-peptide antibodies to immuno-enrich a proteotypic peptide of the target protein, after proteolytic digestion of the sample(s). Importantly, these immuno-MS approaches can involve the use of synthetic stable isotope-labeled standard (SIS) peptides having the exact same amino acid sequence as the endogenous (END) target peptide. The SIS peptides can be spiked into the sample in known amounts and will be co-enriched during the immuno-enrichment. Both SIS and END peptides have the same physicochemical properties and show the same behavior during all steps of the sample preparation and chromatography but can be distinguished by MS due to their differential mass. Therefore, SIS peptides not only enable quantifying endogenous protein concentrations but can also be used as internal standards to control, e.g., immuno-enrichment recovery. This is a crucial control-step that is virtually impossible for anti-protein immuno-enrichment, where even a full-length SIS protein may not represent the exact proteoform(s) present in the sample-of-interest [20,21]. Furthermore, using SIS peptides allows the generic normalization of the END signal and therefore compensates for issues that are often hard to control, such as sample-specific ion suppression, or spray instabilities in ESI [22]. Typically, the most precise and robust quantitation using SIS peptides involves targeted MS, i.e. multiple reaction monitoring (MRM) or parallel reaction monitoring (PRM), where mass spectrometers specifically monitor and quantify specific peptides-of-interest.

The choice of calibration strategy can greatly affect the precision (and accuracy) of protein quantitation assays. While some proteomics studies use only the END/SIS ratio measured in the sample to directly determine protein concentrations, proper quantitation requires a careful characterization of the assay-at-hand, ideally including the assessment of the linear range, the lower limit of quantitation, etc., as well as the generation of a calibration curve in order to deduce the actual END concentration from that END/SIS ratio. The calibration curve directly examines the relationship between the measured signal and the actual peptide quantity, which can demonstrate that the measured concentration is precise, and that the signal is above the lower limit of quantitation (LLOQ), and within the linear range of the assay. When measuring an

unknown sample, all these requirements have to be met to guarantee that the measured signal really reflects a certain quantity of the analyte [23].

External calibration is considered to be a "gold standard" for quantitative MS assays: a synthetic version of the END peptide (often referred to as NAT, for "native") and its SIS are used to generate the calibration curve. While the SIS is kept constant, different levels of NAT are spiked into the individual standards of the calibration curve (see Figure 1a). The same amount of SIS is then also added to all "real" samples with unknown END concentrations. This approach enables the signal to be normalized and corrected for variations in analyte response: once added during sample processing, the SIS peptide reflects all losses from that point forward, including fluctuations in LC-MS response, and consequently corrects the final quantitation.

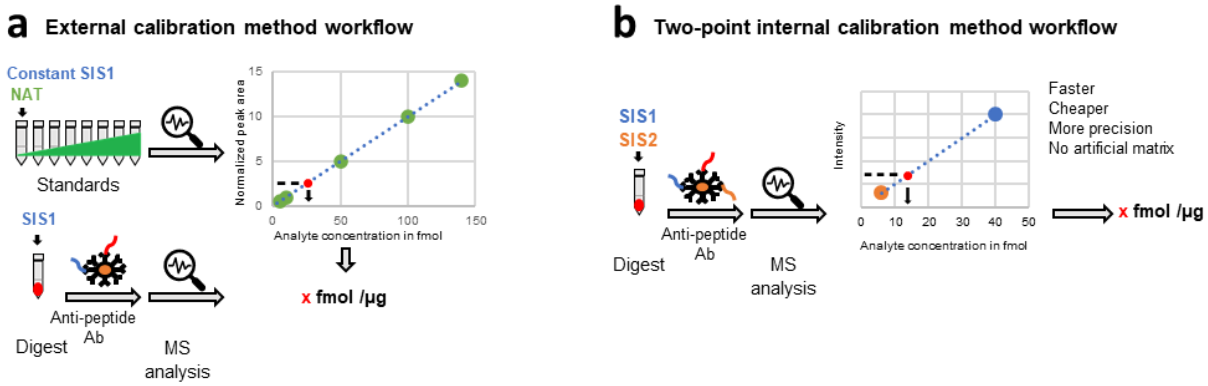

Figure 1: **Comparing external calibration to two-point internal calibration (2-PIC).** Schematic workflows for immuno-MS based protein quantitation. (a) External calibration: multiple standards have different concentrations of NAT in a constant concentration of SIS. Calibration standards are prepared in a surrogate matrix and analyzed together with the sample to determine a calibration curve that is used to calculate the analyte's concentration in real samples. (b) Two-point internal calibration where two different SIS isotopologues that differ in mass are spiked into the real sample at different concentrations, prior to immuno-enrichment, and the two-point internal calibration curve is used to calculate the concentration of the analyte.

External calibration requires the use of a representative sample matrix that, ideally, does not contain endogenous analyte which would interfere with the measurements, particularly at the lower end of the calibration curve. Surrogate matrices are often used for external calibration, based on the assumption that an analyte's LC-MS response is the same in different types of samples [23], thus ignoring a major source of error in external calibration, i.e., matrix effects [24,25]. Because the complete elimination of matrix effects is often either impossible or not feasible in trace analysis, external calibration should be used only when matrix effects can be expected to be low [24].

Recently, we have reported a strategy to compensate for matrix effects in plasma, by using two different SIS isotopologues that differ in mass, in order to prepare an external calibration curve in the exact same matrix without interference from potential END signals [27].

Chiva et al. presented an extension of our approach, where five different isotopically labeled peptide standards were incorporated for internal calibration, and demonstrated its applicability for high precision MRM-based quantitation of Her2 in formalin-fixed paraffin-embedded (FFPE) samples [28].

Here, we present a strategy for the internal calibration of immuno-MRM and immuno-MALDI assays. Mimicking the matrix of iMRM and iMALDI assays in order to generate a representative external calibration curve proved to be challenging, as the background obtained after immuno-enrichment depends strongly on both the antibody used and the sample. Even when external calibration curves were generated from the same sample type after immuno-enrichment, endogenous signals may still interfere [27]. Using surrogate matrices to generate external calibration curves, such as BSA or *E.coli* digests, has previously been shown to be feasible [29] but may not sufficiently represent interference and suppression events occurring in clinical samples, including FFPE specimens, where considerable unanticipated off-target binding of antibodies may occur. Proving that a particular external calibration works for a given combination of immuno-MS assay and patient tissue sample on a case-by-case basis is virtually impossible. As recently argued by Hoofnagle and coworkers, external calibration of each sample batch substantially increases the cost [30] and turnaround time [31], so that the concept of running full calibration curves in each sample batch as "ideal" has been challenged [32]. This practice might be even more questionable for precision-medicine assays which often demand timely analysis and thus are likely to be analyzed individually rather than in large batches. Since iMRM and iMALDI have the great advantage of co-enriching SIS and END peptides with the same efficiency, we evaluated the merit of using two SIS isotopologues at different concentrations in order to quantify the protein of interest using internal calibration (see Figure 1b). Our rationale for the use of only two SIS isotopologues for immuno-MS was to keep the costs for clinical assays low without compromising precision, as (i) generation, purification and quantitation of SIS peptides is costly and (ii) spiked-in SIS will compete with endogenous peptides for antibody-occupancy, thus either reducing peptide recovery or requiring the use of more antibody. We

therefore compared our two-point internal calibration (2-PIC) strategy with the gold-standard, external calibration.

Experimental Procedures

Reagents used, cell lines, cell lysis, and proteolytic digestion are described in the Appendix I.

Samples were analyzed by LC-MRM or iMALDI as described in the Appendix I.

In LC-MS, instrument response is proportional to the concentration (x), and larger deviations at higher analyte concentrations tend to disproportionately influence regression curves (heteroscedasticity). Weighting regression curves using weighted least squares (WLS) significantly reduces the impact of the variance at the upper end of the calibration curve [33], so that $1/x^2$ is the appropriate weighting factor [34]. Thus, SIS peptide peak areas were used for internal and for external calibration with $1/x^2$ weighted linear regression. The 2-PIC calibration curve was generated using WLS through the origin.

For iMALDI, PTEN NAT peptide amounts were determined using either external calibration, or 2-PIC and ordinary least squares regression (OLS) [35].

Sample preparation for the use of 2-PIC for quantifying (i) a constant NAT at different SIS1 and SIS2 levels and (ii) different NAT levels at constant SIS1 and SIS2 levels, using both MRM and iMALDI, are described in the Appendix I, and outlined in Figures 2 and 3, respectively.

Comparison of 2-PIC with external calibration for quanti-fying endogenous PTEN levels in the Colo-205 colon can-cer cell line

The utility of 2-PIC was evaluated for clinical samples, and the precision of quantifying endogenous PTEN was com-pared to external calibration. Sample preparation is de-scribed in the Appendix I.

Results and discussion

This study was designed to determine whether 2-point inter-nal calibration using two different SIS peptides can be used to quantify NAT (or respectively endogenous) peptide/protein levels precisely by immuno-MRM and immuno-MALDI. For this purpose, it is important to address the following questions: (i) does the method generally work with good precision and accuracy, (ii) does a SIS1/SIS2 in-ternal calibration mixture enable the quantitation of differ-ent NAT (or endogenous) levels over a biologically relevant dynamic range, and (iii) how would the quantitation be affected if some real-life samples fall outside the pre-defined calibration curve.

Thus, different standard samples were generated in order to determine whether a constant NAT level could be correctly quantified using different amounts of SIS1 and SIS2, spanning up to two orders of magnitude, even if both SIS standards were either below or above the concentration of the NAT (see Figure 2). Next, standards with fixed amounts of SIS1 and SIS2 were prepared, and we evaluated whether those will allow the precise quantitation of different levels of NAT, again, even if both standards are below/above the NAT concentration (see Figure 3). The second setup better reflects the real-life situation where a specific assay would be developed using a predefined amount of calibrant in order to quantify unknown samples. Finally, we used our 2-PIC method to quantify levels of the tumor suppressor protein PTEN in the Colo-205 cells (see Figure 4). To evaluate the general applicability of 2-PIC, we conducted all experiments for two independent immuno-MS workflows, immuno-MRM and immuno-MALDI. Importantly, these two workflows have completely different sample preparation protocols, target different PTEN peptides (^{48}NNIDDVVR^{55} for iMRM, ^{148}AQEALDFYGEVR^{159} for iMALDI), use two different ionization methods (ESI and MALDI) and two different MS techniques (LC-MRM and MALDI-TOF). These methods are therefore fully orthogonal and importantly have been carried out by two different individuals in two different laboratories (an inter-laboratory comparison).

2-PIC for quantifying a constant NAT at different SIS1 and SIS2 levels

MRM. 2-PIC was used to determine the precision of quantifying a constant 10 fmol NAT spike-in, when different amounts of iMRM SIS1 (NNIDDVV**R**+6 Da) and SIS2 (NNIDDVV**R**+10 Da) were used as standards. For this purpose, three sample sets, A-C, were generated (Figure 2a, 2c).

Sample set A included 3 samples with the following NNIDDVVR SIS1:SIS2 (fmol:fmol) ratios and a constant amount of 10 fmol of NNIDDVVR NAT: (A1) 5:1, (A2) 20:4, and (A3) 40:4. Samples were prepared and measured in triplicate. The amounts of NAT determined based on the internal calibration curves were 9.4±2.1 fmol (A1), 10.6±0.7 fmol (A2), 10.2±1.0 fmol (A3), with relative standard deviations (RSD) of 21.7% (A1), 6.2% (A2), 9.3% (A3). Thus, except for A1, where both standards SIS1 (5 fmol) and SIS2 (1 fmol) were below the 10 fmol NAT, the error was $\leq$10%, and recoveries for all samples were between 94% and 106%.

Sample set B was used to evaluate how well 2-PIC performs when the internal standards span different levels in dynamic range, reflecting changes that might occur in biological samples. Thus, NNIDDVVR NAT and SIS2 were kept constant at 10 fmol and 2 fmol, respectively, while SIS1 was 40 fmol (B1; dynamic range of 20), 60 fmol (B2; dynamic range of 30), and 100 fmol

(B3; dynamic range of 50). Samples were prepared and measured in triplicate. The 10 fmol NAT spike-in was quantified as 9.8±0.3 fmol (B1), 9.3±0.2 fmol (B2), 10.4±0.6 fmol (B3), with RSDs of 2.6%, 2.6%, and 5.9%, respectively. Recoveries were 98±3% (B1), 93±2% (B2), and 104±6% (B3).

In sample set C, the dynamic range of the internal standards was extended to 100. Three samples were prepared in triplicate with the following NNIDDVVR SIS1:SIS2 (fmol:fmol) ratios and a constant amount of 10 fmol of NNIDDVVR NAT: (C1) 100:1, (C2) 500:5, and (C3) 2000:20. The 10 fmol NAT spike-in was quantified as 8.8±0.4 fmol (C1), 8.6±0.1 fmol (C2), 11.2±1.1 fmol (C3), with RSDs of 5.0%, 0.6%, and 9.9%, respectively. Recoveries were 88±4% (C1), 86±1% (C2), and 112±11% (C3).

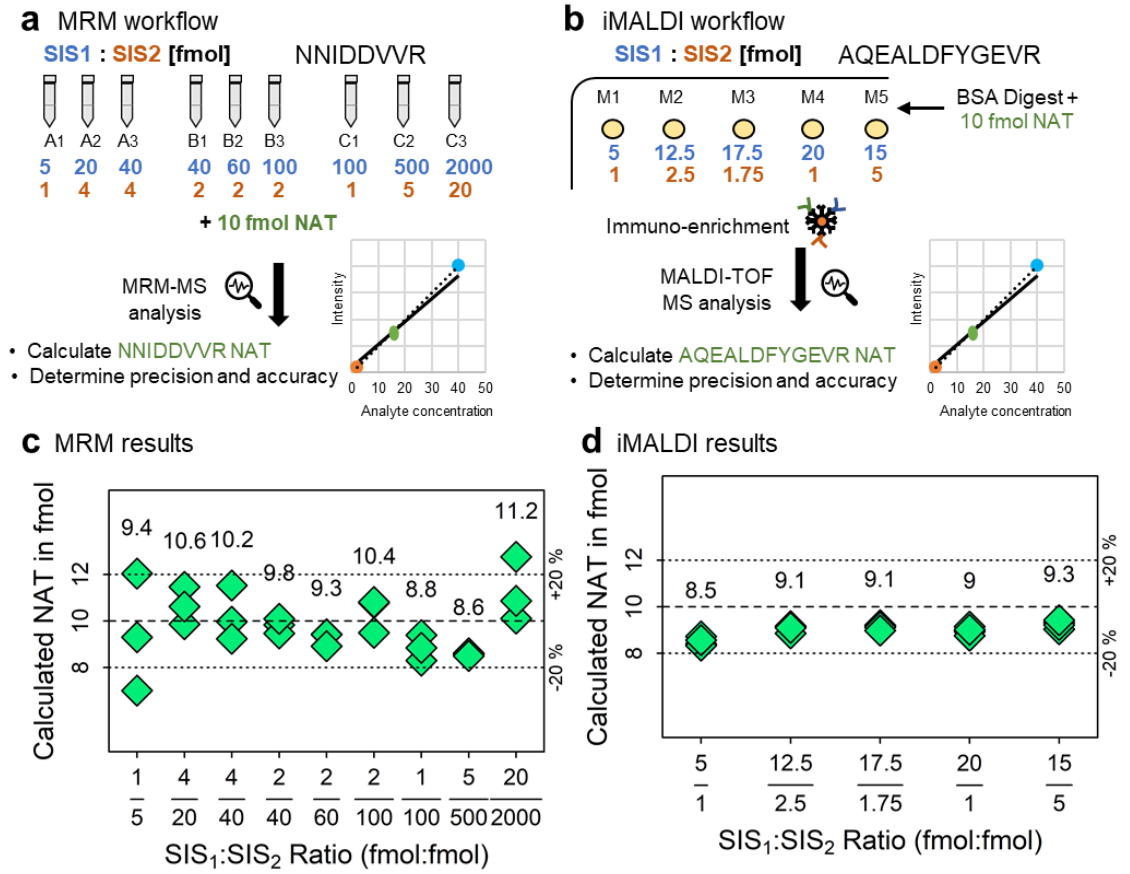

Figure 2: Testing 2-PIC for quantifying a constant NAT level using different SIS1 and SIS2 levels. (a) MRM workflow targeting the PTEN peptide ^{48}NNIDDVVR^{55}. (b) iMALDI workflow targeting the PTEN peptide ^{148}AQEALDFYGEVR^{159}. (c) MRM results of samples A1-A3, B1-B3, C1-C3. NAT levels calculated using 2-PIC are represented as light green rhombuses (N=3). (d) iMALDI results of samples M1-M5. NAT levels calculated using 2-PIC are represented as light green rhombuses (N=4).

iMALDI. To determine if the 2-PIC concept is also applicable to iMALDI assays, which involve a completely different sample preparation protocol and type of MS analysis, five samples, M1-5, were prepared with constant AQEALDFYGEVR NAT (10 fmol) and varying amounts of internal standards (Figure 2b). Because MALDI generally has a smaller linear range than MRM, we adjusted the amounts of iMALDI SIS1 (AQEALDFYGEV**R**+10 Da) and SIS2 (AQEA**L**DFYGEV**R**+17 Da) accordingly, reflecting the PTEN amounts we would expect to find in 10 µg of total protein cell lysate, based on in-house data. Samples M1-M5 had the following AQEALDFYGEVR SIS1:SIS2 ratios (fmol:fmol): (M1) 5:1, (M2) 12.5:2.5, (M3) 17.5:1.75, (M4) 20:1, and (M5) 15:5. The samples were prepared in quadruplicate, using BSA digest as the surrogate sample matrix, followed by analysis using iMALDI (Figure 2d).

The amounts of NAT (10 fmol spike-in) determined based on 2-PIC were 8.5±0.2 fmol (M1), 9.1±0.1 fmol (M2), 9.1±0.1 fmol (M3), 9.0±0.1 fmol (M4), 9.3±0.1 fmol (M5). In all five samples, the NAT levels could be determined with high precision using 2-PIC, with RSDs of 1.8, 1.3, 0.9, 1.6, and 1.5% (Figure 2d) as well as with high accuracy, with the quantified NAT amounts being well within ±20% of the spiked-in concentration. High recoveries were achieved even in cases where (i) SIS1 and SIS2 were both below the NAT amount (M1) with 85±2%, (ii) SIS2 was 20-fold higher than SIS1 (M4) with a 90±1%, and (iii) when SIS1 was only 3-times higher than SIS2 (M5) with 93±1%.

Collectively, these results demonstrate that 2-PIC provides high accuracy and precision for iMALDI-based protein quantitation and is a good alternative to the use of external calibration.

2-PIC for quantifying different NAT levels at constant SIS1 and SIS2 levels

MRM. We next evaluated the precision and accuracy when different levels of NAT were quantified using a fixed SIS1:SIS2 ratio, as would be the case for a fully optimized assay.

Eight different levels of NNIDDVVR NAT spikes (D1: 1 fmol, D2: 2 fmol, D3: 5 fmol, D4: 10 fmol, D5: 20 fmol, D6: 30 fmol, D7: 40 fmol, and D8: 50 fmol) were used to mimic a 50-fold change in PTEN amount, using fixed amounts of 40 fmol SIS1 and 2 fmol SIS2 as 2-PIC standards (Figure 3a). Samples were prepared in triplicate and measured by LC-MRM. In sample D1, the NAT level (1 fmol) was below both internal standards, and in sample D8, the NAT level (50 fmol) was above both internal standards. For all eight samples highly reproducible results were obtained, with the RSD from the triplicate analyses between 1% and 13%, and with a correlation between determined and known NAT levels of r^2= 0.9791 (y= 1.05x–0.23). For D2-

D8, PTEN quantitation was clearly within a 20% cut-off, with recoveries between 83% and 110% (average 103%), while for D1, recovery was 77±2%. Notably, for the D8 sample where 50 fmol NAT was above both SIS standards, the recovery was 97±3% (Figure 3c).

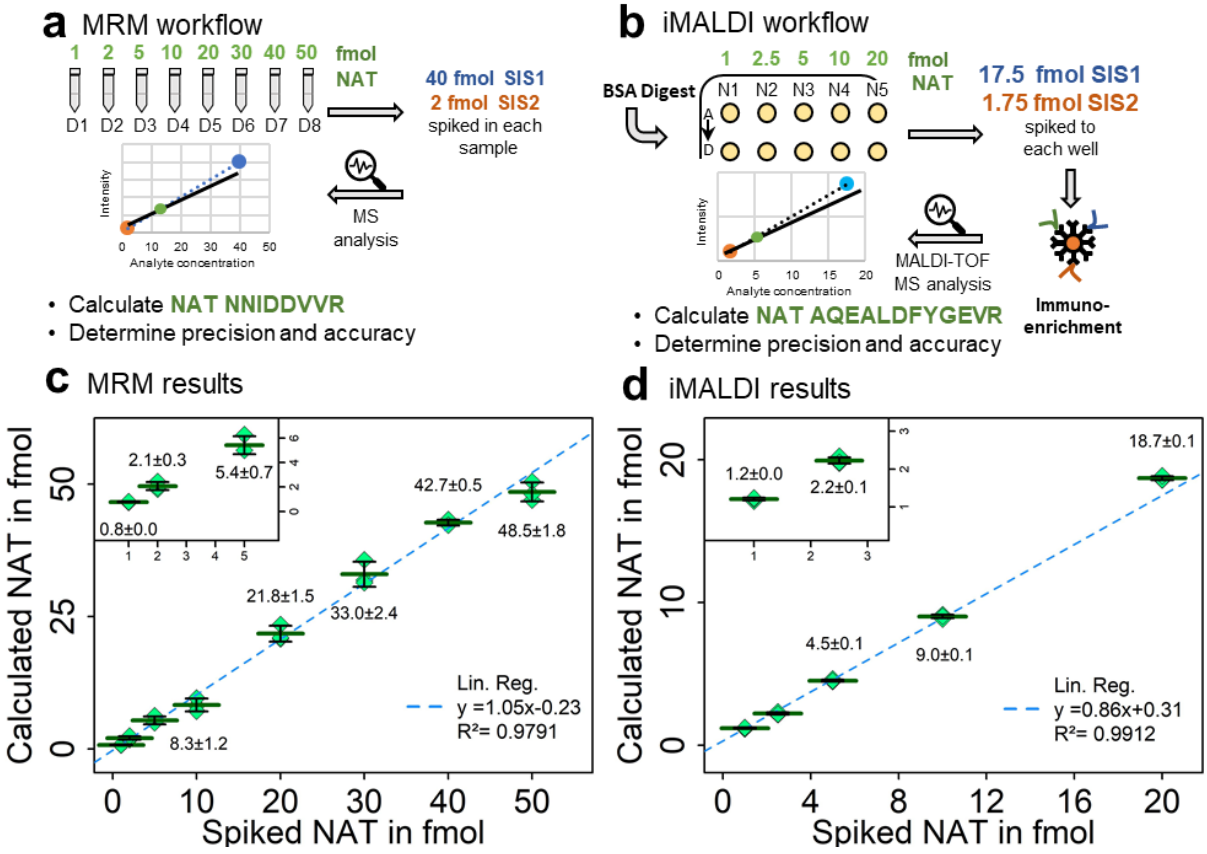

Figure 3: Quantifying different NAT levels using 2-PIC with fixed SIS levels. (a) MRM workflow targeting the PTEN peptide ^{48}NNIDDVVR^{55}. (b) iMALDI workflow targeting the PTEN peptide ^{148}AQEALDFYGEVR^{159}. (c) MRM results of the samples D1-D8. Dashed blue line: $1/x^2$ WLS regression curve. (d) iMALDI results of the samples N1-N5. Dashed blue line: $1/x^2$ WLS regression curve.

These results clearly show that -- given a defined set of SIS1 and SIS2 levels in an optimized assay -- 2-PIC yields accurate and precise results, over a reasonable range of fold-changes that might be expected in a given biological sample.

iMALDI. We prepared another set of 5 samples (N1-N5) with different AQEALDFYGEVR NAT levels (1, 2.5, 5, 10, and 20 fmol) in quadruplicate, using BSA digest as surrogate matrix and 17.5 fmol iMALDI SIS1 and 1.75 fmol SIS2 as the 2-PIC standards (Figure 3b). Again, the NAT level of one sample (N1; 1 fmol NAT) was below the levels of both internal standards, while in the sample N5 (20 fmol NAT) the NAT level was above both internal standards. In all samples, the NAT levels could be quantified with high precision, with RSDs between 0.6% and 3.1%, and

with a good correlation between the experimentally determined and known NAT levels (r^2= 0.9912, y=0.86x+0.31).

For N2-N5 all measurements were within the 20% cutoff, with recoveries between 89% and 93% (average 91%), while for sample N1 (1 fmol NAT), the recovery was 121±3% (Figure 3d).

These results agree with the results from our MRM experiments, and demonstrate the applicability of the 2-PIC strategy for the quantitation of low-abundance proteins.

Comparison of 2-PIC with external calibration for quantifying endogenous PTEN levels in Colo-205 cells

In clinical laboratories, the concept of internal calibration in LC-MS was first introduced for drug monitoring of immunosuppressants [36]. In fact, the Clinical Laboratory Improvement Amendments guidelines do not require a calibration curve for every batch of runs [37]. For targeted proteomics MS methods, internal calibration can increase the throughput, thus reduce expenses while avoiding the dependence on potentially misleading surrogate matrices [30]. Moreover, as clinical laboratories need to analyze small numbers of patient samples when they are received, reducing the workload required for preparing and running the calibrators can be very important. This means that applying internal calibration strategies for targeted proteomics will facilitate its clinical translation.

We therefore compared our 2-PIC strategy to conventional external calibration for their abilities to precisely determine endogenous PTEN expression levels in Colo-205 cells, a cell line that is commonly used to study metastatic colorectal cancer and which shows a down-regulation of PTEN expression compared to other colorectal cell lines [38,39]. Thus, Colo-205 are a good model to test our immuno-MS PTEN assays, because the typically-low endogenous PTEN expression level in normal tissue is further reduced in many cancers. We used both orthogonal workflows, immuno-MRM targeting the peptide ^{48}NNIDDVVR^{55} and immuno-MALDI targeting the peptide ^{148}AQEALDFYGEVR^{159}. To evaluate the robustness of both methods, three different amounts of starting material were used: 10, 15, and 30 µg of total Colo-205 lysate protein, rather than just using the same amount three times. Although one of the advantages of immuno-MS is that the amount of starting material can be scaled-up to improve the detection of low-abundance proteins, relatively low amounts of starting material are often all that can be obtained from clinical samples. Sample preparation, immuno-enrichment, data acquisition, and data analysis were performed as described for the experiments above.

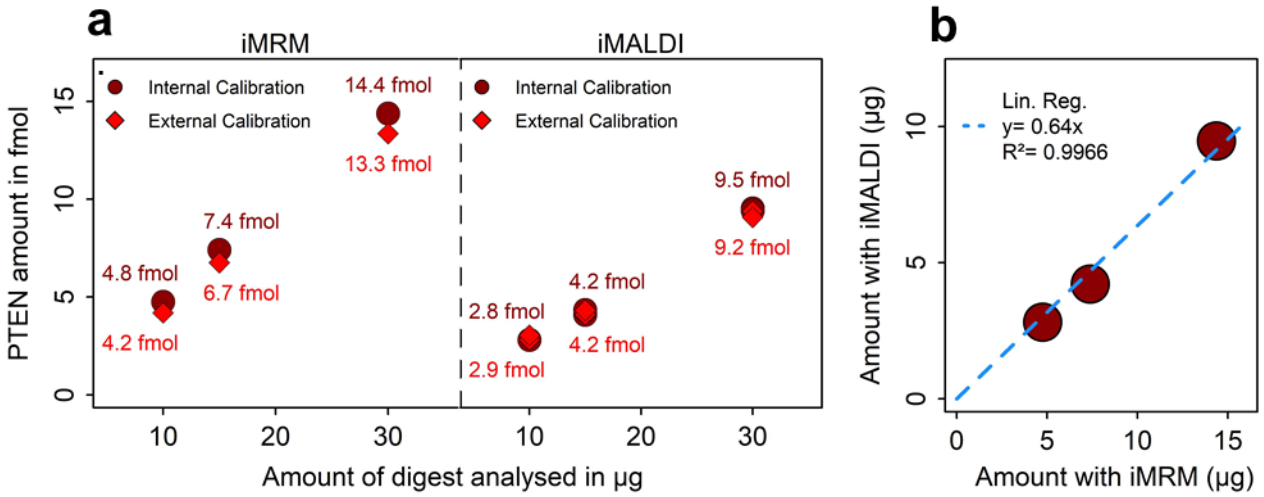

Figure 4: Quantifying endogenous PTEN levels from 10, 15, and 30 µg of Colo205 cell lysate total protein. (a)iMRM and iMALDI measurements. Left: iMRM results. The PTEN peptide NNIDDVVR was immuno-enriched from lysate, followed by MRM analysis. Right: iMALDI results. The PTEN peptide AQEALDFYGEVR was immuno-enriched from lysate, followed by MALDI analysis. (b)Correlation between iMRM and iMALDI results. iMRM and iMALDI show a strong correlation (r^2=0.9966; y=0.64x), although being completely orthogonal methods targeting different PTEN peptides and being conducted by two different individuals in two different laboratories.

For all three amounts of cell lysate (10, 15, and 30 µg of total Colo-205 protein) and both methods (iMRM and iMALDI), the two calibration methods (2-PIC and conventional external calibration) showed good agreement on the determined amounts of endogenous PTEN. For iMRM, the RSDs between 2-PIC and external calibration were 6.4%, 4.6%, and 3.7% using 10 µg, 15 µg, and 30 µg of Colo-205 lysate, respectively, and the iMALDI RSDs were 1.6%, 0.2%, and 1.6%, respectively (Figure 4a). These results demonstrate that both setups are extremely robust and very precise, and that 2-PIC yields results that are fully comparable to those from external calibration, while requiring much less effort, time, antibody, and standards -- and fewer samples analyzed.

Moreover, both methods -- although completely orthogonal and based on two different peptides and anti-peptide antibodies and being performed by two different individuals in two different laboratories -- showed good agreement on the determined amounts of endogenous PTEN when 2-PIC was used, with an average of 0.48±0.01 fmol/µg of total Colo-205 protein for iMRM (RSD of 1.6%) and 0.29±0.02 fmol/µg of total Colo-205 protein for iMALDI (RSD of 5.6%). Using 2-PIC, the endogenous PTEN concentrations determined by iMALDI and iMRM had an

average inter-assay RSD of 25% and these results reflect the good correlation between iMALDI and iMRM for quantifying endogenous PTEN (r^2=0.9966, y=0.64x; (Figure 4b).

For many years, MS researchers have been studying inter-laboratory assay performance and how to manage the resulting imprecision [40-43]. For example, Kuhn et al. demonstrated using a SISCAPA workflow that the overall inter-laboratory %CV, (including protein digestion, desalting, peptide antibody enrichment, and scheduled LC-MRM-MS analysis) was below 25% at or near the LOQ and below 20% at or near the midpoint of the linear range. While Abbatiello et al. studied the reproducibility of MRM assays across 11 laboratories and using 14 LC-MS systems, demonstrating that the median inter-laboratory CV% was <20% across the concentration range tested.

To our knowledge, there are no inter-laboratory precision studies that involved the quantitation of a protein using two completely different MS techniques using two different ionization methods, such as shown here for iMRM and iMALDI. The agreement between the two methods on quantifying endogenous PTEN in Colo-205 cells (RSD=25%; r^2=0.9966; y=0.64x) is comparable to values that have been reported for inter-laboratory variation when using a single method and standardized sample preparation protocols.

Conclusion

Using two completely orthogonal workflows, namely iMRM and iMALDI, targeting two different PTEN peptides, the utility of our 2-PIC strategy for immuno-MS assays was compared with a conventional, multipoint external calibration approach. We found that both the cost and burden of preparing multiple calibration standards with every batch of samples can be reduced, while analytical quality was maintained. Importantly, we demonstrated that even if the difference between the internal standards levels was 100-fold, precise quantitation of the analyte is possible, as long as the standards are in the linear range. Furthermore, 2-PIC allowed quantitation of the analyte in samples with levels below that of the lower internal standard, as well as in samples with levels above the higher internal standard. We also demonstrated that the endogenous PTEN concentrations determined from the cell line Colo-205 using the 2-PIC method were in good agreement with the results obtained using external calibration. Although quantitation of endogenous PTEN in Colo-205 was conducted in two different laboratories by two different individuals, using completely different workflows targeting two different peptides with two

different MS techniques and ionization methods, the results obtained strongly agreed with an RSD of only 25%.

References

1. Distler, U.; Kuharev, J.; Navarro, P.; Tenzer, S., Label-free quantitation in ion mobility-enhanced data-independent acquisition proteomics. *Nat Protoc* **2016,** *11* (4), 795-812.
2. Meier, F.; Geyer, P. E.; Virreira Winter, S.; Cox, J.; Mann, M., BoxCar acquisition method enables single-shot proteomics at a depth of 10,000 proteins in 100 minutes. *Nat Methods* **2018,** *15* (6), 440-448.
3. Mertins, P.; Tang, L. C.; Krug, K.; Clark, D. J.; Gritsenko, M. A.; Chen, L.; Clauser, K. R.; Clauss, T. R.; Shah, P.; Gillette, M. A.; Petyuk, V. A.; Thomas, S. N.; Mani, D. R.; Mundt, F.; Moore, R. J.; Hu, Y.; Zhao, R.; Schnaubelt, M.; Keshishian, H.; Monroe, M. E.; Zhang, Z.; Udeshi, N. D.; Mani, D.; Davies, S. R.; Townsend, R. R.; Chan, D. W.; Smith, R. D.; Zhang, H.; Liu, T.; Carr, S. A., Reproducible workflow for multiplexed deep-scale proteome and phosphoproteome analysis of tumor tissues by liquid chromatography-mass spectrometry. *Nat Protoc* **2018,** *13* (7), 1632-1661.
4. Percy, A. J.; Michaud, S. A.; Jardim, A.; Sinclair, N. J.; Zhang, S.; Mohammed, Y.; Palmer, A. L.; Hardie, D. B.; Yang, J.; LeBlanc, A. M.; Borchers, C. H., Multiplexed MRM-based assays for the quantitation of proteins in mouse plasma and heart tissue. *Proteomics* **2017,** *17* (7).
5. Blank-Landeshammer, B.; Richard, V. R.; Mitsa, G.; Marques, M.; LeBlanc, A.; Kollipara, L.; Feldmann, I.; Couetoux du Tertre, M.; Gambaro, K.; McNamara, S.; Spatz, A.; Zahedi, R. P.; Sickmann, A.; Batist, G.; Borchers, C. H., Proteogenomics of Colorectal Cancer Liver Metastases: Complementing Precision Oncology with Phenotypic Data. *Cancers (Basel)* **2019,** *11* (12).
6. Sobsey, C. A.; Ibrahim, S.; Richard, V. R.; Gaspar, V.; Mitsa, G.; Lacasse, V.; Zahedi, R. P.; Batist, G.; Borchers, C. H., Targeted and Untargeted Proteomics Approaches in Biomarker Development. *Proteomics* **2019**, e1900029.
7. Mnatsakanyan, R.; Shema, G.; Basik, M.; Batist, G.; Borchers, C. H.; Sickmann, A.; Zahedi, R. P., Detecting post-translational modification signatures as potential biomarkers in clinical mass spectrometry. *Expert Rev Proteomics* **2018,** *15* (6), 515-535.
8. Luongo, F.; Colonna, F.; Calapa, F.; Vitale, S.; Fiori, M. E.; De Maria, R., PTEN Tumor-Suppressor: The Dam of Stemness in Cancer. *Cancers (Basel)* **2019,** *11* (8).
9. Berger, A. H.; Knudson, A. G.; Pandolfi, P. P., A continuum model for tumor suppression. *Nature* **2011,** *476* (7359), 163-9.
10. Rosenberger, G.; Bludau, I.; Schmitt, U.; Heusel, M.; Hunter, C. L.; Liu, Y.; MacCoss, M. J.; MacLean, B. X.; Nesvizhskii, A. I.; Pedrioli, P. G. A.; Reiter, L.; Rost, H. L.; Tate, S.; Ting, Y. S.; Collins, B. C.; Aebersold, R., Statistical control of peptide and protein error rates in large-scale targeted data-independent acquisition analyses. *Nat Methods* **2017,** *14* (9), 921-927.
11. Pfammatter, S.; Bonneil, E.; McManus, F. P.; Thibault, P., Accurate Quantitative Proteomic Analyses Using Metabolic Labeling and High Field Asymmetric Waveform Ion Mobility Spectrometry (FAIMS). *J Proteome Res* **2019,** *18* (5), 2129-2138.
12. Jannetto, P. J.; Fitzgerald, R. L., Effective Use of Mass Spectrometry in the Clinical Laboratory. *Clin Chem* **2016,** *62* (1), 92-8.
13. Heaney, L. M.; Jones, D. J.; Suzuki, T., Mass spectrometry in medicine: a technology for the future? *Future Sci OA* **2017,** *3* (3), FSO213.
14. Dou, M.; Clair, G.; Tsai, C. F.; Xu, K.; Chrisler, W. B.; Sontag, R. L.; Zhao, R.; Moore, R. J.; Liu, T.; Pasa-Tolic, L.; Smith, R. D.; Shi, T.; Adkins, J. N.; Qian, W. J.; Kelly, R. T.; Ansong, C.; Zhu,

Y., High-Throughput Single Cell Proteomics Enabled by Multiplex Isobaric Labeling in a Nanodroplet Sample Preparation Platform. *Anal Chem* **2019,** *91* (20), 13119-13127.
15. Nelson, R. W.; Krone, J. R.; Bieber, A. L.; Williams, P., Mass spectrometric immunoassay. *Anal Chem* **1995,** *67* (7), 1153-8.
16. Raska, C. S.; Parker, C. E.; Sunnarborg, S. W.; Pope, R. M.; Lee, D. C.; Glish, G. L.; Borchers, C. H., Rapid and sensitive identification of epitope-containing peptides by direct matrix-assisted laser desorption/ionization tandem mass spectrometry of peptides affinity-bound to antibody beads. *J Am Soc Mass Spectrom* **2003,** *14* (10), 1076-85.
17. Warren, E. N.; Elms, P. J.; Parker, C. E.; Borchers, C. H., Development of a protein chip: a MS-based method for quantitation of protein expression and modification levels using an immunoaffinity approach. *Anal Chem* **2004,** *76* (14), 4082-92.
18. Popp, R.; Basik, M.; Spatz, A.; Batist, G.; Zahedi, R. P.; Borchers, C. H., How iMALDI can improve clinical diagnostics. *Analyst* **2018,** *143* (10), 2197-2203.
19. Anderson, N. L.; Jackson, A.; Smith, D.; Hardie, D.; Borchers, C.; Pearson, T. W., SISCAPA peptide enrichment on magnetic beads using an in-line bead trap device. *Mol Cell Proteomics* **2009,** *8* (5), 995-1005.
20. Solari, F. A.; Dell'Aica, M.; Sickmann, A.; Zahedi, R. P., Why phosphoproteomics is still a challenge. *Mol Biosyst* **2015,** *11* (6), 1487-93.
21. Venne, A. S.; Kollipara, L.; Zahedi, R. P., The next level of complexity: crosstalk of posttranslational modifications. *Proteomics* **2014,** *14* (4-5), 513-24.
22. Hoofnagle, A. N.; Whiteaker, J. R.; Carr, S. A.; Kuhn, E.; Liu, T.; Massoni, S. A.; Thomas, S. N.; Townsend, R. R.; Zimmerman, L. J.; Boja, E.; Chen, J.; Crimmins, D. L.; Davies, S. R.; Gao, Y.; Hiltke, T. R.; Ketchum, K. A.; Kinsinger, C. R.; Mesri, M.; Meyer, M. R.; Qian, W. J.; Schoenherr, R. M.; Scott, M. G.; Shi, T.; Whiteley, G. R.; Wrobel, J. A.; Wu, C.; Ackermann, B. L.; Aebersold, R.; Barnidge, D. R.; Bunk, D. M.; Clarke, N.; Fishman, J. B.; Grant, R. P.; Kusebauch, U.; Kushnir, M. M.; Lowenthal, M. S.; Moritz, R. L.; Neubert, H.; Patterson, S. D.; Rockwood, A. L.; Rogers, J.; Singh, R. J.; Van Eyk, J. E.; Wong, S. H.; Zhang, S.; Chan, D. W.; Chen, X.; Ellis, M. J.; Liebler, D. C.; Rodland, K. D.; Rodriguez, H.; Smith, R. D.; Zhang, Z.; Zhang, H.; Paulovich, A. G., Recommendations for the Generation, Quantitation, Storage, and Handling of Peptides Used for Mass Spectrometry-Based Assays. *Clin Chem* **2016,** *62* (1), 48-69.
23. Honour, J. W., Development and validation of a quantitative assay based on tandem mass spectrometry. *Ann Clin Biochem* **2011,** *48* (Pt 2), 97-111.
24. Villanueva, J.; Carrascal, M.; Abian, J., Isotope dilution mass spectrometry for absolute quantitation in proteomics: concepts and strategies. *J Proteomics* **2014,** *96*, 184-99.
25. Buhrman, D. L.; Price, P. I.; Rudewiczcor, P. J., Quantitation of SR 27417 in human plasma using electrospray liquid chromatography-tandem mass spectrometry: A study of ion suppression. *J Am Soc Mass Spectrom* **1996,** *7* (11), 1099-105.
26. Ciccimaro, E.; Blair, I. A., Stable-isotope dilution LC-MS for quantitative biomarker analysis. *Bioanalysis* **2010,** *2* (2), 311-41.
27. LeBlanc, A.; Michaud, S. A.; Percy, A. J.; Hardie, D. B.; Yang, J.; Sinclair, N. J.; Proudfoot, J. I.; Pistawka, A.; Smith, D. S.; Borchers, C. H., Multiplexed MRM-Based Protein Quantitation Using Two Different Stable Isotope-Labeled Peptide Isotopologues for Calibration. *J Proteome Res* **2017,** *16* (7), 2527-2536.

28. Chiva, C.; Pastor, O.; Trilla-Fuertes, L.; Gamez-Pozo, A.; Fresno Vara, J. A.; Sabido, E., Isotopologue Multipoint Calibration for Proteomics Biomarker Quantitation in Clinical Practice. *Anal Chem* **2019,** *91* (8), 4934-4938.
29. Froehlich, B. C. P., R.; Sobsey, C. A.; Ibrahim, S.; LeBlanc, A.; Mohammed, Y.; Aguilar-Mahecha, A.; Pötz, O.; Spatz, A.; Basik, M.; Batist, G.; Borchers, C.; Zahedi, R. P.; Borchers, C. H., Systematic optimization of the iMALDI workflow for the robust and straightforward quantitation of signalling proteins in cancer cells. **Submitted**.
30. Rule, G. S.; Rockwood, A. L., Improving quantitative precision and throughput by reducing calibrator use in liquid chromatography-tandem mass spectrometry. *Anal Chim Acta* **2016,** *919*, 55-61.
31. Hoffman, M. A.; Schmeling, M.; Dahlin, J. L.; Bevins, N. J.; Cooper, D. P.; Jarolim, P.; Fitzgerald, R. L.; Hoofnagle, A. N., Calibrating from Within: Multipoint Internal Calibration of a Quantitative Mass Spectrometric Assay of Serum Methotrexate. *Clin Chem* **2020,** *66* (3), 474-482.
32. Grant, R. P., The march of the masses. *Clin Chem* **2013,** *59* (6), 871-3.
33. Ma, K.; Vitek, O.; Nesvizhskii, A. I. BMC Bioinf. 2012, 13, S1.
34. Gu, H.; Liu, G.; Wang, J.; Aubry, A. F.; Arnold, M. E., Selecting the correct weighting factors for linear and quadratic calibration curves with least-squares regression algorithm in bioanalytical LC-MS/MS assays and impacts of using incorrect weighting factors on curve stability, data quality, and assay performance. *Anal Chem* **2014,** *86* (18), 8959-66.
35. Cuadros-Rodríguez, L.; Bagur-González, M. G.; Sánchez-Vinas, M.; González-Casado, A.; Gómez-Sáez, A. M., Principles of analytical calibration/quantitation for the separation sciences. *Journal of Chromatography A* **2007,** *1158* (1-2), 33-46.
36. Taylor, P. J.; Hogan, N. S.; Lynch, S. V.; Johnson, A. G.; Pond, S. M., Improved therapeutic drug monitoring of tacrolimus (FK506) by tandem mass spectrometry. *Clin Chem* **1997,** *43* (11), 2189-90.
37. (CMS), C. L. I. A. C. C. f. M. a. M. S., Centers for Medicare and Medicaid Services (CMS). *Available at: https://www.cms.gov/Regulations-and-Guidance/Legislation/CLIA/index.html?redirect=/clia* **Accessed 8/27/18**.
38. Mao, M.; Tian, F.; Mariadason, J. M.; Tsao, C. C.; Lemos, R., Jr.; Dayyani, F.; Gopal, Y. N.; Jiang, Z. Q.; Wistuba, II; Tang, X. M.; Bornman, W. G.; Bollag, G.; Mills, G. B.; Powis, G.; Desai, J.; Gallick, G. E.; Davies, M. A.; Kopetz, S., Resistance to BRAF inhibition in BRAF-mutant colon cancer can be overcome with PI3K inhibition or demethylating agents. *Clin Cancer Res* **2013,** *19* (3), 657-67.
39. Medico, E.; Russo, M.; Picco, G.; Cancelliere, C.; Valtorta, E.; Corti, G.; Buscarino, M.; Isella, C.; Lamba, S.; Martinoglio, B.; Veronese, S.; Siena, S.; Sartore-Bianchi, A.; Beccuti, M.; Mottolese, M.; Linnebacher, M.; Cordero, F.; Di Nicolantonio, F.; Bardelli, A., The molecular landscape of colorectal cancer cell lines unveils clinically actionable kinase targets. *Nat Commun* **2015,** *6*, 7002.
40. Addona, T. A.; Abbatiello, S. E.; Schilling, B.; Skates, S. J.; Mani, D. R.; Bunk, D. M.; Spiegelman, C. H.; Zimmerman, L. J.; Ham, A. J.; Keshishian, H.; Hall, S. C.; Allen, S.; Blackman, R. K.; Borchers, C. H.; Buck, C.; Cardasis, H. L.; Cusack, M. P.; Dodder, N. G.; Gibson, B. W.; Held, J. M.; Hiltke, T.; Jackson, A.; Johansen, E. B.; Kinsinger, C. R.; Li, J.; Mesri, M.; Neubert, T. A.; Niles, R. K.; Pulsipher, T. C.; Ransohoff, D.; Rodriguez, H.; Rudnick, P. A.; Smith, D.; Tabb, D. L.; Tegeler,

T. J.; Variyath, A. M.; Vega-Montoto, L. J.; Wahlander, A.; Waldemarson, S.; Wang, M.; Whiteaker, J. R.; Zhao, L.; Anderson, N. L.; Fisher, S. J.; Liebler, D. C.; Paulovich, A. G.; Regnier, F. E.; Tempst, P.; Carr, S. A., Multi-site assessment of the precision and reproducibility of multiple reaction monitoring-based measurements of proteins in plasma. *Nat Biotechnol* **2009,** *27* (7), 633-41.

41. Prakash, A.; Rezai, T.; Krastins, B.; Sarracino, D.; Athanas, M.; Russo, P.; Ross, M. M.; Zhang, H.; Tian, Y.; Kulasingam, V.; Drabovich, A. P.; Smith, C.; Batruch, I.; Liotta, L.; Petricoin, E.; Diamandis, E. P.; Chan, D. W.; Lopez, M. F., Platform for establishing interlaboratory reproducibility of selected reaction monitoring-based mass spectrometry peptide assays. *J Proteome Res* **2010,** *9* (12), 6678-88.

42. Kuhn, E.; Whiteaker, J. R.; Mani, D. R.; Jackson, A. M.; Zhao, L.; Pope, M. E.; Smith, D.; Rivera, K. D.; Anderson, N. L.; Skates, S. J.; Pearson, T. W.; Paulovich, A. G.; Carr, S. A., Interlaboratory evaluation of automated, multiplexed peptide immunoaffinity enrichment coupled to multiple reaction monitoring mass spectrometry for quantifying proteins in plasma. *Mol Cell Proteomics* **2012,** *11* (6), M111 013854.

43. Abbatiello, S. E.; Schilling, B.; Mani, D. R.; Zimmerman, L. J.; Hall, S. C.; MacLean, B.; Albertolle, M.; Allen, S.; Burgess, M.; Cusack, M. P.; Gosh, M.; Hedrick, V.; Held, J. M.; Inerowicz, H. D.; Jackson, A.; Keshishian, H.; Kinsinger, C. R.; Lyssand, J.; Makowski, L.; Mesri, M.; Rodriguez, H.; Rudnick, P.; Sadowski, P.; Sedransk, N.; Shaddox, K.; Skates, S. J.; Kuhn, E.; Smith, D.; Whiteaker, J. R.; Whitwell, C.; Zhang, S.; Borchers, C. H.; Fisher, S. J.; Gibson, B. W.; Liebler, D. C.; MacCoss, M. J.; Neubert, T. A.; Paulovich, A. G.; Regnier, F. E.; Tempst, P.; Carr, S. A., Large-Scale Interlaboratory Study to Develop, Analytically Validate and Apply Highly Multiplexed, Quantitative Peptide Assays to Measure Cancer-Relevant Proteins in Plasma. *Mol Cell Proteomics* **2015,** *14* (9), 2357-74.

The second manuscript presents the fully-standardized anti-peptide PTEN immune-MRM method as a much-needed tool for the study of PTEN as a potential biomarker in breast cancer. Several breast cancer clinical samples including cell lines, fresh frozen- and formalin-fixed paraffin-embedded (FFPE) tissues were analyzed with the PTEN iMRM assay as well as other conventional techniques including immunohistochemistry and western blot in order to show the correlation between their PTEN quantitation results as well as the superior performance of the PTEN iMRM assay that is particularly relevant for clinical use.

Precise quantitation of PTEN by immuno-MRM: a tool to resolve the breast cancer biomarker controversy.

Sahar Ibrahim[1,2,3], Cathy Lan[4], Catherine Chabot[4], Georgia Mitsa[1,3], Marguerite Buchanan[4], Adriana Aguilar-Mahecha[4], Mounib Elchebly[4], Oliver Poetz[5,6], Alan Spatz[1,4,7,8], Mark Basik[1,4,9], Gerald Batist[4,9], René P. Zahedi[3,10], Christoph H. Borchers[3,9,10*].

[1] Division of Experimental Medicine, McGill University, Montréal, Québec, Canada.

[2] Clinical Pathology Department, National Liver Institute, Menoufia University, Egypt.

[3] Segal Cancer Proteomics Centre, Lady Davis Institute for Medical Research, Jewish General Hospital, McGill University, Montréal, Québec, Canada.

[4] Segal Cancer Center, Lady Davis Institute for Medical Research, Jewish General Hospital, McGill University, Montréal, Québec, Canada.

[5] NMI Natural and Medical Sciences Institute at the University of Tuebingen, Reutlingen, Germany.

[6] SIGNATOPE GmbH, Reutlingen, Germany.[7] Department of Pathology, McGill University, Montréal, Québec, Canada.

[7] Department of Pathology, McGill University, Montréal, Québec, Canada.

[8] Division of Pathology, Department of Laboratory Medicine, McGill University Health Centre, Montréal, Québec, Canada.

[9] Gerald Bronfman Department of Oncology, Jewish General Hospital, McGill University, Montréal, Québec, Canada.

[10] Center for Computational and Data-Intensive Science and Engineering, Skolkovo Institute of Science and Technology, Moscow, Russia).

Introduction

Breast cancer (BC) is a worldwide health burden, with 2.0 million new diagnoses in 2018. BC accounts for one out of four cancer cases in women [1] and in 2019 approximately 41,760 women and 500 men were expected to die from BC in the US alone [2], leading to estimated healthcare costs of 20 billion US dollars in 2018, 34% of which were spent for initial care, 43% for continuing care, and 23% for the last year of life [3].

Current systemic treatment for BC is based on the molecular subtype. For instance, (i) the hormonal receptor positive subtypes luminal A and luminal B are treated mainly with endocrine therapy [4], and (ii) HER2 over-expressing BC is treated mainly with HER2-targeting drugs [5, 6], while for (iii) triple-negative/basal-like BC, chemotherapy was the only approved systemic therapy [7] until the recent approval of immunotherapy. Although more-effective screening programs and treatment options have considerably improved patient outcome, BC remains the leading cause of cancer-related deaths in over 100 countries [1]. This high lethality can be largely explained by the manifestation of *de novo* (or primary) and *acquired* resistance to therapies, which represent a huge challenge for effective and sustainable BC treatment.

The proto-oncogenic phosphatidylinositol-3-kinase (PI3K)/protein kinase B signaling pathway is commonly found to be hyperactive in all BC subtypes [8-10]. Many targeted therapeutics that inhibit the PI3K/AKT pathway were developed as a combinatorial therapy for BC in addition to standard treatments, and are either approved for clinical use [11] or are still being evaluated in clinical trials [12, 13].

The dual-specificity phosphatase and tensin homolog (PTEN) is the main negative regulator of the PI3K/AKT pathway and one of the most important tumor suppressor genes [14], thus playing an important role in cancerogenesis and cancer severity [15 16]. A slight reduction of PTEN protein expression in mice was shown to induce BC, and the extent of PTEN reduction showed a correlation with cancer severity in a dose-dependent manner [17]. From several preclinical and clinical studies, it has been deduced that PTEN protein expression level is a promising potential clinical biomarker in BC, that can be used for prognosis [18 19 20], for prediction of resistance to endocrine [21] and anti-HER2 therapies [22 23, 24], and for selecting patients for combinatorial therapy with PI3K pathway inhibitors [25 26, 27]. However, several other studies have failed to report either an association between PTEN protein levels and prognosis in BC patients [28,29], or an association

with treatment response to various BC therapeutics in clinical trials [23, 24]. Because of these conflicting data, PTEN's role as BC biomarker is still controversial [29 30 24].

Carbognin et al. reasoned that the major source of the conflicting data on PTEN was the lack of standardization of the methods used to determine PTEN expression: Neither the type of assay nor the protocols used for a single type of assay were consistent and reproducible across these studies [31]. PTEN protein is quantified using immunoassays, which, however, are typically low-throughput and associated with a variety of analytical and pre-analytical shortcomings, such as antibody specificity, especially when these antibodies are derived from different sources [32-35]. Immunohistochemistry (IHC) assays are restricted to formalin-fixed paraffin-embedded (FFPE) tissue samples, generally lack standardization, and involve subjective ranking/scoring of results (e.g., H-score, low/medium/high protein levels, % of positive cells). Particularly for PTEN, a cut-off for "PTEN-loss" [36] has not been clearly defined, so that the same biopsy analyzed by different pathologists will likely lead to different or even conflicting interpretations and therapeutic conclusions. Western blotting (WB) suffers from drawbacks similar to those of IHC, and WB allows only relative quantitation of samples that have been analyzed within *a single* batch and has limited precision. Inconsistent results are therefore frequent and derive from the lack of normalization and standardization [37 38]. Reverse Phase Protein Arrays (RPPA) have been used for sensitive high-throughput analysis of PTEN, but the clinical use of RPPA is limited, even in those cases when highly specific antibodies are available and validated, because RPPA platforms and workflows are non-standardized, thus hindering the performance of the large-scale integrative projects needed for biomarker validation [39].

Obviously, there is an urgent need for an improved, robust, accurate, and validated method that allows the standardized and precise quantitation of actual PTEN protein expression in tissue samples (both fresh frozen and FFPE) with high-throughput capacity, and which will therefore allow the clear discrimination of subtle differences in PTEN expression in clinical samples. Only this kind of method will enable the thorough study of PTEN's role as a biomarker for diagnostic and prognostic purposes in precision oncology. Multiple reaction monitoring (MRM) mass spectrometry (MS) is a method that can provide the missing precise and reproducible assessment of PTEN protein expression levels. In recent years, MRM has been increasingly used to evaluate and validate biomarkers because of its (i) accuracy and precision, (ii) high specificity (including the ability to discriminate between various protein isoforms), (iii) reproducibility, and

its capacity for (iv) standardization, (v) automation, and (vi) multiplexing [40]. Once developed and validated, MRM assays are amenable to a wide range of biological samples, including cells and animal models, bodily fluids, fresh-frozen tissue as well as archived FFPE specimens. Because of these characteristics, MRM is believed to be the future alternative to standard antibody-based clinical assays [41].

Once a 'proteotypic' surrogate peptide has been chosen to quantify the target protein after proteolytic digestion, a stable-isotope labeled standard [42] peptide having the same amino acid sequence but incorporated stable isotope labels (i.e. identical physicochemical properties), is spiked into every sample as internal standard. This allows determining the target protein's concentration in any type of sample using fully-standardized, robust, and fast liquid chromatography MRM (LC-MRM) assays. To further boost the sensitivity of MRM for quantifying proteins of extremely low abundance, specific anti-peptide antibodies can be used to co-enrich the target peptide and its SIS prior to MRM. This is referred to as immuno-MRM (iMRM). Because endogenous (END) and SIS peptides are co-enriched with the same efficiency, iMRM allows the fully-standardized and quality-controlled quantitation of proteins with the utmost sensitivity. This is a great advantage over the use of conventional affinity MS workflows using anti-protein antibodies [43].

Here, we present and analytically validate an iMRM method that allows the quantitation of PTEN with high sensitivity and precision. The inclusion of our recent 2-PIC internal calibration strategy greatly facilitates the robust quantitation of clinical specimens. We demonstrate the generic utility of our PTEN-iMRM assay by quantifying endogenous PTEN protein levels in different BC cell lines, fresh frozen tissues, and FFPE tissues. Due to its robustness and performance, we believe that our PTEN-iMRM assay will finally enable the important and urgent study of PTEN's role as a BC biomarker.

Experimental Procedures

Detailed descriptions of all experimental procedures can be found in Appendix II, as well a summary of the used *Reagents* and *Clinical samples* (see also Table S1, Appendix II).

LC-MRM assay development. The PTEN prototypic peptide NNIDDVVR^{2+} (m/z 472.7434) was selected (see Table S2, Appendix II) to be targeted by LC-MRM method that was developed and optimized on an Agilent 6495A triple-quadrupole MS. Skyline-Daily software 19.1 was used to

select y5 as a quantifier, and y4, y6, and b3 as qualifier-fragment ions for NNIDDVVR in NAT and SIS forms (Table S4, Appendix II). Collision energies (CE) were optimized for each transition with the help of Skyline-Daily, using a dwell time of 10 ms for each transition. The fully optimized LC and MS parameters are summarized in (Table S5, Appendix II).

The LC-MRM validation, including the *Response curve*, the *Method repeatability test*, and the *Method selectivity test* are described in the Appendix II, as well as the *Determination of the anti-*NNIDDVVR peptide immuno-enrichment recovery, the PTEN iMRM method accuracy test, and the Western blot analysis of PDX-derived cell lines.

Quantitation of PTEN protein levels in cell lines using immuno-MRM. Protein was extracted from cell lines and their total protein concentration was determined as described in Appendix II. For the cell lines T670, P129, and P132, 20 µg of total protein lysate were used, while different amounts of total protein lysate were used for the commercial cell lines that were prepared in triplicate (8 µg MCF7, 10 µg BT474, 10 µg MDA-231, 14 µg MDA-231+EGF). Samples were subjected to reduction, alkylation, digestion, immuno-enrichment for NNIDDVVR analyzed by LC-MRM, as described above. Endogenous PTEN concentrations were determined using our 2-PIC strategy [44] and the LC-MRM PTEN results of the in-house cell lines were compared to the western blot data for PTEN and pHER2.

FFPE sectioning and staining are described in the Appendix II.

Quantitation of PTEN levels in FFPE cores using Immuno-MRM. Guided by the IHC results, three 1.0-mm diameter cores were punched out of each block and transferred to separate reaction tubes, to be used as analytical triplicates. Each core was deparaffinized and rehydrated followed by protein extraction as described in Appendix II. Samples containing either 20, 30, or 50 µg protein from the tissue lysate were prepared and subjected to reduction, alkylation, digestion, and immuno-enrichment for NNIDDVVR as described above for cell line samples. Samples were analyzed by LC-MRM as described above. Endogenous PTEN concentrations were determined using our 2-PIC strategy [44] and are reported in fmol per 10 µg of protein, which can be more precisely determined than for instance actual tumor tissue volume or weight.

The embedding of PDX-derived fresh-frozen tissue samples in OCT is described in the Appendix II.

Quantitation of PTEN levels in fresh frozen OCT blocks using immuno-MRM. Protein extraction from fresh frozen OCT blocks was performed as described in ***SI***. Eighty µg of each lysate were subjected to reduction, alkylation, digestion and immuno-enrichment for NNIDDVVR as described in Appendix II. Samples were analyzed by LC-MRM and Endogenous PTEN concentrations were determined as described above.

PTEN western blot analysis of fresh frozen tissue samples is described in the Appendix II.

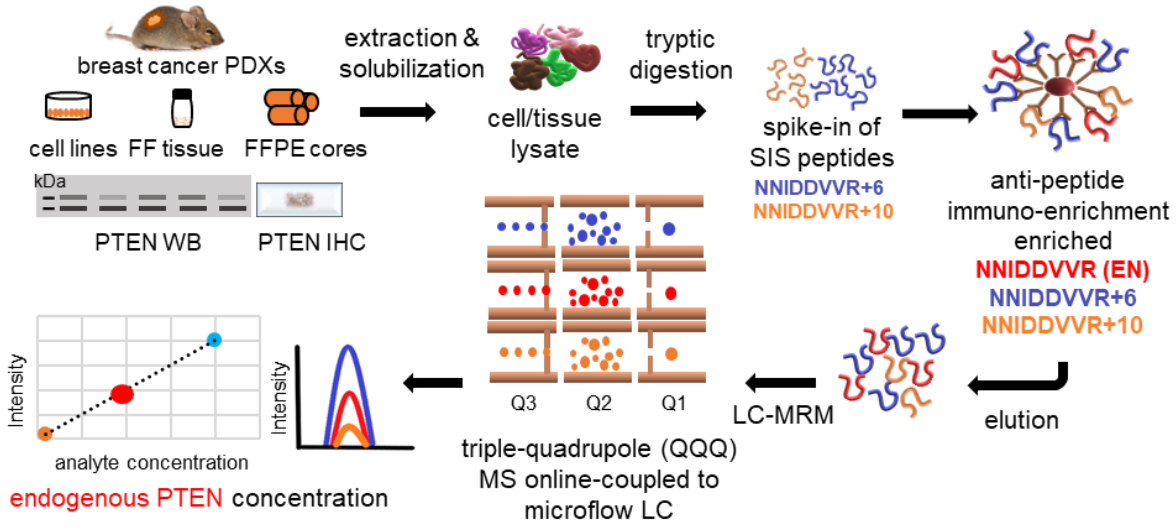

Figure 1. Quantitation of PTEN using anti-peptide immuno-MRM. BC PDX models were used to generate different sample types, cell lines, FF and FFPE tissue. While PTEN expression in cell lines and fresh frozen (FF) tissue samples was determined using WB, FFPE tissue samples were analyzed by PTEN IHC. For all samples, proteins were extracted, followed by tryptic digestion to release the endogenous target peptide NNIDDVVR (red). SIS variants 1 (NNIDDV**V**R+6 Da, blue) and 2 (NNIDDVV**R**+10 Da, orange) were spiked into the samples prior to anti-NNIIDDVVR immuno-enrichment. The eluates were analyzed by LC-MRM, and the endogenous PTEN levels were determined using our two-point internal calibration (2-PIC) and are reported in fmol per 10 µg of total extracted protein, which can be more precisely determined than, for example, the actual tumor tissue volume or weight.

Results and discussion

We present here an immuno-MRM method for the precise quantitation of PTEN protein concentrations in clinical samples. Our assay will enable researchers to finally shed light on PTEN's controversial role as a BC biomarker (Figure 1) and may also be directly useful for improving patient stratification.

Our initial goal was to (i) develop and optimize a robust assay that provides high sensitivity to allow PTEN quantitation in different types of samples, including FFPE cores, and to (ii) validate

that this assay offers good precision (CV<20%) and accuracy (80-120%). However, after optimizing the conditions for a PTEN LC-MRM assay and validating its performance, we observed that the LLOQ of the assay was insufficient to measure PTEN in different cell lines, even when loading digests corresponding to 100 µg of total protein on-column. These results indicated the need for a more sensitive assay. This is particularly relevant when analyzing BC and other tumors where PTEN is known to be down-regulated compared to healthy tissues, and even more because the extent of this down-regulation correlates with disease severity. Although nano-LC-MS/MS can provide higher sensitivity than our micro-LC-MRM setup, micro-flow LC-MRM is considerably more robust, requires substantially less maintenance, allows a higher throughput with very short and reproducible gradients, and requires less costly equipment [45].

We, therefore, developed an assay that combines micro-LC-MRM with prior anti-peptide immuno-enrichment for PTEN quantitation, in order to synergize the sensitivity, specificity, precision, and confidence of the two methods. To demonstrate the performance and added value of our novel assay, we compared it with the two methods currently being used to assess PTEN levels -- IHC and WB -- for their abilities to precisely quantify differences in PTEN protein expression.

The PTEN surrogate peptide NNIDDVVR was selected as ideal target to develop a highly sensitive LC-MRM method, after querying proteomics databases, enforcing specific sequence and peptide criteria [46], and analyzing recPTEN by DDA to validate a good signal response. The LC-MRM method for NNIDDVVR was developed on an Agilent 6495 triple quadrupole and the LC conditions and collision energies for individual MRM transitions were optimized to reduce analysis time and improve sensitivity.

PTEN LC-MRM method validation

To validate the resulting 11-min LC-MRM method, we followed the guidelines of the Clinical Proteomic Tumor Analysis Consortium [47] for MRM assays [42]. We prepared a calibration curve with 0.27-270 fmol of NNIDDVV<u>R</u> SIS2 and constant 5 fmol of NNIDDV<u>V</u>R SIS1 peptide on-column in mCRC FFPE protein digest background to mimic the post-immuno-enrichment matrix. Plotting the SIS2:SIS1 peak area ratios against the amount of SIS2 spike-in shows a good r^2 of 0.9965 by linear regression (Figure S1b, Appendix II). Fitting the data points to a power function confirmed a good linearity ($y= 0.1344x^{1.0257}$; exponent of x should be between 0.95 and

1.05 [42]; (Figure 2a). The lower limits of detection (LLOD) and quantitation (LLOQ) were determined as 0.45 fmol (CV 17.7%) and 0.90 fmol (CV 6.8%) on-column, respectively.

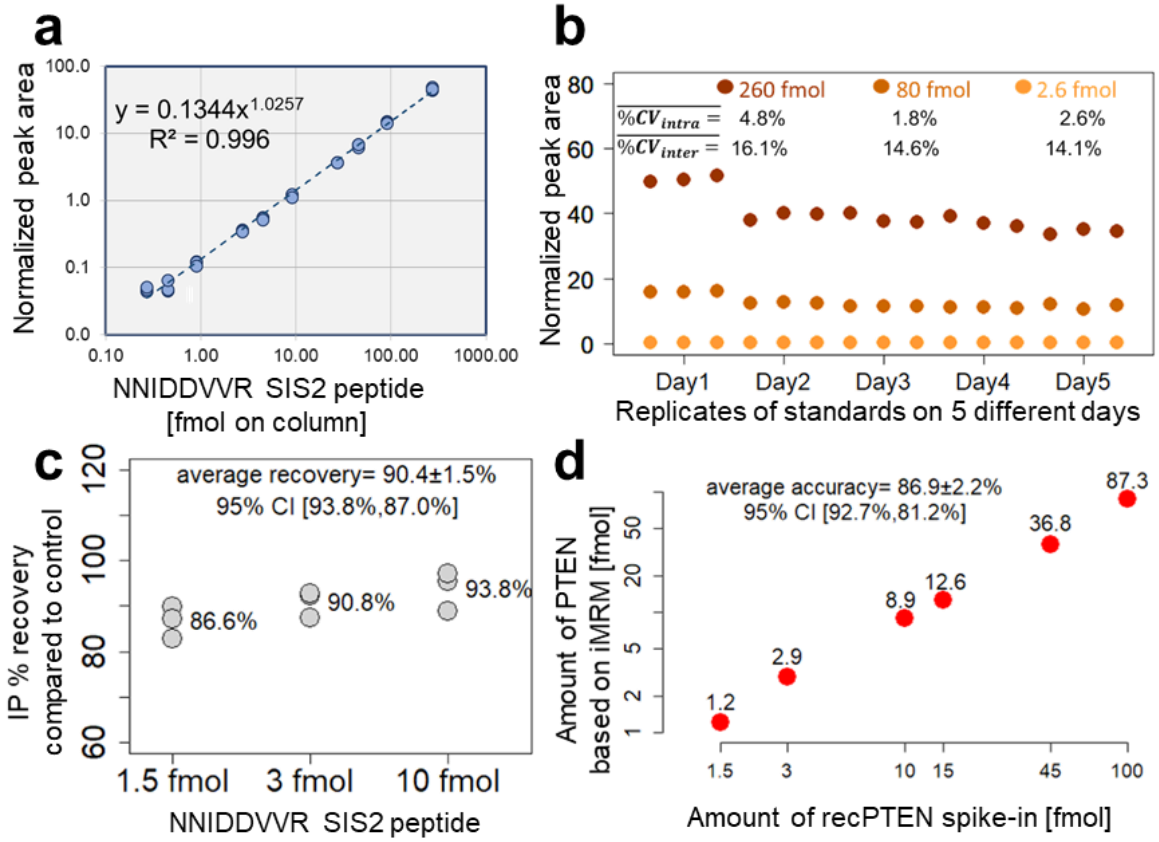

Figure 2. Validation of the PTEN immuno-MRM assay. (a) LC-MRM calibration curve for NNIDDVVR with increasing SIS2 amounts in a constant SIS1 level. Y-axis: Normalized SIS2 peak area (SI2/SIS peak area ratio). A power function was fitted to the data. (b) Repeatability test, measuring three different levels of NNIDDVV**R** SIS2 in a constant matrix of 1 µg of total tissue protein digest and 5 fmol of SIS1. (c) Recovery (%) of SIS2 anti-peptide IP from tissue lysate digest. (d) Accuracy of the immuno-MRM assay determined after spiking CRC FFPE tissue with recombinant PTEN (recPTEN). CI = confidence interval.

Next, we assessed the inter- and intra-day reproducibility of our LC-MRM assay in accordance with the CPTAC guidelines [42]. Three different standards with varying SIS2 (low: 0.26 fmol/µL, med: 8.0 fmol/µL, high: 26.0 fmol/µL) and constant SIS1 (0.5 fmol/µL) concentrations spiked-into a matrix of tissue digest were freshly prepared each day, for 5 different days (i.e. two different calendar days with samples prepared ≥16 h apart). Per standard (low/medium/high), three aliquots were analyzed in random order by LC-MRM and their normalized SIS2 peak areas were compared. The average intra-day assay %CVs were 2.6% (low), 1.9% (medium), and 4.8% (high). Inter-assay variabilities over 5 days were determined as 14.1% (low), 14.5% (medium),

and 15.4% (high), respectively, yielding a total variability of 14.3% for the low, 14.6% for the medium, and 16.1% for the high SIS2 concentrations (Figure 2b).

To assess the selectivity of our LC-MRM assay in accordance with CPTAC guidelines, we used six biological matrix replicates spiked with 0, 40, and 80 fmol of SIS2 and 10 fmol of SIS1 in 10 µg of total protein digest. The total %CVs were 9.5% and 6.7% for the 40 and 80 fmol samples, respectively (Figure S1b, Appendix II). The results from duplicate injections for each sample were averaged and were plotted on the linear scale for each biological replicate, and the slopes of the resulting lines for all biological replicates were less than 4.8% away from the mean of all slopes (Figure S1c, Appendix II).

LC-MRM alone is not sufficiently sensitive to quantify PTEN in tissue samples.

Having validated our PTEN LC-MRM assay, we analyzed a set of seven different cell lines to determine their endogenous PTEN levels, but despite the high sensitivity of our assay all endogenous PTEN levels were below both the LLOQ and even the LLOD (data not shown). These results indicate that a direct quantitation of PTEN from cell or tissue lysate is likely not feasible, in particular because PTEN protein levels are expected to inversely correlate with disease severity.

Immuno-MRM boosts the sensitivity of PTEN quantitation and shows high accuracy.

We decided to generate an anti-peptide antibody targeted against our proteotypic PTEN peptide NNIDDVVR, in order to develop an immuno-mass spectrometry assay with superior sensitivity, as we have previously done to quantify other cancer signaling proteins, such as AKT1, AKT2[48], and PI3K [49], by immuno-MALDI mass spectrometry.

To assess the recovery of the anti-NNIDDVVR immuno-enrichment step, three standards were prepared in quadruplicate with varying amounts of SIS2 (NNIDDVV**R**+10 Da) peptide: 0.15, 0.3, or 1.0 fmol/µL in 0.1 µg/µL matrix of tissue lysate digest. Three 10-µL aliquots of each standard were used for immuno-precipitation (IP) while the fourth aliquot was used as control (no IP). Immediately before LC-MRM injection, all IP and control samples were spiked with 40 fmol of SIS1 to be used as normalizer. The %recovery was determined to be 87, 91, and 94% for the 1.5, 3, and 10 fmol samples, respectively (Figure 2c), with an average recovery of 90%.

To assess the overall accuracy of the complete iMRM assay, we spiked four samples of 7.5 µg total protein lysate from a kidney-FFPE sample with 0, 1.5, 3, 10, 15, 45, or 100 fmol of

recPTEN. The corrected PTEN levels determined were 1.2, 2.9, 8.9, 12.6, 36.8, and 87.3 fmol resulting in accuracies of 83, 97, 89, 84, 82, and 87%, respectively (Figure 2d) with an average accuracy of 87%.

iMRM outperforms western blotting for quantifying PTEN in cell lines.

To test the efficacy of our PTEN iMRM assay, we quantified PTEN in different BC patient cell lines, three of which were HER2-positive and derived from either a patient's tumor (T670) or its PDXs (P129 and P132) (Figure 3b). We compared the iMRM PTEN levels obtained from a sample input of 20 µg of total protein with WB results obtained from 50 µg of total protein, with all WBs being performed on the same day, on the same gel, and by the same individual, to reduce technical variation. Notably, PTEN could be barely detected by WB in T670 (2% band intensity compared to the loading control in WB; 1.2 fmol/10 µg by iMRM), while P132 showed a moderate PTEN expression (38%; 3.8 fmol/10 µg), and P129 the highest (60%; 9.0 fmol/10 µg) PTEN expression (Figure 3). These results indicate that in the ideal and non-authentic 'standardized' situation, WB results correlate well with our iMRM assay (r^2=0.893; y=6.988x-0.510), while iMRM has the advantage of providing actual protein *concentrations* rather than arbitrary intensities from densitometric measurements. This is an important requirement to allow cross-laboratory comparisons of data. Interestingly, our data indicate a potential inverse correlation between PTEN iMRM expression levels and HER2-$Tyr^{1221/1222}$ phosphorylation (r^2=0.9597; y=-2.3489x–44.360), which is an established measure of HER2 receptor activity (Figure S2a, Appendix II)[50]. This inverse correlation needs to be further investigated on a larger scale, together with total HER2 protein levels to evaluate whether PTEN concentration, as determined by iMRM, may be used as predictive biomarker for anti-HER2 therapy. The activation status of phospho-HER2 is commonly used as an indicator of the activity of the PI3K/AKT/mTOR pathway and has been shown to potentially correlate with the response to trastuzumab [50]. Using IHC, no correlation has been observed between PTEN and phosho-HER2 in HER2-positive early-stage BC patients treated with adjuvant chemotherapy or trastuzumab [50], which may be a consequence of the aforementioned limitations inherent in IHC. Notably, our method allowed PTEN quantitation from20 µg of total protein in T670, while WB on 50 µg of total protein did not yield any PTEN-band for T670 (Figure 3a and 3b).

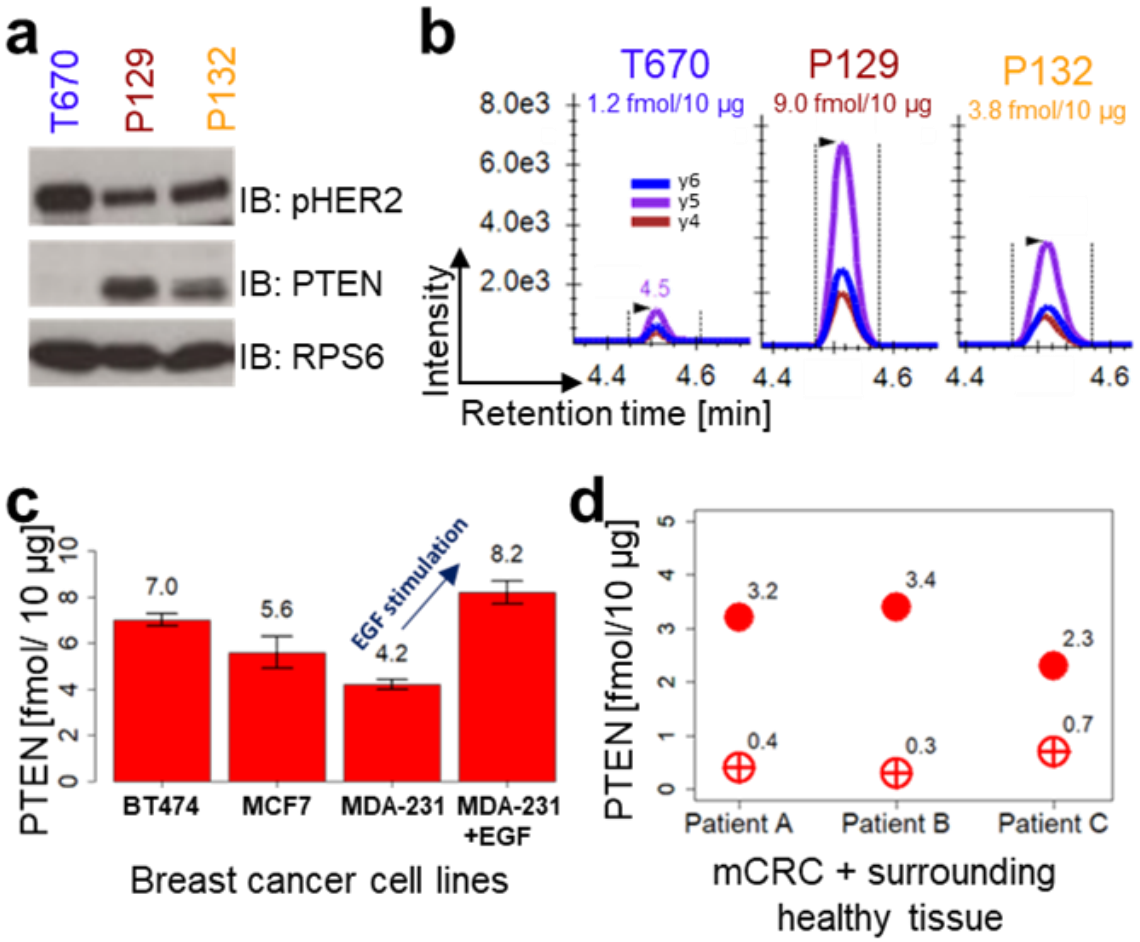

Figure 3. PTEN protein expression levels determined in BC cell lines and tissues. (a) WB analysis of HER2-positive cell lines derived from a patient tumor (T670) or PDXs thereof (P129, P132). Absent (T760), high (P129), and moderate (P132) levels of PTEN inversely correlate with the levels of phosphorylated HER2 (pHER2$^{Tyr1221/1222}$). RPS6=loading control. The original WB is available at Figure S3a, Appendix II. (b) iMRM signals and concentrations of endogenous PTEN in the same cell lines. Notably, T670 PTEN can be quantified as 1.2 fmol/10 µg by iMRM, despite using lower protein input (20 µg for iMRM vs. 50 µg for WB). (c) PTEN concentrations determined by iMRM in commercial cell lines of different BC subtypes, luminal B (BT474), luminal A (MCF7), triple negative basal (MDA-231), and EGF-treated MDA-231 (MDA-231+EGF). (d) PTEN levels determined in mCRC (⊕) and surrounding liver tissue (●) from three different patients. PTEN concentrations in all mCRC samples were considerably below that of T670 cells, which were PTEN-negative according to WB.

We next analyzed, in triplicate, three commercially available cell lines representing different BC subtypes, luminal B BT474, luminal A MCF7, triple negative basal MDA-MB-231 (MDA-231), as well as EGF-stimulated MDA-231 (MDA-231+EGF) (Figure 3c). The average PTEN concentrations determined by iMRM were 7.0±0.3, 5.6±0.7, 4.2±0.2, and 8.2±0.5 fmol for BT474, MCF7, MDA-231, and MDA-231+EGF, respectively, with all %CVs below 6%. MDA-231+EGF showed an approximately 2-fold increase of PTEN compared to MDA-231, indicating an impact of EGF-treatment in augmenting PTEN expression. The small difference in PTEN

expression that we observed between BT474 (7.0 fmol/10 µg) and MCF7 (5.6 fmol/10 µg) agrees well with data from Pfeiler et al., who determined their relative PTEN expression by WB [51]. Interestingly, the authors also reported a stronger response to trastuzumab and to the EGFR-inhibitor ZD1839 in BT-474 cells compared to MCF7 cells, while both cell lines showed approximately the same response to 4-OH tamoxifen [51]. In contrast, Mittendorf et al. reported higher PTEN expression in MCF7 rather than in BT474 cells, also using WB [52]. These conflicting results document the limitations and the lack of standardization of WB, which cannot provide intra- and inter-laboratory reproducibility, in contrast to iMRM as we have demonstrated here. Guaranteeing a high and, most importantly, a known level of reproducibility is essential for any meta-analysis study.

PTEN iMRM determines the difference of PTEN concentrations in tumor and healthy tissue samples.

We next evaluated the capacity of our iMRM assay to quantify PTEN levels in actual tumor tissues. We, therefore, analyzed mCRC and surrounding tissues from three different patients. PTEN concentrations in the three tumors were 0.4, 0.3, and 0.7 fmol/10 µg of total protein, while the matched surrounding liver tissues showed significantly higher concentrations of 3.2, 3.4, and 2.3 fmol/10 µg, corresponding to an 8-, 11-, and 3-fold downregulation of PTEN in tumor tissue, respectively (Figure 3d). PTEN expression estimated from proteome-wide analyses was almost identical, 3.91 (for normal colon) and 3.78 (for normal liver) according to ProteomicsDB data [53], clearly confirming that the difference in PTEN expression between mCRC and surrounding liver tissue observed by our iMRM method is indeed related to the tumorigenic downregulation of PTEN rather than to tissue-specific differences in PTEN expression.

Absolute iMRM PTEN levels correlate with relative WB data in fresh frozen PDX tissue samples.

To show the capacity of our assay to better discriminate BC patients according to different PTEN protein levels, we decided to apply PTEN iMRM to samples where a higher variability of PTEN expression can be expected. Therefore, we analyzed samples derived from HER2+ BC PDX models (13 samples in triplicate), including biological replicates.

Three pieces of 0.5 mm thickness were cut from each PDX sample, embedded in OCT and for each PDX sample the piece with the best viable tumor content (>70% based on H&E staining) was selected for analysis by both PTEN WB and PTEN iMRM (Figure 4a). All PTEN WB

analyses were performed on the same day, on the same gel, and by the same individual to minimize the inherently high variation of WB analysis. Relative band densities were normalized to the lowest band intensity (sample P2b) and correlate well with actual PTEN concentrations (fmol/10 µg) determined by iMRM (r^2=0.728; y=1.0769x+0.1878) (Figure 4b). iMRM results showed CVs from technical replicates ranging from 1.8% to 11.4%, while RSDs between biological replicates were 22.6% (P2a/b), 4.8% (P5a/b), 11.7% (P6a/b/c/d), and 4.6% (7a/b).

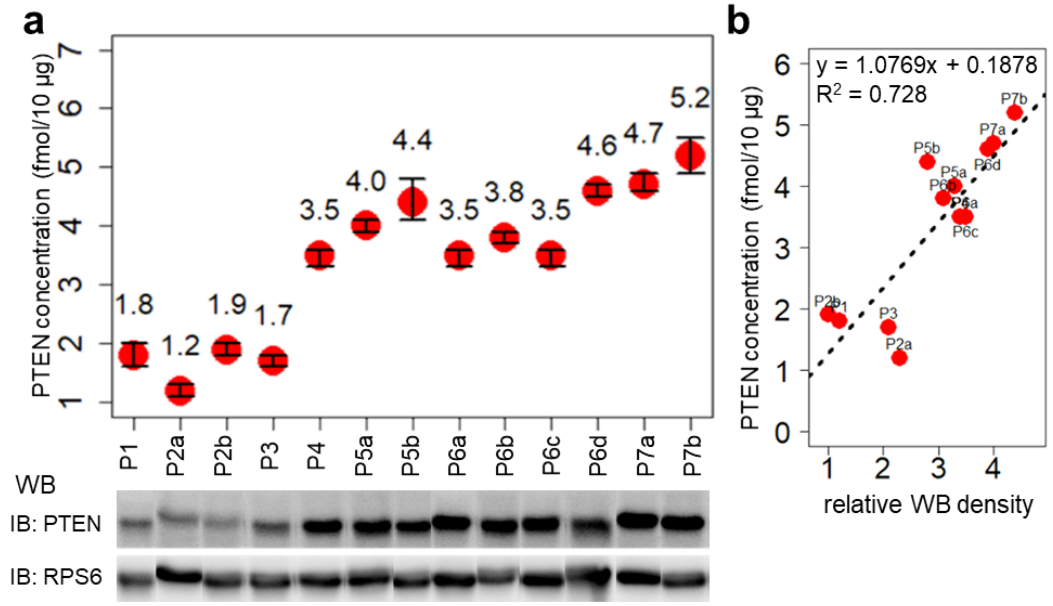

Figure 4. PTEN quantified by iMRM and WB in fresh frozen tissue samples of BC PDXs. (a) PTEN concentrations determined by iMRM (n=3) and the corresponding WB bands for PTEN and the loading control RPS6. (b) Good correlation between iMRM PTEN concentrations and relative PTEN WB density normalized to sample P2a. (r^2=0.728; y=1.0769x+0.1878). The original WB is available at Figure S3b, Appendix II.

Next, FFPE blocks of the 7 BC PDX samples were analyzed by PTEN IHC. To minimize the variability and subjectivity commonly associated with the interpretation of IHC data, the analysis was performed by a single experienced pathologist all at once. PTEN expression was scored semi-quantitatively from negative to high (-, +, ++, +++) to guide the punching of three cores from each FFPE block, which were analyzed as analytical replicates by PTEN-iMRM. iMRM PTEN concentrations were consistent *(i)* across biological replicates, P7a/b (5.7±0.1 fmol/10 µg total protein; Figure 5a), P5a/b (2.1±0.3), P6a/b/c/d (2.7±1.0 fmol/10 µg total protein; Figure S4, Appendix II), and P2a/b (0.7±0.0 fmol/10 µg total protein), *(ii)* across technical replicates with an average %CV of 24% for the three cores analyzed per PDX sample (Figure 5c), and *(iii)* generally showed the same trend as the IHC classification. Notably, not only did iMRM allow

the quantitation of PTEN in four samples that were IHC-negative (P1, P2a/b, P3), but, more importantly, differences between these samples could also be precisely determined, with P1 (0.1±0.01 fmol/10 µg total protein) showing a much lower PTEN concentration than P2a (0.7±0.3 fmol/10 µg total protein; Figure 5b), P2b (0.8±0.4 fmol/10 µg total protein) and P3 (0.9±0.2 fmol/10 µg total protein). These data underline the superior sensitivity and precision of the iMRM that allows, for the first time, the discrimination of subtle differences in absolute PTEN protein expression levels in a standardized manner, which is essential for enabling future inter-laboratory comparison studies.

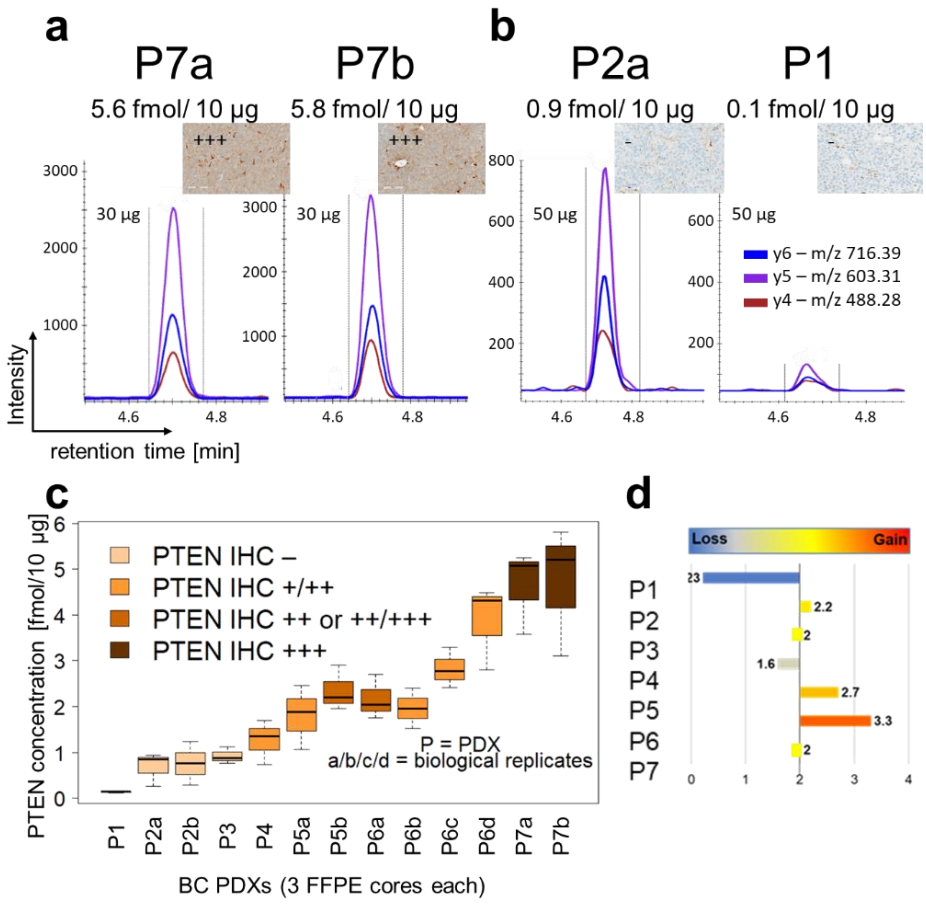

Figure 5. PTEN protein levels in FFPE PDX BC samples. Endogenous PTEN NNIDDVVR peptide signal acquired by iMRM and corresponding IHC classification from negative "-" to high "+++". (a) Biological replicates P7a/b with the highest PTEN levels for both iMRM and IHC. (b) While P2a and P1 were IHC-negative, PTEN was well-detected by iMRM with a 9-fold difference in concentration between both samples. (c) Correlation between iMRM PTEN concentrations and IHC classification. Box plots represent iMRM concentrations of three cores per sample, a vertical line goes through the box at the median and the whiskers go from each quartile to the minimum and the maximum. PTEN concentrations and box colours representing semi-quantitative IHC results (d) PTEN gene copy number determined from biological replicates of fresh frozen samples P1-7.

To evaluate how PTEN protein quantitation can complement genomic data, we analyzed copy number variations (CNVs) in biological replicates of our PDX samples by Cytoscan HD analysis. We observed 0.23 copies of the PTEN gene for P1, indicating a loss of PTEN gene (Figure 5d). Thus, the PTEN protein level determined by iMRM (0.1±0.01 fmol/10 µg total protein) may indeed reflect background levels of PTEN derived from mouse stromal cells where the target peptide has 100% sequence homology with the human sequence -- which underscores the high sensitivity of the assay. In general, the protein levels derived from IHC and iMRM PTEN (Figure 5c) do not agree well with PTEN CNVs (r^2=0.1498; y=0.5979x+0.457; Figure 5d; Figure S5a, Appendix II). For example, the PTEN protein concentration in P7 (4.7±0.9 fmol/10 µg total protein) differed substantially from the protein concentrations in P2a, P2b, and P3 (0.7-0.9 fmol/10 µg) even though all subjects had 2.0 copies of the PTEN gene, which indicates that neither a loss nor a gain of the PTEN gene occurred. On the other hand, PTEN concentrations in P4 (1.3±0.5 fmol/10 µg) and P6 (P6: 2.7±0.9 fmol/10 µg) showed some correlation with PTEN copy number (P4: 1.6; P6: 3.3). Since proteins are the major drug targets and aberrant pathway activity manifests on the protein level, these data clearly confirm the concept of proteogenomics, that genome-only analyses may often not be sufficient to capture the phenotype of a tumor and to make optimal treatment decisions [47].

We also analyzed FFPE cores and pieces of fresh frozen tissues that were obtained from the same BC PDX samples, and observed a good correlation of PTEN protein levels determined by iMRM in FFPE cores and matching fresh frozen tissue (r^2=0.7671; y=0.773x+1.6891; Figure S5b, Appendix II). We, however, observed differences in *absolute* concentrations between FFPE and fresh-frozen samples, which may be related to differences in their tumor content. The FFPE cores were punched from regions of interest that were mapped onto FFPE blocks [54], as guided by H&E and PTEN IHC results. In contrast, tumor sections/pieces often include tissue that is more heterogeneous in cell preservation and composition [54], even though sections of the fresh-frozen tissues were examined by H&E to assure >70% viable tumor content. The resulting variability in the content of non-viable or non-tumor tissue can severely impact the determined PTEN concentrations, in particular since PTEN protein expression is considerably higher in healthy tissue, as we demonstrated for mCRC and healthy surrounding tissues. Specifically, in samples with very low PTEN concentrations (P1-3), the tumor microenvironment and/or surrounding tissue (such as fat cells) can lead to increased levels of detected PTEN.

Conclusion

We developed and validated a new immuno-MRM method for the precise quantitation of the potential BC biomarker and main negative regulator of the PI3K/AKT/mTOR pathway, PTEN. Despite excellent performance metrics, a direct LC-MRM method targeting the proteotypic PTEN peptide NNIDDVVR lacked the required sensitivity to quantify PTEN in cells and tissues. Our LC-MRM method showed very good linearity over a very wide range of PTEN amounts on-column (0.27 to 270 fmol), with an LOD of 0.45 fmol, and an LLOQ of 0.9 fmol, as well as a high reproducibility with intra-day variations <5% and inter-day variations <15%, except for the highest tested PTEN level of 260 fmol with 16.1%.

To increase the sensitivity of our assay, we incorporated an anti-peptide immuno-enrichment step prior to the LC-MRM analysis, and we obtained an average NNIDDVVR peptide recovery in tumor tissue digest of 86.1%. We successfully applied our iMRM assay to quantify PTEN in different cell lines, fresh frozen tissues, and FFPE tissues. PTEN concentrations were consistent across biological replicates and were in a good agreement with both semi-quantitative IHC and WB results that were obtained under ideal conditions that are not achievable in clinical laboratories. Notably, iMRM allowed the quantitation and even the clear differentiation of PTEN levels across samples that were deemed to be PTEN-negative by both IHC and WB, even though smaller sample amounts were used for iMRM compared to WB.

The accuracy of an iMRM assay may be affected, e.g., by the selection of the tissue locus, protein extraction yields, digestion efficiency, and peptide binding capacity. Our results, however, show that different cores from the same block and even biological replicates (figure 5c) show a low variation in PTEN levels. Non-optimal protein extraction can be compensated for by normalization to total extracted protein, which is also more precise than measuring, e.g., tissue weight or volume, and the good correlation with orthogonal WB- and IHC-based PTEN quantitation emphasizes a good overall performance of the applied protocol. The chosen peptide NNIDDVVR has a predicted digestion efficiency of almost 100% for both termini and we could not observe missed- or mis-cleavages in our DDA data. Nevertheless, a sophisticated digestion control as reported by Burkhart et al. [55], the addition of MRM transitions for control proteins similar to loading controls in WB analyses, or the acquisition of MS1 survey scans in high resolution instrumentation for parallel reaction monitoring (PRM) will further increase the confidence for a high digestion efficiency. Notably, the target peptide NNIDDVVR could

undergo deamidation [56], for which we have not seen major evidence in our data. Finally, we used the exact same protocol (including a fixed amount of antibody) to enrich 1-200 fmol NAT PTEN with high precision, demonstrating a sufficient dynamic range of the reported protocol to analyze biological samples. Overloading of the antibody with target peptide can be, importantly, directly evidenced by decreased intensities of the SIS standards. Nevertheless, we strongly advise researchers to first test the approximate concentrations of a novel sample matrix, before adjusting the SIS levels or the sample input for the final assay

The PTEN protein levels determined by both IHC and iMRM do not correlate with PTEN copy number data, demonstrating the shortcomings of using the PTEN genotype to determine the tumor PTEN phenotype. In contrast, PTEN iMRM enabled the detection of differences in PTEN concentrations in clinical samples, thus paving the way to correlating these differences with individual patient responses to therapy. Our iMRM assay therefore fills the gap that currently prevents the evaluation of PTEN as a potential BC biomarker, not only for prognosis but also to guide precision oncology. In the future, we will apply PTEN iMRM to a larger cohort of BC patients to evaluate whether there is, indeed, a clinically significant correlation between PTEN protein concentration and a patient's prognosis and response to different therapeutics.

References

1. Bray, F.; Ferlay, J.; Soerjomataram, I.; Siegel, R. L.; Torre, L. A.; Jemal, A., Global cancer statistics 2018: GLOBOCAN estimates of incidence and mortality worldwide for 36 cancers in 185 countries. *CA Cancer J Clin* **2018,** *68* (6), 394-424.

2. Howlader N, N. A., Krapcho M, Miller D, Brest A, Yu M, Ruhl J, Tatalovich Z,; Mariotto A, L. D., Chen HS, Feuer EJ, Cronin KA (eds). SEER Cancer Statistics Review, 1975-2016, National Cancer Institute. **Posted to the SEER web site, April 2019.**

3. Mariotto, A. B.; Yabroff, K. R.; Shao, Y.; Feuer, E. J.; Brown, M. L., Projections of the cost of cancer care in the United States: 2010-2020. *J Natl Cancer Inst* **2011,** *103* (2), 117-28.

4. Bihani, T.; Patel, H. K.; Arlt, H.; Tao, N.; Jiang, H.; Brown, J. L.; Purandare, D. M.; Hattersley, G.; Garner, F., Elacestrant (RAD1901), a Selective Estrogen Receptor Degrader (SERD), Has Antitumor Activity in Multiple ER(+) Breast Cancer Patient-derived Xenograft Models. *Clin Cancer Res* **2017,** *23* (16), 4793-4804.

5. Batoo, S.; Bayraktar, S.; Al-Hattab, E.; Basu, S.; Okuno, S.; Gluck, S., Recent advances and optimal management of human epidermal growth factor receptor-2-positive early-stage breast cancer. *J Carcinog* **2019,** *18*, 5.

6. Kotecki, N.; Gombos, A.; Awada, A., Adjuvant therapeutic approaches of HER2-positive breast cancer with a focus on neratinib maleate. *Expert Rev Anticancer Ther* **2019,** *19* (6), 447-454.

7. Tutt, A.; Tovey, H.; Cheang, M. C. U.; Kernaghan, S.; Kilburn, L.; Gazinska, P.; Owen, J.; Abraham, J.; Barrett, S.; Barrett-Lee, P.; Brown, R.; Chan, S.; Dowsett, M.; Flanagan, J. M.; Fox, L.; Grigoriadis, A.; Gutin, A.; Harper-Wynne, C.; Hatton, M. Q.; Hoadley, K. A.; Parikh, J.; Parker, P.; Perou, C. M.; Roylance, R.; Shah, V.; Shaw, A.; Smith, I. E.; Timms, K. M.; Wardley, A. M.; Wilson, G.; Gillett, C.; Lanchbury, J. S.; Ashworth, A.; Rahman, N.; Harries, M.; Ellis, P.; Pinder, S. E.; Bliss, J. M., Carboplatin in BRCA1/2-mutated and triple-negative breast cancer BRCAness subgroups: the TNT Trial. *Nat Med* **2018,** *24* (5), 628-637.

8. Martin, H. L.; Smith, L.; Tomlinson, D. C., Multidrug-resistant breast cancer: current perspectives. *Breast Cancer (Dove Med Press)* **2014,** *6*, 1-13.

9. Li, G.; Guo, J.; Shen, B. Q.; Yadav, D. B.; Sliwkowski, M. X.; Crocker, L. M.; Lacap, J. A.; Phillips, G. D. L., Mechanisms of Acquired Resistance to Trastuzumab Emtansine in Breast Cancer Cells. *Mol Cancer Ther* **2018,** *17* (7), 1441-1453.

10. Ponde, N.; Brandao, M.; El-Hachem, G.; Werbrouck, E.; Piccart, M., Treatment of advanced HER2-positive breast cancer: 2018 and beyond. *Cancer Treat Rev* **2018,** *67*, 10-20.

11. Vasan, N.; Toska, E.; Scaltriti, M., Overview of the relevance of PI3K pathway in HR-positive breast cancer. *Ann Oncol* **2019,** *30 Suppl 10*, x3-x11.

12. Costa, R. L. B.; Han, H. S.; Gradishar, W. J., Targeting the PI3K/AKT/mTOR pathway in triple-negative breast cancer: a review. *Breast Cancer Res Treat* **2018,** *169* (3), 397-406.

13. Wisinski, K. B.; Tevaarwerk, A. J.; Burkard, M. E.; Rampurwala, M.; Eickhoff, J.; Bell, M. C.; Kolesar, J. M.; Flynn, C.; Liu, G., Phase I Study of an AKT Inhibitor (MK-2206) Combined with Lapatinib in Adult Solid Tumors Followed by Dose Expansion in Advanced HER2+ Breast Cancer. *Clin Cancer Res* **2016,** *22* (11), 2659-67.

14. Bazzichetto, C.; Conciatori, F.; Pallocca, M.; Falcone, I.; Fanciulli, M.; Cognetti, F.; Milella, M.; Ciuffreda, L., PTEN as a Prognostic/Predictive Biomarker in Cancer: An Unfulfilled Promise? *Cancers (Basel)* **2019,** *11* (4).

15. Malaney, P.; Uversky, V. N.; Dave, V., PTEN proteoforms in biology and disease. *Cell Mol Life Sci* **2017,** *74* (15), 2783-2794.

16. Luongo, F.; Colonna, F.; Calapa, F.; Vitale, S.; Fiori, M. E.; De Maria, R., PTEN Tumor-Suppressor: The Dam of Stemness in Cancer. *Cancers (Basel)* **2019,** *11* (8).

17. Berger, A. H.; Knudson, A. G.; Pandolfi, P. P., A continuum model for tumor suppression. *Nature* **2011,** *476* (7359), 163-9.

18. Alimonti, A.; Carracedo, A.; Clohessy, J. G.; Trotman, L. C.; Nardella, C.; Egia, A.; Salmena, L.; Sampieri, K.; Haveman, W. J.; Brogi, E.; Richardson, A. L.; Zhang, J.; Pandolfi, P. P., Subtle variations in Pten dose determine cancer susceptibility. *Nat Genet* **2010,** *42* (5), 454-8.

19. Zhang, H. Y.; Liang, F.; Jia, Z. L.; Song, S. T.; Jiang, Z. F., PTEN mutation, methylation and expression in breast cancer patients. *Oncol Lett* **2013,** *6* (1), 161-168.

20. Wang, L. L.; Hao, S.; Zhang, S.; Guo, L. J.; Hu, C. Y.; Zhang, G.; Gao, B.; Zhao, J. J.; Jiang, Y.; Tian, W. G.; Wang, J.; Luo, D. L., PTEN/PI3K/AKT protein expression is related to clinicopathological features and prognosis in breast cancer with axillary lymph node metastases. *Hum Pathol* **2017,** *61*, 49-57.

21. Phuong, N. T.; Kim, S. K.; Lim, S. C.; Kim, H. S.; Kim, T. H.; Lee, K. Y.; Ahn, S. G.; Yoon, J. H.; Kang, K. W., Role of PTEN promoter methylation in tamoxifen-resistant breast cancer cells. *Breast Cancer Res Treat* **2011,** *130* (1), 73-83.

22. Rimawi, M. F.; De Angelis, C.; Contreras, A.; Pareja, F.; Geyer, F. C.; Burke, K. A.; Herrera, S.; Wang, T.; Mayer, I. A.; Forero, A.; Nanda, R.; Goetz, M. P.; Chang, J. C.; Krop, I. E.; Wolff, A. C.; Pavlick, A. C.; Fuqua, S. A. W.; Gutierrez, C.; Hilsenbeck, S. G.; Li, M. M.; Weigelt, B.; Reis-Filho, J. S.; Kent Osborne, C.; Schiff, R., Low PTEN levels and PIK3CA mutations predict resistance to neoadjuvant lapatinib and trastuzumab without chemotherapy in patients with HER2 over-expressing breast cancer. *Breast Cancer Res Treat* **2018,** *167* (3), 731-740.

23. Loibl, S.; Darb-Esfahani, S.; Huober, J.; Klimowicz, A.; Furlanetto, J.; Lederer, B.; Hartmann, A.; Eidtmann, H.; Pfitzner, B.; Fasching, P. A.; Tiemann, K.; Jackisch, C.; Mehta, K.; von Minckwitz, G.; Untch, M.; Denkert, C., Integrated Analysis of PTEN and p4EBP1 Protein Expression as Predictors for pCR in HER2-Positive Breast Cancer. *Clin Cancer Res* **2016,** *22* (11), 2675-83.

24. Jones, R. H.; Casbard, A.; Carucci, M.; Cox, C.; Butler, R.; Alchami, F.; Madden, T. A.; Bale, C.; Bezecny, P.; Joffe, J.; Moon, S.; Twelves, C.; Venkitaraman, R.; Waters, S.;

Foxley, A.; Howell, S. J., Fulvestrant plus capivasertib versus placebo after relapse or progression on an aromatase inhibitor in metastatic, oestrogen receptor-positive breast cancer (FAKTION): a multicentre, randomised, controlled, phase 2 trial. *Lancet Oncol* **2020,** *21* (3), 345-357.

25. Juric, D.; Castel, P.; Griffith, M.; Griffith, O. L.; Won, H. H.; Ellis, H.; Ebbesen, S. H.; Ainscough, B. J.; Ramu, A.; Iyer, G.; Shah, R. H.; Huynh, T.; Mino-Kenudson, M.; Sgroi, D.; Isakoff, S.; Thabet, A.; Elamine, L.; Solit, D. B.; Lowe, S. W.; Quadt, C.; Peters, M.; Derti, A.; Schegel, R.; Huang, A.; Mardis, E. R.; Berger, M. F.; Baselga, J.; Scaltriti, M., Convergent loss of PTEN leads to clinical resistance to a PI(3)Kalpha inhibitor. *Nature* **2015,** *518* (7538), 240-4.

26. Andre, F.; Hurvitz, S.; Fasolo, A.; Tseng, L. M.; Jerusalem, G.; Wilks, S.; O'Regan, R.; Isaacs, C.; Toi, M.; Burris, H.; He, W.; Robinson, D.; Riester, M.; Taran, T.; Chen, D.; Slamon, D., Molecular Alterations and Everolimus Efficacy in Human Epidermal Growth Factor Receptor 2-Overexpressing Metastatic Breast Cancers: Combined Exploratory Biomarker Analysis From BOLERO-1 and BOLERO-3. *J Clin Oncol* **2016,** *34* (18), 2115-24.

27. Oliveira, M.; Saura, C.; Nuciforo, P.; Calvo, I.; Andersen, J.; Passos-Coelho, J. L.; Gil Gil, M.; Bermejo, B.; Patt, D. A.; Ciruelos, E.; de la Pena, L.; Xu, N.; Wongchenko, M.; Shi, Z.; Singel, S. M.; Isakoff, S. J., FAIRLANE, a double-blind placebo-controlled randomized phase II trial of neoadjuvant ipatasertib plus paclitaxel for early triple-negative breast cancer. *Ann Oncol* **2019,** *30* (8), 1289-1297.

28. Perez, E. A.; Dueck, A. C.; McCullough, A. E.; Chen, B.; Geiger, X. J.; Jenkins, R. B.; Lingle, W. L.; Davidson, N. E.; Martino, S.; Kaufman, P. A.; Kutteh, L. A.; Sledge, G. W.; Harris, L. N.; Gralow, J. R.; Reinholz, M. M., Impact of PTEN protein expression on benefit from adjuvant trastuzumab in early-stage human epidermal growth factor receptor 2-positive breast cancer in the North Central Cancer Treatment Group N9831 trial. *J Clin Oncol* **2013,** *31* (17), 2115-22.

29. Nuciforo, P. G.; Aura, C.; Holmes, E.; Prudkin, L.; Jimenez, J.; Martinez, P.; Ameels, H.; de la Pena, L.; Ellis, C.; Eidtmann, H.; Piccart-Gebhart, M. J.; Scaltriti, M.; Baselga, J., Benefit to neoadjuvant anti-human epidermal growth factor receptor 2 (HER2)-targeted therapies in HER2-positive primary breast cancer is independent of phosphatase and tensin homolog deleted from chromosome 10 (PTEN) status. *Ann Oncol* **2015,** *26* (7), 1494-500.

30. Kim, S. B.; Wildiers, H.; Krop, I. E.; Smitt, M.; Yu, R.; Lysbet de Haas, S.; Gonzalez-Martin, A., Relationship between tumor biomarkers and efficacy in TH3RESA, a phase III study of trastuzumab emtansine (T-DM1) vs. treatment of physician's choice in previously treated HER2-positive advanced breast cancer. *Int J Cancer* **2016,** *139* (10), 2336-42.

31. Carbognin, L.; Miglietta, F.; Paris, I.; Dieci, M. V., Prognostic and Predictive Implications of PTEN in Breast Cancer: Unfulfilled Promises but Intriguing Perspectives. *Cancers (Basel)* **2019,** *11* (9).

32. Hoofnagle, A. N.; Wener, M. H., The fundamental flaws of immunoassays and potential solutions using tandem mass spectrometry. *J Immunol Methods* **2009,** *347* (1-2), 3-11.

33. Saper, C. B., A guide to the perplexed on the specificity of antibodies. *J Histochem Cytochem* **2009,** *57* (1), 1-5.

34. Mnatsakanyan, R.; Shema, G.; Basik, M.; Batist, G.; Borchers, C. H.; Sickmann, A.; Zahedi, R. P., Detecting post-translational modification signatures as potential biomarkers in clinical mass spectrometry. *Expert Rev Proteomics* **2018,** *15* (6), 515-535.

35. Popp, R.; Basik, M.; Spatz, A.; Batist, G.; Zahedi, R. P.; Borchers, C. H., How iMALDI can improve clinical diagnostics. *Analyst* **2018,** *143* (10), 2197-2203.

36. Hocking, C.; Hardingham, J. E.; Broadbridge, V.; Wrin, J.; Townsend, A. R.; Tebbutt, N.; Cooper, J.; Ruszkiewicz, A.; Lee, C.; Price, T. J., Can we accurately report PTEN status in advanced colorectal cancer? *BMC Cancer* **2014,** *14*, 128.

37. Aebersold, R.; Burlingame, A. L.; Bradshaw, R. A., Western blots versus selected reaction monitoring assays: time to turn the tables? *Mol Cell Proteomics* **2013,** *12* (9), 2381-2.

38. Butler, T. A. J.; Paul, J. W.; Chan, E. C.; Smith, R.; Tolosa, J. M., Misleading Westerns: Common Quantification Mistakes in Western Blot Densitometry and Proposed Corrective Measures. *Biomed Res Int* **2019,** *2019*, 5214821.

39. Byron, A., Reproducibility and Crossplatform Validation of Reverse-Phase Protein Array Data. *Adv Exp Med Biol* **2019,** *1188*, 181-201.

40. Sobsey, C. A.; Ibrahim, S.; Richard, V. R.; Gaspar, V.; Mitsa, G.; Lacasse, V.; Zahedi, R. P.; Batist, G.; Borchers, C. H., Targeted and Untargeted Proteomics Approaches in Biomarker Development. *Proteomics* **2019**, e1900029.

41. Fredolini, C.; Bystrom, S.; Pin, E.; Edfors, F.; Tamburro, D.; Iglesias, M. J.; Haggmark, A.; Hong, M. G.; Uhlen, M.; Nilsson, P.; Schwenk, J. M., Immunocapture strategies in translational proteomics. *Expert Rev Proteomics* **2016,** *13* (1), 83-98.

42. Whiteaker, J. R.; Halusa, G. N.; Hoofnagle, A. N.; Sharma, V.; MacLean, B.; Yan, P.; Wrobel, J. A.; Kennedy, J.; Mani, D. R.; Zimmerman, L. J.; Meyer, M. R.; Mesri, M.; Rodriguez, H.; Clinical Proteomic Tumor Analysis, C.; Paulovich, A. G., CPTAC Assay Portal: a repository of targeted proteomic assays. *Nat Methods* **2014,** *11* (7), 703-4.

43. Zhang, B.; Whiteaker, J. R.; Hoofnagle, A. N.; Baird, G. S.; Rodland, K. D.; Paulovich, A. G., Clinical potential of mass spectrometry-based proteogenomics. *Nat Rev Clin Oncol* **2019,** *16* (4), 256-268.

44. Ibrahim, S.; Froehlich, B. C.; Aguilar-Mahecha, A.; Aloyz, R.; Poetz, O.; Basik, M.; Batist, G.; Zahedi, R. P.; Borchers, C. H., Using Two Peptide Isotopologues as Internal Standards for the Streamlined Quantification of Low-Abundance Proteins by Immuno-MRM and Immuno-MALDI. *Anal Chem* **2020,** *92* (18), 12407-12414.

45. Percy, A. J.; Chambers, A. G.; Yang, J.; Domanski, D.; Borchers, C. H., Comparison of standard- and nano-flow liquid chromatography platforms for MRM-based quantitation of putative plasma biomarker proteins. *Anal Bioanal Chem* **2012,** *404* (4), 1089-101.

46. Mohammed, Y.; Domanski, D.; Jackson, A. M.; Smith, D. S.; Deelder, A. M.; Palmblad, M.; Borchers, C. H., PeptidePicker: a scientific workflow with web interface for

selecting appropriate peptides for targeted proteomics experiments. *J Proteomics* **2014,** *106*, 151-61.

47. Zhang, B.; Wang, J.; Wang, X.; Zhu, J.; Liu, Q.; Shi, Z.; Chambers, M. C.; Zimmerman, L. J.; Shaddox, K. F.; Kim, S.; Davies, S. R.; Wang, S.; Wang, P.; Kinsinger, C. R.; Rivers, R. C.; Rodriguez, H.; Townsend, R. R.; Ellis, M. J.; Carr, S. A.; Tabb, D. L.; Coffey, R. J.; Slebos, R. J.; Liebler, D. C.; Nci, C., Proteogenomic characterization of human colon and rectal cancer. *Nature* **2014,** *513* (7518), 382-7.

48. Popp, R.; Li, H.; LeBlanc, A.; Mohammed, Y.; Aguilar-Mahecha, A.; Chambers, A. G.; Lan, C.; Poetz, O.; Basik, M.; Batist, G.; Borchers, C. H., Immuno-Matrix-Assisted Laser Desorption/Ionization Assays for Quantifying AKT1 and AKT2 in Breast and Colorectal Cancer Cell Lines and Tumors. *Anal Chem* **2017,** *89* (19), 10592-10600.

49. Froehlich, B. C.; Popp, R.; Sobsey, C. A.; Ibrahim, S.; LeBlanc, A. M.; Mohammed, Y.; Aguilar-Mahecha, A.; Poetz, O.; Chen, M. X.; Spatz, A.; Basik, M.; Batist, G.; Zahedi, R. P.; Borchers, C. H., Systematic Optimization of the iMALDI Workflow for the Robust and Straightforward Quantification of Signaling Proteins in Cancer Cells. *Proteomics Clin Appl* **2020,** *14* (5), e2000034.

50. Jensen, J. D.; Knoop, A.; Laenkholm, A. V.; Grauslund, M.; Jensen, M. B.; Santoni-Rugiu, E.; Andersson, M.; Ewertz, M., PIK3CA mutations, PTEN, and pHER2 expression and impact on outcome in HER2-positive early-stage breast cancer patients treated with adjuvant chemotherapy and trastuzumab. *Ann Oncol* **2012,** *23* (8), 2034-42.

51. Pfeiler, G.; Horn, F.; Lattrich, C.; Klappenberger, S.; Ortmann, O.; Treeck, O., Apoptotic effects of signal transduction inhibitors on human tumor cells with different PTEN expression. *Oncol Rep* **2007,** *18* (5), 1305-9.

52. Mittendorf, E. A.; Philips, A. V.; Meric-Bernstam, F.; Qiao, N.; Wu, Y.; Harrington, S.; Su, X.; Wang, Y.; Gonzalez-Angulo, A. M.; Akcakanat, A.; Chawla, A.; Curran, M.; Hwu, P.; Sharma, P.; Litton, J. K.; Molldrem, J. J.; Alatrash, G., PD-L1 expression in triple-negative breast cancer. *Cancer Immunol Res* **2014,** *2* (4), 361-70.

53. Schmidt, T.; Samaras, P.; Frejno, M.; Gessulat, S.; Barnert, M.; Kienegger, H.; Krcmar, H.; Schlegl, J.; Ehrlich, H. C.; Aiche, S.; Kuster, B.; Wilhelm, M., ProteomicsDB. *Nucleic Acids Res* **2018,** *46* (D1), D1271-D1281.

54. Patel, P. G.; Selvarajah, S.; Boursalie, S.; How, N. E.; Ejdelman, J.; Guerard, K. P.; Bartlett, J. M.; Lapointe, J.; Park, P. C.; Okello, J. B.; Berman, D. M., Preparation of Formalin-fixed Paraffin-embedded Tissue Cores for both RNA and DNA Extraction. *J Vis Exp* **2016,** (114).

55. Burkhart, J. M.; Schumbrutzki, C.; Wortelkamp, S.; Sickmann, A.; Zahedi, R. P., Systematic and quantitative comparison of digest efficiency and specificity reveals the impact of trypsin quality on MS-based proteomics. *J Proteomics* **2012,** *75* (4), 1454-62.

56. Mikkat, S.; Kischstein, T.; Kreutzer, M.; Glocker, M. O., Mass spectrometric peptide analysis of 2DE-separated mouse spinal cord and rat hippocampus proteins suggests an NGxG motif of importance for in vivo deamidation. *Electrophoresis* **2013,** *34* (11), 1610-8.

In the third manuscript, I used the PTEN iMRM assay to analyze several fresh frozen tissue samples of patients with colorectal cancer, hepatocellular carcinoma and different benign hepatic disorders where PTEN protein have been demonstrated to be a promising biomarker candidate. As I found a high variation of PTEN levels, precise PTEN quantitation with our iMRM assay will allow a better patient stratification in these disorders/cancers, and hence will help providing more accurately personalized care to patients

PTEN quantitation by immuno-MRM and patient stratification in several cancers/diseases.

Sahar Ibrahim[1,2,3], Marguerite Buchanan[4], Adriana Aguilar-Mahecha[4], Alan Spatz[1,4,5,6], Mark Basik[1,4,7], Gerald Batist[1,4,7], René P. Zahedi[3,8], Christoph H. Borchers[3,7,8*].

[1] Division of Experimental Medicine, McGill University, Montréal, Québec, Canada.

[2] Clinical Pathology Department, National Liver Institute, Menoufia University, Egypt.

[3] Segal Cancer Proteomics Centre, Lady Davis Institute for Medical Research, Jewish General Hospital, McGill University, Montréal, Québec, Canada.

[4] Segal Cancer Center, Lady Davis Institute for Medical Research, Jewish General Hospital, McGill University, Montréal, Québec, Canada.

[5] Department of Pathology, McGill University, Montréal, Québec, Canada.

[6] Division of Pathology, Department of Laboratory Medicine, McGill University Health Centre, Montréal, Québec, Canada.

[7] Gerald Bronfman Department of Oncology, Jewish General Hospital, McGill University, Montréal, Québec, Canada.

[8] Center for Computational and Data-Intensive Science and Engineering, Skolkovo Institute of Science and Technology, Moscow, Russia).

Introduction

Phosphatase and Tensin Homolog deleted on Chromosome 10 (PTEN) is a dual phosphatase with both protein and lipid phosphatase activities. For instance, PTEN dephosphorylates phosphatidylinositol-3, 4, 5-phosphate (PIP_3) which is a critical second messenger mediating the signal of several growth factors. PIP_3-dephosphorylation established PTEN as the main negative regulator of the PI3K/AKT pathway and as a tumor suppressor with growth and survival regulatory functions (see Figure 1). In recent years, two other functions of PTEN have attracted significant attention: its roles in maintaining chromosomal stability and in metabolic regulation. Nuclear PTEN is involved in a variety of processes, including maintenance of the heterochromatin structure and genome stability, DNA repair, cell-cycle control, gene expression, and DNA replication [1, 2]. Through both a PI3K/AKT pathway-dependent and in an independent manner, PTEN has been found to be involved in the regulation of several aspects of metabolism as well as mitochondrial energy production [3]. The underlying mechanisms of these functions of PTEN, as well as their physiological and pathological impact, are still being studied. Importantly, these novel functions of PTEN have shed a light on the close relationship between downregulated PTEN expression levels and the occurrence and severity of several benign and malignant disorders. Indeed, in PTEN deficient disorders/ tumors, no other biomarkers in the PI3K/AKT pathway (such as phospho-AKT) can predict or precisely correlate with the various effects of PTEN deficiency [4].

With regard to PTEN's nuclear functions, in some cancer subtypes, PTEN deficiency has been found to be associated with the loss of expression of mismatch repair (MMR) proteins and thus microsatellite instability (MSI) [5, 6]. DNA MMR is a highly conserved process, involved in restoring DNA integrity after the occurrence of mismatch errors during DNA replication, recombination, or iatrogenic damage. The MMR mechanism is highly regulated and is maintained by four proteins: mutL homologue 1 (MLH1), mutS homologue 2 (MSH2), mutS homologue 6 (MSH6), and postmeiotic segregation increased 2 (PMS2). The absence or dysfunction of one or more of these proteins is defined as deficient MMR (dMMR) -- otherwise it is considered to be proficient MMR (pMMR). dMMR can be clinically determined using immunohistochemistry (IHC) analysis of the previously mentioned proteins or by detecting MSI. Microsatellites are repetitive DNA sequences with a unit length ranging from one to six bases distributed along both coding and noncoding regions of the genome. They are highly

polymorphic among subjects but are stable in each individual. The repetitive nature of these regions makes them particularly sensitive to mismatch errors. An accumulation of mutations in these repeats is referred to as microsatellite instability-High (MSI-H), which can be determined by the analysis of polyA microsatellites. Thus, MSI is a marker of dMMR and is a characteristic of a hypermutable cellular state. Up to 15% of sporadic colon cancers show dMMR/MSI-H which has been found to be associated with poor differentiation, BRAF V600E mutation, and poor survival in metastatic CRC [7]. Recently, dMMR/MSI-H tumors, irrespective of cancer type, were found to be more sensitive to immune checkpoint inhibitors (CPIs) , many of which are already in clinical trials, particularly PD-1 and PD-L1 inhibitors, [8 9, 10]. Several studies have shed light on the correlation between the dMMR/MSI-H tumors and loss of PTEN expression, for example, in breast cancer, endometrial carcinoma, and colorectal cancer [6, 11]. Moreover, several studies have shown that cancer cell intrinsic PD-L1 expression in breast cancer and colorectal cancer increases as a result of PTEN-loss [12, 13]. Lopez et al., have proposed a novel diagnostic algorithm where PTEN expression analysis can be employed to identify pMMR breast cancers [6]. All these findings suggest that PTEN expression analysis should be useful for better stratifying breast cancer and colon cancer patients, for example, according to the tumor mutational burden and for selecting the patients who would respond to immune CPIs.

Many recent studies have focused on the role of PTEN and PTEN-regulated signals in metabolic regulation. This includes the role of PTEN in glycolysis, gluconeogenesis, glycogen synthesis, and lipid metabolism, as well as mitochondrial metabolism [3] (see Figure 1), which make the PTEN status an important effector not only in many metabolic disorders but in cancers as well. Cancer cells preferentially consume glucose and glutamine to fuel uncontrolled cell proliferation and they process intermediate metabolites for lipid and protein synthesis, which drives tumorigenesis [14]. Metabolic reprogramming is a hallmark of tumor cells, being highly important in certain subtypes such as liver-cancer cells, where energetic metabolism shifts from oxidative phosphorylation to aerobic glycolysis, i.e., the Warburg effect. This metabolic rewiring plays an important role in the maintenance of malignancies by conferring tumor cells advantages of proliferation and survival [15]. Through both PI3K/AKT pathway-dependent and independent ways, PTEN provides tumor suppression by opposing the Warburg effect, and PTEN-deficient tumors manifest a glycolytic phenotype [16]. Recently, Qian et al., have found that PTEN directly interacts with and dephosphorylates phosphoglycerate kinase 1 (PGK1), thus inhibiting

glycolysis [17], while, in mitochondria, the PTENα isoform induces cytochrome c oxidase activity and ATP production [18]. In addition, PTEN inhibits lipogenesis while induces gluconeogenesis and triglyceride metabolism [19]. Therefore, PTEN plays a critical role in both glucose and lipid metabolism where PTEN downregulation was found to induce hepatic insulin resistance, steatosis, steatohepatitis, and hepatocellular carcinoma [20]. Moreover, hepatic PTEN expression is altered in liver diseases associated with obesity, metabolic syndrome, viral infection, and alcohol consumption. In these hepatic disorders, PTEN regulation and its pro-apoptotic ability are altered and this, in turn, enhances the process of tumor formation. In other words, PTEN expression affects the prognosis of these hepatic disorders and their progression into liver cancer. In this regard, it is now clear that -- instead of mutations or deletions -- dysregulations of PTEN expression by a wide variety of mechanisms, including the action of metabolic factors, toxins, or viral components, is plays a crucial role in the development and/or progression of multiple types of hepatic dysfunction, uncontrolled hepatocyte proliferation, and cancer development. Therefore, my PTEN iMRM assay -- presented in Chapter 2 as a robust tool to quantify and study PTEN in breast cancer -- can be used for the study of hepatic disorders and hepatocellular carcinoma (HCC) as well as metastatic colorectal cancer in liver. Thus, this assay can be used on patient samples to study the PTEN levels associated with in these disorders and to determine variations in PTEN levels among patients and, possibly, to obtain prognostic read-outs.

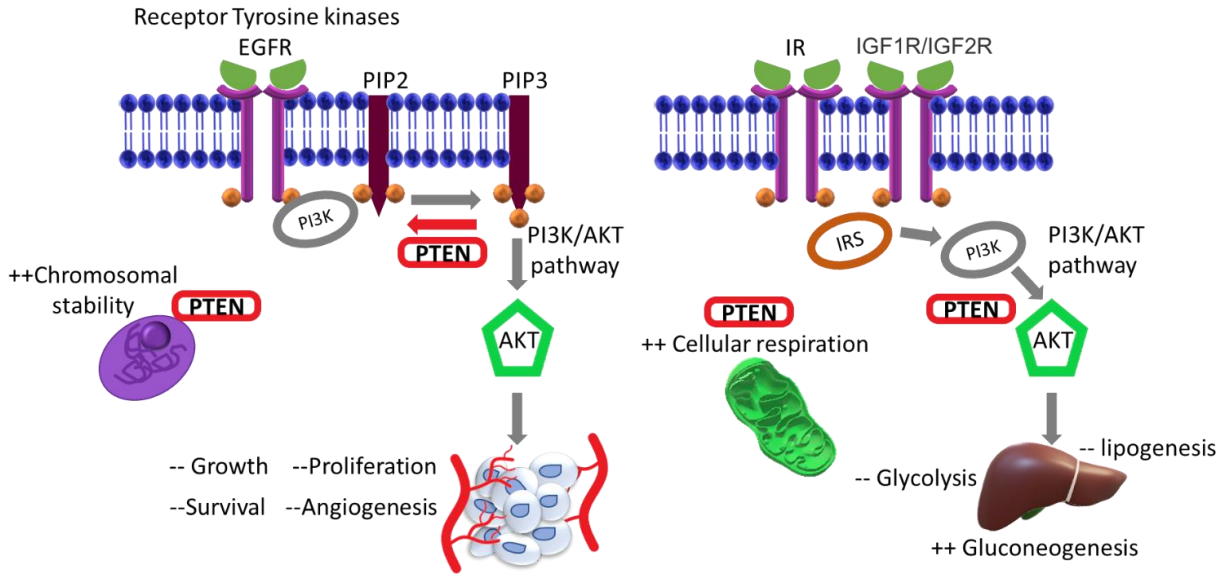

Figure 1. The functions of the tumor suppressor PTEN, both dependent and independent of the PI3K/AKT pathway. EGFR: epidermal growth factor receptor, IR: insulin receptor, IGF1R: insulin like growth factor 1 receptor.

Experimental Procedures

Reagents: see Appendix II for a summary of the reagents used.

Clinical samples:

Fresh-frozen tissue samples were collected from patients with hepatic metastases of colorectal cancer (mCRC), hepatocellular carcinoma and hepatic benign disorders (See Table 1). The patients were recruited at the Jewish General Hospital (JGH; Montreal, QC) and provided informed consent for participation in the JGH central biobank, protocol 10-153, which was reviewed and approved by the local Research Ethics Board (REB). The JGH biobank is affiliated with the Réseau de recherche sur le cancer (RRCancer) of the Fonds de recherche du Québec – Santé (FRQS) and with the Canadian Tumor Repository Network (CTRNet).

Embedding of PDX-derived Fresh Frozen tissue samples embedded in Optimal cutting temperature (OCT) compound:

A small piece of tissue (approximately 0.5 cm^3) was cut from each patient's sample on a sterile agar plate placed over dry ice and the pieces were transferred to labeled cryomolds and carefully covered with cryogel, OCT, snap-frozen in isopentane (2-Methylbutane Millipore)/dry ice (-60 to -70°C), and then transferred to a −80 °C freezer.

Cryosections of tissues were made with a cryostat (CM3050 S Research, Leica Biosystems). The frozen tissue was cut into 4-µm thick sections that were immediately mounted onto slides. After fixation in 10% formalin, the sections were stained with H&E and examined by Dr. Alan Spatz under a light microscope to verify the quality of the tissue sections, and to determine the cell viability as a %, the tumor-tissue content in mCRC and HCC samples, and the hepatic pathological disorders of non-neoplastic liver tissue.

Table 1: Patient samples used in analysis.

Samples analyzed	Type of tissue	Tumor size at time of diagnosis [cm of largest dimension]	Molecular testing and markers
p* A	mCRC	3.0	KRAS mutation-negative**
p B	mCRC	2.5	**KRAS mutation-positive** **dMMR : positive*** **
p C	mCRC	2.0	KRAS mutation-negative **dMMR : positive**
p D	mCRC	4.5	KRAS mutation-negative
p E	mCRC	5.3	KRAS mutation-negative
p F	mCRC	3.6	KRAS mutation-negative
p G	HCC	3.2	AFP: Negative **CEA: Positive****
p H	HCC	2.7	AFP: Negative*****
p I	HCC	3.8	AFP: Negative
p J	HCC	1.3	AFP: Negative
p K	HCC	3.5	AFP: Negative
p L	HCC	4.0	AFP: Negative
FL1	Fatty liver		
FL2	Fatty liver		
FL3	Fatty liver		
FL4	Fatty liver		
FL5	Fatty liver		
FL6	Fatty liver		
FL7	Fatty liver, cirrhosis	-	-
FL8	Fatty liver, Hepatitis		
H1	Hepatitis	-	-

H2	Hepatitis	-	-
H3	Hepatitis	-	-
H4	Hepatitis		

*p: patient; **KRAS: Kirsten rat sarcoma virus; KRAS mutation-negative: wild-type; ***dMMR positive: absence or dysfunction of one or more of four mismatch repair proteins, mutL homologue 1 (MLH1), mutS homologue 2 (MSH2), mutS homologue 6 (MSH6), and postmeiotic segregation increased 2 (PMS2). ****CEA: carcinoembryonic antigen; CEA positive: CEA blood level ≥ 20 ng/mL; *****AFP: alpha-fetoprotein; AFP negative: AFP blood level between 10 and 20 ng/mL.

Quantitation of PTEN levels in fresh frozen OCT blocks using immuno-MRM: As described in Appendix II, protein extraction from fresh frozen OCT blocks was performed and followed by ethanol precipitation and total protein quantitation using the Bicinchoninic acid (BCA) assay. Fifty µg total protein from each lysate was subjected to reduction, alkylation, digestion, and immuno-enrichment for NNIDDVVR as described in Appendix II. Samples were analyzed by LC-MRM as described in Appendix II.

Endogenous PTEN concentrations were determined using our laboratory's 2-PIC strategy [21] and are reported in fmol per 10 µg of protein, which can be more precisely determined than either actual tumor tissue volume or weight.

PTEN concentration correction:

The pathological examination of the H&E slides made from the OCT-embedded blocks revealed different tumor contents for the cancer samples, so the measured PTEN concentrations are derived from different quantitative compositions of healthy and cancer tissue. Laser Capture Microdissection (LCM) allows precise separation and examination of a cell subpopulation of a surgically obtained tissue sample. Therefore, LCM is increasingly used in cancer research. However, the LCM technique has some limitations that discouraged its use in my experiments. These limitations include that (i) it is an expensive technique and the fact that it is not available in all research centers, (ii) it is time-consuming, and multiple slides per sample would have had to be microdissect in order to collect sufficient protein for the iMRM analysis, (iii) it is a complicated technique, so it needs specialized expertise, and (iv) the quality of microdissected tissue is easily affected by several factors, such as fixatives and staining reagents, dehydration of

sections because of the absence of coverslips, and mounting medium onto sections. For these reasons, I used a correction factor to be able to determine the PTEN concentrations in the cancerous portion of the sample. This formula uses the % tumor content of each sample to correct the experimentally determined PTEN concentration to account for the unaffected hepatic tissue surrounding the tumor. The average PTEN concentration in unaffected hepatic tissue is 3 fmol/ 10 µg, as determined in Chapter 2 from from samples from three different patient.

$$Corrected\ PTEN = (measured\ PTEN\ in\ \text{fmol}/10\ \mu\text{g} - [(100 - tumor\ content\ \%)x\ 3\ fmol/10\ \mu g]\ )\ x \frac{100}{tumorcontent\%}$$

Measured PTEN is the average PTEN concentration determined by iMRM using three analytical replicates of the respective sample.

Example: In patient sample C [22], the measured PTEN average is 1.8 fmol/10 µg (100% of the sample). The tumor content % of pC is 60%. Hence the remaining surrounding 40% of the sample content represent the PTEN expression from healthy tissue which is 3 fmol/10 µg (40% x 3=1.2). Then the 60% should have PTEN expression equal to 1 fmol/10 µg which is the corrected PTEN, in another words, the actual PTEN concentration in the tumor tissue.

It is important to mention here that I am totally aware of the limitations of using this formula. The main two limitations are (i) the limited number of normal liver tissue samples used to determine the average PTEN expression in order to compensate for the potential variation of PTEN levels of healthy tissues, and (ii) considering that the liver tissue surrounding the tumor is always normal. In reality, in cancers -- especially in HCC -- the surrounding liver tissue may be affected by many other pathological disorders, including those that are considered to be risk factors for cancer development.

Results and discussion:

In the previous chapter, I presented the determination of PTEN protein concentrations using my robust iMRM assay which was validated and showed consistent results with other protein quantitation techniques (i.e., IHC and WB) in clinical samples. In this chapter, I show further applications of this assay for the analysis of several fresh-frozen tissue samples from patients with mCRC, HCC, and non-neoplastic hepatic disorders, in order to determine the PTEN protein

concentrations and their variation in these disorders, and how these PTEN levels relate to the patients clinicopathological data.

PTEN protein levels and hepatic metastases of colorectal cancer (mCRC):

In CRC, metastasis is one of the most common causes of death, of which liver metastasis is the most fatal. Therefore, in order to reduce the mortality of patients, early diagnosis of CRC liver metastasis, as well as use of targeted therapeutics for more efficient prevention/elimination of these metastases, are of highest importance. For PTEN quantitation from hepatic metastases of CRC (Figure 2a), the corrected PTEN concentrations in the tumors were between 0.3 and 2.0 fmol/ 10 µg. The sample from patient B (pB) showed the lowest PTEN concentration among the mCRC samples (0.3 fmol/ 10 µL) and was the only sample that was positive for KRAS mutations. Several studies on endometrial carcinomas, colorectal cancer, and biliary tract malignancies [23-25] showed a marked synergy between PTEN downregulation and KRAS mutation in activating both the ERK–MAPK cascade and the PI3K pathway. This explains why mutant KRAS alone was insufficient to cause neoplasia in mouse models. In other words, while the PI3K pathway is activated by mutated KRAS, an additional loss of the 'stop' function of PTEN may need to be overcome for cancer manifestation. In CRC, PTEN alterations have been found to be more frequently correlated with right-sided tumors, MSI, BRAF mutations, lymph-node metastases, and a higher tumor stage [26]. Samples pB and pC, which had the lowest PTEN concentration of all of the samples (0.3 and 1 fmol/ 10 µg respectively), showed loss expression of the MMR proteins (MLH1, MSH2, MSH6, and PMS2) determined by IHC. This important finding supports the results of previous studies that have demonstrated the association between loss of PTEN and dMMR[6, 11] which can guide patient selection for immune CPIs. Atreya et al. demonstrated, using IHC, that there is concordant PTEN expression (positive/negative) in CRC primary and liver metastasis tumor pairs and that loss of PTEN expression is associated with poor survival of CRC patients with liver-only metastases [27]. This means that the PTEN concentrations determined in these CRC liver metastases could reflect the PTEN status of the CRC primary tumors. To the best of my knowledge, there is no study that correlates PTEN concentrations with the tumor size of CRC hepatic metastases. In my study, PTEN concentrations also showed no correlation with the tumor size of the hepatic metastases as determined by imaging at time of diagnosis (r^2=0.0876; y=0.6696x+2.7244) (Figure 2b).

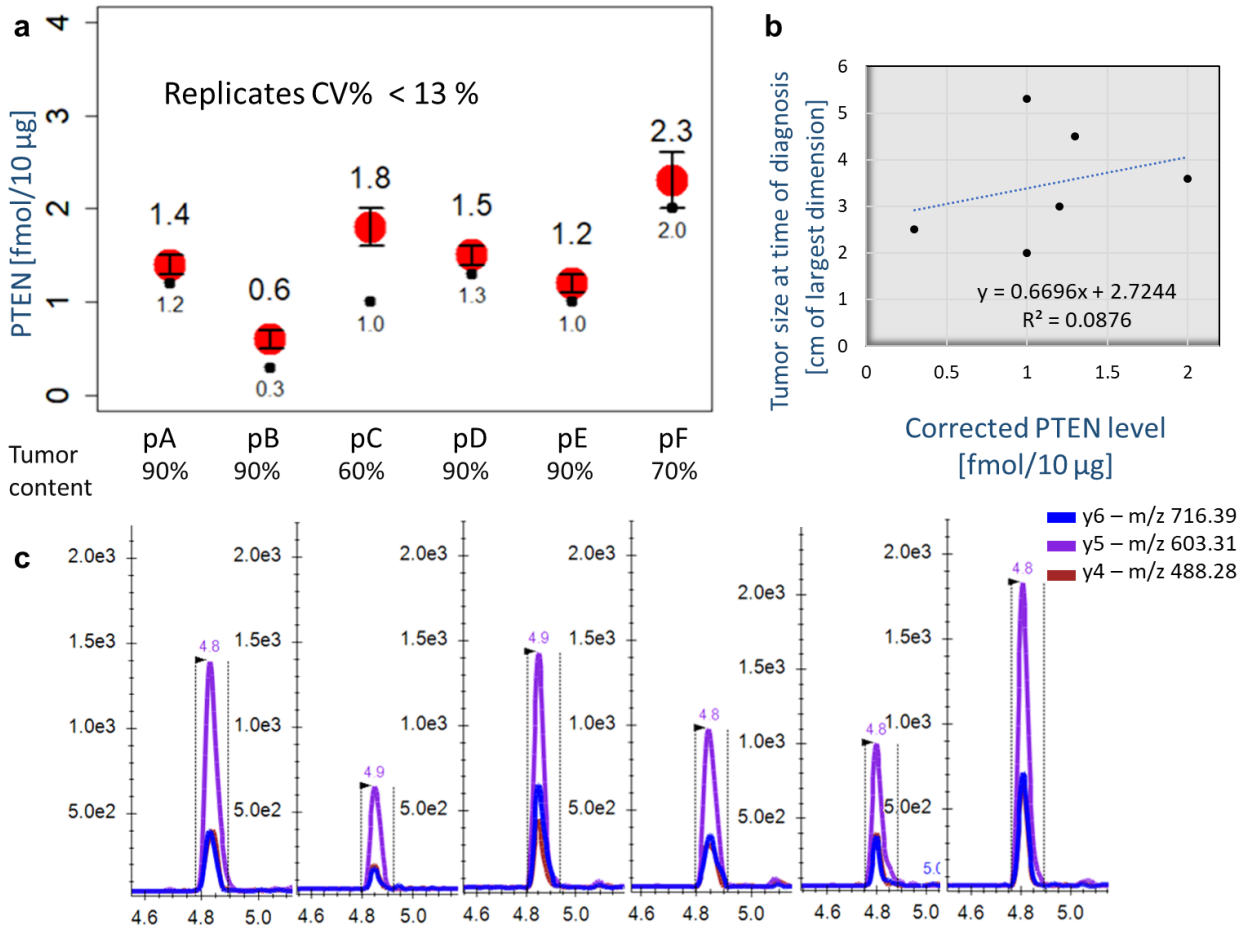

Figure 2. PTEN quantified by iMRM in patient samples of fresh-frozen tissue from hepatic metastases from colorectal cancer. (a) PTEN concentrations determined by iMRM (error bars are the ±SD of 3 analytical replicates for each sample). The dark small circle is the corrected PTEN level calculated from the average PTEN level determined and the tumor content %. (b) No correlation was found between iMRM PTEN concentrations and tumor size determined by imaging at the time of diagnosis. (r^2=0.0876; y=0.6696x+2.7244). (c) Endogenous PTEN NNIDDVVR peptide signals acquired by iMRM in samples pA-pF.

PTEN protein levels in hepatocellular carcinoma (HCC):

PTEN plays a key role in hepatocarcinogenesis and in HCC prognosis and recurrence. PTEN expression was found to be inversely related to increased expression of some HCC tumor markers such as epithelial cell adhesion molecule (EpCAM). In HCC samples (Figure 3a), the PTEN concentrations were between 1.3/10 µg and 3.1 fmol/10 µg, determined after correction for the % tumor content in each sample. All of the samples were α-fetoprotein (AFP) negative which means that the AFP level was < 20 ng/mL; the most commonly used cut-off value to differentiate HCC patients from healthy adults. The fetal-specific glycoprotein alpha-fetoprotein

(AFP) is primarily produced by the liver of the fetus. The serum AFP concentration drops rapidly after birth, and its synthesis in adulthood is repressed. Due to tumor excretion, AFP serum levels are elevated in more than half of HCC patients and it has become the most widely used biomarker for HCC diagnosis [28]. HCC with normal levels of AFP (AFP-negative) is not easily detected due to a lack of ideal biomarkers and this diagnosis thus mainly relies on imaging, which sometimes involves complex and expensive techniques. Imaging also may lack the required sensitivity and/or specificity, as most AFP-negative HCC tumors are small and, in early-stage HCC, exhibit a better prognosis. Therefore, finding new blood biomarkers for the diagnosis of AFP-negative HCC in clinical practice has been a critical issue for the early treatment and prognosis improvement of HCC [29].

Regarding serum carcinoembryonic antigen [30], the sample from patient G (pG) was positive for serum carcinoembryonic antigen and showed the lowest PTEN concentration (1.3 fmol/10 µg), while the average PTEN level of samples that were CEA negative was 2.3 fmol/10 µg. Except for AFP, no other significant association has been previously shown between increased expression levels of tumor markers in serum, including CEA, and lower PTEN expression in HCC patients [31]. Despite being a CRC tumor marker [32], CEA is also used as an indicator of tumor progression in a variety of other carcinomas. In HCC, high CEA patients had a significantly lower rate of disease-free survival (DFS) compared with normal CEA patients [33]. Therefore, in the pG sample, the low PTEN concentration associated with a positive CEA may indicate a high degree of tumor progression and may indicate a poor prognosis.

Zhou and Li have found that PTEN expression was negatively associated with liver-function grading: the higher the PTEN expression, the lower the liver function grading. Moreover, PTEN was significant in predicting the occurrence, development, and prognosis of liver cancer [31]. Here, PTEN concentration showed a moderate negative correlation with the HCC tumor size as determined by imaging at time of diagnosis (r^2=0.5955; y=-1.1931x+5.5936) (Figure 3b). This means the lower the PTEN concentration, the larger the volume of the tumor. Tumor size is a known prognostic factor in HCC, with larger tumors typically leading to worse prognosis. Therefore, tumor size has been included in most surgical staging systems for HCC, such as the American Joint Committee on Cancer (AJCC), TNM (Tumor, Node, Metastasis) staging), and

the Japan Integrated Staging Score [34-36] The negative correlation between PTEN protein concentration and tumor size indicates that PTEN may serve as a prognostic biomarker in HCC.

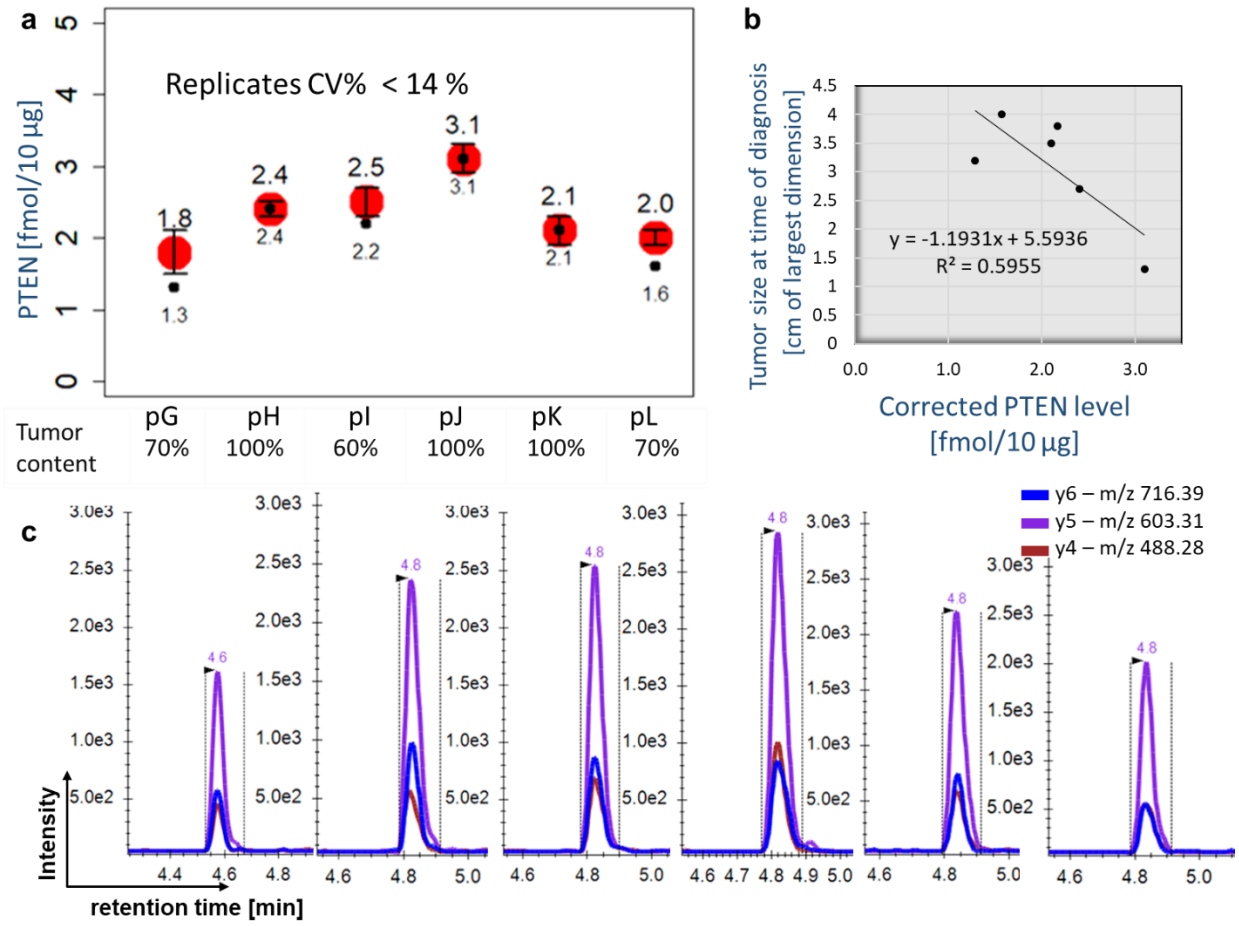

Figure 3. PTEN quantified by iMRM in fresh-frozen hepatocellular carcinoma. (a) PTEN concentrations determined by iMRM (error bars are the ±SD of 3 analytical replicates for each sample). The dark small circle is the corrected PTEN level calculated from the average PTEN level determined and the %. tumor content. (b) A moderate negative correlation was found between iMRM PTEN concentrations and tumor size determined by imaging at the time of diagnosis. (r^2=0.5955; y=1.1931x+5.5936). (c) Endogenous PTEN NNIDDVVR peptide signals acquired by iMRM in samples pG-pL.

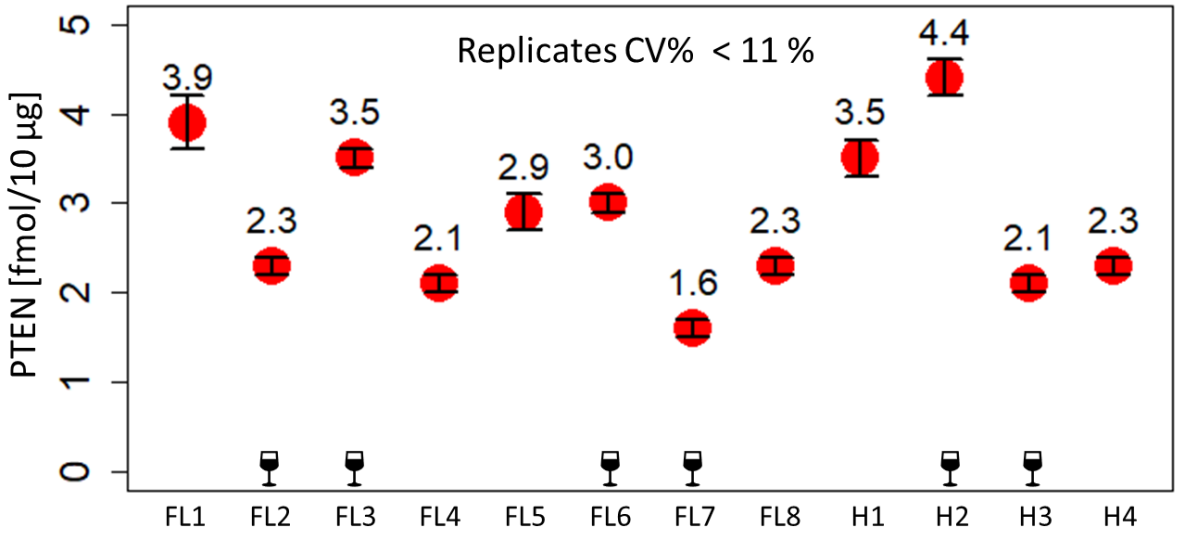

Figure 3. PTEN quantified by iMRM in liver fresh-frozen tissue samples from patients with non-neoplastic hepatic disorders (e.g., fatty liver, hepatitis, cirrhosis). 🍷 sign represents history of alcohol intake.

PTEN protein levels and hepatic disorders:

High variation in PTEN expression was found in samples of patients with non-neoplastic hepatic disorders, where PTEN concentrations ranged from 1.6 to 4.4 fmol/ 10 µg (Figure 3) with %CVs of < 11%. In patients with fatty liver (FL1 to FL8), PTEN concentrations ranged from 1.6 to 3.9 fmol/ 10 µg, where FL7 is fatty liver with cirrhosis while FL8 is for fatty liver with hepatitis. It has been demonstrated that PTEN expression is downregulated in the liver of obese humans and rodent models developing hepatic steatosis [37], as well as in cultured hepatocytes exposed to free fatty acids [38]. Several studies have supported these data and have indicated that PTEN downregulation represents an early event in non-alcoholic fatty liver disease (NAFLD). Moreover, the degree of PTEN downregulation correlates with the degree of steatosis and contributes to its development. Interestingly, sample FL7 that showed the lowest PTEN concentration (1.6 fmol/ 10 µg) among all non-neoplastic hepatic tissue samples analyzed, also suffered from sever alcoholic liver cirrhosis. This clinical finding agrees with a study on a rat model of cirrhosis, where expression of PTEN in rat liver tissues was negatively correlated with liver fibrosis [39].

Samples FL2, FL3, FL6, FL7, H2, and H3 are from patients with a history of varying levels of alcohol intake. Patient FL7 drank heavily (6 fl.oz. of scotch per day), while other patients drank alcohol only occasionally, and H2 self-reported to have quit drinking alcohol two years prior to the surgery. Patient H2 had the highest PTEN concentration (4.4 fmol/ 10 µg) among all non-

neoplastic hepatic tissue samples analyzed. This may indicate that PTEN was upregulated during recovery from alcohol intake, and that there was a reversal of its associated hepatic histopathological changes. This, however, does not agree with some other studies that showed an increase in PTEN expression in ethanol-exposed hepatic cells [40, 41].

Conclusion

In conclusion, I have been able to perform PTEN quantitation using my iMRM assay on a set of patient samples. These patients were suffering from different cancers and diseases, including hepatocellular carcinoma (HCC), hepatic metastatic lesions of colorectal carcinomas (CRC), and non-neoplastic hepatic disorders including fatty liver disease and viral hepatitis. PTEN expression levels showed a high variation between patients. Interestingly, mCRC samples showed the lowest average PTEN concentration (1.1 fmol/ 10 µg), where samples with the lowest PTEN concentrations were associated with positive KRAS mutations and deficient MMR proteins. This sheds light on the capability of PTEN to be used (i) for better CRC patient stratification, (ii) as a prognostic biomarker where low PTEN concentration may indicate a bad prognosis, and (iii) as a predictive biomarker that can helps to select patients for other therapeutic options, including PI3K/AKT pathway inhibitors and immune check point inhibitors.

The average PTEN concentration in HCC samples (2.1 fmol/ 10 µg) was lower than in samples with non-neoplastic hepatic diseases (2.8 fmol/ 10 µg). Furthermore, PTEN levels were found to be negatively correlated with HCC tumor size, as determined by imaging at the time of diagnosis -- i.e., the larger the tumor, the lower the PTEN level -- which is an indication of poor prognosis (and vice versa). Interestingly, samples from patients that had severe hepatic cirrhosis showed the lowest PTEN concentrations. Therefore, the precise determination of PTEN expression levels in these hepatic diseases (and throughout the course of these diseases) may greatly and fundamentally improve our understanding of these diseases and their progression into HCC. In addition, this may help to lay the groundwork for developing a reference PTEN expression level that can differentiate hepatic patients with a high risk of developing cancer (i.e., patients who we can refer to as "pre-neoplastic") from those with a low risk.

References:

1. Gong, L.; Govan, J. M.; Evans, E. B.; Dai, H.; Wang, E.; Lee, S. W.; Lin, H. K.; Lazar, A. J.; Mills, G. B.; Lin, S. Y., Nuclear PTEN tumor-suppressor functions through maintaining heterochromatin structure. *Cell Cycle* **2015,** *14* (14), 2323-32.
2. Fan, X.; Kraynak, J.; Knisely, J. P. S.; Formenti, S. C.; Shen, W. H., PTEN as a Guardian of the Genome: Pathways and Targets. *Cold Spring Harb Perspect Med* **2020,** *10* (9).
3. Chen, C. Y.; Chen, J.; He, L.; Stiles, B. L., PTEN: Tumor Suppressor and Metabolic Regulator. *Front Endocrinol (Lausanne)* **2018,** *9*, 338.
4. Milella, M.; Falcone, I.; Conciatori, F.; Cesta Incani, U.; Del Curatolo, A.; Inzerilli, N.; Nuzzo, C. M.; Vaccaro, V.; Vari, S.; Cognetti, F.; Ciuffreda, L., PTEN: Multiple Functions in Human Malignant Tumors. *Front Oncol* **2015,** *5*, 24.
5. Djordjevic, B.; Barkoh, B. A.; Luthra, R.; Broaddus, R. R., Relationship between PTEN, DNA mismatch repair, and tumor histotype in endometrial carcinoma: retained positive expression of PTEN preferentially identifies sporadic non-endometrioid carcinomas. *Mod Pathol* **2013,** *26* (10), 1401-12.
6. Lopez, G.; Noale, M.; Corti, C.; Gaudioso, G.; Sajjadi, E.; Venetis, K.; Gambini, D.; Runza, L.; Costanza, J.; Pesenti, C.; Grossi, F.; Maggi, S.; Ferrero, S.; Bosari, S.; Fusco, N., PTEN Expression as a Complementary Biomarker for Mismatch Repair Testing in Breast Cancer. *Int J Mol Sci* **2020,** *21* (4).
7. Jin, Z.; Sanhueza, C. T.; Johnson, B.; Nagorney, D. M.; Larson, D. W.; Mara, K. C.; Harmsen, W. C.; Smyrk, T. C.; Grothey, A.; Hubbard, J. M., Outcome of Mismatch Repair-Deficient Metastatic Colorectal Cancer: The Mayo Clinic Experience. *Oncologist* **2018,** *23* (9), 1083-1091.
8. Zhao, P.; Li, L.; Jiang, X.; Li, Q., Mismatch repair deficiency/microsatellite instability-high as a predictor for anti-PD-1/PD-L1 immunotherapy efficacy. *J Hematol Oncol* **2019,** *12* (1), 54.
9. Andre, T.; Shiu, K. K.; Kim, T. W.; Jensen, B. V.; Jensen, L. H.; Punt, C.; Smith, D.; Garcia-Carbonero, R.; Benavides, M.; Gibbs, P.; de la Fouchardiere, C.; Rivera, F.; Elez, E.; Bendell, J.; Le, D. T.; Yoshino, T.; Van Cutsem, E.; Yang, P.; Farooqui, M. Z. H.; Marinello, P.; Diaz, L. A., Jr.; Investigators, K.-. Pembrolizumab in Microsatellite-Instability-High Advanced Colorectal Cancer. *N Engl J Med* **2020,** *383* (23), 2207-2218.
10. Le, D. T.; Kim, T. W.; Van Cutsem, E.; Geva, R.; Jager, D.; Hara, H.; Burge, M.; O'Neil, B.; Kavan, P.; Yoshino, T.; Guimbaud, R.; Taniguchi, H.; Elez, E.; Al-Batran, S. E.; Boland, P. M.; Crocenzi, T.; Atreya, C. E.; Cui, Y.; Dai, T.; Marinello, P.; Diaz, L. A., Jr.; Andre, T., Phase II Open-Label Study of Pembrolizumab in Treatment-Refractory, Microsatellite Instability-High/Mismatch Repair-Deficient Metastatic Colorectal Cancer: KEYNOTE-164. *J Clin Oncol* **2020,** *38* (1), 11-19.
11. Nelson, G. S.; Pink, A.; Lee, S.; Han, G.; Morris, D.; Ogilvie, T.; Duggan, M. A.; Kobel, M., MMR deficiency is common in high-grade endometrioid carcinomas and is associated with an unfavorable outcome. *Gynecol Oncol* **2013,** *131* (2), 309-14.
12. Song, M.; Chen, D.; Lu, B.; Wang, C.; Zhang, J.; Huang, L.; Wang, X.; Timmons, C. L.; Hu, J.; Liu, B.; Wu, X.; Wang, L.; Wang, J.; Liu, H., PTEN loss increases PD-L1 protein expression and affects the correlation between PD-L1 expression and clinical parameters in colorectal cancer. *PLoS One* **2013,** *8* (6), e65821.

13. Yang, R.; Cai, T. T.; Wu, X. J.; Liu, Y. N.; He, J.; Zhang, X. S.; Ma, G.; Li, J., Tumor YAP1 and PTEN expression correlates with tumor-associated myeloid suppressor cell expansion and reduced survival in colorectal cancer. *Immunology* **2018,** *155* (2), 263-272.
14. Yang, L.; Venneti, S.; Nagrath, D., Glutaminolysis: A Hallmark of Cancer Metabolism. *Annu Rev Biomed Eng* **2017,** *19*, 163-194.
15. Nakagawa, H.; Hayata, Y.; Kawamura, S.; Yamada, T.; Fujiwara, N.; Koike, K., Lipid Metabolic Reprogramming in Hepatocellular Carcinoma. *Cancers (Basel)* **2018,** *10* (11).
16. Cordero-Espinoza, L.; Hagen, T., Increased concentrations of fructose 2,6-bisphosphate contribute to the Warburg effect in phosphatase and tensin homolog (PTEN)-deficient cells. *J Biol Chem* **2013,** *288* (50), 36020-8.
17. Qian, X.; Li, X.; Shi, Z.; Xia, Y.; Cai, Q.; Xu, D.; Tan, L.; Du, L.; Zheng, Y.; Zhao, D.; Zhang, C.; Lorenzi, P. L.; You, Y.; Jiang, B. H.; Jiang, T.; Li, H.; Lu, Z., PTEN Suppresses Glycolysis by Dephosphorylating and Inhibiting Autophosphorylated PGK1. *Mol Cell* **2019,** *76* (3), 516-527 e7.
18. Liang, H.; He, S.; Yang, J.; Jia, X.; Wang, P.; Chen, X.; Zhang, Z.; Zou, X.; McNutt, M. A.; Shen, W. H.; Yin, Y., PTENalpha, a PTEN isoform translated through alternative initiation, regulates mitochondrial function and energy metabolism. *Cell Metab* **2014,** *19* (5), 836-48.
19. Piguet, A. C.; Dufour, J. F., PI(3)K/PTEN/AKT pathway. *J Hepatol* **2011,** *54* (6), 1317-9.
20. Matsuda, S.; Kobayashi, M.; Kitagishi, Y., Roles for PI3K/AKT/PTEN Pathway in Cell Signaling of Nonalcoholic Fatty Liver Disease. *ISRN Endocrinol* **2013,** *2013*, 472432.
21. Ibrahim, S.; Froehlich, B. C.; Aguilar-Mahecha, A.; Aloyz, R.; Poetz, O.; Basik, M.; Batist, G.; Zahedi, R. P.; Borchers, C. H., Using Two Peptide Isotopologues as Internal Standards for the Streamlined Quantitation of Low-Abundance Proteins by Immuno-MRM and Immuno-MALDI. *Anal Chem* **2020,** *92* (18), 12407-12414.
22. Howlader N, N. A., Krapcho M, Miller D, Brest A, Yu M, Ruhl J, Tatalovich Z,; Mariotto A, L. D., Chen HS, Feuer EJ, Cronin KA (eds). SEER Cancer Statistics Review, 1975-2016, National Cancer Institute. **Posted to the SEER web site, April 2019.**
23. Marsh, V.; Davies, E. J.; Williams, G. T.; Clarke, A. R., PTEN loss and KRAS activation cooperate in murine biliary tract malignancies. *J Pathol* **2013,** *230* (2), 165-73.
24. Davies, E. J.; Marsh Durban, V.; Meniel, V.; Williams, G. T.; Clarke, A. R., PTEN loss and KRAS activation leads to the formation of serrated adenomas and metastatic carcinoma in the mouse intestine. *J Pathol* **2014,** *233* (1), 27-38.
25. Kim, T. H.; Wang, J.; Lee, K. Y.; Franco, H. L.; Broaddus, R. R.; Lydon, J. P.; Jeong, J. W.; Demayo, F. J., The Synergistic Effect of Conditional Pten Loss and Oncogenic K-ras Mutation on Endometrial Cancer Development Occurs via Decreased Progesterone Receptor Action. *J Oncol* **2010,** *2010*, 139087.
26. Salvatore, L.; Calegari, M. A.; Loupakis, F.; Fassan, M.; Di Stefano, B.; Bensi, M.; Bria, E.; Tortora, G., PTEN in Colorectal Cancer: Shedding Light on Its Role as Predictor and Target. *Cancers (Basel)* **2019,** *11* (11).
27. Atreya, C. E.; Sangale, Z.; Xu, N.; Matli, M. R.; Tikishvili, E.; Welbourn, W.; Stone, S.; Shokat, K. M.; Warren, R. S., PTEN expression is consistent in colorectal cancer primaries and metastases and associates with patient survival. *Cancer Med* **2013,** *2* (4), 496-506.
28. Sauzay, C.; Petit, A.; Bourgeois, A. M.; Barbare, J. C.; Chauffert, B.; Galmiche, A.; Houessinon, A., Alpha-foetoprotein (AFP): A multi-purpose marker in hepatocellular carcinoma. *Clin Chim Acta* **2016,** *463*, 39-44.

29. Wang, T.; Zhang, K. H., New Blood Biomarkers for the Diagnosis of AFP-Negative Hepatocellular Carcinoma. *Front Oncol* **2020,** *10*, 1316.
30. Laurent-Puig, P.; Cayre, A.; Manceau, G.; Buc, E.; Bachet, J. B.; Lecomte, T.; Rougier, P.; Lievre, A.; Landi, B.; Boige, V.; Ducreux, M.; Ychou, M.; Bibeau, F.; Bouche, O.; Reid, J.; Stone, S.; Penault-Llorca, F., Analysis of PTEN, BRAF, and EGFR status in determining benefit from cetuximab therapy in wild-type KRAS metastatic colon cancer. *J Clin Oncol* **2009,** *27* (35), 5924-30.
31. Zhou, J.; Li, X., Association of PTEN expression with liver function and inflammatory changes in patients with liver cancer after chemotherapy. *Oncol Lett* **2018,** *16* (5), 6633-6637.
32. Gonzalez-Pons, M.; Cruz-Correa, M., Colorectal Cancer Biomarkers: Where Are We Now? *Biomed Res Int* **2015,** *2015*, 149014.
33. Yoshikawa, M.; Morine, Y.; Ikemoto, T.; Imura, S.; Higashijima, J.; Iwahashi, S.; Saito, Y. U.; Takasu, C.; Yamada, S.; Ishikawa, D.; Teraoku, H.; Takata, A.; Yoshimoto, T.; Shimada, M., Elevated Preoperative Serum CEA Level Is Associated with Poor Prognosis in Patients with Hepatocellular Carcinoma Through the Epithelial-Mesenchymal Transition. *Anticancer Res* **2017,** *37* (3), 1169-1175.
34. Pons, F.; Varela, M.; Llovet, J. M., Staging systems in hepatocellular carcinoma. *HPB (Oxford)* **2005,** *7* (1), 35-41.
35. Minagawa, M.; Ikai, I.; Matsuyama, Y.; Yamaoka, Y.; Makuuchi, M., Staging of hepatocellular carcinoma: assessment of the Japanese TNM and AJCC/UICC TNM systems in a cohort of 13,772 patients in Japan. *Ann Surg* **2007,** *245* (6), 909-22.
36. Goh, B. K.; Teo, J. Y.; Chan, C. Y.; Lee, S. Y.; Jeyaraj, P.; Cheow, P. C.; Chow, P. K.; Ooi, L. L.; Chung, A. Y., Importance of tumor size as a prognostic factor after partial liver resection for solitary hepatocellular carcinoma: Implications on the current AJCC staging system. *J Surg Oncol* **2016,** *113* (1), 89-93.
37. Vinciguerra, M.; Veyrat-Durebex, C.; Moukil, M. A.; Rubbia-Brandt, L.; Rohner-Jeanrenaud, F.; Foti, M., PTEN down-regulation by unsaturated fatty acids triggers hepatic steatosis via an NF-kappaBp65/mTOR-dependent mechanism. *Gastroenterology* **2008,** *134* (1), 268-80.
38. Vinciguerra, M.; Sgroi, A.; Veyrat-Durebex, C.; Rubbia-Brandt, L.; Buhler, L. H.; Foti, M., Unsaturated fatty acids inhibit the expression of tumor suppressor phosphatase and tensin homolog (PTEN) via microRNA-21 up-regulation in hepatocytes. *Hepatology* **2009,** *49* (4), 1176-84.
39. Zheng, L.; Chen, X.; Guo, J.; Sun, H.; Liu, L.; Shih, D. Q.; Zhang, X., Differential expression of PTEN in hepatic tissue and hepatic stellate cells during rat liver fibrosis and its reversal. *Int J Mol Med* **2012,** *30* (6), 1424-30.
40. Shulga, N.; Hoek, J. B.; Pastorino, J. G., Elevated PTEN levels account for the increased sensitivity of ethanol-exposed cells to tumor necrosis factor-induced cytotoxicity. *J Biol Chem* **2005,** *280* (10), 9416-24.
41. Shearn, C. T.; Smathers, R. L.; Backos, D. S.; Reigan, P.; Orlicky, D. J.; Petersen, D. R., Increased carbonylation of the lipid phosphatase PTEN contributes to Akt2 activation in a murine model of early alcohol-induced steatosis. *Free Radic Biol Med* **2013,** *65*, 680-692.

The fourth manuscript presents one of the most important potential applications of my PTEN iMRM assay which is testing the predictive role of PTEN in response to different cancer therapeutics. I therefore used the PTEN iMRM assay to test some triple negative breast cancer-PDXs treated with paclitaxel and carboplatin to evaluate whether or not there was a clinically significant correlation between PTEN protein concentration and response to treatment.

PTEN quantitation by immuno-MRM and the response of triple negative breast cancer to paclitaxel and carboplatin.

Sahar Ibrahim[1,2,3], Marguerite Buchanan[4], Adriana Aguilar-Mahecha[4], Alan Spatz[1,4,5,6], Mark Basik[1,4,7], Gerald Batist[1,4,7], René P. Zahedi[3,8], Christoph H. Borchers[3,7,8*].

[1] Division of Experimental Medicine, McGill University, Montréal, Québec, Canada.

[2] Clinical Pathology Department, National Liver Institute, Menoufia University, Egypt.

[3] Segal Cancer Proteomics Centre, Lady Davis Institute for Medical Research, Jewish General Hospital, McGill University, Montréal, Québec, Canada.

[4] Segal Cancer Center, Lady Davis Institute for Medical Research, Jewish General Hospital, McGill University, Montréal, Québec, Canada.

[5] Department of Pathology, McGill University, Montréal, Québec, Canada.

[6] Division of Pathology, Department of Laboratory Medicine, McGill University Health Centre, Montréal, Québec, Canada.

[7] Gerald Bronfman Department of Oncology, Jewish General Hospital, McGill University, Montréal, Québec, Canada.

[8] Center for Computational and Data-Intensive Science and Engineering, Skolkovo Institute of Science and Technology, Moscow, Russia).

Introduction

Triple-negative breast cancer (TNBC) is an aggressive subtype of breast cancer that is routinely diagnosed whenever the cancer cells pathologically lack expression of the estrogen receptor (ER), progesterone receptor (PR), and human epidermal growth factor receptor 2 (HER2) [1]. TNBC accounts for approximately 10-20% of all breast cancers and tends to be more common in women between aged 20 to 39, who are African Americans, or carriers of germline BRCA (BReast CAncer genes) and PALB2 (Partner And Localizer Of BRCA2) mutations [2]. Due to its special molecular phenotype, TNBC is not sensitive to endocrine therapy or molecular targeted therapies such as Anti-HER2 therapeutics. Therefore, chemotherapy is the main systemic treatment. Interestingly, there is a great difference in treatment response and clinical outcomes among TNBC patients. This is largely because TNBC is a highly diverse group of cancers with a substantial tumor heterogeneity among patients. Much effort has been made to reveal the molecular complexity behind this heterogenicity in order to better predict treatment response and clinical outcome as well as to select new targeted therapies [1]. In 2011, Lehmann et al. [3] used gene expression profiles to divide TNBC into six subtypes: basal-like 1 (BL1), basal-like 2 (BL2), mesenchymal (M), mesenchymal stem-like (MSL), immunomodulatory (IM), and luminal androgen receptor (LAR). 'Omics' technologies have revealed that the BL1 and BL2 subtypes usually express epidermal growth factor receptor (EGFR) and basal cytokeratins such as CK5/6, CK14 and CK17, while the LAR subtype usually has high androgen receptor (AR) expression [4]. Numerous studies have demonstrated that PTEN deficiency is a frequent and critical TNBC molecular abnormality, conferring a selective advantage for aggressiveness, drug resistance, and poor prognosis [5-8]. Interestingly, some studies showed that PTEN deficiency is more likely in the BL1 subtype.

Combined p53 and PTEN deficiency accounts for 21–28 % of all TNBC and is associated with a more aggressive phenotype with higher therapy resistance. Certain molecular findings have been determined only in TNBC with combined p53 and PTEN deficiency, suggesting the involvement of a unique molecular signaling pathway, which may be distinct from the deficiency of p53 or PTEN alone [6-8].

Regarding TNBC systemic treatment, there are several promising new targets and new agents that already have been approved or are being tested in clinical trials. For example, PARP inhibitors have been approved to treat advanced-stage TNBC patients with a germline BRCA1/2 mutation [9]. Interestingly, PTEN deficiency was suggested to cause the chromosomal instability in TNBC and therefore, TNBC with low expression levels of PTEN can be sensitized for PARP1 inhibitors, independent of BRCA mutations [10]. Regarding the use of immunotherapy to treat TNBC, randomized phase III clinical trials have now demonstrated a favorable benefit-risk ratio for the addition of the PD-L1 antibody atezolizumab or the PD-1 antibody pembrolizumab to standard chemotherapy for both early high-risk and metastatic TNBC basal-like immune-activated and the immunomodulatory subtypes [11]. Barroso-Sousa et al., have demonstrated that in TNBC, PTEN alterations are associated with resistance to anti-PD-1/L1 therapies and shorter survival [12]. AKT inhibitors are other very promising new therapeutics to be used in TNBCs with PIK3CA/AKT pathway hyperactivation, which accounts for 25% of all TNBCs and which is mainly caused by PTEN loss [13, 14].

Despite all these new treatment options, chemotherapy, in particular with anthracycline, platinum and taxanes, remains the standard therapeutic approach for TNBC at all stages as neoadjuvant, adjuvant, and metastatic treatment. Many studies have shown significant benefit of chemotherapy, particularly dose dense and dose intensive regimens in TNBC. Interestingly, TNBC is particularly sensitive to specific types of chemotherapy [15]. TNBCs that harbor BRCA gene mutations are especially susceptible to DNA-damaging compounds such as platinum derivatives cisplatin and carboplatin [16]. The basal-like TNBC subtypes have an enriched expression of proliferation-related genes, implying its susceptibility to antimitotic agents such as taxanes [17].

Carboplatin has replaced cisplatin as they share efficacy, but carboplatin has less and more tolerable side effects. Addition of carboplatin to neoadjuvant chemotherapy in TNBC has been demonstrated to (i) increase the pathological complete response rate [18] and (ii) improve disease-free and overall survival in patients [19]. Moreover, metastatic TNBC patients, especially those with germline BRCA1/2 mutations, may also benefit from carboplatin treatment [20]. In advanced/metastatic TNBC patients (regardless of BRCA status) previously treated with an

anthracycline with or without a taxane in the neoadjuvant or adjuvant setting, carboplatin demonstrated comparable efficacy with docetaxel with a more favourable toxicity profile [21]. Several studies have demonstrated the role of specific mRNAs that downregulate PTEN and induce cisplatin chemoresistance in ovarian cancer cells [22-24]. However, no corresponding studies involving carboplatin response and PTEN expression level have been conducted in TNBC.

Conventional taxanes such as paclitaxel (PTX) and docetaxel have been demonstrated to be particularly more active in endocrine receptor-negative tumors, and to be among the most active agents for metastatic TNBC. Therefore, they are indicated as the first-line treatment of metastatic TNBC and are commonly used in adjuvant therapy [25]. PTX is a promoter of microtubule polymerization and a radio-sensitizing agent. Paclitaxel promotes the assembly of microtubules from tubulin dimers and stabilizes microtubules by preventing depolymerization. This stability results in the inhibition of the normal dynamic reorganization of the microtubule network that is essential for vital interphase, transportation, and mitotic cellular functions. Recent studies have indicated that paclitaxel induces programmed cell death (apoptosis) in cancer cells by binding to the apoptosis-inhibiting Bcl-2 (B-cell leukemia 2) and thus arrests its function. Compared with docetaxel, PTX has a lower myelosuppressive effect and can be used in patients with mild to moderate hepatic dysfunction [26]. PTX use as adjuvant and neoadjuvant therapy in TNBC showed significant clinical benefits [15]. However, the response rate is relatively low, and many patients become resistant due to either disease recurrence within 6 months of completion of adjuvant or neoadjuvant treatment, or tumor progression that occurs during treatment and up to 3 months after the last dose. The relatively high PTX resistance rate in TNBC underscores the need for a biomarker that can predict resistance to PTX and hence can be used to select patients for new therapeutics that overcome this resistance.

Several reports showed that PTEN downregulation may be involved in PTX resistance and hence might be used as predictive biomarker for response [27]. PTEN was presented in other studies as a target to overcome PTX resistance, through activating its regulators cyclin B1 or miR-22 [28, 29]. Furthermore, AKT inhibitors added to PTX in several clinical trials showed greater treatment benefit in early or metastatic TNBC patients with PTEN deficiency. In these patients AKT inhibitors were able to reverse PTX resistance caused by PTEN deficiency 30-32.

As presented and discussed in chapter two, the PTEN iMRM assay outperforms immunohistochemistry with its many well-known drawbacks. I, therefore, hypothesized that the PTEN iMRM assay may not only reveal that PTEN protein expression has a prognostic value in BC but that it also has a predictive value for treatment response, such as for PTX treatment. Therefore, I analyzed BC PDXs treated with paclitaxel or carboplatin in order to study the correlation between their response data and the PTEN protein concentrations.

The PDX technology has been increasingly used in cancer research since its development[33]. This can be largely attributed to several advantages including: (i) a better availability than patient tumors: PDX models are an excellent alternative to patient tumors which often are of limited availability, quantity, and quality. (ii) preservation of the tumor architecture, heterogeneity, stromal and extracellular components: PDX models retain the interactions between the tumor and its microenvironment [34]. All these tumor characteristics are even more preserved with orthotopic PDXs than with heterotopic ones [35]. This is an important difference to cell line xenografts where *in-vitro* culture of patient samples leads to the generation of a cell line from a subpopulation of the original patient's tumor after being subjected to culture selection and adaptation to artificial conditions [34]. (iii) Simulation of the original patient tumor's properties for up to 5 passages, which has been evaluated on the transcriptome, proteome, and genome level [36].

However, the development of PDX models is costly and technically difficult with low engraftment success rates (not all engrafted mice develop the tumor) and low growth rates[37]. Importantly, as immunodeficient mice are used, PDX models do not preserve the interactions between the tumor and the immune system. In order to address this issue, PDX mice with human hematopoietic and immune systems (humanized PDX) were developed and became a powerful tool for the analysis of tumor–immune system interactions and the evaluation of immunotherapy response [38]. It is worth noting that while ordinary PDXs are already very costly, the exorbitant cost of humanized PDX limits their use to specific research purposes, such as immunotherapy response.

Experimental Procedures

Reagents: Summary of the used Reagents (see Appendix II).

Clinical samples and methodology:

The TNBC patients consented to sample collection for the JGH breast biobank (protocol #05-006) and PDX generation was performed under protocol (#14-168). All protocols were approved by the JGH Research Ethics Committee. Pieces of breast tumors were implanted in the mammary fat pads of NSG female mice (6–7-week-old). Tumor growth was monitored biweekly with calipers. Once the tumors reached 2000 mm^3, the mice were sacrificed and tumor tissue was collected and stored in liquid nitrogen, formalin (for paraffin embedding) or in DMSO as live tissue to expand the PDX biobank. Those parent untreated PDX tumors were used for PTEN protein quantitation by our iMRM assay and for the PTEN copy number variant analysis by CytoScan-HD (see Appendix II) in order to predict the response to drug treatment in the following PDX passages. Frozen PDX tumors were embedded in OCT and one cryosection was obtained for H&E staining. A pathologist determined the percent tumor cellularity and necrosis in each tumor sample. Samples were taken for CytoScan-HD analysis if they contained at least 50% tumor cells. Slices from the FFPE blocks were used for immunohistochemistry using mouse monoclonal anti-Mitochondria antibody (ab92824) from Abcam (Cambridge, USA) to validate the presence of human tumor cells in each model. All PDXs models were confirmed to carry human tumors. Furthermore, H&E staining from Sigma Aldrich (Oakville, Canada) was used verify the quality of the tissue and the homogeneity of the tumor under a light microscope. Guided by the H&E staining, three 1.0-mm diameter cores were punched out of each FFPE block and transferred to separate reaction tubes, to be used as technical triplicates. Each core was deparaffinized and rehydrated, followed by protein extraction as described in Appendix II. Samples containing either 20 or 30 µg total tissue lysate protein were prepared and subjected to reduction, alkylation, digestion, and immuno-enrichment for NNIDDVVR as described in Appendix II for cell line samples. Samples were analyzed by LC-MRM as described in Appendix II. Endogenous PTEN concentrations were determined using our 2-PIC strategy and are reported in fmol per 10 µg of protein, which can be more precisely determined than for instance actual tumor tissue volume or weight. This is due to several reasons including (i) total protein concentration can be measured with higher analytical precision than methods to obtain the tumor volume or weight that require a manual readout, which is difficult to achieve for the low weights and small volumes of these core samples. (ii) the actual tumor content in FFPE cores of a given size/volume can vary a lot. In fact, sometimes these cores can be 90% empty and contain only 10% tumor tissue, while another core can be 50/50, etc.

In the following PDX passages, mice were injected intraperitoneally once a week with either 40 mg of carboplatin per kg of body weight or 20 mg/kg paclitaxel (see Figure 1) and treatment was continued for at least 21 days.

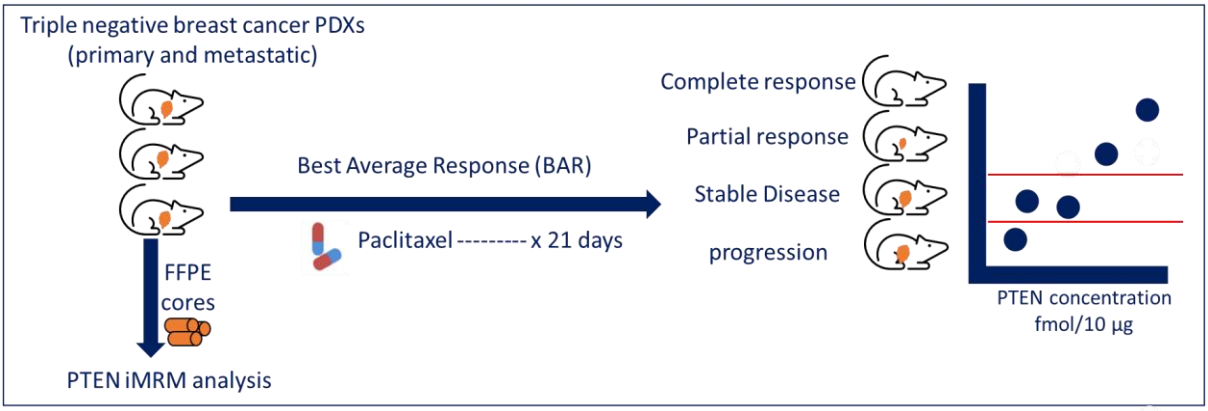

Figure 1. Schematic experimental design for evaluating the relationship between the response of TNBC PDXs to paclitaxel treatment and their PTEN protein levels as quantified by iMRM.

Gao et al., described in detail the determination of treatment response [39]. In summary, the % tumor volume change at time point t (ΔVol_t) in reference to the baseline volume (*V_initial*) was determined as shown in the following equation:

$$\%\ tumor\ volume\ change\ =\ \Delta Vol\_t =\ 100\% \times ((V\_t - V\_initial)\ /\ V\_initial)$$

The Best Response (BR) is defined as the minimum value of ΔVolt_t for t ≥ 10 days. For each time point t, the average ΔVol_t was calculated, and the Best Average Response (BAR) was defined as the minimum ΔVol_t over a period of 21 days (see Table 1).

Table 1: Patient samples used to study the potential correlation between PTX-response and PTEN expression.

Samples	PDX	Paclitaxel BAR 21 days	Carboplatin BAR 21 days	Tumor type
P1	BM-152	-76	-80	metastatic
P2	T-779	-51	-85	primary
P3	T-846	-47	-86	primary
P4	BM-126	-31	77	metastatic
P5a	T-691	-29	-69	primary
P5b	T-692	-29	-69	primary
P6	T-904	-12	31	primary
P7	BM-156	-8	11	metastatic
P8	BM-209	-7	18	metastatic
P9	T-684 in	2	59	primary
P10	T-960	10	160	primary
P11	T-802	30	42	primary
P12a	T-786 skin	34	49	primary
P12b	T-789	34	171	primary
P13	BM-236-2	47	49	metastatic
P14	BM-163	50	50	metastatic
P15	BM-204	60	31	metastatic

Results and discussion:

In chapter two, a robust iMRM assay was presented for precise quantitation of PTEN protein concentrations. The assay was validated and showed consistent results with other protein quantitation techniques (IHC and WB) in clinical samples. In this chapter, I further applied this assay to analyze FFPE cores from PDXs that were derived from different patients' primary and metastatic TNBC tumors.

In this study, PDXs were treated with paclitaxel or carboplatin and their responses were reported as percent decrease or increase in tumor size, based on the best average response [39]. By studying

the correlation between PTEN protein concentrations of these PDXs samples and their response data to both therapeutics, we shed the light on the predictive role of PTEN to breast cancer therapeutics and how PTEN iMRM assay will help studying this role in order to put an end to the controversy about it.

PTEN protein quantitation and genomic data

The copy number variations (CNVs) were determined in biological replicates of the PDX samples that were used for iMRM. Four samples P2, P6, P9 and P10 showed a loss of the PTEN gene where the CNV of PTEN was equal to 1.0, 0.3, 1.4 and 1.3 respectively. Five samples P4, P7, P12a, P12b and P15 showed no gain nor loss while the rest showed a gain of the PTEN gene where CNV ranged from 2.1 to 4. Interestingly, in P6, 0.3 copies of the PTEN gene indicated a loss of the PTEN gene (Figure 2b), while the PTEN protein level determined by iMRM was 0.1±0.01 fmol/10 µg total protein. The protein measurement may indeed reflect background levels of PTEN that are derived from mouse stromal cells, as the target peptide has 100% sequence homology with the human sequence. This result underscores the high sensitivity of the assay. In general, the protein levels derived from the PTEN iMRM (Figure 2a) do not agree with PTEN CNVs (r^2=0.0855; y=0.1218x + 1.843). For example, the PTEN protein concentrations in P4 and P7 (3.7±0.9 and 2.2±0.2 fmol/10 µg total protein respectively) differed substantially from the protein concentrations in P12a and P15 (0.7±0.2 and 0.5±0.1 fmol/10 µg respectively) although all subjects had 2.0 copies of the PTEN gene, which indicates that neither a loss nor a gain of the PTEN gene occurred. On the other hand, PTEN concentrations in P2 (0.4±0.1 fmol/10 µg) and P3 (8.1±1.1 fmol/10 µg) showed some correlation with PTEN copy number (P4: 1.0; P6: 3.0). These data clearly confirm the concept of proteogenomics, that genome-only analyses may often not be sufficient to capture the phenotype of a tumor and to make optimal treatment decisions. Such low correlation between the CNV of a gene and the change at the protein levels were previously shown in many studies involved several cancer subtypes [40-42].

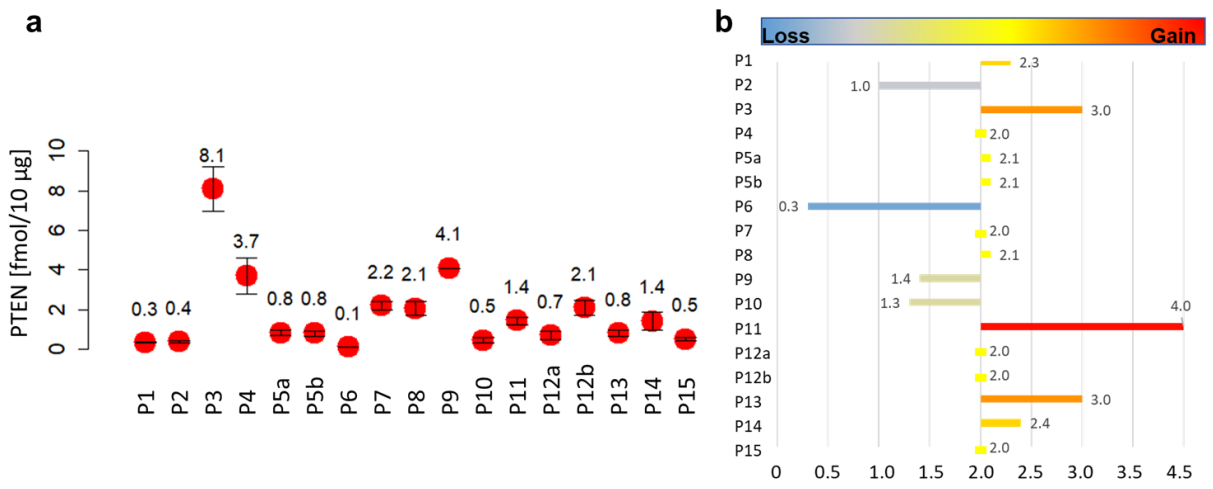

Figure 2. PTEN quantified by iMRM in FFPE cores of PDXs derived from primary and metastatic TNBC patient samples. Error bars are the ±SD of 3 technical replicates (three cores per sample).

High precision and agreement of biological replicates

All samples were analyzed by PTEN-iMRM in a single blind experiment, i.e., no information about the individual samples was provided by the biobank to avoid any bias that may be raised from handling related samples such as primary, metastatic, or biological replicates together. Moreover, determination of total protein concentrations in each extracted core sample was performed with BCA analysis in two separate 96 plates. Samples were randomly divided into four analytical batches and sample preparation and iMRM analysis were performed in four subsequent weeks, using one batch each. As previously shown, our assay again achieved a high precision, with the iMRM PTEN concentrations of biological replicates, such as P5a and P5b, being almost identical (0.83± 0.1 and 0.79±0.1 fmol/10 µg total protein), despite having been analyzed in two separate batches.

Tumor heterogeneity

Samples P12a and P12b are from two different PDXs that were derived from the same patient but from two distinct areas of the primary tumor. P12a, from the part of tumor extended to the skin, showed PTEN concentration (0.71±0.2 fmol/10 µg total protein) lower than P12b which is from the internal part of the breast tumor (2.08±0.4 fmol/10 µg total protein). It's important to mention that all samples tumor content and histopathological homogeneity were confirmed by both the H&E and the IHC of the human mitochondria. Due to the high precision of the iMRM assay discussed above, such a variation in protein expression as determined here for PTEN can

be suggested to be related to the intra-tumoral heterogeneity (also known as intra-lesion heterogeneity) or a variation of the tumor microenvironment content in the two different sections of the tumor. In general, tumor heterogeneity, either being inter-tumor or intra-tumor, is a consequence of differences in (i) cancer-cell-intrinsic parameters, such as genetic profile, interaction between the genome, epigenome/transcriptome and proteome, migration and invasion capabilities, (ii) extrinsic microenvironmental factors such as tumor hypoxia and the extent of vascularisation, interactions between cancer cells and cells of the tumor stroma, such as endothelial cells, pericytes, fibroblasts, and the contribution of a variety of tumor-infiltrating cells of the innate and the adaptive immune systems [43]. Samples P12a and P12b showed the same PTEN CNV (2.0), and hence their heterogeneity in PTEN protein level is likely to be related to transcriptional and post-transcriptional mechanisms.

PTEN iMRM concentrations and paclitaxel response

Eight out of the sixteen different PDXs showed a response to paclitaxel treatment, four of them having a BAR ≤ -30%, while the other four had a BAR between zero and -30%. The PTEN iMRM concentrations and the paclitaxel response data did not show any correlation using Pearson's correlation analysis (r^2=0.1383; y=-0.021x + 1.9337). For example, P5a and P5b had the same PTEN iMRM concentration as P13 (0.8 fmol/10 µg total protein), but had a greatly different paclitaxel response (BAR 21 days= -29% for P5a/b and 47% for P13). The same holds true for P10 and P15, with PTEN iMRM concentrations of 0.5 fmol/10 µg total protein, and paclitaxel BAR 21 days= 10% and 60%, respectively. Moreover, samples with higher PTEN iMRM concentrations such as P3 and P4 (8.1 and 3.7 fmol/10 µg total protein) showed a weaker response than P1 and P2 with lower PTEN concentrations (0.3 and 0.4 fmol/10 µg total protein respectively).

However, when all samples, metastatic and primary divided into two groups, resistant and responsive to treatment and paclitaxel response is plotted against PTEN iMRM concentrations, the two groups can be distinguished. When performing a correlation analysis for the primary and metastatic samples, separately, the iMRM PTEN concentrations determined in the metastatic samples (P4, P7, P8, P13, P14, P15) showed a very good correlation with their paclitaxel response [Pearson's correlation (r^2=0.8633; y=-0.028x + 2.3131) (Figure 3), Spearman's Rank Correlation (r_s= 0.9429; T-test = 5.7 and P-value <= 0.005)]. Despite the limited statistical power owing to the low number of samples these interesting results are supported by Zhang et al., who

have found that taxol might be more efficacious in PTEN-positive glioblastoma than in PTEN-negative glioblastoma, that showed associated increases in p-Akt and VEGF helping in maintaining survival and angiogenesis, respectively [44]. However, in a retrospective study performed by Rescigno et al. studied the relation between the antitumor activity of docetaxel in metastatic castration-resistant prostate cancer (CRPC) patients and IHC PTEN expression; there was no difference between PTEN loss and PTEN positive groups in their response to docetaxel, which was evaluated radiologically as well as clinically using progression free survival and prostate-specific antigen levels[45].

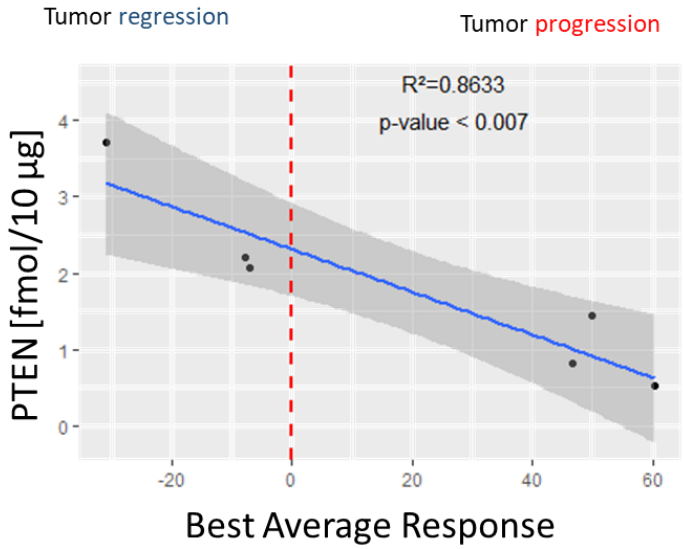

Figure 3. Correlation of PTEN concentrations in TNBC PDXs and their paclitaxel response. Response was determined as percent decrease (tumor regression) or increase (tumor progression) in tumor size. Pearson's correlation of the paclitaxel response and the PTEN concentrations of the metastatic samples.

PTEN iMRM concentrations and carboplatin response

Only four out of sixteen different PDXs showed response to carboplatin treatment, all of them having BARs ≤ -30%. The PTEN iMRM concentrations and the carboplatin response data did not show any correlation using Pearson's correlation analysis (r^2=0.011; y=-0.0026x + 1.8276). in the responsive samples, P1, P2 and P5a and P5b have low PTEN concentrations (0.3, 0.4, and 0.8 fmol/10 µg total protein, respectively), while P3 has a considerably higher PTEN concentration (8.1 fmol/10 µg total protein). The iMRM PTEN concentrations determined in metastatic samples (P1, P4, P7, P8, P13, P14 and P15) showed a weak correlation with their

carboplatin response [Pearson's correlation (r^2=0.3154; y=0.0133x + 1.2918) (Figure 4). It is worth noting that only 4 PDXs were responsive to carboplatin, which is considered as a weakness in the correlation study.

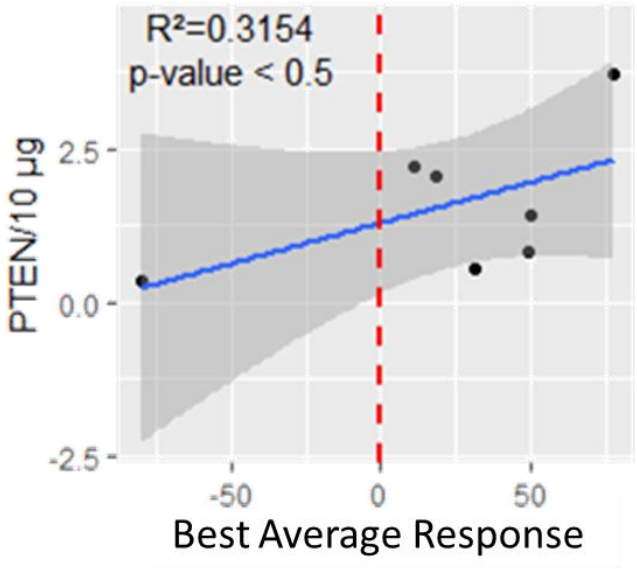

Figure 4. Correlation study of PTEN concentrations of TNBC PDXs and their carboplatin response determined as percent decrease (tumor regression) or increase (tumor progression) in tumor size. Pearson's correlation of the carboplatin response and the PTEN concentrations of the metastatic samples only.

Conclusion

The PTEN iMRM method coupled with the two-point internal calibration allows absolute quantitation as well as fine discrimination of the different PTEN protein levels of TNBC PDXs. The PDXs samples showed a high variability in PTEN levels, ranging from 0.1 – 8.1 fmol/10 µg, which underlines the high sensitivity of iMRM assay, in comparison to IHC or WB, especially needed with clinical samples. The sixteen PDXs are used for studying the response to paclitaxel and carboplatin where eight were responsive to paclitaxel and only four were responsive to carboplatin. The metastatic samples PTEN protein levels showed a very good correlation with paclitaxel response and no correlation with carboplatin response. The main limitation in this correlation study is the restricted number of PDXs. I do not consider using unhumanised and heterotopic PDXs as a limitation factor as several studies have demonstrated that ordinary PDXs

can simulate the original patients' tumors in their response to chemotherapeutics and hence could be used in drug response studies as long as it's not immunotherapy.

Another important limitation is related to the sample itself. Despite core selection was used to ensure very high tumor content, the PTEN expression level determined is the net result of the sum of PTEN expression levels of different components of the bulk tumor sample including tumor cells, tumor stem cells, normal cells, matrix cells and several types of immune cells. It is worth noted that the recent progress and future prospects of the single-cell MS-based proteomics gives the hope to enable precise protein quantitation of the individual tumor cells and assess the intra-lesion tumor heterogeneity.

References:

1. Yin, L.; Duan, J. J.; Bian, X. W.; Yu, S. C., Triple-negative breast cancer molecular subtyping and treatment progress. *Breast Cancer Res* **2020,** *22* (1), 61.
2. Howard, F. M.; Olopade, O. I., Epidemiology of Triple-Negative Breast Cancer: A Review. *Cancer J* **2021,** *27* (1), 8-16.
3. Lehmann, B. D.; Bauer, J. A.; Chen, X.; Sanders, M. E.; Chakravarthy, A. B.; Shyr, Y.; Pietenpol, J. A., Identification of human triple-negative breast cancer subtypes and preclinical models for selection of targeted therapies. *J Clin Invest* **2011,** *121* (7), 2750-67.
4. da Silva, J. L.; Rodrigues, F. R.; de Mesquita, G. G.; Fernandes, P. V.; Thuler, L. C. S.; de Melo, A. C., Triple-Negative Breast Cancer: Assessing the Role of Immunohistochemical Biomarkers on Neoadjuvant Treatment. *Breast Cancer (Dove Med Press)* **2021,** *13*, 31-44.
5. Cocco, S.; Piezzo, M.; Calabrese, A.; Cianniello, D.; Caputo, R.; Lauro, V. D.; Fusco, G.; Gioia, G. D.; Licenziato, M.; De Laurentiis, M., Biomarkers in Triple-Negative Breast Cancer: State-of-the-Art and Future Perspectives. *Int J Mol Sci* **2020,** *21* (13).
6. Gasparyan, M.; Lo, M. C.; Jiang, H.; Lin, C. C.; Sun, D., Combined p53- and PTEN-deficiency activates expression of mesenchyme homeobox 1 (MEOX1) required for growth of triple-negative breast cancer. *J Biol Chem* **2020,** *295* (34), 12188-12202.
7. Liu, J. C.; Voisin, V.; Wang, S.; Wang, D. Y.; Jones, R. A.; Datti, A.; Uehling, D.; Al-awar, R.; Egan, S. E.; Bader, G. D.; Tsao, M.; Mak, T. W.; Zacksenhaus, E., Combined deletion of Pten and p53 in mammary epithelium accelerates triple-negative breast cancer with dependency on eEF2K. *EMBO Mol Med* **2014,** *6* (12), 1542-60.
8. Wang, S.; Liu, J. C.; Kim, D.; Datti, A.; Zacksenhaus, E., Targeted Pten deletion plus p53-R270H mutation in mouse mammary epithelium induces aggressive claudin-low and basal-like breast cancer. *Breast Cancer Res* **2016,** *18* (1), 9.
9. Papadimitriou, M.; Mountzios, G.; Papadimitriou, C. A., The role of PARP inhibition in triple-negative breast cancer: Unraveling the wide spectrum of synthetic lethality. *Cancer Treat Rev* **2018,** *67*, 34-44.
10. Rieckhoff, J.; Meyer, F.; Classen, S.; Zielinski, A.; Riepen, B.; Wikman, H.; Petersen, C.; Rothkamm, K.; Borgmann, K.; Parplys, A. C., Exploiting Chromosomal Instability of PTEN-Deficient Triple-Negative Breast Cancer Cell Lines for the Sensitization against PARP1 Inhibition in a Replication-Dependent Manner. *Cancers (Basel)* **2020,** *12* (10).
11. Emens, L. A., Immunotherapy in Triple-Negative Breast Cancer. *Cancer J* **2021,** *27* (1), 59-66.
12. Barroso-Sousa, R.; Keenan, T. E.; Pernas, S.; Exman, P.; Jain, E.; Garrido-Castro, A. C.; Hughes, M.; Bychkovsky, B.; Umeton, R.; Files, J. L.; Lindeman, N. I.; MacConaill, L. E.; Hodi, F. S.; Krop, I. E.; Dillon, D.; Winer, E. P.; Wagle, N.; Lin, N. U.; Mittendorf, E. A.; Van Allen, E. M.; Tolaney, S. M., Tumor Mutational Burden and PTEN Alterations as Molecular Correlates of Response to PD-1/L1 Blockade in Metastatic Triple-Negative Breast Cancer. *Clin Cancer Res* **2020,** *26* (11), 2565-2572.
13. Carey, L. A., Finding the positive in triple-negative breast cancer. *Nat Cancer* **2021,** *2*, 476–478.
14. Martorana, F.; Motta, G.; Pavone, G.; Motta, L.; Stella, S.; Vitale, S. R.; Manzella, L.; Vigneri, P., AKT Inhibitors: New Weapons in the Fight Against Breast Cancer? *Front Pharmacol* **2021,** *12*, 662232.
15. Isakoff, S. J., Triple-negative breast cancer: role of specific chemotherapy agents. *Cancer J* **2010,** *16* (1), 53-61.

16. Caramelo, O.; Silva, C.; Caramelo, F.; Frutuoso, C.; Almeida-Santos, T., The effect of neoadjuvant platinum-based chemotherapy in BRCA mutated triple negative breast cancers - systematic review and meta-analysis. *Hered Cancer Clin Pract* **2019,** *17*, 11.
17. Wu, Q.; Siddharth, S.; Sharma, D., Triple Negative Breast Cancer: A Mountain Yet to Be Scaled Despite the Triumphs. *Cancers (Basel)* **2021,** *13* (15).
18. von Minckwitz, G.; Schneeweiss, A.; Loibl, S.; Salat, C.; Denkert, C.; Rezai, M.; Blohmer, J. U.; Jackisch, C.; Paepke, S.; Gerber, B.; Zahm, D. M.; Kummel, S.; Eidtmann, H.; Klare, P.; Huober, J.; Costa, S.; Tesch, H.; Hanusch, C.; Hilfrich, J.; Khandan, F.; Fasching, P. A.; Sinn, B. V.; Engels, K.; Mehta, K.; Nekljudova, V.; Untch, M., Neoadjuvant carboplatin in patients with triple-negative and HER2-positive early breast cancer (GeparSixto; GBG 66): a randomised phase 2 trial. *Lancet Oncol* **2014,** *15* (7), 747-56.
19. Iwase, M.; Ando, M.; Aogi, K.; Aruga, T.; Inoue, K.; Shimomura, A.; Tokunaga, E.; Masuda, N.; Yamauchi, H.; Yamashita, T.; Iwata, H., Long-term survival analysis of addition of carboplatin to neoadjuvant chemotherapy in HER2-negative breast cancer. *Breast Cancer Res Treat* **2020,** *180* (3), 687-694.
20. Isakoff, S. J.; Mayer, E. L.; He, L.; Traina, T. A.; Carey, L. A.; Krag, K. J.; Rugo, H. S.; Liu, M. C.; Stearns, V.; Come, S. E.; Timms, K. M.; Hartman, A. R.; Borger, D. R.; Finkelstein, D. M.; Garber, J. E.; Ryan, P. D.; Winer, E. P.; Goss, P. E.; Ellisen, L. W., TBCRC009: A Multicenter Phase II Clinical Trial of Platinum Monotherapy With Biomarker Assessment in Metastatic Triple-Negative Breast Cancer. *J Clin Oncol* **2015,** *33* (17), 1902-9.
21. Zhang, J.; Fan, M.; Xie, J.; Wang, Z.; Wang, B.; Zhang, S.; Wang, L.; Cao, J.; Tao, Z.; Li, T.; Hu, X., Chemotherapy of metastatic triple negative breast cancer: Experience of using platinum-based chemotherapy. *Oncotarget* **2015,** *6* (40), 43135-43.
22. Fu, X.; Tian, J.; Zhang, L.; Chen, Y.; Hao, Q., Involvement of microRNA-93, a new regulator of PTEN/Akt signaling pathway, in regulation of chemotherapeutic drug cisplatin chemosensitivity in ovarian cancer cells. *FEBS Lett* **2012,** *586* (9), 1279-86.
23. Yang, H.; Kong, W.; He, L.; Zhao, J. J.; O'Donnell, J. D.; Wang, J.; Wenham, R. M.; Coppola, D.; Kruk, P. A.; Nicosia, S. V.; Cheng, J. Q., MicroRNA expression profiling in human ovarian cancer: miR-214 induces cell survival and cisplatin resistance by targeting PTEN. *Cancer Res* **2008,** *68* (2), 425-33.
24. Chen, Q.; Qin, R.; Fang, Y.; Li, H., Berberine Sensitizes Human Ovarian Cancer Cells to Cisplatin Through miR-93/PTEN/Akt Signaling Pathway. *Cell Physiol Biochem* **2015,** *36* (3), 956-65.
25. Lebert, J. M.; Lester, R.; Powell, E.; Seal, M.; McCarthy, J., Advances in the systemic treatment of triple-negative breast cancer. *Curr Oncol* **2018,** *25* (Suppl 1), S142-S150.
26. Weaver, B. A., How Taxol/paclitaxel kills cancer cells. *Mol Biol Cell* **2014,** *25* (18), 2677-81.
27. Chan, J. J.; Tan, T. J. Y.; Dent, R. A., Novel therapeutic avenues in triple-negative breast cancer: PI3K/AKT inhibition, androgen receptor blockade, and beyond. *Ther Adv Med Oncol* **2019,** *11*, 1758835919880429.
28. Ou, Y.; Ma, L.; Ma, L.; Huang, Z.; Zhou, W.; Zhao, C.; Zhang, B.; Song, Y.; Yu, C.; Zhan, Q., Overexpression of cyclin B1 antagonizes chemotherapeutic-induced apoptosis through PTEN/Akt pathway in human esophageal squamous cell carcinoma cells. *Cancer Biol Ther* **2013,** *14* (1), 45-55.

29. Li, J.; Zhang, Y.; Zhao, J.; Kong, F.; Chen, Y., Overexpression of miR-22 reverses paclitaxel-induced chemoresistance through activation of PTEN signaling in p53-mutated colon cancer cells. *Mol Cell Biochem* **2011,** *357* (1-2), 31-8.
30. Kim, S. B.; Dent, R.; Im, S. A.; Espie, M.; Blau, S.; Tan, A. R.; Isakoff, S. J.; Oliveira, M.; Saura, C.; Wongchenko, M. J.; Kapp, A. V.; Chan, W. Y.; Singel, S. M.; Maslyar, D. J.; Baselga, J.; investigators, L., Ipatasertib plus paclitaxel versus placebo plus paclitaxel as first-line therapy for metastatic triple-negative breast cancer (LOTUS): a multicentre, randomised, double-blind, placebo-controlled, phase 2 trial. *Lancet Oncol* **2017,** *18* (10), 1360-1372.
31. Oliveira, M.; Saura, C.; Nuciforo, P.; Calvo, I.; Andersen, J.; Passos-Coelho, J. L.; Gil Gil, M.; Bermejo, B.; Patt, D. A.; Ciruelos, E.; de la Pena, L.; Xu, N.; Wongchenko, M.; Shi, Z.; Singel, S. M.; Isakoff, S. J., FAIRLANE, a double-blind placebo-controlled randomized phase II trial of neoadjuvant ipatasertib plus paclitaxel for early triple-negative breast cancer. *Ann Oncol* **2019,** *30* (8), 1289-1297.
32. Schmid, P.; Abraham, J.; Chan, S.; Wheatley, D.; Brunt, A. M.; Nemsadze, G.; Baird, R. D.; Park, Y. H.; Hall, P. S.; Perren, T.; Stein, R. C.; Mangel, L.; Ferrero, J. M.; Phillips, M.; Conibear, J.; Cortes, J.; Foxley, A.; de Bruin, E. C.; McEwen, R.; Stetson, D.; Dougherty, B.; Sarker, S. J.; Prendergast, A.; McLaughlin-Callan, M.; Burgess, M.; Lawrence, C.; Cartwright, H.; Mousa, K.; Turner, N. C., Capivasertib Plus Paclitaxel Versus Placebo Plus Paclitaxel As First-Line Therapy for Metastatic Triple-Negative Breast Cancer: The PAKT Trial. *J Clin Oncol* **2020,** *38* (5), 423-433.
33. Hidalgo, M.; Amant, F.; Biankin, A. V.; Budinska, E.; Byrne, A. T.; Caldas, C.; Clarke, R. B.; de Jong, S.; Jonkers, J.; Maelandsmo, G. M.; Roman-Roman, S.; Seoane, J.; Trusolino, L.; Villanueva, A., Patient-derived xenograft models: an emerging platform for translational cancer research. *Cancer Discov* **2014,** *4* (9), 998-1013.
34. Sulaiman, A.; Wang, L., Bridging the divide: preclinical research discrepancies between triple-negative breast cancer cell lines and patient tumors. *Oncotarget* **2017,** *8* (68), 113269-113281.
35. Hoffman, R. M., Patient-derived orthotopic xenografts: better mimic of metastasis than subcutaneous xenografts. *Nat Rev Cancer* **2015,** *15* (8), 451-2.
36. Zhang, X.; Claerhout, S.; Prat, A.; Dobrolecki, L. E.; Petrovic, I.; Lai, Q.; Landis, M. D.; Wiechmann, L.; Schiff, R.; Giuliano, M.; Wong, H.; Fuqua, S. W.; Contreras, A.; Gutierrez, C.; Huang, J.; Mao, S.; Pavlick, A. C.; Froehlich, A. M.; Wu, M. F.; Tsimelzon, A.; Hilsenbeck, S. G.; Chen, E. S.; Zuloaga, P.; Shaw, C. A.; Rimawi, M. F.; Perou, C. M.; Mills, G. B.; Chang, J. C.; Lewis, M. T., A renewable tissue resource of phenotypically stable, biologically and ethnically diverse, patient-derived human breast cancer xenograft models. *Cancer Res* **2013,** *73* (15), 4885-97.
37. Hernandez, M. C.; Yang, L.; Leiting, J. L.; Sugihara, T.; Bergquist, J. R.; Ivanics, T.; Graham, R.; Truty, M. J., Successful Secondary Engraftment of Pancreatic Ductal Adenocarcinoma and Cholangiocarcinoma Patient-Derived Xenografts After Previous Failed Primary Engraftment. *Transl Oncol* **2019,** *12* (1), 69-75.
38. Okada, S.; Vaeteewoottacharn, K.; Kariya, R., Application of Highly Immunocompromised Mice for the Establishment of Patient-Derived Xenograft (PDX) Models. *Cells* **2019,** *8* (8).
39. Gao, H.; Korn, J. M.; Ferretti, S.; Monahan, J. E.; Wang, Y.; Singh, M.; Zhang, C.; Schnell, C.; Yang, G.; Zhang, Y.; Balbin, O. A.; Barbe, S.; Cai, H.; Casey, F.; Chatterjee, S.;

Chiang, D. Y.; Chuai, S.; Cogan, S. M.; Collins, S. D.; Dammassa, E.; Ebel, N.; Embry, M.; Green, J.; Kauffmann, A.; Kowal, C.; Leary, R. J.; Lehar, J.; Liang, Y.; Loo, A.; Lorenzana, E.; Robert McDonald, E., 3rd; McLaughlin, M. E.; Merkin, J.; Meyer, R.; Naylor, T. L.; Patawaran, M.; Reddy, A.; Roelli, C.; Ruddy, D. A.; Salangsang, F.; Santacroce, F.; Singh, A. P.; Tang, Y.; Tinetto, W.; Tobler, S.; Velazquez, R.; Venkatesan, K.; Von Arx, F.; Wang, H. Q.; Wang, Z.; Wiesmann, M.; Wyss, D.; Xu, F.; Bitter, H.; Atadja, P.; Lees, E.; Hofmann, F.; Li, E.; Keen, N.; Cozens, R.; Jensen, M. R.; Pryer, N. K.; Williams, J. A.; Sellers, W. R., High-throughput screening using patient-derived tumor xenografts to predict clinical trial drug response. *Nat Med* **2015,** *21* (11), 1318-25.

40. Tyanova, S.; Albrechtsen, R.; Kronqvist, P.; Cox, J.; Mann, M.; Geiger, T., Proteomic maps of breast cancer subtypes. *Nat Commun* **2016,** *7*, 10259.

41. Zhang, B.; Wang, J.; Wang, X.; Zhu, J.; Liu, Q.; Shi, Z.; Chambers, M. C.; Zimmerman, L. J.; Shaddox, K. F.; Kim, S.; Davies, S. R.; Wang, S.; Wang, P.; Kinsinger, C. R.; Rivers, R. C.; Rodriguez, H.; Townsend, R. R.; Ellis, M. J.; Carr, S. A.; Tabb, D. L.; Coffey, R. J.; Slebos, R. J.; Liebler, D. C.; Nci, C., Proteogenomic characterization of human colon and rectal cancer. *Nature* **2014,** *513* (7518), 382-7.

42. Geiger, T.; Cox, J.; Mann, M., Proteomic changes resulting from gene copy number variations in cancer cells. *PLoS Genet* **2010,** *6* (9), e1001090.

43. Luond, F.; Tiede, S.; Christofori, G., Breast cancer as an example of tumor heterogeneity and tumor cell plasticity during malignant progression. *Br J Cancer* **2021,** *125* (2), 164-175.

44. Zhang, R.; Banik, N. L.; Ray, S. K., Differential sensitivity of human glioblastoma LN18 (PTEN-positive) and A172 (PTEN-negative) cells to Taxol for apoptosis. *Brain Res* **2008,** *1239*, 216-25.

45. Rescigno, P.; Lorente, D.; Dolling, D.; Ferraldeschi, R.; Rodrigues, D. N.; Riisnaes, R.; Miranda, S.; Bianchini, D.; Zafeiriou, Z.; Sideris, S.; Ferreira, A.; Figueiredo, I.; Sumanasuriya, S.; Mateo, J.; Perez-Lopez, R.; Sharp, A.; Tunariu, N.; de Bono, J. S., Docetaxel Treatment in PTEN- and ERG-aberrant Metastatic Prostate Cancers. *Eur Urol Oncol* **2018,** *1* (1), 71-77.

Comprehensive discussion

This thesis focusses on PTEN, the tumor-suppressor protein that is most commonly downregulated and silenced in cancer and other benign disorders, and the development of a precise and sensitive quantitation method for its expression in tissues. I hypothesize that a highly sensitive, robust MS-based assay for PTEN protein quantitation will overcome the drawbacks of other commonly used techniques, such as IHC, and will therefore allow researchers to better study PTEN's potential role as a prognostic/predictive biomarker in some cancer subtypes and hepatic disorders. My goal was (i) to develop an MRM assay and a calibration strategy that would allow precise and robust PTEN quantitation in different types of tissue samples including small FFPE cores, (ii) to confirm that this assay was highly sensitive and offered good precision (CV<20%) and accuracy (>80%), (iii) to use this validated iMRM method to quantify PTEN in different clinical specimen and test its efficacy compared to WB and IHC to ensure the robustness of our assay, and (iv) to further use this assay to study different clinical samples from different tumors and disorders in order test PTEN's prognostic/predictive role in different disorders.

The PTEN peptide NNIDDVVR was selected as the surrogate peptide and the ideal target after querying databases, enforcing specific sequence and peptide criteria, and analyzing recombinant PTEN by DDA. Interestingly, this peptide can be used to quantify PTEN from both human and mice as they share the same peptide sequence. This allows the assay to be used in analyzing samples from mice which are the most commonly used animal models in medical research.

Because liquid-chromatography triple-quadrupole mass spectrometry (LC-MS/MS) is the most prevalent tandem MS instrument currently used in clinical laboratories, an LC-MRM method for NNIDDVVR was developed and optimized on an Agilent 6495A triple quadrupole mass spectrometer, where the microflow LC conditions and collision energies for individual MRM transitions were optimized. This will facilitate the adoption of the assay by clinical laboratories as soon as PTEN's role as a biomarker has been validated and the clinical benefits have been established.

As an important step to improve confidence in the data as well as the assay robustness, the two-point internal calibration (2-PIC) strategy was developed as a better alternative to external calibration, the most commonly used calibration strategy with MRM, where surrogate matrices

are often used due to limitations in available sample material from patients. Using surrogate matrices, however, has inherent limitations for the analysis of clinical specimens, as there are often substantial variations in the sample matrix and sample amounts. The 2-PIC strategy, which is based on the use of two isotopologues spiked into each sample at two different concentrations as internal calibrators, will be very useful in increasing the robustness and precision of immuno-MS assays where mimicking the matrix is very challenging, as the background obtained after immuno-enrichment strongly depends on both the antibody used as well as the sample at hand. Through a series of experiments with the PTEN MRM, the 2-PIC strategy has demonstrated great flexibility and robustness and has yielded accurate and precise results over a reasonable range of fold-changes between the two isotopologues – covering the concentration ranges that might be expected for an analyte in a given biological sample. Moreover, quantitation of PTEN in 10 µg, 15 µg, and 30 µg of Colo-205 cell lysate by PTEN iMRM, using 2-PIC and external calibration, yielded very similar results. PTEN concentrations were determined as 0.48, 0.49, and 0.48 fmol/µg with 2-PIC (r^2= 0.998) and 0.42, 0.45, and 0.44 fmol/µg with external calibration (r^2= 0.998), with average RSDs between 2-PIC and external calibration of only 6.4%, 4.6%, and 3.7%), without requiring a surrogate matrix or additional patient material for calibration, while concurrently reducing instrument time and cost.

In this work, a fully standardized PTEN MRM assay using 2-PIC calibration has been introduced and provides PTEN quantitation with high sensitivity and precision. The performance of the assay was tested with a series of experiments presented in the Clinical Proteomic Tumor Analysis Consortium (CPTAC) guidelines[155]. The LC-MRM method showed very good linearity over a very wide range of PTEN amounts on-column (0.27 to 270 fmol), with an LOD of 0.45 fmol, and an LLOQ of 0.9 fmol, as well as high reproducibility with intra-day variations <5% and inter-day variations <16%. The LLOQ, however, was insufficient to measure PTEN in different cell lines, when digests corresponding to 100 µg of total protein were loaded on-column. Moreover, PTEN protein levels are expected to inversely correlate with disease severity.

Therefore, to boost the sensitivity of our assay, I incorporated an anti-peptide immuno-enrichment step preceding the LC-MRM analysis. With the addition of this immuno-enrichment step, the average NNIDDVVR peptide recovery in tumor tissue digest was 90%. The complete

PTEN immuno-MRM (iMRM) assay showed an average accuracy of 87%, as determined from samples with 1.5, 3, 10, 15, 45, and 100 fmol recPTEN.

The PTEN iMRM assay has been used to successfully quantify PTEN in cell lines, fresh frozen-, and formalin-fixed paraffin-embedded (FFPE) cancer tissues. PTEN levels were quantified in six different breast cancer cell lines. Three of these cell lines were HER2-positive and derived from a patient's tumor (T670) or PDXs thereof (P129, P132), where the PTEN iMRM results correlated well with the PTEN WB and inversely correlated with WB results of phosphorylated HER2 (pHER2-Tyr1221/1222) protein. The other three cell lines were commercially available cell lines from luminal A (MCF7), luminal B (BT474), and triple negative basal (MDA-MB-231) BC subtypes, after being stimulated with EGF. The average PTEN concentrations were 7.0±0.3, 5.6±0.7, 4.2±0.2, and 8.2±0.5 fmol for BT474, MCF7, MDA-231, and MDA-231+EGF, respectively, with all %CVs below 6%. MDA-231+EGF showed an approximately 2-fold increase of PTEN compared to MDA-231, indicating an impact of EGF-treatment in augmenting PTEN expression.

The difference in PTEN expression between tumor and healthy surroundings was clearly demonstrated when the PTEN iMRM assay was used to test patient fresh-frozen tissue samples from metastatic colorectal cancer (mCRC) versus the surrounding tissues. The surrounding liver tissues showed significantly higher concentrations of PTEN, which corresponded to an 8-, 11-, and 3-fold down-regulation of PTEN in the matched tumor tissues. This is a significant clinical finding that not only shows the downregulation of PTEN expression in tumor tissue, but also the variation in PTEN expression in patients with same cancer subtype compared to normal surrounding tissue. It is important to note here that the PTEN expression in normal colon tissue was almost identical to that found in proteome-wide data from ProteomicsDB. Thus, I can conclude that the difference in PTEN expression found between mCRC, and surrounding liver tissue observed by the PTEN iMRM method is indeed related to the tumorigenic down-regulation of PTEN rather than to any tissue-specific difference in PTEN expression.

The PTEN iMRM assay outperformed both WB and IHC and showed superior sensitivity. iMRM allowed the quantitation and even the clear differentiation of PTEN levels across samples that were deemed PTEN-negative by both IHC and WB, even though lower sample amounts were used for iMRM than for WB. This was shown above with the patient-derived cell line

T760, where the PTEN WB shows an absent band while its iMRM PTEN was quantified as 1.2 fmol/10 µg, despite using a lower protein amount (20 µg for iMRM vs. 50 µg for WB).

In order to precisely compare the PTEN iMRM assay with PTEN IHC and WB, I analyzed thirteen fresh-frozen tissue samples derived from HER2+ BC PDX models, including biological replicates. Samples were provided as: (i) PDX-derived fresh-frozen tissue samples embedded in OCT and analyzed with both iMRM and WB. For the PTEN WB bands, the relative PTEN expression was obtained by densitometric measurements and normalization to the respective RPS6 bands. (ii) FFPE blocks with slices taken first to perform PTEN IHC analysis and investigated by a single pathologist altogether to minimize any variability and subjectivity associated with the interpretation of IHC data. PTEN staining intensity was scored semi-quantitatively from negative to high (-, +, ++, and +++).

Three cores per block were analyzed using our iMRM assay to determine PTEN concentration. Interestingly, the PTEN concentrations determined with iMRM were consistent across biological replicates and were in a good agreement with both the semi-quantitative IHC and WB results which were obtained under ideal conditions that are not translatable into clinical laboratories. Compared to WB, the PTEN concentrations in fmol/10 µg determined by iMRM correlated well (r^2=0.7236; y = 1.3752x - 1.1643) with the relative PTEN expression results of WB analysis of the same samples. For the FFPE samples, iMRM PTEN concentrations determined were consistent i) across biological replicates, e.g. 5.7±0.1 fmol/10 µg (PTEN-IHC-high) and 0.7±0.0 fmol/10 µg (PTEN-IHC-low); (ii) across technical replicates with an average %CV of 24% for three cores analyzed from the same FFPE block; and (iii) generally showed the same trend as the IHC classification.

In order to shed the light on the prognostic role of PTEN using the now validated and fully standardized iMRM assay, I analyzed several patients' samples with mCRC, HCC, and non-neoplastic hepatic disorders. Interestingly, the variation in PTEN expression was more prominent in non-neoplastic hepatic disorders (where PTEN concentrations ranged from 1.6 to 4.4 fmol/ 10 µL) than in mCRC and HCC (where PTEN concentrations ranged from 0.3 to 2.0 and 1.3 to 3.1 fmol/ 10 µL respectively). I believe that my iMRM assay could have a critical clinical impact in the diagnosis of these disorders and cancer subtypes, where it may provide

better patient stratification and hence improve patient management through enabling a more personalized treatment.

In the mCRC samples analyzed, the lowest PTEN expression was associated with KRAS mutation and expression of MMR proteins. This clinical finding supports the probable inverse correlation that has been previously observed between PTEN expression and an mCRC patient's prognosis. In HCC, PTEN concentrations showed a moderate negative correlation with the tumor size as determined by imaging at time of diagnosis (r^2=0.5955; y=-1.1931x+5.5936). This means the lower PTEN concentration, the larger the volume of the tumor -- which is used in most staging system to indicate a later stage and hence a worse prognosis. Regarding the non-neoplastic hepatic disorders, the high variation of PTEN expression levels in the samples may greatly change our understanding of these disorders and their progression into cancer. Also, it may support the introduction of a new term, such as "pre-neoplastic", to better describe patients with PTEN expression levels lower than certain limit.

Finally, the PTEN iMRM assay has been used to analyze core samples from FFPE PDXs derived from primary and metastatic triple-negative BC samples. The mice were then treated with paclitaxel and carboplatin, and the regression in tumor size was evaluated over 21 days. The FFPE samples derived from paclitaxel-treated metastatic TNBC PDXs showed a very good correlation (r^2=0.86) between PTEN iMRM concentration and treatment-response. More samples still have to be analyzed, however, to confirm these initial results and to validate the use of PTEN as a clinically relevant biomarker of a BC patient's prognosis and response to therapy.

In addition, in this work I shed the light on the use of the PTEN genotype compared with the PTEN protein level to determine a tumor's PTEN phenotype. Here, the PTEN copy number variations (CNVs) were determined using Cytoscan HD analysis of biological replicates of the thirteen HER2+ BC PDXs, as well as the sixteen triple negative BC PDX samples mentioned above. Interestingly, no good correlation was observed between the PTEN copy number data and the PTEN protein levels determined by IHC, WB, or iMRM, demonstrating the shortcomings of using the PTEN genotype alone to determine the tumor PTEN phenotype. In contrast, PTEN iMRM enables the detection of even slight differences in PTEN concentrations in clinical samples.

There are several advantages and prospective applications of this new PTEN iMRM assay. The PTEN iMRM assay can be multiplexed with other iMRM assays. This multiplexing has been done successfully by many groups including ours[156, 157]. There are many potential targets, either inside or outside the PI3K/AKT pathway, to be considered --- resulting in possible multiplexed assays such as PI3K, AKT, S6K, GSK3β, cyclin D1, PD1, and/or PD-L1 with PTEN. Some steps in the Borchers laboratory have been already taken to start multiplexing the iMRM assays for PTEN and PD-L1. In oncology, such an assay will be very valuable in (i) verifying the regulation of PTEN on PD-L1, (ii) determining the effect of PTEN on the correlation between PD-L1 expression and clinical parameters in many cancer subtypes, especially CRC, and (iii) determining the role of PTEN loss as a mechanism responsible for resistance to anti PD-1/PD-L1 treatment. So that combinatorial strategies between PD-1/PD-L1 inhibitors and PI3K/AKT-targeting drugs can be used as an effective strategy to overcome resistance to immune checkpoint inhibition.

In addition to multiplexing, the assay can easily be modified to quantify PTEN in plasma samples. PTEN and its isoform PTEN-L can be found in extracellular fluid, either being a component of exosomes or through secretion, respectively, and hence can be found in serum and plasma. In fact, using my iMRM assay, I was able to detect endogenous PTEN from normal pooled plasma. A few groups have previously studied PTEN in serum/plasma where they compared PTEN levels in a control group with those in acute myeloid leukemia [60, 158] or gestational diabetes mellitus (GDM)[159] patients using either WB or ELISA. However, the techniques used in these studies lack the standardization, specificity, and sensitivity required to validate PTEN as a blood-based biomarker. In other words, more studies using an accurate and reproducible quantitative method are needed to ensure that the plasma/serum PTEN concentrations reflect the actual changes in tissue PTEN expression levels before the analysis of plasma or serum can replace tissue biopsy samples taken by invasive, often risky and painful procedures.

Despite that the robustness that PTEN iMRM assay shows, and the many advantages that it has already demonstrated, two main limitations should be taken into consideration when using the assay for PTEN quantitation from tissue. The first limitation is sampling. Surgical sampling of tumors does not allow the precise determination of the tumor cell PTEN expression even after ensuring the high tumor content of FFPE cores. The PTEN expression level determined is

therefore the net result of the sum of PTEN expression levels of different components of the bulk tumor sample, including tumor cells, tumor stem cells, normal cells, matrix cells, and several types of immune cells. It is worth noting that recent progress in single-cell MS-based proteomics give hope for the precise protein quantitation of individual tumor cells and better assessment of intra-lesion tumor heterogeneity. The second limitation is related to the assay's requirement for a significant amount of manual sample handling that can adversely affect throughput and reproducibility. Therefore, what I am currently working on now is the optimization of the PTEN iMRM workflow on an automated liquid-handling platform such as the Agilent Bravo. Automation of sample handling improves throughput and reduces analytical variability, and will be essential for the successful adoption of the assay by clinical laboratories.

Conclusion

After years of arduous work and dedicated effort, I am now able to conclude that my hypothesis was correct as I have succeeded in developing a fully standardized highly sensitive and robust anti-peptide immuno-multiple reaction monitoring mass spectrometry (iMRM) assay for PTEN quantitation. This new iMRM method overcomes the drawbacks of other commonly used techniques, such as IHC, and therefore will allow researchers to better study PTEN's potential role as a prognostic/predictive biomarker in some cancer subtypes and hepatic disorders. This assay includes an 11-min micro-flow LC-MRM analysis on a triple-quadrupole mass spectrometer,and showed very good linearity over a very wide range of PTEN amounts on-column (0.27 to 270 fmol), with an LOD of 0.45 fmol, and an LLOQ of 0.9 fmol, as well as a high reproducibility with intra-day variations of <5% and inter-day variations of <15%. The assay is designed to be coupled with a two-point internal calibration (2PIC) strategy that uses two peptide isotopologues as internal standards. The 2PIC method reduces instrument time and cost, and, more importantly, is able to overcome the inherent limitations of multi-point external calibration, specifically in regard to immuno-mass spectrometry assays used for the analysis of precious and scarce patients' tissue samples for the streamlined quantitation of low-abundance proteins.

PTEN iMRM assay using the 2-PIC strategy has proven to be a very precise tool for the quantitation of PTEN concentrations in cell lines, fresh frozen-, and formalin-fixed paraffin-embedded (FFPE) tissues, down to 0.1 fmol/10 µg of extracted protein, with high inter- and intra-day precision (6.3% CV). Moreover, this method makes it possible to discriminate subtle differences in PTEN protein expression in a standardized manner. PTEN protein levels in HER2+ BC patient-derived xenografts (PDX) samples that were determined by iMRM outperform the semi-quantitative IHC and WB methods produced under standardized conditions while the results of the 3 methods correlate very well. Importantly, iMRM allowed me to precisely quantify PTEN levels in samples that were deemed to be PTEN-negative by IHC or WB, while using substantially less tumor tissue.

Interesting clinical findings were obtained when the PTEN iMRM assay was used to analyze samples from patient with different cancers and diseases, including hepatocellular carcinoma (HCC), hepatic metastatic lesions of colorectal carcinomas (CRC), and non-neoplastic hepatic disorders including fatty liver disease and viral hepatitis. It should be noted that the mCRC

patients whose samples showed lowest average PTEN concentration were associated with positive KRAS mutations and deficient MMR proteins. Another important finding was that PTEN levels were found to be negatively correlated with HCC tumor size. This result was confirmed by imaging techniques at the time of diagnosis, i.e., the larger the tumor size was, the lower the PTEN level. Thus, a low PTEN level is likely to be a useful indicator of poor prognosis, and vice versa. In addition, the samples from patients suffering from severe hepatic cirrhosis showed the lowest PTEN concentrations of all of the patient samples.

The PTEN iMRM assay was also used to determine the PTEN protein levels in triple-negative BC PDX samples from micethat were treated with paclitaxel and carboplatin, in order to compare the PTEN concentrations with the PDXs' response to therapy. In these studies, I found that metastatic tumors showed a very good correlation (r^2=0.86) between paclitaxel response and the determined PTEN concentrations. This correlation will, however, require further study with higher statistical power.

Finally, after seeing the advantages and the potential applications of PTEN-level determination with my PTEN iMRM assay, it is my belief that this assay will prove to be highly valuable in medical practice and will enable researchers to finally validate its clinical usefulness and to confirm its prognostic ability to improve the better stratification of patients with a variety of different diseases and cancers.

Appendix I

Reagents

Reagents were obtained from Sigma Aldrich (Oakville, Canada), if not stated otherwise. The Bicinchoninic acid assay (BCA) kit was obtained from Thermo Scientific (Ottawa, Canada). Trypsin/Lys-C Mix, MS Grade was from Promega (Madison, USA), while TLCK treated trypsin, was purchased from Worthington (Lakewood, USA). Microcon-30 kDa Centrifugal Filters were purchased from Millipore-Sigma (Oakville, Canada). LC-MS grade acetonitrile (ACN) and water were purchased from VWR International (Montreal, Canada) and Honeywell B&J Brand (Muskegon, USA), respectively. Acetic acid was purchased from Honeywell Fluka (Montreal, Canada).

The iMRM SIS2 (NNIDDVVR+10 Da; bold letters indicate stable-isotope labeled amino acids; the total mass shift in Da is given) peptide, as well as the iMALDI NAT (AQEALDFYGEVR) and SIS1 (AQEALDFYGEV**R**+10 Da) peptides were synthesized at the University of Victoria Genome BC Proteomics Centre (Victoria, BC, Canada), and their purities and concentrations were determined by capillary zone electrophoresis and amino acid analysis, respectively.[207, 208] The iMRM NAT (NNIDDVVR) and SIS1 (NNIDDVV**R**+6 Da) and the iMALDI SIS2 (AQEA**L**DFYGEV**R**+17 Da) peptides were purchased from Synpeptides (Shanghai, China). Anti-NNIDDVVR and anti-AQEALDFYGEVR rabbit polyclonal antibodies were obtained from Signatope (Reutlingen, Germany). Protein A Dynabeads and Protein G Dynabeads were purchased from Invitrogen (Ottawa, Canada).

Cell lines samples and sample digestion

Colon adenocarcinoma Colo-205 cells were second-passage cells obtained from ATCC. Cells were mycoplasma-free and 6.66 x 10^6 cells were seeded in 10 cm dishes, and cultured in RPMI-1640 medium (ATCC 30-2001) with 10% FBS at 37°C in 5% CO_2. Cells were collected at 80% confluence within 24 h of seeding, washed with D-PBS, trypsinized (0.25% trypsin), centrifuged at 12,000 x g for 5 min, and the pellet was collected.

The Colo-205 cell pellet was washed 3 times with 1 mL of 50 mM Tris buffer (pH 8.5) and spun down at 15,000 x g for 1 min at 4 °C. Then the pellet was re-suspended in 400 µL of 2% sodium deoxycholate in 50 mM Tris, vortexed for 30 s before being centrifuged at

18,000 x g for 30 min at 4 °C. The supernatant was transferred into an Eppendorf LoBind microcentrifuge tube, and a 10 µL aliquot was used to determine total protein concentration by BCA, following the manufacturer's protocol. Twenty-µL aliquots were then prepared.

For iMRM, 7 µL of lysate (equivalent to 60 µg of total protein) were reduced with 10 mM Dithiothreitol (DTT) for 30 minutes at 56 °C, with shaking. After cooling on ice, free Cys residues were alkylated with 25 mM of iodoacetamide (IAA), incubated at 22 °C for 30 min in the dark, followed by quenching with 5 mM of DTT. Prior to proteolytic digestion, sodium deoxycholate[209] was diluted to a final concentration of below 0.3% with freshly[210] prepared 8 M urea, 100 mM TRIS-HCl, pH 7.8. The sample was then transferred to a molecular weight cutoff spin filter (Microcon-30 kDa Centrifugal Filter Unit, Millipore) for filter-aided sample preparation.[211, 212] After centrifugation at 13,500 x g for 15 minutes, the sample was washed 3 times with 200 µL of 8 M urea, 100 mM TRIS-HCl, followed by another 3 washes with 200 µL of 50 mM ammonium bicarbonate (AmBic). The filter device was transferred into a fresh LoBind microcentrifuge tube and 100 µL of 30 ng/µL Trypsin/LysC in 50 mM AmBic were added (1:20 protein:enzyme, w:w). The sample was incubated overnight at 37 °C, under gentle shaking. The generated peptides were collected by centrifugation at 13,500 x g for 15 minutes, followed by a wash with 50 µL of 50 mM AmBic, and another wash with 50 µL of dH_2O. The sample was dried in a Speedvac and reconstituted in 60 µL of 1x PBS supplemented with 0.003% CHAPS (PBSC), followed by vortexing for 1 min.

For iMALDI, the Colo-205 lysate was diluted using 20 mM TRIS+0.015% CHAPS (TRIS+C) to a final concentration of 0.5 µg/µL in a 1.5 mL Axygen MaxRecovery tube. For proteolytic digestion, aliquots of 105 µL were prepared in triplicate. The samples were denatured by adding 10.5 µL 10% DOC in 200 mM TRIS, pH 8.1 (DOC2), to a final DOC2 concentration of 0.91%, followed by incubation at 60 °C for 30 min. Then, 10.5 µL of 10 µg/µL trypsin in 1 mM HCl (1:2, w:w protein:enzyme) were added, followed by incubation at 37 °C for 1 h. The digestion was quenched by adding 10.5 µL of 850 µM Nα-Tosyl-L-lysine chloromethyl ketone hydrochloride (TLCK).

In addition, bovine serum albumin (BSA) digest was prepared as surrogate matrix for the experiments described below by first preparing a 10 mL BSA solution at a concentration of

0.1 µg/µL in TRIS+C in a Falcon® 15 mL conical centrifuge tube. The sample was digested as described above, using 1 mL 10% DOC2 for denaturation, 1 mL 2 µg/µL trypsin solution (1:2 protein:enzyme) for digestion and 1 mL 170 µM TLCK for quenching.

LC-MRM analysis

Samples were analyzed on an Agilent 6495 triple-quadrupole MS, coupled online to an Agilent 1290 Infinity UHPLC system via an ESI source with Agilent Jet Stream technology, in the positive ion mode. The capillary and nozzle voltages were set at 3500 V and 300 V, respectively. Peptides were separated using an Agilent RRHD Eclipse Plus C18 column (2.1 mm inner diameter × 150 mm length, 1.8 µm particle size), maintained at 50 °C, using a binary gradient at a flow rate of 0.4 mL/min. Mobile phases A and B consisted of 0.1% formic acid (FA), and 0.1% FA in ACN, respectively. 11-min multistep gradient was as follows. 0 min: 2 % B, 1 min: 3 % B, 8 min: 35 % B, 9.5 min: 85 % B, 10 min: 85 % B, 10.5 min, 2 % B, 11 min: 2 % B. The UHPLC system was interfaced to an Agilent 6495 triple quadrupole mass spectrometer where the peptide ions y6, y5, y4 and b3 were targeted with an MRM method using collisional energies of 19, 17, 19, and 13, respectively. MRM data was quantified with Skyline-Daily 19.1.[213, 214] Peak picking was manually checked, and data was exported to Excel.

iMALDI

Liquid handling including the washing of unconjugated beads, the addition of standards and beads to the samples, as well as the final bead washing, matrix spotting, and spot washing was done on an Agilent Bravo 96LT liquid handling platform (Santa Clara, USA).

Protein G Dynabeads were aliquoted into in an Axygen® 96-well 1.1 mL deep well plate and washed 7x with 25:75 ACN:PBS+0.015 % CHAPS (PBSC2) and 3x PBSC2 buffer, using 10x the original bead slurry volume. Afterward, beads were resuspended in the original volume of PBSC2, anti-AQEALDFYGEVR rabbit polyclonal antibodies (pAb) were added (0.2 µg pAb per 30 µg beads), and the tubes were incubated while being rotating at room temperature for 1 h. The coupled beads were stored at 4 °C while rotating, until use. Immediately before use, the coupled beads were washed 3x with PBSC2, as described above, and resuspended in PBSC2, using 10x

the original bead volume. Protein and cell lysate digests, prepared as described in the main method section, were used as the samples. Aliquots of 130 µL were prepared in in an Axygen® 96-well 1.1 mL Deep Well Plate.

A mixture of iMALDI SIS1 (AQEALDFYGEV**R**+10 Da) and SIS2 (AQEALDFYGEV**R**+17 Da) peptides was prepared and spiked into each sample as the internal standards. Next, 30 µg of antibody-coupled beads (0.2 µg antibody per replicate) were added to each sample, followed by a 1-h incubation at room temperature while shaking at 1000 RPM on a Microplate Vortex 120V ADV (Thermo Fisher, Ottawa, Canada).

After incubation, the antigen-antibody-bead complex was magnetically separated from the sample and washed 1x with 70 µL PBSC2 and 3x with 80 µL 5 mM AmBic. The beads were resuspended in 10 µL 5 mM AmBic and spotted onto a 2600 µm µFocus MALDI target (Hudson Surface Technologies, Suwon, South Korea). After the spots were dried, 1.5 µL of matrix (3 mg/mL α-cyano-4-hydroxycinnamic acid, 7 mM ammonium citrate in 70% ACN, 0.1% trifluoroacetic acid (TFA)) were added and dried using a fan. The spots were then washed 3x with 10 µL 7 mM ammonium citrate.

The MALDI plates were analyzed on a Bruker Microflex LRT (Bremen, Germany) in reflectron positive ion mode (RP). One thousand laser shots per spot, were accumulated in 25-shot intervals using a 'random walk' pattern. The data was analyzed using FlexAnalysis (v3.4, Build 70). Mass spectra were smoothed using Savitzky Golay (1 cycle, Peak width= 0.2 Da and TopHat baseline subtraction). Peaks were detected using Snap (SNAP average composition set to Averagine). Mass lists were exported and analyzed using R.[215, 216]

External calibration

To generate an external calibration curve for iMRM, eight different standard samples were created by mixing different concentrations of iMRM SIS2 (NNIDDVVR+10 Da) peptide to a constant concentration of 2 fmol/µL of SIS1 (NNIDDVVR+6 Da) in 0.1% FA, resulting in SIS2 concentrations of 0.025, 0.05, 0.125, 0.25, 0.42, 1.67, 3.33, 6.67 fmol/µL. Then, 20 µL of each standard sample were injected and analyzed by LC-MRM in triplicate, as described above.

To generate an external calibration curve for iMALDI, six standards were created with varying amounts of AQEALDFYGEVR NAT peptide in PBSC2: 0.03, 0.063, 0.125, 0.25, 0.5, and 1.0

fmol/µL. A SIS2 (AQEALDFYGEVR+17 Da) peptide standard, with a concentration of 0.088 fmol/µL, was prepared similarly.

Aliquots of 130 µL BSA digest, prepared as described above, were used as the surrogate sample matrix yielding 10 µg total protein per aliquot. These samples were spiked with 20 µL iMALDI NAT standard and 20 µL SIS2 standard, resulting in constant SIS2 amounts of 1.75 fmol per replicate and varying NAT amounts of 0.6, 1.25, 2.5, 5, 10, and 50 fmol per replicate. Three technical replicates were prepared for each standard. The samples were analyzed using iMALDI as described above.

References

1. Kuzyk, M. A.; Parker, C. E.; Domanski, D.; Borchers, C. H. In *Methods Mol. Biol.*, 2013, pp 53-82.
2. Percy, A. J.; Chambers, A. G.; Parker, C. E.; Borchers, C. H. *Methods Mol. Biol.* **2013**, *1000*, 167-189.
3. Proc, J. L.; Kuzyk, M. A.; Hardie, D. B.; Yang, J.; Smith, D. S.; Jackson, A. M.; Parker, C. E.; Borchers, C. H. *J. Proteome Res.* **2010**, *9*, 5422-5437.
4. Kollipara, L.; Zahedi, R. P. *Proteomics* **2013**, *13*, 941-944.
5. Manza, L. L.; Stamer, S. L.; Ham, A. J.; Codreanu, S. G.; Liebler, D. C. *Proteomics* **2005**, *5*, 1742-1745.
6. Wiśniewski, J. R.; Zougman, A.; Nagaraj, N.; Mann, M. *Nat Methods* **2009**, *6*, 359-362.
7. MacCoss_laboratory. *Skyline-daily*, ttps://proteome.gs.washington.edu/software/test/brendanx/Skyline-test/; Vol. 2019.
8. MacLean, B.; Tomazela, D. M.; Shulman, N.; Chambers, M.; Finney, G. L.; Frewen, B.; Kern, R.; Tabb, D. L.; Liebler, D. C.; MacCoss, M. J. *Bioinformatics* **2010**, *26*, 966-968.
9. Ihaka, R.; Gentleman, R. *Journal of Computational and Graphical Statistics* **1996**, *5*, 299-314.
10. R_Development_Core_Team. http://www.R-project.org/, Vienna, Austria, 2009.

Appendix II

Reagents

Reagents were obtained from Sigma Aldrich (Oakville, Canada), if not stated otherwise. The bicinchoninic acid assay (BCA) kit was obtained from Thermo Scientific (Ottawa, Canada). Trypsin/Lys-C Mix, MS Grade as well as Sequencing Grade Modified Trypsin were purchased from Promega (Madison, USA). Microcon-30 kDa Centrifugal Filters were purchased from Millipore-Sigma (Oakville, Canada). Solid-phase extraction (SPE) cartridges (Oasis HLB 10 mg) were purchased from Waters (Brossard, Canada). LC-MS grade acetonitrile (ACN) and water were purchased from VWR International (Montreal, Canada) and Honeywell B&J Brand (Muskegon, USA), respectively. Acetic acid was purchased from Honeywell Fluka (Montreal, Canada). All solutions used for automated IHC were obtained from Ventana Medical System, Roche (Laval, Canada) except for the mounting medium that was obtained from Eukitt, Honeywell Fluka (Montreal, Canada). MCF7 cells were obtained from ATCC (HTB-22), and Dulbecco's Modified Eagle's medium DMEM as well as heat-inactivated fetal bovine serum (FBS) were purchased from Wisent Bioproducts. Tissue-Tek Optimum cutting temperature (OCT) compound used to embed fresh frozen tissue blocks was purchased from Sakura (Torrance, USA).

The iMRM NAT (NNIDDVVR) and SIS1 (NNIDDV**V**R+6 Da; bold letters indicate stable-isotope labeled amino acids; the total mass shift in Da is given) were purchased from Synpeptide (Shanghai, China). The iMRM SIS2 (NNIDDVV**R**+10 Da) peptide was synthesized at the University of Victoria Genome BC Proteomics Centre (Victoria, BC, Canada). Peptide purity and concentration were determined by capillary zone electrophoresis and amino acid analysis, respectively [217] [218]. Rabbit polyclonal anti-NNIDDVVR peptide antibodies were obtained from Signatope [219] (Reutlingen, Germany). Protein A Dynabeads were purchased from Invitrogen (Ottawa, Canada). For PTEN IHC, rabbit monoclonal anti-PTEN (Clone138G6) was purchased from Cell Signaling Technology (Danvers, USA). The recombinant PTEN (ab84765) was purchased from Abcam (Cambridge, USA).

Clinical samples

Fresh-frozen tumor tissue and surrounding healthy tissue samples were collected from patients with hepatic metastases of colorectal cancer (mCRC). The patients were recruited at the Jewish General Hospital (JGH; Montreal, QC) and provided informed consent to participate in the JGH central biobank, protocol 10-153, which was reviewed and approved by the local Research Ethics Board (REB). The JGH biobank is affiliated with the Réseau de recherche sur le cancer (RRCancer) of the FRQS and with the Canadian Tumor Repository Network (CTRNet). Patient derived xenografts (PDX) were established from tumor tissue collected from primary or metastatic breast tumors. Patients were recruited at the JGH and provided informed consent to participate in the JGH breast biobank, protocol 05-006, which was reviewed and approved by the local Research Ethics Board (REB). All animal procedures were done in accordance with the Lady Davis Institute/McGill University animal care committee guidelines. In summary, 3-mm pieces of tumor tissue were implanted into the mammary fat pads of 4-6 week female, immunodeficient NSG mice (NOD. Cg-Prkdc ^{scid} Il2rg^{tm1Wjl}/SzJ) from Jackson Labs. Tumor growth was monitored by caliper measurements and once tumors reached at least 1000 mm^3, PDX tissue was harvested for the establishment of cell lines (such as P132 and P129) according to the Schlegel protocol [205].

Pieces of the PDX tissue samples (Supplementary Table S1) were stored snap-frozen in liquid nitrogen and extracted DNA was sent for CytoScan-HD analysis at Centre for Applied Genomics (Sick Kids Hospital, Toronto, ON). The Affymetrix Chromosome Analysis Suite [64] software was used for the visualization of copy number changes and molecular analysis was performed. Pieces of the same tissue samples were fixed in 10% neutral buffered formalin, washed, stored in 70% ethanol and sent for paraffin embedding at the Lady Davis Institute Pathology Core Facility.

A patient-derived cell line (T670) was established from a Her2+ primary breast tumor obtained at the time of surgery. The patient provided informed consent to have her tumor collected as part of the JGH breast biobank (05-006). Conditional reprogramming and cell culture were performed according to the Schlegel protocol[205].

Cell lines MDA-MB-231, MCF7, and BT-474 were obtained from ATCC (American Type Culture Collection, atcc.org) and were cultured at the JGH according to the manufacturer's

protocols. MDA-MB-231 cells were incubated with 10 ng/mL human recombinant EGF in 0.25% fetal bovine serum (FBS) for 10 min at 37 °C.

All established cell lines were regularly verified for mycoplasma contamination and confirmed free of mycoplasma. When cells reached 80% confluence, cells were scraped on ice, and the pellet was obtained by low-speed centrifugation.

Table S1: PDX samples used in this study.

Samples analyzed	PDXs Models*	Mouse number
P1	T-817	10005
P2a**	BM-156	360
P2b	BM-156	359
P3	T-786	357
P4	T-670	788
P5a	T654	174
P5b	T654	776
P6a	BM-120	518
P6b	BM-120	507
P6c	BM-120	548
P6d	BM-120	525
P7a	BM-126	371
P7b	BM-126	369

*PDXs models as established [205, 220].

**a, b, c, d: different biological replicates

LC-MRM assay development

The UniProt knowledgebase [221], Peptide Atlas [222] , the ExPASy PeptideCutter tool [223], and PeptidePicker [224] were used to select peptides that are *(i)* unique to PTEN, *(ii)* exist in all PTEN isoforms, *(iii)* while lacking any known posttranslational modifications or natural variants. [223] The peptide length had to be between 7-20 amino acids, excluding methionine (M) and cysteine (C) residues, N-terminal glutamine (Q), aspartic acid paired with proline or glycine (DP or DG), asparagine–glycine (NG) and glutamine–glycine (QG) pairs, as well as sequential proline (P) and serine (S) residues. *(v)* Furthermore, in Peptide Atlas, the selected peptides had to have a good

Empirical Suitability Score (ESS) and Empirical Observability Score (EOS) in data dependent acquisition [24] experiments. *(vi)* The peptides also had to have a predicted trypsin digestion efficiency above 95% at both their N- and C- terminal ends according to ExPASy PeptideCutter. The selection of candidate peptides was then screened for the high V-scores obtained from PeptidePicker. Next, a tryptic digest of recombinant PTEN (recPTEN) was analyzed by DDA on a Q-Exactive plus mass spectrometer (Thermo Scientific) with subsequent data analysis using Proteome Discoverer 2.0 (Thermo Scientific). Based on our DDA data we selected three peptides (AQEALDFYGEVR, IYSSNSGPTR, and NNIDDVVR) as best candidates among the previously in-silico selected surrogate peptides (supplementary Table S2). After the LC-MRM conditions for all three peptides were optimized, we observed a considerably better response and higher signal/noise for the finally selected peptide $NNIDDVVR^{2+}$ (m/z 472.7434), as exemplified Figure S1a, which shows the MRM traces for all three peptides (unscheduled run) when analyzing 50 fmol of recombinant PTEN after digestion with trypsin.

Table S2: Three peptide candidates for LC-MRM. Three peptides were selected as potential LC-MRM candidates based on both in-silico and DDA data analysis of recPTEN digest. SNP= single-nucleotide polymorphism.

Peptide sequence	Best charge state	Peptide length	Calc. Trypsin Eff. (%)	V-score	ESS	Single gene locus	PTMs	Natural variants
AQEALDFYGEVR	2+	12	100/84.5	0.77	0.83	yes	none	SNP at 155: Y to C & at 158: V to L
IYSSNSGPTR	2+	10	100/90.9	0.441	0.76	yes	none	SNP at 227: S to F
NNIDDVVR	2+	8	100/100	0.609	0.47	yes	none	none

Table S3: Optimized MRM transitions. Stable isotope-labeled amino acids in the SIS peptides as well as the quantifier transitions used are labeled in bold. CE= collision energy.

Peptide Sequence (variant)	**Precursor ion, m/z (Q1)**	**Charge state**	**Fragment ion, m/z (Q3)**	**Charge state**	**CE**
NNIDDVVR (NAT/END)	472.74	+2	**y5 - 603.31**	+1	19
			y6 - 716.39	+1	17
			y4 - 488.28	+1	19
			b3 - 342.18	+1	13
NNIDDVVR + 6 Da (SIS1)	475.75	+2	**y5 - 609.32**	+1	19
			y6 - 722.41	+1	17
			y4 - 494.30	+1	19
			b3 - 342.18	+1	13
NNIDDVVR + 10 Da (SIS2)	477.75	+2	**y5 - 613.32**	+1	19
			y6 - 726.40	+1	17
			y4 - 498.29	+1	19
			b3 - 342.18	+1	13

Table S4: LC and MS parameters of the PTEN LC-MRM method.

LC Parameters	
LC type	Agilent 1290 Infinity UHPLC system
Type of the Column	Agilent RRHD Eclipse Plus C18 column (2.1 mm inner diameter × 150 mm length, 1.8 µm particle size)
Column Temperature	50 °C
Mobile Phases	mobile phases A and B consisting of 0.1% formic acid (FA), and 0.1% FA in acetonitrile (ACN)
Flow rate	0.4 mL/min
Duration	11-min
Gradient steps	0 min: 2 % B, 1 min: 3 % B, 8 min: 35 % B, 9.5 min: 85 % B, 10 min: 85 % B, 10.5 min, 2 % B, 11 min: 2 % B.
MS Parameters	
MS type	Agilent 6495A triple-quadrupole
Ion source	ESI source with Agilent Jet Stream technology.
The capillary voltage	3500 V
The nozzle voltage	300 V
The dwell time	10 millisecond for each transition

LC-MRM response curve

A tryptic digest prepared from metastatic colon cancer liver FFPE tissue was prepared as matrix (matrix A) as follows: 200 µg of total protein lysate (in 2 % sodium deoxycholate (SDC), 10 mM dithiothreitol (DTT) in 50 mM Tris-HCl, pH 8.5) were incubated with iodoacetamide (IAA; final concentration of 25 mM) at 22 °C for 30 min in the dark, followed by quenching with 5 mM of DTT. Prior to proteolytic digestion, SDC was diluted to a final concentration <0.3% with freshly prepared urea buffer[210] (8 M urea in 100 mM TRIS-HCl, pH 7.8). The sample was then transferred to a molecular weight cutoff spin filter (Microcon-30 kDa Centrifugal Filter Unit, Millipore) for filter-aided sample preparation [206, 225]. After centrifugation at 13,500 x g for 15 minutes, the sample was washed three times with 200 µL of 8 M urea, 100 mM TRIS-HCl, followed by another three washes with 200 µL of 50 mM ammonium bicarbonate (AmBic). The filter device was transferred to a fresh protein LoBind microcentrifuge tube and Trypsin/LysC in 50 mM AmBic was added (1:20 protein:enzyme, w:w). The sample was incubated overnight at 37 °C, with gentle shaking. The peptides generated were collected by centrifugation at 13,500 x g for 15 minutes, followed by a wash with 50 µL of 50 mM AmBic, and another wash with 50

µL of H_2O (HPLC grade). The digest was dried under vacuum and reconstituted in 200 µL of 0.1 %FA (FC=1mg/mL) and aliquots were made and stored at -80 °C.

1. Ten standards were prepared as serial dilutions of SIS2 (NNIDDVV**R**+10 Da) peptide using 0.001 µg/µL matrix A in 0.1% FA: 0.27, 0.45, 0.9, 2.7, 4.5, 9, 27, 45, 90, 270 fmol/µL. Then, 5 µL of each standard was spiked into 40 µL of 0.125 µg/µL matrix digest. Blank matrix samples were prepared by adding 5 µL of 0.1% FA to 40 µL of 0.125 µg/µL matrix digest. Then, 5 µL of 10 fmol/µL SIS1 (NNIDDV**V**R+6 Da) peptide in 0.1% FA were added to each sample including blank matrix samples. The resulting 50-µL samples contained 0.027, 0.045, 0.09, 0.27, 0.45, 0.9, 2.7, 4.5, 9, or 27 fmol/µL SIS2 (NNIDDVVR+10 Da) and 1 fmol/µL SIS1 (NNIDDVVR+6 Da), in 0.1 µg/µL matrix digest. Ten µL of each resulting sample were then analyzed in triplicate by LC-MRM, as described above. Each replicate curve was acquired by injecting samples from low to high concentrations, using independently prepared replicates. Blank samples were injected three times prior to the first curve and two times prior to the following curves. A calibration curve was generated using the SIS2 to SIS1 peak area ratio, plotted against the SIS1 amounts on column, and linearity was checked by fitting a power function to the data ($y=Ax^n$, where y=peak area ratio, and x=the amount on column, where n should be > 0.95 and < 1.05). The lower limit of detection (LLOD) was defined as the lowest amount spike-in that showed a signal-to-noise (S/N) > 3. The lower limit of quantitation (LLOQ) was defined as the lowest spike-in at which the coefficient of variation (% CV) was less than 20% and the S/N was $\geq$10.

LC-MRM method repeatability test

Three concentrations of SIS2 (NNIDDVV**R**+10 Da) peptide in 0.001 µg/µL matrix A were prepared in 0.1% FA: 2.6, 80, 260 fmol/µL (low, med, high). Each day for five different days, 5 µL of each sample (low, medium, high) was spiked freshly into 40 µL of 0.125 mg/mL matrix digest that was used in the response curve experiment. Then, 5 µL of solution containing 5 fmol/µL SIS1 (NNIDDV**V**R+6 Da) peptide and 0.001 µg/µL matrix A in 0.1% FA were added to each sample. Ten µL of each resulting sample were then analyzed in triplicate by LC-MRM as described above. The samples were injected in a randomized fashion with blank samples before low-SIS2-level samples.

For each concentration, the *intra-assay variability* over 5 days was calculated by determining first the %CV of the three replicates analyzed on each day and then the mean %CV over the entire five days, i.e. the average *intra-assay* $\%CV_{intra}$ at the low standard level would be (repl=replicate, d=day):

$$\overline{\%\boldsymbol{CV}_{\boldsymbol{intra}}} = \frac{\mathbf{1}}{\mathbf{5}} \times \left(\%\boldsymbol{CV}_{\boldsymbol{d1\ repl1-3}} + \%\boldsymbol{CV}_{\boldsymbol{d2\ repl1-3}} + \%\boldsymbol{CV}_{\boldsymbol{d3\ repl1-3}} + \%\boldsymbol{CV}_{\boldsymbol{d4\ repl1-3}} + \%\boldsymbol{CV}_{\boldsymbol{d5\ repl1-3}}\right)$$

The *inter-assay variability* was calculated at each concentration by determining the %CV over all first injections across the five days, then the second injection, and then the third. These three %CVs were averaged to determine the *average inter-assay* $\%CV_{inter}$ as follows:

$$\overline{\%\boldsymbol{CV}_{\boldsymbol{inter}}} = \frac{\mathbf{1}}{\mathbf{3}} \times \left(\%\boldsymbol{CV}_{\boldsymbol{repl1\ d1-5}} + \%\boldsymbol{CV}_{\boldsymbol{repl2\ d1-5}} + \%\boldsymbol{CV}_{\boldsymbol{repl3\ d1-5}}\right)$$

The *total variability* $\%CV_{total}$ of the assay was calculated as follows:

$$\%\boldsymbol{CV}_{\boldsymbol{total}} = \sqrt{\overline{\%\boldsymbol{CV}_{\boldsymbol{intra}}}^{2} + \overline{\%\boldsymbol{CV}_{\boldsymbol{inter}}}^{2}}$$

LC-MRM method selectivity test

Tryptic digests of six different FFPE tissue samples from colon cancer metastases in the liver, including the one used in the response curve and repeatability test experiments, were used as matrix biological replicates**.** From each of the six biological replicates of matrix (10 µg total protein digest in 24 µL), three samples were prepared in duplicate as summarized in supplementary Table S5). Ten µL of each sample were then analyzed by LC-MRM as described above, in randomized order on the same day.

The LC-MRM data was analyzed with Skyline-Daily 19.1. For each sample, the results of duplicate injections were averaged, and then the SIS2/SIS1 peak-area ratios were calculated. Thus, for each of the biological replicates, three points with known SIS2 concentrations (0, 40, and 80 fmol) and their normalized peak areas were used to plot a linear regression. The slopes of the regression lines of each of the biological replicate curves were determined and the mean of these 6 slopes was determined. The slopes of all biological matrix replicates had to be within 10% of this mean to pass the selectivity test.

Table S5: Pipetting scheme of the selectivity test samples. Three samples were analyzed for each of the six biological replicates.

	Matrix A 1 mg/mL	Blank 0.1% FA	Standard A SIS2(NNIDDVVR+10 Da) [80 fmol/µL]	Standard B SIS2(NNIDDVVR+10 Da) [40 fmol/µL]	FC of SIS2 [fmol//µL]	Standard C SIS1(NNIDDVVR+6 Da) [10 fmol/µL]
Sample 1	24 µL	3 µL	-	-	0	3 µL
Sample 2	24 µL	-	3 µL	-	8	3 µL
Sample 3	24 µL	-	-	3 µL	4	3 µL

Determination of the anti-NNIDDVVR peptide immuno-enrichment recovery

The day before the immuno-enrichment, Protein A Dynabead slurry (Invitrogen, 2.8 µm, 30 µg/µL) was transferred to a fresh 2 mL tube, and the beads were washed three times and resuspended in PBS supplemented with 0.003% CHAPS (PBSC) using 10x the original bead slurry volume. Anti-NNIDDVVR rabbit polyclonal antibody was added (0.5 µg Ab per 30 µg beads), and the tube was incubated overnight at 4 °C, with shaking.

The following steps were performed in a cold room using a pre-cooled magnetic rack and pre-cooled PBSC: The antibody-coupled beads were washed three times with PBSC and then reconstituted in the PBSC, using 10x the original bead slurry volume in both cases. Twenty µL of the reconstituted antibody-bead complex (i.e. 1 µg of antibody) per sample was used for immuno-enrichment.

Four standard solutions were prepared in quadruplicate with varying amounts of SIS2 (NNIDDVV**R**+10 Da) peptide: 0.15, 0.3 and 1.0 fmol/µL in 0.1 µg/µL matrix A. Three replicates of each standard solution were used for the immuno-precipitation experiments (IP 1-3) while the fourth replicate was without IP (control). For samples IP1-3, 10 µL of the standard solution was transferred to a new 2 mL tube with 70 µL PBSC and 20 µL of the reconstituted antibody-bead complex, and incubated overnight at 4 °C, with shaking. After magnetic separation, the supernatant was discarded, and the beads were washed with 200 µL of PBSC, followed by 200 µL of 0.1x PBSC, and finally with 200 µL of H_2O. The affinity-bound peptides were eluted for 2 min with 20 µL of 3% ACN, 5% acetic acid, 50 mM citrate spiked with 40

fmol of SIS1 (NNIDDV**V**R+6 Da). For the control samples, 10 µL from each standard solution were added to 10 µL of 3% ACN, 5% acetic acid, 50 mM citrate spiked with 40 fmol SIS1. All samples were analyzed using LC-MRM as described above.

PTEN immuno-MRM method accuracy test

Seven samples were prepared to assess the accuracy of our assay, each sample containing 7.5 µg of total protein from a colorectal-cancer FFPE-tissue protein extract (in 2% SDC, 50 mM Tris-HCl, 10 mM DTT, pH 8.5) and spiked with different amount of recombinant PTEN (0, 1, 3, 10, 15, 45, 100 fmol). Three standard solutions (10, 1, and 0.1 fmol/µL, in 50 mM AmBic) of recombinant PTEN (recPTEN) were prepared from a recPTEN stock solution of 0.1 µg/µL. The samples were prepared by adding 0, 10, 30 µL of 0.1 fmol/µL recPTEN (0, 1, and 3 fmol recPTEN samples), 10 and 15 µL of 1 fmol/µL recPTEN (10 and 15 fmol recPTEN samples), and 4.5, and 10 µL of 10 fmol/µL recPTEN (45 and 100 fmol recPTEN samples).

The Samples were reduced with 10 mM DTT for 30 minutes at 56 °C and, after cooling on ice, free Cys residues were alkylated with 25 mM IAA at 22 °C for 30 min in the dark, followed by quenching with 5 mM of DTT. Prior to proteolytic digestion, SDC was diluted to a final concentration <0.3% with freshly prepared 8 M urea [210], 100 mM TRIS-HCl, pH 7.8. The samples were then transferred to molecular weight cutoff spin filters (Microcon-30 kDa Centrifugal Filter Unit, Millipore) for filter-aided sample preparation [206, 225]. After centrifugation at 13,500 x g for 15 minutes, each sample was washed three times with 200 µL of 8 M urea, 100 mM TRIS-HCl, followed by another three washes with 200 µL of 50 mM ammonium bicarbonate (AmBic). Each filter device was transferred into a fresh protein LoBind microcentrifuge tube and Trypsin/LysC in 50 mM AmBic was added (1:20 protein:enzyme, w:w). The sample was incubated overnight at 37 °C, under gentle shaking. The generated peptides were collected by centrifugation at 13,500 x g for 15 minutes, followed by a wash with 50 µL of 50 mM AmBic, and another wash with 50 µL of H_2O. A mixture of SIS1 (NNIDDV**V**R+6 Da) and SIS2 (NNIDDVV**R**+10 Da) peptides was prepared to add 2 fmol of SIS2 and 40 fmol of SIS1 to each sample [226]. Samples were dried in a Speedvac. Dried samples were resolubilized using 80 µL 1x PBSC and incubated with 20 µL of the reconstituted antibody-bead complex, prepared as described above, overnight at 4 °C, while shaking. Bead separation, washing, and peptide elution were performed as described above. PTEN concentrations were determined using our 2-PIC strategy [226] and the PTEN amount quantified

from the samples without recPTEN spike-in was subtracted from the other three samples to compensate for the endogenous PTEN level in the FFPE tissue extract.

Western blot analysis of PDX derived cell lines.

Cells from CRC-T-670, CRC-PDX-132, and CRC-PDX-129 cultures were harvested for lysis and protein extraction as previously reported [198]. 50 µg of protein extract were separated on sodium dodecyl sulfate (SDS)-polyacrylamide gels. The protein was transferred onto nitrocellulose membranes and probed with primary anti PTEN antibody (Rabbit mAb CST: 9188T, dilution 1000), anti phospho-Her-2 (TYR1221/1222) antibody (Rabbit mAb CST: 2243S, dilution 1000), RPS6 antibody (Mouse mAb CST: 74459, dilution 3000) and two secondary antibodies; anti-Rabbit IgG, HRP-liked antibody (CST: 7074s, dilution 3000) for PTEN and pHer2 while anti-Mouse IgG, HRP-liked antibody (CST: 7076s, dilution 3000) was used for RPS6. Proteins were visualized by enhanced chemiluminescence (ECL) (Amersham Biosciences).

Quantitation of PTEN protein levels in cell lines using immuno-MRM

Cell line pellets were washed 3 times with 1 mL of 50 mM Tris buffer (pH 8.5) and spun down at 15,000 x g for 1 min at 4 °C. The pellet was re-suspended in 400 µL of 2% SDC in 50 mM Tris-HCl, vortexed for 30 s, followed by centrifugation at 18,000 x g for 30 min at 4 °C. The supernatant was transferred to an Eppendorf protein LoBind microcentrifuge tube, and a 10-µL aliquot was used to determine total protein concentration based on BCA, following the manufacturer's protocol. Next, 20-µL aliquots were prepared.

FFPE sectioning and staining

FFPE thin section tissue processing, IHC, and hematoxylin and eosin (H&E) staining were performed at the Lady Davis Institute-Research Pathology Facility (JGH, Montreal). Two 4-µm thick tissue sections were cut from each FFPE block, placed on SuperFrost/Plus slides (Leica) and dried overnight at 37 °C. One slide from each block, was stained with H&E from Sigma Aldrich (Oakville, Canada) and observed under a light microscope to verify the quality of the

tissue and the homogeneity of the tumor. The other slide was loaded onto the Discovery XT Autostainer (Ventana Medical System) for PTEN IHC staining. De-paraffinization, heat-induced epitope retrieval (CC1 prediluted solution, standard protocol), and PTEN-immunostaining were performed following the recommended protocol for immunohistochemistry staining using Ventana Discovery XT. Rabbit monoclonal anti-PTEN antibody (diluted 1:40 with physiologic saline solution) was used as the primary antibody and incubated for 32 min at 37 °C. The OmniMap anti-Rb HRP was used as the secondary antibody while ChromoMap-DAB was used as the chromogen. A negative control was performed by omitting the primary antibody. Slides were counterstained with Hematoxylin for 8 min, blued with Bluing Reagent for 8 min, removed from the autostainer, washed in warm soapy water, dehydrated with graded series of ethanol alcohols, cleared in xylene, and mounted with mounting medium (Eukitt, Fluka Analytical). The slides were covered with a glass coverslip and stored in the dark at room temperature until imaged and examined under a light microscope, to score PTEN expression and to determine the percentage of necrosis.

Quantitation of PTEN levels in FFPE cores using Immuno-MRM

Each core was deparaffinized and rehydrated as using a solvent-free procedure [227]. Briefly, hot dH_2O (80 °C) was used for deparaffinization, followed by homogenization in a new tube with FFPE-lysis buffer (2 % SDC, 10 mM DTT in 50 mM Tris-HCl, pH 8.5) using a BioMasher Disposable tissue grinder from Kimble Chase (Sigma Aldrich). Samples were incubated for 20 min at 99 °C, then for 2 h at 80 °C with gentle shaking. The lysate was centrifuged at 4 °C, 18,000 g for 15 min and the supernatant was transferred to a fresh Eppendorf LoBind microcentrifuge tube. A 10-µL aliquot was used to determine total protein concentration by BCA.

Embedding of PDX-derived Fresh Frozen tissue samples in OCT

Each of the 13 fresh-frozen tissue samples was cut into three pieces on a sterile agar plate placed over dry ice and the pieces were transferred to labeled cryomolds and carefully covered with

cryogel, OCT, snap-frozen in isopentane (2-Methylbutane Millipore)/dry ice (-60 to -70°C), and then transferred to a −80 °C freezer.

Cryosections of tissues were made with a cryostat (CM3050 S Research, Leica Biosystems). The frozen tissue was cut into 4-µm thick sections that were immediately mounted onto slides. After fixation in 10% formalin, the sections were stained with H&E and examined under a light microscope to verify the quality of the tissue sections and the cell viability in %. For each of the 13 samples, the OCT-embedded fresh frozen tissue piece having the best viable tumor tissue content (> 70%) was selected to be further analyzed by PTEN-iMRM and WB.

Quantitation of PTEN levels in fresh frozen OCT blocks using immuno-MRM

Protein extraction from fresh frozen OCT blocks was performed as described by Blank-Landeshammer et al. [149]. Briefly, excess OCT around the tissue block was removed with a scalpel without compromising the embedded tissue. Each frozen tissue sample was then transferred into a 1.5 mL tube to which 300 µL of extraction buffer (4% SDS, 150 mM NaCl, 50 mM Tris-HCl, pH 8.5) were added. The samples were carefully ground using a BioMasher Disposable tissue grinder and homogenized using an ultrasonicator (Fisher Scientific Dismembrator 500) until completely suspended. Samples were incubated at 37 °C for 30 min while shaking. The lysate was centrifuged at 20 °C, 18,000 g for 30 min and the supernatant was transferred into an Eppendorf LoBind microcentrifuge tube. A 10-µL aliquot was used to determine the total protein concentration using BCA, following the manufacturer's protocol. Twenty-five-µL aliquots were prepared and stored at -80 °C.

Eighty µg of each lysate was reduced with 10 mM DTT for 30 minutes at 56 °C, while shaking. After cooling on ice, free Cys residues were alkylated with 30 mM IAA at 22 °C for 30 min in the dark. The samples were then diluted 10-fold with ice-cold ethanol and incubated at -80 °C for 2 hours. After centrifugation for 30 min at 4 °C, 12,000 x g, the supernatant was carefully discarded. The pellets were washed with 500_µL of ice-cold acetone. After another step of centrifugation for 30 min at 4 °C, 12,000 x g, the supernatants were carefully discarded, and pellets were set to dry under a laminar flow hood. Pellets were resolubilized in 160 µL of 6 M GuHCl, 50 mM AmBic, vortexed thoroughly and kept on ice. Aliquots of the lysate that were

equivalent to 10 or 20 µg of total protein were transferred to LoBind microcentrifuge tubes and guanidinium chloride (GuHCl) was diluted with 50 mM AmBic, 0.2 mM $CaCl_2$ to a final concentration of 0.2 M. Trypsin/LysC resolublized in 50 mM AmBic was added (1:20 protein:enzyme, w:w) and incubated at 37 °C, overnight, under gentle shaking. After acidification using 10% TFA (final concentration of 0.5% TFA), the samples were centrifuged at 14,000 xg for 5 min and the supernatant was then transferred to a LoBind microcentrifuge tube. Two fmol of SIS2 and 40 fmol of SIS1 were added to each sample for 2-PIC and samples were dried in a SpeedVac. Samples were immuno-enriched for NNIDDVVR peptides, analyzed by LC-MRM and endogenous PTEN concentrations as described above.

PTEN WB analysis of Fresh Frozen tissue samples

From each of the same fresh-frozen tissue samples that had been used for the PTEN immuno-MRM PTEN, 50 µg of total protein extract were separated by sodium dodecyl sulfate (SDS)-polyacrylamide gels. Proteins were transferred onto nitrocellulose membranes and probed with primary anti PTEN antibody (Rabbit mAb RAY: 88119 dilutiuon 250), RPS6 antibody (Mouse mAb CST: 74459, dilution 4000) and two secondary antibodies; anti-Rabbit IgG, HRP-liked antibody (CST: 7074s at dilution 3000) for PTEN while anti-Mouse IgG, HRP-liked antibody (CST: 7076s, dilution 3000) was used for RPS6. Proteins were visualized by enhanced chemiluminescence (ECL) (Amersham Biosciences), and the band densities were analyzed using the Image J software 1.8.0_112. PTEN intensities were normalized to RPS6 which was used as loading control, as shown previously [228]

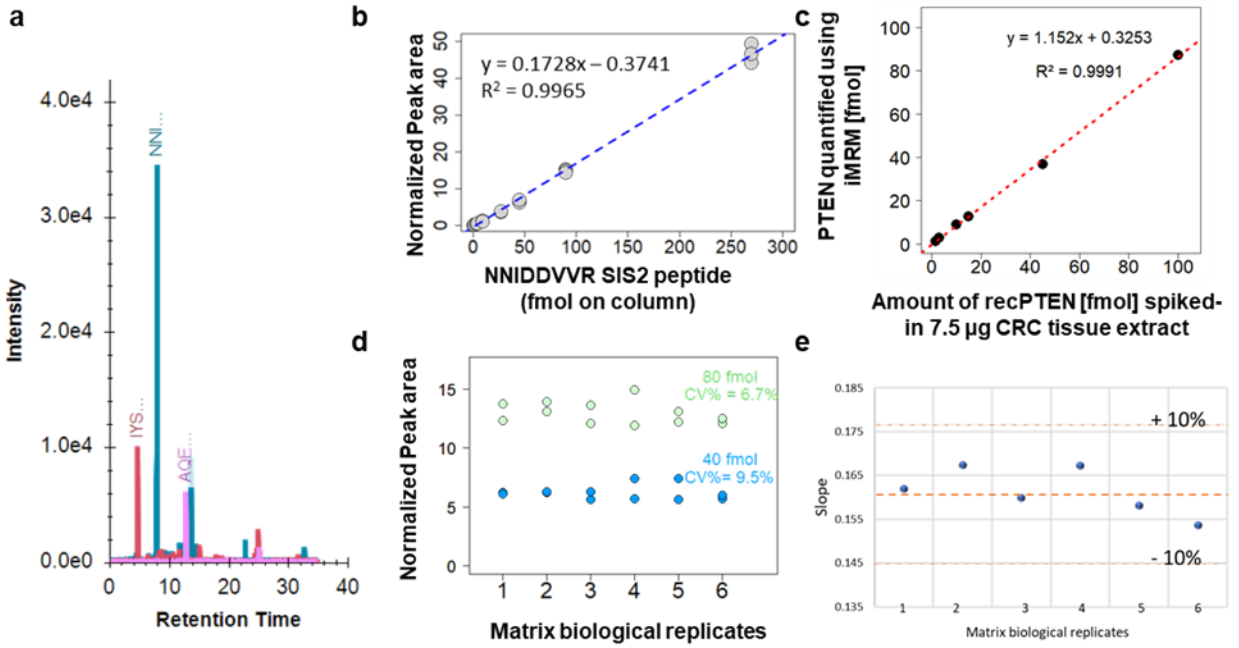

Figure S1. Development and validation of the PTEN MRM assay. (A) Unscheduled MRM traces of the three best candidate peptides according to DDA (table S2; unscheduled run). 50 fmol of recombinant PTEN were analyzed post-digestion with trypsin and after optimizing the LC-MRM conditions for all 3 peptides. We saw a considerably better response and signal/noise for the finally selected peptide NNIDDVVR^{2+} (m/z 472.743). (B) LC-MRM calibration curve with linear regression for NNIDDVVR with increasing SIS2 amounts in a constant SIS1 level. Y-axis: Normalized SIS2 peak area (normalized SIS2/SIS peak area ratio). (C) Correlation between the amount of recPTEN spiked-in and the iMRM PTEN level quantified in 4 different samples. Each sample has different level of recPTEN (0, 1.5, 3, 10, 15, 45 or 100 fmol) spiked into 7.5 µg total protein of a CRC FFPE tissue extract. The recPTEN and the quantified iMRM PTEN correlate well (r^2= 0.9991; y= 1.152x + 0.3253). (D) Selectivity test. 0, 40, and 80 fmol of SIS2 was spiked into six different CRC tumor tissues and measured by iMRM in duplicate, each. The total %CVs were 9.5% and 6.7% for the 40 and 80 fmol samples, respectively. (E) Selectivity test. The slopes of the regression lines for the six biological replicates were determined and compared. All slopes were within the 10% of their means.

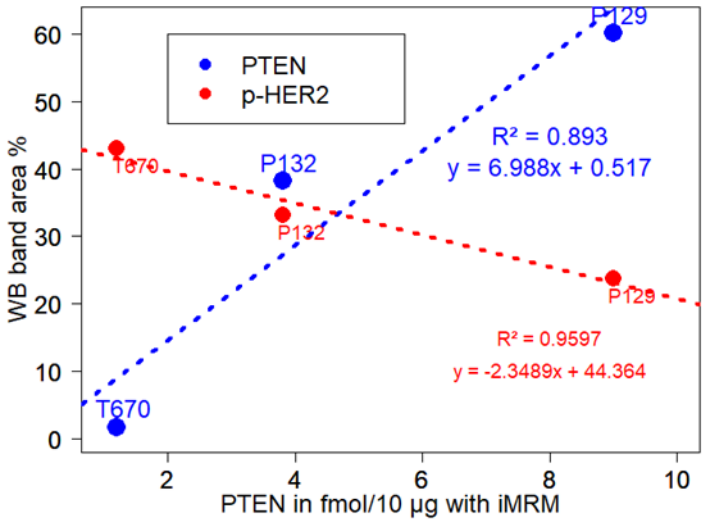

Figure S2. PTEN quantitation in cell lines. iMRM PTEN concentrations in 3 different cell lines correlate with PTEN WB band intensities (blue) and inversely correlate with HER2 phosphorylation (pHER2, red).

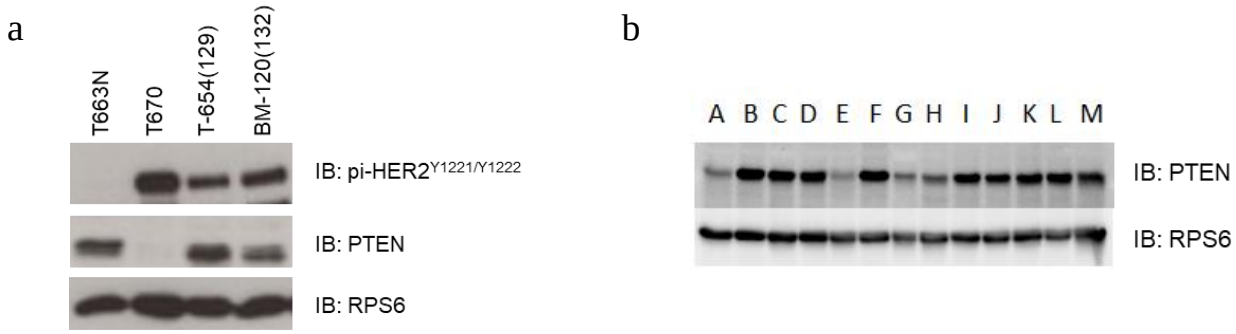

Figure S3. The original WB bands. (A) HER2 BC cell lines for PTEN, the housekeeping protein RPS6 and the phosphorylated HER2. (B) BC PDXs fresh frozen samples for PTEN as well as the housekeeping protein RPS6.

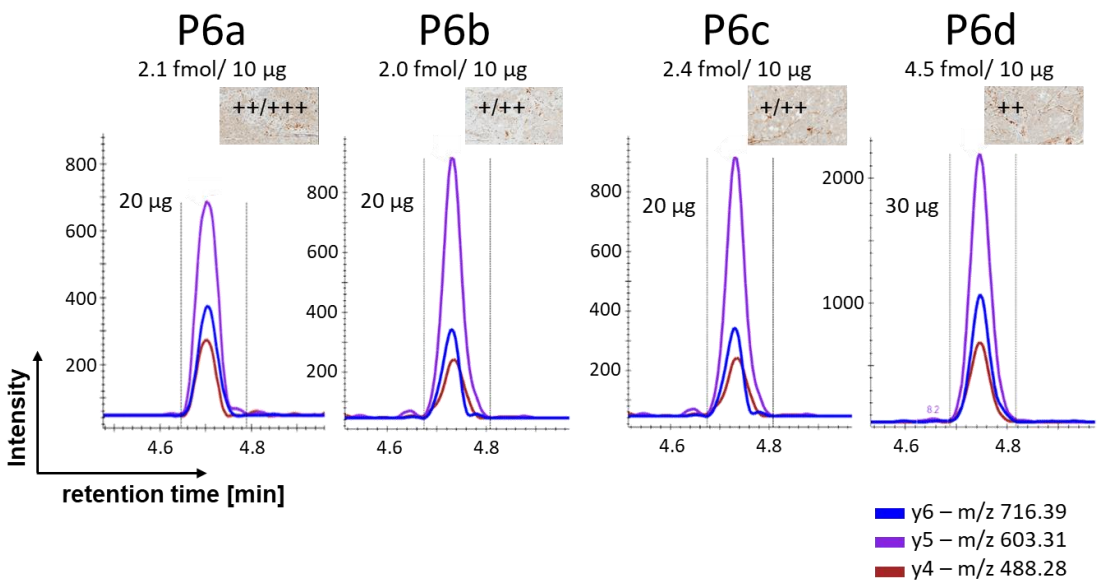

Figure S4. PTEN protein levels in FFPE PDX BC samples. Endogenous PTEN NNIDDVVR peptide signal acquired by iMRM and corresponding IHC classification from negative "-" to high "+++". Biological replicates P6a,b,c,d with moderate PTEN-IHC levels.

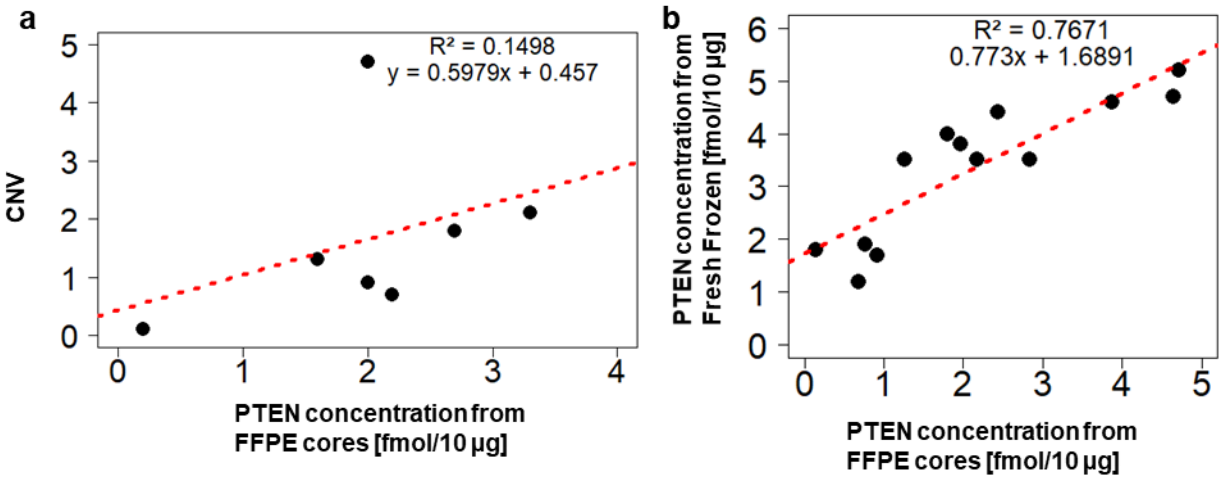

Figure S5. PTEN quantitation in BC PDX samples (a) Correlation between iMRM PTEN concentrations in FFPE cores with PTEN copy number variants (CNVs) determined for non-drug-treated replicates of the same samples. The weak correlation (r^2=0.1498; y=0.5979x-0.457) reflects the shortcomings of genomics to determine the actual PTEN tumor status. (b) Correlation between the iMRM PTEN concentrations derived from FFPE cores and matching fresh-frozen tissue samples.

References

1. Percy AJ, Chambers AG, Parker CE, Borchers CH. 2013. *Methods Mol Biol* 1000: 167-89
2. Kuzyk MA, Parker CE, Domanski D, Borchers CH. 2013. *Methods Mol Biol* 1023: 53-82
3. Hoeppe S, Schreiber TD, Planatscher H, Zell A, Templin MF, et al. 2011. *Mol Cell Proteomics* 10: M110 002857
4. Liu X, Krawczyk E, Suprynowicz FA, Palechor-Ceron N, Yuan H, et al. 2017. *Nat Protoc* 12: 439-51
5. UniProt Consortium T. 2018. *Nucleic Acids Res* 46: 2699
6. Deutsch EW, Sun Z, Campbell D, Kusebauch U, Chu CS, et al. 2015. *J Proteome Res* 14: 3461-73
7. Gasteiger E, Gattiker A, Hoogland C, Ivanyi I, Appel RD, Bairoch A. 2003. *Nucleic Acids Res* 31: 3784-8
8. Mohammed Y, Borchers CH. 2015. *J Proteomics* 129: 93-7
9. Kollipara L, Zahedi RP. 2013. *Proteomics* 13: 941-4
10. Manza LL, Stamer SL, Ham AJ, Codreanu SG, Liebler DC. 2005. *Proteomics* 5: 1742-5
11. Wisniewski JR, Zougman A, Nagaraj N, Mann M. 2009. *Nat Methods* 6: 359-62
12. Ibrahim SF, B. C. P.; Aguilar-Mahecha, A.; Aloyz, R.; Pötz, O.; Basik, M.; Batist, G.; Zahedi, R. P.; Borchers, C. Epub ahead of print.
13. Popp R, Li H, LeBlanc A, Mohammed Y, Aguilar-Mahecha A, et al. 2017. *Anal Chem* 89: 10592-600
14. Georgia Mitsa QG, Christophe Goncalves, Sam Preston, Adriana Aguilar-Mahecha, Naciba Benlimame, Mark Basik, Alan Spatz, Gerald Batist, Wilson H. Miller Jr, Sonia V. del Rincon, Rene P. Zahedi, Christoph H. Borchers. To be submitted soon.
15. Blank-Landeshammer B, Richard VR, Mitsa G, Marques M, LeBlanc A, et al. 2019. *Cancers (Basel)* 11
16. Enganti R, Cho SK, Toperzer JD, Urquidi-Camacho RA, Cakir OS, et al. 2017. *Front Plant Sci* 8: 2210
17. Whiteaker JR, Halusa GN, Hoofnagle AN, Sharma V, MacLean B, et al. 2014. *Nat Methods* 11: 703-4

References:

1. Fan, X.; Kraynak, J.; Knisely, J. P. S.; Formenti, S. C.; Shen, W. H., PTEN as a Guardian of the Genome: Pathways and Targets. *Cold Spring Harb Perspect Med* **2020,** *10* (9).
2. Conciatori, F.; Bazzichetto, C.; Falcone, I.; Ciuffreda, L.; Ferretti, G.; Vari, S.; Ferraresi, V.; Cognetti, F.; Milella, M., PTEN Function at the Interface between Cancer and Tumor Microenvironment: Implications for Response to Immunotherapy. *Int J Mol Sci* **2020,** *21* (15).
3. Chen, C. Y.; Chen, J.; He, L.; Stiles, B. L., PTEN: Tumor Suppressor and Metabolic Regulator. *Front Endocrinol (Lausanne)* **2018,** *9*, 338.
4. Fusco, N.; Sajjadi, E.; Venetis, K.; Gaudioso, G.; Lopez, G.; Corti, C.; Rocco, E. G.; Criscitiello, C.; Malapelle, U.; Invernizzi, M., PTEN Alterations and Their Role in Cancer Management: Are We Making Headway on Precision Medicine? *Genes (Basel)* **2020,** *11* (7).
5. Berger, A. H.; Knudson, A. G.; Pandolfi, P. P., A continuum model for tumor suppression. *Nature* **2011,** *476* (7359), 163-9.
6. Carbognin, L.; Miglietta, F.; Paris, I.; Dieci, M. V., Prognostic and Predictive Implications of PTEN in Breast Cancer: Unfulfilled Promises but Intriguing Perspectives. *Cancers (Basel)* **2019,** *11* (9).
7. Roh, W.; Chen, P. L.; Reuben, A.; Spencer, C. N.; Prieto, P. A.; Miller, J. P.; Gopalakrishnan, V.; Wang, F.; Cooper, Z. A.; Reddy, S. M.; Gumbs, C.; Little, L.; Chang, Q.; Chen, W. S.; Wani, K.; De Macedo, M. P.; Chen, E.; Austin-Breneman, J. L.; Jiang, H.; Roszik, J.; Tetzlaff, M. T.; Davies, M. A.; Gershenwald, J. E.; Tawbi, H.; Lazar, A. J.; Hwu, P.; Hwu, W. J.; Diab, A.; Glitza, I. C.; Patel, S. P.; Woodman, S. E.; Amaria, R. N.; Prieto, V. G.; Hu, J.; Sharma, P.; Allison, J. P.; Chin, L.; Zhang, J.; Wargo, J. A.; Futreal, P. A., Integrated molecular analysis of tumor biopsies on sequential CTLA-4 and PD-1 blockade reveals markers of response and resistance. *Sci Transl Med* **2017,** *9* (379).
8. Gygi, S. P.; Rochon, Y.; Franza, B. R.; Aebersold, R., Correlation between protein and mRNA abundance in yeast. *Mol Cell Biol* **1999,** *19* (3), 1720-30.
9. Gry, M.; Rimini, R.; Stromberg, S.; Asplund, A.; Ponten, F.; Uhlen, M.; Nilsson, P., Correlations between RNA and protein expression profiles in 23 human cell lines. *BMC Genomics* **2009,** *10*, 365.
10. Schwanhausser, B.; Busse, D.; Li, N.; Dittmar, G.; Schuchhardt, J.; Wolf, J.; Chen, W.; Selbach, M., Global quantification of mammalian gene expression control. *Nature* **2011,** *473* (7347), 337-42.
11. Swindell, W. R.; Remmer, H. A.; Sarkar, M. K.; Xing, X.; Barnes, D. H.; Wolterink, L.; Voorhees, J. J.; Nair, R. P.; Johnston, A.; Elder, J. T.; Gudjonsson, J. E., Proteogenomic analysis of psoriasis reveals discordant and concordant changes in mRNA and protein abundance. *Genome Med* **2015,** *7* (1), 86.
12. Kosti, I.; Jain, N.; Aran, D.; Butte, A. J.; Sirota, M., Cross-tissue Analysis of Gene and Protein Expression in Normal and Cancer Tissues. *Sci Rep* **2016,** *6*, 24799.
13. Edfors, F.; Danielsson, F.; Hallstrom, B. M.; Kall, L.; Lundberg, E.; Ponten, F.; Forsstrom, B.; Uhlen, M., Gene-specific correlation of RNA and protein levels in human cells and tissues. *Mol Syst Biol* **2016,** *12* (10), 883.
14. Chen, G.; Gharib, T. G.; Huang, C. C.; Taylor, J. M.; Misek, D. E.; Kardia, S. L.; Giordano, T. J.; Iannettoni, M. D.; Orringer, M. B.; Hanash, S. M.; Beer, D. G., Discordant protein and mRNA expression in lung adenocarcinomas. *Mol Cell Proteomics* **2002,** *1* (4), 304-13.

15. Lundberg, E.; Fagerberg, L.; Klevebring, D.; Matic, I.; Geiger, T.; Cox, J.; Algenas, C.; Lundeberg, J.; Mann, M.; Uhlen, M., Defining the transcriptome and proteome in three functionally different human cell lines. *Mol Syst Biol* **2010,** *6*, 450.
16. Pillai-Kastoori, L.; Heaton, S.; Shiflett, S. D.; Roberts, A. C.; Solache, A.; Schutz-Geschwender, A. R., Antibody validation for Western blot: By the user, for the user. *J Biol Chem* **2020,** *295* (4), 926-939.
17. Saper, C. B., A guide to the perplexed on the specificity of antibodies. *J Histochem Cytochem* **2009,** *57* (1), 1-5.
18. Morales-Betanzos, C. A.; Lee, H.; Gonzalez Ericsson, P. I.; Balko, J. M.; Johnson, D. B.; Zimmerman, L. J.; Liebler, D. C., Quantitative Mass Spectrometry Analysis of PD-L1 Protein Expression, N-glycosylation and Expression Stoichiometry with PD-1 and PD-L2 in Human Melanoma. *Mol Cell Proteomics* **2017,** *16* (10), 1705-1717.
19. Powers, A. D.; Palecek, S. P., Protein analytical assays for diagnosing, monitoring, and choosing treatment for cancer patients. *J Healthc Eng* **2012,** *3* (4), 503-534.
20. Goldstein, N. S.; Hewitt, S. M.; Taylor, C. R.; Yaziji, H.; Hicks, D. G.; Members of Ad-Hoc Committee On Immunohistochemistry, S., Recommendations for improved standardization of immunohistochemistry. *Appl Immunohistochem Mol Morphol* **2007,** *15* (2), 124-33.
21. Shuford, C. M.; Walters, J. J.; Holland, P. M.; Sreenivasan, U.; Askari, N.; Ray, K.; Grant, R. P., Absolute Protein Quantification by Mass Spectrometry: Not as Simple as Advertised. *Anal Chem* **2017,** *89* (14), 7406-7415.
22. Gillette, M. A.; Carr, S. A., Quantitative analysis of peptides and proteins in biomedicine by targeted mass spectrometry. *Nat Methods* **2013,** *10* (1), 28-34.
23. Mohammed, Y.; Domanski, D.; Jackson, A. M.; Smith, D. S.; Deelder, A. M.; Palmblad, M.; Borchers, C. H., PeptidePicker: a scientific workflow with web interface for selecting appropriate peptides for targeted proteomics experiments. *J Proteomics* **2014,** *106*, 151-61.
24. Peyrou, M.; Clement, S.; Maier, C.; Bourgoin, L.; Branche, E.; Conzelmann, S.; Kaddai, V.; Foti, M.; Negro, F., PTEN protein phosphatase activity regulates hepatitis C virus secretion through modulation of cholesterol metabolism. *J Hepatol* **2013,** *59* (3), 420-6.
25. Zhang, B.; Wang, J.; Wang, X.; Zhu, J.; Liu, Q.; Shi, Z.; Chambers, M. C.; Zimmerman, L. J.; Shaddox, K. F.; Kim, S.; Davies, S. R.; Wang, S.; Wang, P.; Kinsinger, C. R.; Rivers, R. C.; Rodriguez, H.; Townsend, R. R.; Ellis, M. J.; Carr, S. A.; Tabb, D. L.; Coffey, R. J.; Slebos, R. J.; Liebler, D. C.; Nci, C., Proteogenomic characterization of human colon and rectal cancer. *Nature* **2014,** *513* (7518), 382-7.
26. Alimonti, A.; Carracedo, A.; Clohessy, J. G.; Trotman, L. C.; Nardella, C.; Egia, A.; Salmena, L.; Sampieri, K.; Haveman, W. J.; Brogi, E.; Richardson, A. L.; Zhang, J.; Pandolfi, P. P., Subtle variations in Pten dose determine cancer susceptibility. *Nat Genet* **2010,** *42* (5), 454-8.
27. Zhang, H. Y.; Liang, F.; Jia, Z. L.; Song, S. T.; Jiang, Z. F., PTEN mutation, methylation and expression in breast cancer patients. *Oncol Lett* **2013,** *6* (1), 161-168.
28. Wang, L. L.; Hao, S.; Zhang, S.; Guo, L. J.; Hu, C. Y.; Zhang, G.; Gao, B.; Zhao, J. J.; Jiang, Y.; Tian, W. G.; Wang, J.; Luo, D. L., PTEN/PI3K/AKT protein expression is related to clinicopathological features and prognosis in breast cancer with axillary lymph node metastases. *Hum Pathol* **2017,** *61*, 49-57.

29. Ersahin, T.; Tuncbag, N.; Cetin-Atalay, R., The PI3K/AKT/mTOR interactive pathway. *Mol Biosyst* **2015,** *11* (7), 1946-54.
30. Liu, R.; Chen, Y.; Liu, G.; Li, C.; Song, Y.; Cao, Z.; Li, W.; Hu, J.; Lu, C.; Liu, Y., PI3K/AKT pathway as a key link modulates the multidrug resistance of cancers. *Cell Death Dis* **2020,** *11* (9), 797.
31. Miricescu, D.; Totan, A.; Stanescu, S., II; Badoiu, S. C.; Stefani, C.; Greabu, M., PI3K/AKT/mTOR Signaling Pathway in Breast Cancer: From Molecular Landscape to Clinical Aspects. *Int J Mol Sci* **2020,** *22* (1).
32. Fruman, D. A.; Chiu, H.; Hopkins, B. D.; Bagrodia, S.; Cantley, L. C.; Abraham, R. T., The PI3K Pathway in Human Disease. *Cell* **2017,** *170* (4), 605-635.
33. Meric-Bernstam, F.; Gonzalez-Angulo, A. M., Targeting the mTOR signaling network for cancer therapy. *J Clin Oncol* **2009,** *27* (13), 2278-87.
34. Cai, S. L.; Tee, A. R.; Short, J. D.; Bergeron, J. M.; Kim, J.; Shen, J.; Guo, R.; Johnson, C. L.; Kiguchi, K.; Walker, C. L., Activity of TSC2 is inhibited by AKT-mediated phosphorylation and membrane partitioning. *J Cell Biol* **2006,** *173* (2), 279-89.
35. Mikkat, S.; Kischstein, T.; Kreutzer, M.; Glocker, M. O., Mass spectrometric peptide analysis of 2DE-separated mouse spinal cord and rat hippocampus proteins suggests an NGxG motif of importance for in vivo deamidation. *Electrophoresis* **2013,** *34* (11), 1610-8.
36. LoRusso, P. M., Inhibition of the PI3K/AKT/mTOR Pathway in Solid Tumors. *J Clin Oncol* **2016,** *34* (31), 3803-3815.
37. Lee, Y. R.; Chen, M.; Pandolfi, P. P., The functions and regulation of the PTEN tumor suppressor: new modes and prospects. *Nat Rev Mol Cell Biol* **2018,** *19* (9), 547-562.
38. Jerde, T. J., Phosphatase and Tensin Homologue: Novel Regulation by Developmental Signaling. *J Signal Transduct* **2015,** *2015*, 282567.
39. Kalli, A. C.; Devaney, I.; Sansom, M. S., Interactions of phosphatase and tensin homologue (PTEN) proteins with phosphatidylinositol phosphates: insights from molecular dynamics simulations of PTEN and voltage sensitive phosphatase. *Biochemistry* **2014,** *53* (11), 1724-32.
40. Taylor, J.; Abdel-Wahab, O., PTEN isoforms with dual and opposing function. *Nat Cell Biol* **2019,** *21* (11), 1306-1308.
41. Wang, L.; Cho, Y. L.; Tang, Y.; Wang, J.; Park, J. E.; Wu, Y.; Wang, C.; Tong, Y.; Chawla, R.; Zhang, J.; Shi, Y.; Deng, S.; Lu, G.; Wu, Y.; Tan, H. W.; Pawijit, P.; Lim, G. G.; Chan, H. Y.; Zhang, J.; Fang, L.; Yu, H.; Liou, Y. C.; Karthik, M.; Bay, B. H.; Lim, K. L.; Sze, S. K.; Yap, C. T.; Shen, H. M., PTEN-L is a novel protein phosphatase for ubiquitin dephosphorylation to inhibit PINK1-Parkin-mediated mitophagy. *Cell Res* **2018,** *28* (8), 787-802.
42. Liang, H.; Chen, X.; Yin, Q.; Ruan, D.; Zhao, X.; Zhang, C.; McNutt, M. A.; Yin, Y., PTENbeta is an alternatively translated isoform of PTEN that regulates rDNA transcription. *Nat Commun* **2017,** *8*, 14771.
43. Nguyen, H. N.; Afkari, Y.; Senoo, H.; Sesaki, H.; Devreotes, P. N.; Iijima, M., Mechanism of human PTEN localization revealed by heterologous expression in Dictyostelium. *Oncogene* **2014,** *33* (50), 5688-96.
44. Qian, X.; Li, X.; Shi, Z.; Xia, Y.; Cai, Q.; Xu, D.; Tan, L.; Du, L.; Zheng, Y.; Zhao, D.; Zhang, C.; Lorenzi, P. L.; You, Y.; Jiang, B. H.; Jiang, T.; Li, H.; Lu, Z., PTEN Suppresses Glycolysis by Dephosphorylating and Inhibiting Autophosphorylated PGK1. *Mol Cell* **2019,** *76* (3), 516-527 e7.

45. Zhang, S.; Huang, W. C.; Li, P.; Guo, H.; Poh, S. B.; Brady, S. W.; Xiong, Y.; Tseng, L. M.; Li, S. H.; Ding, Z.; Sahin, A. A.; Esteva, F. J.; Hortobagyi, G. N.; Yu, D., Combating trastuzumab resistance by targeting SRC, a common node downstream of multiple resistance pathways. *Nat Med* **2011,** *17* (4), 461-9.
46. Shi, Y.; Wang, J.; Chandarlapaty, S.; Cross, J.; Thompson, C.; Rosen, N.; Jiang, X., PTEN is a protein tyrosine phosphatase for IRS1. *Nat Struct Mol Biol* **2014,** *21* (6), 522-7.
47. Kuchay, S.; Giorgi, C.; Simoneschi, D.; Pagan, J.; Missiroli, S.; Saraf, A.; Florens, L.; Washburn, M. P.; Collazo-Lorduy, A.; Castillo-Martin, M.; Cordon-Cardo, C.; Sebti, S. M.; Pinton, P.; Pagano, M., PTEN counteracts FBXL2 to promote IP3R3- and Ca(2+)-mediated apoptosis limiting tumor growth. *Nature* **2017,** *546* (7659), 554-558.
48. Zhao, D.; Lu, X.; Wang, G.; Lan, Z.; Liao, W.; Li, J.; Liang, X.; Chen, J. R.; Shah, S.; Shang, X.; Tang, M.; Deng, P.; Dey, P.; Chakravarti, D.; Chen, P.; Spring, D. J.; Navone, N. M.; Troncoso, P.; Zhang, J.; Wang, Y. A.; DePinho, R. A., Synthetic essentiality of chromatin remodelling factor CHD1 in PTEN-deficient cancer. *Nature* **2017,** *542* (7642), 484-488.
49. Song, M. S.; Salmena, L.; Pandolfi, P. P., The functions and regulation of the PTEN tumor suppressor. *Nat Rev Mol Cell Biol* **2012,** *13* (5), 283-96.
50. Aquila, S.; Santoro, M.; Caputo, A.; Panno, M. L.; Pezzi, V.; De Amicis, F., The Tumor Suppressor PTEN as Molecular Switch Node Regulating Cell Metabolism and Autophagy: Implications in Immune System and Tumor Microenvironment. *Cells* **2020,** *9* (7).
51. Song, M.; Chen, D.; Lu, B.; Wang, C.; Zhang, J.; Huang, L.; Wang, X.; Timmons, C. L.; Hu, J.; Liu, B.; Wu, X.; Wang, L.; Wang, J.; Liu, H., PTEN loss increases PD-L1 protein expression and affects the correlation between PD-L1 expression and clinical parameters in colorectal cancer. *PLoS One* **2013,** *8* (6), e65821.
52. Zhao, L.; Li, C.; Liu, F.; Zhao, Y.; Liu, J.; Hua, Y.; Liu, J.; Huang, J.; Ge, C., A blockade of PD-L1 produced antitumor and antimetastatic effects in an orthotopic mouse pancreatic cancer model via the PI3K/Akt/mTOR signaling pathway. *Onco Targets Ther* **2017,** *10*, 2115-2126.
53. Parikh, A. R.; Ali, S. M.; Schrock, A. B.; Albacker, L. A.; Miller, V. A.; Stephens, P. J.; Crilley, P.; Markman, M., Response to rapamycin analogs but not PD-1 inhibitors in PTEN-mutated metastatic non-small-cell lung cancer with high tumor mutational burden. *Lung Cancer (Auckl)* **2018,** *9*, 45-47.
54. Chen, H.; Chong, W.; Teng, C.; Yao, Y.; Wang, X.; Li, X., The immune response-related mutational signatures and driver genes in non-small-cell lung cancer. *Cancer Sci* **2019,** *110* (8), 2348-2356.
55. Cai, J.; Li, R.; Xu, X.; Zhang, L.; Lian, R.; Fang, L.; Huang, Y.; Feng, X.; Liu, X.; Li, X.; Zhu, X.; Zhang, H.; Wu, J.; Zeng, M.; Song, E.; He, Y.; Yin, Y.; Li, J.; Li, M., CK1alpha suppresses lung tumor growth by stabilizing PTEN and inducing autophagy. *Nat Cell Biol* **2018,** *20* (4), 465-478.
56. Milella, M.; Falcone, I.; Conciatori, F.; Cesta Incani, U.; Del Curatolo, A.; Inzerilli, N.; Nuzzo, C. M.; Vaccaro, V.; Vari, S.; Cognetti, F.; Ciuffreda, L., PTEN: Multiple Functions in Human Malignant Tumors. *Front Oncol* **2015,** *5*, 24.
57. Hobert, J. A.; Eng, C., PTEN hamartoma tumor syndrome: an overview. *Genet Med* **2009,** *11* (10), 687-94.
58. Bermudez Brito, M.; Goulielmaki, E.; Papakonstanti, E. A., Focus on PTEN Regulation. *Front Oncol* **2015,** *5*, 166.

59. Chia, Y. C.; Catimel, B.; Lio, D. S.; Ang, C. S.; Peng, B.; Wu, H.; Zhu, H. J.; Cheng, H. C., The C-terminal tail inhibitory phosphorylation sites of PTEN regulate its intrinsic catalytic activity and the kinetics of its binding to phosphatidylinositol-4,5-bisphosphate. *Arch Biochem Biophys* **2015,** *587*, 48-60.
60. Chen, L.; Liu, S.; Tao, Y., Regulating tumor suppressor genes: post-translational modifications. *Signal Transduct Target Ther* **2020,** *5* (1), 90.
61. Xia, Q.; Ali, S.; Liu, L.; Li, Y.; Liu, X.; Zhang, L.; Dong, L., Role of Ubiquitination in PTEN Cellular Homeostasis and Its Implications in GB Drug Resistance. *Front Oncol* **2020,** *10*, 1569.
62. Chen, Z.; Dempsey, D. R.; Thomas, S. N.; Hayward, D.; Bolduc, D. M.; Cole, P. A., Molecular Features of Phosphatase and Tensin Homolog (PTEN) Regulation by C-terminal Phosphorylation. *J Biol Chem* **2016,** *291* (27), 14160-14169.
63. Hess, D. T.; Stamler, J. S., Regulation by S-nitrosylation of protein post-translational modification. *J Biol Chem* **2012,** *287* (7), 4411-8.
64. Meng, Z.; Jia, L. F.; Gan, Y. H., PTEN activation through K163 acetylation by inhibiting HDAC6 contributes to tumor inhibition. *Oncogene* **2016,** *35* (18), 2333-44.
65. Matunis, M. J.; Guzzo, C. M., SUMO, PTEN and Tumor Suppression. *Pigment Cell Melanoma Res* **2012**.
66. Ojo, D.; Wu, Y.; Bane, A.; Tang, D., A role of SIPL1/SHARPIN in promoting resistance to hormone therapy in breast cancer. *Biochim Biophys Acta Mol Basis Dis* **2018,** *1864* (3), 735-745.
67. Cao, J.; Wan, L.; Hacker, E.; Dai, X.; Lenna, S.; Jimenez-Cervantes, C.; Wang, Y.; Leslie, N. R.; Xu, G. X.; Widlund, H. R.; Ryu, B.; Alani, R. M.; Dutton-Regester, K.; Goding, C. R.; Hayward, N. K.; Wei, W.; Cui, R., MC1R is a potent regulator of PTEN after UV exposure in melanocytes. *Mol Cell* **2013,** *51* (4), 409-22.
68. Lima-Fernandes, E.; Enslen, H.; Camand, E.; Kotelevets, L.; Boularan, C.; Achour, L.; Benmerah, A.; Gibson, L. C.; Baillie, G. S.; Pitcher, J. A.; Chastre, E.; Etienne-Manneville, S.; Marullo, S.; Scott, M. G., Distinct functional outputs of PTEN signalling are controlled by dynamic association with beta-arrestins. *EMBO J* **2011,** *30* (13), 2557-68.
69. van Diepen, M. T.; Parsons, M.; Downes, C. P.; Leslie, N. R.; Hindges, R.; Eickholt, B. J., MyosinV controls PTEN function and neuronal cell size. *Nat Cell Biol* **2009,** *11* (10), 1191-6.
70. Carlberg, C.; Velleuer, E., Tumor Suppressor Genes and Cell Fate Control. In *Cancer Biology: How Science Works*, Springer International Publishing: Cham, 2021; pp 29-40.
71. Salmena, L.; Carracedo, A.; Pandolfi, P. P., Tenets of PTEN tumor suppression. *Cell* **2008,** *133* (3), 403-14.
72. Bray, F.; Ferlay, J.; Soerjomataram, I.; Siegel, R. L.; Torre, L. A.; Jemal, A., Global cancer statistics 2018: GLOBOCAN estimates of incidence and mortality worldwide for 36 cancers in 185 countries. *CA Cancer J Clin* **2018,** *68* (6), 394-424.
73. Bihani, T.; Patel, H. K.; Arlt, H.; Tao, N.; Jiang, H.; Brown, J. L.; Purandare, D. M.; Hattersley, G.; Garner, F., Elacestrant (RAD1901), a Selective Estrogen Receptor Degrader (SERD), Has Antitumor Activity in Multiple ER(+) Breast Cancer Patient-derived Xenograft Models. *Clin Cancer Res* **2017,** *23* (16), 4793-4804.
74. Batoo, S.; Bayraktar, S.; Al-Hattab, E.; Basu, S.; Okuno, S.; Gluck, S., Recent advances and optimal management of human epidermal growth factor receptor-2-positive early-stage breast cancer. *J Carcinog* **2019,** *18*, 5.

75. Kotecki, N.; Gombos, A.; Awada, A., Adjuvant therapeutic approaches of HER2-positive breast cancer with a focus on neratinib maleate. *Expert Rev Anticancer Ther* **2019,** *19* (6), 447-454.
76. Lehmann, B. D.; Bauer, J. A.; Chen, X.; Sanders, M. E.; Chakravarthy, A. B.; Shyr, Y.; Pietenpol, J. A., Identification of human triple-negative breast cancer subtypes and preclinical models for selection of targeted therapies. *J Clin Invest* **2011,** *121* (7), 2750-67.
77. Tutt, A.; Tovey, H.; Cheang, M. C. U.; Kernaghan, S.; Kilburn, L.; Gazinska, P.; Owen, J.; Abraham, J.; Barrett, S.; Barrett-Lee, P.; Brown, R.; Chan, S.; Dowsett, M.; Flanagan, J. M.; Fox, L.; Grigoriadis, A.; Gutin, A.; Harper-Wynne, C.; Hatton, M. Q.; Hoadley, K. A.; Parikh, J.; Parker, P.; Perou, C. M.; Roylance, R.; Shah, V.; Shaw, A.; Smith, I. E.; Timms, K. M.; Wardley, A. M.; Wilson, G.; Gillett, C.; Lanchbury, J. S.; Ashworth, A.; Rahman, N.; Harries, M.; Ellis, P.; Pinder, S. E.; Bliss, J. M., Carboplatin in BRCA1/2-mutated and triple-negative breast cancer BRCAness subgroups: the TNT Trial. *Nat Med* **2018,** *24* (5), 628-637.
78. Martin, H. L.; Smith, L.; Tomlinson, D. C., Multidrug-resistant breast cancer: current perspectives. *Breast Cancer (Dove Med Press)* **2014,** *6*, 1-13.
79. Fu, X.; Creighton, C. J.; Biswal, N. C.; Kumar, V.; Shea, M.; Herrera, S.; Contreras, A.; Gutierrez, C.; Wang, T.; Nanda, S.; Giuliano, M.; Morrison, G.; Nardone, A.; Karlin, K. L.; Westbrook, T. F.; Heiser, L. M.; Anur, P.; Spellman, P.; Guichard, S. M.; Smith, P. D.; Davies, B. R.; Klinowska, T.; Lee, A. V.; Mills, G. B.; Rimawi, M. F.; Hilsenbeck, S. G.; Gray, J. W.; Joshi, A.; Osborne, C. K.; Schiff, R., Overcoming endocrine resistance due to reduced PTEN levels in estrogen receptor-positive breast cancer by co-targeting mammalian target of rapamycin, protein kinase B, or mitogen-activated protein kinase kinase. *Breast Cancer Res* **2014,** *16* (5), 430.
80. Ponde, N.; Brandao, M.; El-Hachem, G.; Werbrouck, E.; Piccart, M., Treatment of advanced HER2-positive breast cancer: 2018 and beyond. *Cancer Treat Rev* **2018,** *67*, 10-20.
81. Li, G.; Guo, J.; Shen, B. Q.; Yadav, D. B.; Sliwkowski, M. X.; Crocker, L. M.; Lacap, J. A.; Phillips, G. D. L., Mechanisms of Acquired Resistance to Trastuzumab Emtansine in Breast Cancer Cells. *Mol Cancer Ther* **2018,** *17* (7), 1441-1453.
82. Pascual, J.; Turner, N. C., Targeting the PI3-kinase pathway in triple-negative breast cancer. *Ann Oncol* **2019,** *30* (7), 1051-1060.
83. Ciruelos Gil, E. M., Targeting the PI3K/AKT/mTOR pathway in estrogen receptor-positive breast cancer. *Cancer Treat Rev* **2014,** *40* (7), 862-71.
84. Lee, J. J.; Loh, K.; Yap, Y. S., PI3K/Akt/mTOR inhibitors in breast cancer. *Cancer Biol Med* **2015,** *12* (4), 342-54.
85. Costa, R. L. B.; Han, H. S.; Gradishar, W. J., Targeting the PI3K/AKT/mTOR pathway in triple-negative breast cancer: a review. *Breast Cancer Res Treat* **2018,** *169* (3), 397-406.
86. Razavi, P.; Dickler, M. N.; Shah, P. D.; Toy, W.; Brown, D. N.; Won, H. H.; Li, B. T.; Shen, R.; Vasan, N.; Modi, S.; Jhaveri, K.; Caravella, B. A.; Patil, S.; Selenica, P.; Zamora, S.; Cowan, A. M.; Comen, E.; Singh, A.; Covey, A.; Berger, M. F.; Hudis, C. A.; Norton, L.; Nagy, R. J.; Odegaard, J. I.; Lanman, R. B.; Solit, D. B.; Robson, M. E.; Lacouture, M. E.; Brogi, E.; Reis-Filho, J. S.; Moynahan, M. E.; Scaltriti, M.; Chandarlapaty, S., Alterations in PTEN and ESR1 promote clinical resistance to alpelisib plus aromatase inhibitors. *Nat Cancer* **2020,** *1* (4), 382-393.
87. Kim, S. B.; Dent, R.; Im, S. A.; Espie, M.; Blau, S.; Tan, A. R.; Isakoff, S. J.; Oliveira, M.; Saura, C.; Wongchenko, M. J.; Kapp, A. V.; Chan, W. Y.; Singel, S. M.;

Maslyar, D. J.; Baselga, J.; investigators, L., Ipatasertib plus paclitaxel versus placebo plus paclitaxel as first-line therapy for metastatic triple-negative breast cancer (LOTUS): a multicentre, randomised, double-blind, placebo-controlled, phase 2 trial. *Lancet Oncol* **2017,** *18* (10), 1360-1372.
88. Lopez, G.; Noale, M.; Corti, C.; Gaudioso, G.; Sajjadi, E.; Venetis, K.; Gambini, D.; Runza, L.; Costanza, J.; Pesenti, C.; Grossi, F.; Maggi, S.; Ferrero, S.; Bosari, S.; Fusco, N., PTEN Expression as a Complementary Biomarker for Mismatch Repair Testing in Breast Cancer. *Int J Mol Sci* **2020,** *21* (4).
89. Burnett, J. P.; Korkaya, H.; Ouzounova, M. D.; Jiang, H.; Conley, S. J.; Newman, B. W.; Sun, L.; Connarn, J. N.; Chen, C. S.; Zhang, N.; Wicha, M. S.; Sun, D., Trastuzumab resistance induces EMT to transform HER2(+) PTEN(-) to a triple negative breast cancer that requires unique treatment options. *Sci Rep* **2015,** *5*, 15821.
90. Perez, E. A.; Dueck, A. C.; McCullough, A. E.; Chen, B.; Geiger, X. J.; Jenkins, R. B.; Lingle, W. L.; Davidson, N. E.; Martino, S.; Kaufman, P. A.; Kutteh, L. A.; Sledge, G. W.; Harris, L. N.; Gralow, J. R.; Reinholz, M. M., Impact of PTEN protein expression on benefit from adjuvant trastuzumab in early-stage human epidermal growth factor receptor 2-positive breast cancer in the North Central Cancer Treatment Group N9831 trial. *J Clin Oncol* **2013,** *31* (17), 2115-22.
91. Nuciforo, P. G.; Aura, C.; Holmes, E.; Prudkin, L.; Jimenez, J.; Martinez, P.; Ameels, H.; de la Pena, L.; Ellis, C.; Eidtmann, H.; Piccart-Gebhart, M. J.; Scaltriti, M.; Baselga, J., Benefit to neoadjuvant anti-human epidermal growth factor receptor 2 (HER2)-targeted therapies in HER2-positive primary breast cancer is independent of phosphatase and tensin homolog deleted from chromosome 10 (PTEN) status. *Ann Oncol* **2015,** *26* (7), 1494-500.
92. Kim, S. B.; Wildiers, H.; Krop, I. E.; Smitt, M.; Yu, R.; Lysbet de Haas, S.; Gonzalez-Martin, A., Relationship between tumor biomarkers and efficacy in TH3RESA, a phase III study of trastuzumab emtansine (T-DM1) vs. treatment of physician's choice in previously treated HER2-positive advanced breast cancer. *Int J Cancer* **2016,** *139* (10), 2336-42.
93. Jones, R. H.; Casbard, A.; Carucci, M.; Cox, C.; Butler, R.; Alchami, F.; Madden, T. A.; Bale, C.; Bezecny, P.; Joffe, J.; Moon, S.; Twelves, C.; Venkitaraman, R.; Waters, S.; Foxley, A.; Howell, S. J., Fulvestrant plus capivasertib versus placebo after relapse or progression on an aromatase inhibitor in metastatic, oestrogen receptor-positive breast cancer (FAKTION): a multicentre, randomised, controlled, phase 2 trial. *Lancet Oncol* **2020,** *21* (3), 345-357.
94. Lech, G.; Slotwinski, R.; Slodkowski, M.; Krasnodebski, I. W., Colorectal cancer tumor markers and biomarkers: Recent therapeutic advances. *World J Gastroenterol* **2016,** *22* (5), 1745-55.
95. Sawai, H.; Yasuda, A.; Ochi, N.; Ma, J.; Matsuo, Y.; Wakasugi, T.; Takahashi, H.; Funahashi, H.; Sato, M.; Takeyama, H., Loss of PTEN expression is associated with colorectal cancer liver metastasis and poor patient survival. *BMC Gastroenterol* **2008,** *8*, 56.
96. Lin, M. S.; Huang, J. X.; Chen, W. C.; Zhang, B. F.; Fang, J.; Zhou, Q.; Hu, Y.; Gao, H. J., Expression of PPARgamma and PTEN in human colorectal cancer: An immunohistochemical study using tissue microarray methodology. *Oncol Lett* **2011,** *2* (6), 1219-1224.
97. Li, X. H.; Zheng, H. C.; Takahashi, H.; Masuda, S.; Yang, X. H.; Takano, Y., PTEN expression and mutation in colorectal carcinomas. *Oncol Rep* **2009,** *22* (4), 757-64.

98. Zhou, X. P.; Loukola, A.; Salovaara, R.; Nystrom-Lahti, M.; Peltomaki, P.; de la Chapelle, A.; Aaltonen, L. A.; Eng, C., PTEN mutational spectra, expression levels, and subcellular localization in microsatellite stable and unstable colorectal cancers. *Am J Pathol* **2002,** *161* (2), 439-47.
99. Tracy, T. S.; Chaudhry, A. S.; Prasad, B.; Thummel, K. E.; Schuettz, E. G.; Zhong , X.-B.; Tien , Y.-C.; Jeong, H.; Pan, X.; Shireman, L. M.; Tay-Sontheimer, J.; Lin, Y. S., Interindividual Variability in Cytochrome P450-Mediated Drug Metabolism. *Drug Metabolism and Disposition* **2016,** *44* (3), 343-51.
100. Gao, H.; Korn, J. M.; Ferretti, S.; Monahan, J. E.; Wang, Y.; Singh, M.; Zhang, C.; Schnell, C.; Yang, G.; Zhang, Y.; Balbin, O. A.; Barbe, S.; Cai, H.; Casey, F.; Chatterjee, S.; Chiang, D. Y.; Chuai, S.; Cogan, S. M.; Collins, S. D.; Dammassa, E.; Ebel, N.; Embry, M.; Green, J.; Kauffmann, A.; Kowal, C.; Leary, R. J.; Lehar, J.; Liang, Y.; Loo, A.; Lorenzana, E.; Robert McDonald, E., 3rd; McLaughlin, M. E.; Merkin, J.; Meyer, R.; Naylor, T. L.; Patawaran, M.; Reddy, A.; Roelli, C.; Ruddy, D. A.; Salangsang, F.; Santacroce, F.; Singh, A. P.; Tang, Y.; Tinetto, W.; Tobler, S.; Velazquez, R.; Venkatesan, K.; Von Arx, F.; Wang, H. Q.; Wang, Z.; Wiesmann, M.; Wyss, D.; Xu, F.; Bitter, H.; Atadja, P.; Lees, E.; Hofmann, F.; Li, E.; Keen, N.; Cozens, R.; Jensen, M. R.; Pryer, N. K.; Williams, J. A.; Sellers, W. R., High-throughput screening using patient-derived tumor xenografts to predict clinical trial drug response. *Nat Med* **2015,** *21* (11), 1318-25.
101. Frattini, M.; Saletti, P.; Romagnani, E.; Martin, V.; Molinari, F.; Ghisletta, M.; Camponovo, A.; Etienne, L. L.; Cavalli, F.; Mazzucchelli, L., PTEN loss of expression predicts cetuximab efficacy in metastatic colorectal cancer patients. *Br J Cancer* **2007,** *97* (8), 1139-45.
102. Laurent-Puig, P.; Cayre, A.; Manceau, G.; Buc, E.; Bachet, J. B.; Lecomte, T.; Rougier, P.; Lievre, A.; Landi, B.; Boige, V.; Ducreux, M.; Ychou, M.; Bibeau, F.; Bouche, O.; Reid, J.; Stone, S.; Penault-Llorca, F., Analysis of PTEN, BRAF, and EGFR status in determining benefit from cetuximab therapy in wild-type KRAS metastatic colon cancer. *J Clin Oncol* **2009,** *27* (35), 5924-30.
103. Sood, A.; McClain, D.; Maitra, R.; Basu-Mallick, A.; Seetharam, R.; Kaubisch, A.; Rajdev, L.; Mariadason, J. M.; Tanaka, K.; Goel, S., PTEN gene expression and mutations in the PIK3CA gene as predictors of clinical benefit to anti-epidermal growth factor receptor antibody therapy in patients with KRAS wild-type metastatic colorectal cancer. *Clin Colorectal Cancer* **2012,** *11* (2), 143-50.
104. Locker, G. Y.; Hamilton, S.; Harris, J.; Jessup, J. M.; Kemeny, N.; Macdonald, J. S.; Somerfield, M. R.; Hayes, D. F.; Bast, R. C., Jr.; Asco, ASCO 2006 update of recommendations for the use of tumor markers in gastrointestinal cancer. *J Clin Oncol* **2006,** *24* (33), 5313-27.
105. Schmoll, H. J.; Van Cutsem, E.; Stein, A.; Valentini, V.; Glimelius, B.; Haustermans, K.; Nordlinger, B.; van de Velde, C. J.; Balmana, J.; Regula, J.; Nagtegaal, I. D.; Beets-Tan, R. G.; Arnold, D.; Ciardiello, F.; Hoff, P.; Kerr, D.; Kohne, C. H.; Labianca, R.; Price, T.; Scheithauer, W.; Sobrero, A.; Tabernero, J.; Aderka, D.; Barroso, S.; Bodoky, G.; Douillard, J. Y.; El Ghazaly, H.; Gallardo, J.; Garin, A.; Glynne-Jones, R.; Jordan, K.; Meshcheryakov, A.; Papamichail, D.; Pfeiffer, P.; Souglakos, I.; Turhal, S.; Cervantes, A., ESMO Consensus Guidelines for management of patients with colon and rectal cancer. a personalized approach to clinical decision making. *Ann Oncol* **2012,** *23* (10), 2479-2516.
106. Sepulveda, A. R.; Hamilton, S. R.; Allegra, C. J.; Grody, W.; Cushman-Vokoun, A. M.; Funkhouser, W. K.; Kopetz, S. E.; Lieu, C.; Lindor, N. M.; Minsky, B. D.; Monzon, F.

A.; Sargent, D. J.; Singh, V. M.; Willis, J.; Clark, J.; Colasacco, C.; Rumble, R. B.; Temple-Smolkin, R.; Ventura, C. B.; Nowak, J. A., Molecular Biomarkers for the Evaluation of Colorectal Cancer: Guideline From the American Society for Clinical Pathology, College of American Pathologists, Association for Molecular Pathology, and the American Society of Clinical Oncology. *J Clin Oncol* **2017,** *35* (13), 1453-1486.
107. Price, T. J.; Hardingham, J. E.; Lee, C. K.; Townsend, A. R.; Wrin, J. W.; Wilson, K.; Weickhardt, A.; Simes, R. J.; Murone, C.; Tebbutt, N. C., Prognostic impact and the relevance of PTEN copy number alterations in patients with advanced colorectal cancer (CRC) receiving bevacizumab. *Cancer Med* **2013,** *2* (3), 277-85.
108. Salvatore, L.; Calegari, M. A.; Loupakis, F.; Fassan, M.; Di Stefano, B.; Bensi, M.; Bria, E.; Tortora, G., PTEN in Colorectal Cancer: Shedding Light on Its Role as Predictor and Target. *Cancers (Basel)* **2019,** *11* (11).
109. Tian, M.; Wang, J.; Liu, S.; Li, X.; Li, J.; Yang, J.; Zhang, C.; Zhang, W., Hepatic HuR protects against the pathogenesis of non-alcoholic fatty liver disease by targeting PTEN. *Cell Death Dis* **2021,** *12* (3), 236.
110. Sun, Y.; Yu, M.; Qu, M.; Ma, Y.; Zheng, D.; Yue, Y.; Guo, S.; Tang, L.; Li, G.; Zheng, W.; Wang, M.; Guo, D.; Li, C., Hepatitis B virus-triggered PTEN/beta-catenin/c-Myc signaling enhances PD-L1 expression to promote immune evasion. *Am J Physiol Gastrointest Liver Physiol* **2020,** *318* (1), G162-G173.
111. Tang, J.; Xiao, X.; Jiang, Y.; Tian, Y.; Peng, Z.; Yang, M.; Xu, Z.; Gong, G., miR-3 Encoded by Hepatitis B Virus Downregulates PTEN Protein Expression and Promotes Cell Proliferation. *J Hepatocell Carcinoma* **2020,** *7*, 257-269.
112. Wu, Q.; Li, Z.; Mellor, P.; Zhou, Y.; Anderson, D. H.; Liu, Q., The role of PTEN - HCV core interaction in hepatitis C virus replication. *Sci Rep* **2017,** *7* (1), 3695.
113. Wu, Q.; Li, Z.; Liu, Q., Treatment with PTEN-Long protein inhibits hepatitis C virus replication. *Virology* **2017,** *511*, 1-8.
114. Yang, J. D.; Hainaut, P.; Gores, G. J.; Amadou, A.; Plymoth, A.; Roberts, L. R., A global view of hepatocellular carcinoma: trends, risk, prevention and management. *Nat Rev Gastroenterol Hepatol* **2019,** *16* (10), 589-604.
115. Singal, A. G.; Pillai, A.; Tiro, J., Early detection, curative treatment, and survival rates for hepatocellular carcinoma surveillance in patients with cirrhosis: a meta-analysis. *PLoS Med* **2014,** *11* (4), e1001624.
116. Chauhan, R.; Lahiri, N., Tissue- and Serum-Associated Biomarkers of Hepatocellular Carcinoma. *Biomark Cancer* **2016,** *8* (Suppl 1), 37-55.
117. Peyrou, M.; Bourgoin, L.; Foti, M., PTEN in liver diseases and cancer. *World J Gastroenterol* **2010,** *16* (37), 4627-33.
118. Wan, X. W.; Jiang, M.; Cao, H. F.; He, Y. Q.; Liu, S. Q.; Qiu, X. H.; Wu, M. C.; Wang, H. Y., The alteration of PTEN tumor suppressor expression and its association with the histopathological features of human primary hepatocellular carcinoma. *J Cancer Res Clin Oncol* **2003,** *129* (2), 100-6.
119. Zhou, J.; Li, X., Association of PTEN expression with liver function and inflammatory changes in patients with liver cancer after chemotherapy. *Oncol Lett* **2018,** *16* (5), 6633-6637.
120. Wang, J.; Xu, B., Targeted therapeutic options and future perspectives for HER2-positive breast cancer. *Signal Transduct Target Ther* **2019,** *4*, 34.
121. Medico, E.; Russo, M.; Picco, G.; Cancelliere, C.; Valtorta, E.; Corti, G.; Buscarino, M.; Isella, C.; Lamba, S.; Martinoglio, B.; Veronese, S.; Siena, S.; Sartore-Bianchi, A.;

Beccuti, M.; Mottolese, M.; Linnebacher, M.; Cordero, F.; Di Nicolantonio, F.; Bardelli, A., The molecular landscape of colorectal cancer cell lines unveils clinically actionable kinase targets. *Nat Commun* **2015,** *6*, 7002.
122. Bazzichetto, C.; Conciatori, F.; Pallocca, M.; Falcone, I.; Fanciulli, M.; Cognetti, F.; Milella, M.; Ciuffreda, L., PTEN as a Prognostic/Predictive Biomarker in Cancer: An Unfulfilled Promise? *Cancers (Basel)* **2019,** *11* (4).
123. Li, H.; Liu, Z. Y.; Wu, N.; Chen, Y. C.; Cheng, Q.; Wang, J., PARP inhibitor resistance: the underlying mechanisms and clinical implications. *Mol Cancer* **2020,** *19* (1), 107.
124. Fraser, M.; Zhao, H.; Luoto, K. R.; Lundin, C.; Coackley, C.; Chan, N.; Joshua, A. M.; Bismar, T. A.; Evans, A.; Helleday, T.; Bristow, R. G., PTEN deletion in prostate cancer cells does not associate with loss of RAD51 function: implications for radiotherapy and chemotherapy. *Clin Cancer Res* **2012,** *18* (4), 1015-27.
125. Sandhu, S. K.; Schelman, W. R.; Wilding, G.; Moreno, V.; Baird, R. D.; Miranda, S.; Hylands, L.; Riisnaes, R.; Forster, M.; Omlin, A.; Kreischer, N.; Thway, K.; Gevensleben, H.; Sun, L.; Loughney, J.; Chatterjee, M.; Toniatti, C.; Carpenter, C. L.; Iannone, R.; Kaye, S. B.; de Bono, J. S.; Wenham, R. M., The poly(ADP-ribose) polymerase inhibitor niraparib (MK4827) in BRCA mutation carriers and patients with sporadic cancer: a phase 1 dose-escalation trial. *Lancet Oncol* **2013,** *14* (9), 882-92.
126. Bian, X.; Gao, J.; Luo, F.; Rui, C.; Zheng, T.; Wang, D.; Wang, Y.; Roberts, T. M.; Liu, P.; Zhao, J. J.; Cheng, H., PTEN deficiency sensitizes endometrioid endometrial cancer to compound PARP-PI3K inhibition but not PARP inhibition as monotherapy. *Oncogene* **2018,** *37* (3), 341-351.
127. Dillon, L. M.; Miller, T. W., Therapeutic targeting of cancers with loss of PTEN function. *Curr Drug Targets* **2014,** *15* (1), 65-79.
128. Allott, E. H.; Ebot, E. M.; Stopsack, K. H.; Gonzalez-Feliciano, A. G.; Markt, S. C.; Wilson, K. M.; Ahearn, T. U.; Gerke, T. A.; Downer, M. K.; Rider, J. R.; Freedland, S. J.; Lotan, T. L.; Kantoff, P. W.; Platz, E. A.; Loda, M.; Stampfer, M. J.; Giovannucci, E.; Sweeney, C. J.; Finn, S. P.; Mucci, L. A., Statin Use Is Associated with Lower Risk of PTEN-Null and Lethal Prostate Cancer. *Clin Cancer Res* **2020,** *26* (5), 1086-1093.
129. Poliseno, L.; Salmena, L.; Zhang, J.; Carver, B.; Haveman, W. J.; Pandolfi, P. P., A coding-independent function of gene and pseudogene mRNAs regulates tumor biology. *Nature* **2010,** *465* (7301), 1033-8.
130. Sturgeon, C. M.; Viljoen, A., Analytical error and interference in immunoassay: minimizing risk. *Ann Clin Biochem* **2011,** *48* (Pt 5), 418-32.
131. Prichard, J. W., Overview of automated immunohistochemistry. *Arch Pathol Lab Med* **2014,** *138* (12), 1578-82.
132. Fedchenko, N.; Reifenrath, J., Different approaches for interpretation and reporting of immunohistochemistry analysis results in the bone tissue - a review. *Diagn Pathol* **2014,** *9*, 221.
133. Kim, S. W.; Roh, J.; Park, C. S., Immunohistochemistry for Pathologists: Protocols, Pitfalls, and Tips. *J Pathol Transl Med* **2016,** *50* (6), 411-418.
134. Yamashita, S., Heat-induced antigen retrieval: mechanisms and application to histochemistry. *Prog Histochem Cytochem* **2007,** *41* (3), 141-200.
135. Lee, H. G.; Jo, J.; Hong, H. H.; Kim, K. K.; Park, J. K.; Cho, S. J.; Park, C., State-of-the-art housekeeping proteins for quantitative western blotting: Revisiting the first draft of the human proteome. *Proteomics* **2016,** *16* (13), 1863-7.

136. Aebersold, R.; Burlingame, A. L.; Bradshaw, R. A., Western blots versus selected reaction monitoring assays: time to turn the tables? *Mol Cell Proteomics* **2013,** *12* (9), 2381-2.
137. Carr, S. A.; Abbatiello, S. E.; Ackermann, B. L.; Borchers, C.; Domon, B.; Deutsch, E. W.; Grant, R. P.; Hoofnagle, A. N.; Huttenhain, R.; Koomen, J. M.; Liebler, D. C.; Liu, T.; MacLean, B.; Mani, D. R.; Mansfield, E.; Neubert, H.; Paulovich, A. G.; Reiter, L.; Vitek, O.; Aebersold, R.; Anderson, L.; Bethem, R.; Blonder, J.; Boja, E.; Botelho, J.; Boyne, M.; Bradshaw, R. A.; Burlingame, A. L.; Chan, D.; Keshishian, H.; Kuhn, E.; Kinsinger, C.; Lee, J. S.; Lee, S. W.; Moritz, R.; Oses-Prieto, J.; Rifai, N.; Ritchie, J.; Rodriguez, H.; Srinivas, P. R.; Townsend, R. R.; Van Eyk, J.; Whiteley, G.; Wiita, A.; Weintraub, S., Targeted peptide measurements in biology and medicine: best practices for mass spectrometry-based assay development using a fit-for-purpose approach. *Mol Cell Proteomics* **2014,** *13* (3), 907-17.
138. Chen, Y.; Wang, F.; Xu, F.; Yang, T., Mass Spectrometry-Based Protein Quantification. *Adv Exp Med Biol* **2016,** *919*, 255-279.
139. Dupree, E. J.; Jayathirtha, M.; Yorkey, H.; Mihasan, M.; Petre, B. A.; Darie, C. C., A Critical Review of Bottom-Up Proteomics: The Good, the Bad, and the Future of this Field. *Proteomes* **2020,** *8* (3).
140. Parker, C. E.; Pearson, T. W.; Anderson, N. L.; Borchers, C. H., Mass-spectrometry-based clinical proteomics--a review and prospective. *Analyst* **2010,** *135* (8), 1830-8.
141. Fredolini, C.; Bystrom, S.; Pin, E.; Edfors, F.; Tamburro, D.; Iglesias, M. J.; Haggmark, A.; Hong, M. G.; Uhlen, M.; Nilsson, P.; Schwenk, J. M., Immunocapture strategies in translational proteomics. *Expert Rev Proteomics* **2016,** *13* (1), 83-98.
142. Shi, T.; Song, E.; Nie, S.; Rodland, K. D.; Liu, T.; Qian, W. J.; Smith, R. D., Advances in targeted proteomics and applications to biomedical research. *Proteomics* **2016,** *16* (15-16), 2160-82.
143. Picotti, P.; Aebersold, R., Selected reaction monitoring-based proteomics: workflows, potential, pitfalls and future directions. *Nat Methods* **2012,** *9* (6), 555-66.
144. Percy, A. J.; Chambers, A. G.; Smith, D. S.; Borchers, C. H., Standardized protocols for quality control of MRM-based plasma proteomic workflows. *J Proteome Res* **2013,** *12* (1), 222-33.
145. Sobsey, C. A.; Ibrahim, S.; Richard, V. R.; Gaspar, V.; Mitsa, G.; Lacasse, V.; Zahedi, R. P.; Batist, G.; Borchers, C. H., Targeted and Untargeted Proteomics Approaches in Biomarker Development. *Proteomics* **2019**, e1900029.
146. Boja, E.; Rivers, R.; Kinsinger, C.; Mesri, M.; Hiltke, T.; Rahbar, A.; Rodriguez, H., Restructuring proteomics through verification. *Biomark Med* **2010,** *4* (6), 799-803.
147. Wiita, A. P.; Seaman, J. E.; Wells, J. A., Global analysis of cellular proteolysis by selective enzymatic labeling of protein N-termini. *Methods Enzymol* **2014,** *544*, 327-58.
148. Keerthikumar, S.; Mathivanan, S., Proteotypic Peptides and Their Applications. *Methods Mol Biol* **2017,** *1549*, 101-107.
149. Hoofnagle, A. N.; Whiteaker, J. R.; Carr, S. A.; Kuhn, E.; Liu, T.; Massoni, S. A.; Thomas, S. N.; Townsend, R. R.; Zimmerman, L. J.; Boja, E.; Chen, J.; Crimmins, D. L.; Davies, S. R.; Gao, Y.; Hiltke, T. R.; Ketchum, K. A.; Kinsinger, C. R.; Mesri, M.; Meyer, M. R.; Qian, W. J.; Schoenherr, R. M.; Scott, M. G.; Shi, T.; Whiteley, G. R.; Wrobel, J. A.; Wu, C.; Ackermann, B. L.; Aebersold, R.; Barnidge, D. R.; Bunk, D. M.; Clarke, N.; Fishman, J. B.; Grant, R. P.; Kusebauch, U.; Kushnir, M. M.; Lowenthal, M. S.; Moritz, R. L.; Neubert, H.; Patterson, S. D.; Rockwood, A. L.; Rogers, J.; Singh, R. J.; Van Eyk, J. E.;

Wong, S. H.; Zhang, S.; Chan, D. W.; Chen, X.; Ellis, M. J.; Liebler, D. C.; Rodland, K. D.; Rodriguez, H.; Smith, R. D.; Zhang, Z.; Zhang, H.; Paulovich, A. G., Recommendations for the Generation, Quantification, Storage, and Handling of Peptides Used for Mass Spectrometry-Based Assays. *Clin Chem* **2016,** *62* (1), 48-69.
150. Shi, T.; Qian, W. J., Antibody-free PRISM-SRM for multiplexed protein quantification: is this the new competition for immunoassays in bioanalysis? *Bioanalysis* **2013,** *5* (3), 267-9.
151. Whiteaker, J. R.; Halusa, G. N.; Hoofnagle, A. N.; Sharma, V.; MacLean, B.; Yan, P.; Wrobel, J. A.; Kennedy, J.; Mani, D. R.; Zimmerman, L. J.; Meyer, M. R.; Mesri, M.; Boja, E.; Carr, S. A.; Chan, D. W.; Chen, X.; Chen, J.; Davies, S. R.; Ellis, M. J.; Fenyo, D.; Hiltke, T.; Ketchum, K. A.; Kinsinger, C.; Kuhn, E.; Liebler, D. C.; Liu, T.; Loss, M.; MacCoss, M. J.; Qian, W. J.; Rivers, R.; Rodland, K. D.; Ruggles, K. V.; Scott, M. G.; Smith, R. D.; Thomas, S.; Townsend, R. R.; Whiteley, G.; Wu, C.; Zhang, H.; Zhang, Z.; Rodriguez, H.; Paulovich, A. G., Using the CPTAC Assay Portal to Identify and Implement Highly Characterized Targeted Proteomics Assays. *Methods Mol Biol* **2016,** *1410*, 223-36.
152. Nelson, R. W.; Krone, J. R.; Bieber, A. L.; Williams, P., Mass spectrometric immunoassay. *Anal Chem* **1995,** *67* (7), 1153-8.
153. Becker, J. O.; Hoofnagle, A. N., Replacing immunoassays with tryptic digestion-peptide immunoaffinity enrichment and LC-MS/MS. *Bioanalysis* **2012,** *4* (3), 281-90.
154. Pino, L. K.; Searle, B. C.; Huang, E. L.; Noble, W. S.; Hoofnagle, A. N.; MacCoss, M. J., Calibration Using a Single-Point External Reference Material Harmonizes Quantitative Mass Spectrometry Proteomics Data between Platforms and Laboratories. *Anal Chem* **2018,** *90* (21), 13112-13117.
155. Chiva, C.; Pastor, O.; Trilla-Fuertes, L.; Gamez-Pozo, A.; Fresno Vara, J. A.; Sabido, E., Isotopologue Multipoint Calibration for Proteomics Biomarker Quantification in Clinical Practice. *Anal Chem* **2019,** *91* (8), 4934-4938.
156. Mani, D. R.; Abbatiello, S. E.; Carr, S. A., Statistical characterization of multiple-reaction monitoring mass spectrometry (MRM-MS) assays for quantitative proteomics. *BMC Bioinformatics* **2012,** *13 Suppl 16*, S9.
157. Cortese, M.; Gigliobianco, M. R.; Magnoni, F.; Censi, R.; Di Martino, P. D., Compensate for or Minimize Matrix Effects? Strategies for Overcoming Matrix Effects in Liquid Chromatography-Mass Spectrometry Technique: A Tutorial Review. *Molecules* **2020,** *25* (13).
158. Hoffman, M. A.; Schmeling, M.; Dahlin, J. L.; Bevins, N. J.; Cooper, D. P.; Jarolim, P.; Fitzgerald, R. L.; Hoofnagle, A. N., Calibrating from Within: Multipoint Internal Calibration of a Quantitative Mass Spectrometric Assay of Serum Methotrexate. *Clin Chem* **2020,** *66* (3), 474-482.
159. Anderson, N. L.; Anderson, N. G.; Haines, L. R.; Hardie, D. B.; Olafson, R. W.; Pearson, T. W., Mass spectrometric quantitation of peptides and proteins using Stable Isotope Standards and Capture by Anti-Peptide Antibodies (SISCAPA). *J Proteome Res* **2004,** *3* (2), 235-44.
160. LeBlanc, A.; Michaud, S. A.; Percy, A. J.; Hardie, D. B.; Yang, J.; Sinclair, N. J.; Proudfoot, J. I.; Pistawka, A.; Smith, D. S.; Borchers, C. H., Multiplexed MRM-Based Protein Quantitation Using Two Different Stable Isotope-Labeled Peptide Isotopologues for Calibration. *J Proteome Res* **2017,** *16* (7), 2527-2536.
161. Froehlich, B. C.; Popp, R.; Sobsey, C. A.; Ibrahim, S.; LeBlanc, A. M.; Mohammed, Y.; Aguilar-Mahecha, A.; Poetz, O.; Chen, M. X.; Spatz, A.; Basik, M.; Batist, G.; Zahedi, R. P.; Borchers, C. H., Systematic Optimization of the iMALDI Workflow for the Robust and

Straightforward Quantification of Signaling Proteins in Cancer Cells. *Proteomics Clin Appl* **2020,** *14* (5), e2000034.
162. Grant, R. P., The march of the masses. *Clin Chem* **2013,** *59* (6), 871-3.
163. Whiteaker, J. R.; Halusa, G. N.; Hoofnagle, A. N.; Sharma, V.; MacLean, B.; Yan, P.; Wrobel, J. A.; Kennedy, J.; Mani, D. R.; Zimmerman, L. J.; Meyer, M. R.; Mesri, M.; Rodriguez, H.; Clinical Proteomic Tumor Analysis, C.; Paulovich, A. G., CPTAC Assay Portal: a repository of targeted proteomic assays. *Nat Methods* **2014,** *11* (7), 703-4.
164. Keshishian, H.; Burgess, M. W.; Gillette, M. A.; Mertins, P.; Clauser, K. R.; Mani, D. R.; Kuhn, E. W.; Farrell, L. A.; Gerszten, R. E.; Carr, S. A., Multiplexed, Quantitative Workflow for Sensitive Biomarker Discovery in Plasma Yields Novel Candidates for Early Myocardial Injury. *Mol Cell Proteomics* **2015,** *14* (9), 2375-93.
165. Froehlich, B. C.; Popp, R.; Sobsey, C. A.; Ibrahim, S.; LeBlanc, A.; Mohammed, Y.; Buchanan, M.; Aguilar-Mahecha, A.; Potz, O.; Chen, M. X.; Spatz, A.; Basik, M.; Batist, G.; Zahedi, R. P.; Borchers, C. H., A multiplexed, automated immuno-matrix assisted laser desorption/ionization mass spectrometry assay for simultaneous and precise quantitation of PTEN and p110alpha in cell lines and tumor tissues. *Analyst* **2021,** *146* (21), 6566-6575.
166. Wu, J.; Song, Y., Expression and clinical significance of serum MMP-7 and PTEN levels in patients with acute myeloid leukemia. *Oncol Lett* **2018,** *15* (3), 3447-3452.
167. Li, Y. Y.; Xiao, R.; Li, C. P.; Huangfu, J.; Mao, J. F., Increased plasma levels of FABP4 and PTEN is associated with more severe insulin resistance in women with gestational diabetes mellitus. *Med Sci Monit* **2015,** *21*, 426-31.